2019

Compound-Specific Isotope Analysis of Amino Acids in Biological Tissues: Applications in Forensic Entomology, Food Authentication and Soft-Biometrics in Humans

Mayara Patricia Viana de Matos
West Virginia University, mavianademattos@mix.wvu.edu

Compound-Specific Isotope Analysis of Amino Acids in Biological Tissues: Applications in Forensic Entomology, Food Authentication and Soft-Biometrics in Humans

Mayara Patrícia Viana de Matos

Dissertation submitted to the Eberly College of Arts and Sciences
at West Virginia University
in partial fulfillment of the requirements
for the degree of

Doctor of Philosophy
in
Biology

Glen P. Jackson, Ph.D., Committee Chair
Clifton P. Bishop, Ph.D.
Jennifer E. Gallagher, Ph.D.
Shikha Sharma, Ph.D.
Stephen J. Valentine, Ph.D.

Department of Biology

Morgantown, West Virginia
2019

Keywords: stable isotope analysis (SIA), compound-specific isotope analysis (CSIA), IRMS, entomology, food authentication, soft-biometrics, human hair, forensics

ABSTRACT

Compound-Specific Isotope Analysis of Amino Acids in Biological Tissues: Applications in Forensic Entomology, Food Authentication and Soft-Biometrics in Humans

Mayara Patrícia Viana de Matos

In this work we demonstrate the power of compound-specific isotope analysis (CSIA) to analyze proteinaceous biological materials in three distinct forensic applications, including: 1) linking necrophagous blow flies in different life stages to their primary carrion diet; 2) identifying the harvesting area of oysters for food authentication purposes; and 3) the ability to predict biometric traits about humans from their hair.

In the first application, we measured the amino-acid-level fractionation that occurs at each major life stage of *Calliphora vicina* (Robineau-Desvoidy) (Diptera: Calliphoridae) blow flies. Adult blow flies oviposited on raw pork muscle, beef muscle, or chicken liver. Larvae, pupae and adult blow flies from each carrion were selected for amino acid CSIA. Canonical discriminant analysis showed that flies were correctly classified to specific carrion types in 100% (original rules) and 96.8% (leave-one-out cross-validation [LOOCV]) of cases. Regarding life stages, we obtained 100% and 71% of correct classification in original rules and LOOCV, respectively. Most of the essential amino acids did not significantly change between life stages (at 95% CI). However, some non-essential (Ala, Ser, and Glu) and conditionally essential amino acids (Gly and Pro) were isotopically depleted in the adult stage. Except for the essential amino acids, the amino acids in larvae and pupae were enriched in ^{13}C and adult blow flies were depleted in ^{13}C relative to the carrion on which they fed. These results make it possible to exclude potential sources of carrion as larval food. In addition, amino-acid-specific IRMS could help inform entomologists whether a fly has just arrived from another location to feed on a corpse or has emerged from a pupa whose feedstock was the corpse.

Regarding the source inference of oysters, we investigated the bulk, amino-acid compound-specific stable isotopes, cadmium and lead concentrations of the popular Eastern oyster, *Crassostrea virginica*. This species has been one of the most popular species for the oyster harvesting business in the United States, despite its claimed reduced availability due to excessive harvesting and some parasitic diseases. The results from specimens collected from different Gulf of Mexico bays were subjected to multivariate statistical analysis to assess whether we could predict the oysters' harvest area. Our results indicate that the combination of trace elements and isotope ratios can predict geographic provenance of oysters with greater than 70% correct classification using LOOCV, which is superior to using only CSIA or only trace elements. The $\delta^{13}C$ values of serine and glycine could also discriminate between two adjacent harvest areas within the same Apalachicola bay. One of these areas is fishable in the winter season and the other is fishable in the summer season, so the ability to differentiate oysters from these two areas is a valuable capability for the Florida Department of Agriculture, which is responsible for enforcement. The use of chemical signatures to identify harvest areas is a valuable tool to protect consumers from food fraud, food-borne diseases and to help regulatory agencies enforce harvesting regulations.

Finally, we describe the use of amino-acid CSIA and amino acid quantitation of scalp hair of American individuals to predict soft biometrics in humans. We measured the isotope ratios and respective quantities of 13 amino acid peaks. Correlation analysis of the multivariate data provided the degree of correlation between essential and non-essential amino acids with factors such sex and age of the hair donors. The isotope ratios of each amino acid were first corrected for the extent of C_4-based carbon in the diet to reveal relationships between metabolic or phenotypic factors and the isotope ratios of ^{13}C in the amino acids in the hair shafts. Multivariate analysis revealed that the sex of a donor could be correctly predicted with cross-validated accuracies of 80% and 89% using the

isotope ratios or quantities of amino acids, respectively. The continuous dependent variables of donor age and body mass index (BMI) were also predicted using the amino acid isotope ratios or quantities, but the predictions were not as reliable as for sex determination. Unexpectedly, the $\delta^{13}C$ values of hair reflected the frequency of alcohol consumption in two groups of subjects.

DEDICATION

I dedicate this work to my loved parents, Margarida and Matos, who always supported my decisions and encouraged me to be resilient in every moment of my life. Access to education is the best gift one can receive; thank you for making all the sacrifices to make sure I could have it.

"Dedico este trabalho aos meus amados pais, Margarida e Matos, os quais sempre apoiaram minhas decisões e me encorajaram a ser persistente em todos os momentos da minha vida. Ter acesso à educação é o melhor presente que alguém pode receber; obrigada por fazer todos os sacríficios para garantir que eu a recebesse."

ACKNOWLEDGMENTS

Firstly, I would like to thank my advisor, Dr. Glen Jackson, for all these years of learning opportunities in his research group. I joined WVU aiming to be part of his lab and was very happy when he accepted me despite my initial struggles in the university. Dr. Jackson fully supported my decision to transfer from Chemistry to the Biology department and, since then, I aimed to give my best and prove that I could do much better in this new place. I thank Dr. Jackson for all the time he invested in my scientific development, for allowing me to take initiative towards my work, for introducing me to other scientists, for improving my written and oral scientific skills with valuable tips, and for treating me and my work colleagues with constant respect and appreciation.

I want to thank my committee members: Dr. Clifton Bishop, Dr. Jennifer Gallagher, Dr. Shikha Sharma, and Dr. Stephen Valentine for the time they dedicated reviewing this dissertation, as well as for the extra advice during informal conversations. This work certainly gained value after including their expert insights.

I also acknowledge the scientists from the Center for Food Safety and Applied Nutrition (Methods Development Branch) of the Food and Drug Administration at College Park, MD, in special Dr. Brad Mangrum and Dr. Lowri DeJager. During two short internships in their facility, I could run some of my samples, which allowed me to graduate within the scheduled deadline. They were also very kind to provide any lab supplies I needed for the experiments, while also allowing me to acquire some experience in different instruments. I will always be grateful for the opportunity!

I am also thankful to the faculty and staff of the Department of Biology and the Department of Forensic and Investigative Science (FIS) for always providing a scientific and friendly environment for the students. From the Biology department, a special thanks to Dr. Clifton Bishop and Dr. Rita Rio who were extremely helpful during my transferring period from the Chemistry department. From the FIS, a big thanks to William (Bill) Cunningham for being such a nice, proactive and helpful person.

A big thanks to the members of my research group, some of the nicest and smartest people I had the chance to work with throughout these years. In random order, the grads Halle Edwards, Zach Sasiene, Tyler Davidson, Praneeth Mario Mendis, Tom Hakey, Caitlyn Lear; and the undergrads Isaac Willis, Sarah Chaffman and Sam Mehnert. Thanks for the great times in the lab, for being so cooperative, and for holding such a good work environment despite the struggles with instruments and experiments. It was much easier to pass through grad student life being surrounded by such great people. I also thank the former group members Dr. William (Billy) Hoffman, Dr. Feng Jin and Dr. Pengfei Li for their contribution in my first years in the group. To my out-of-lab friends, who at some point contributed to the success of this work by providing the emotional support and happy moments that I so much needed outside the laboratory, thanks to all of you!

Finally, I would like to say thanks to my family for all the love, support and encouragement in this journey far away from home. You are the responsible for the solid base I needed to build anything in my life. Thanks for believing I could do it, even when, for many times, I did not believe it myself. Without you I would not have gone this far!

TABLE OF CONTENTS

TABLE OF FIGURES

LIST OF TABLES

LIST OF SYMBOLS / ABBREVIATIONS

δ - Delta

m/z – Mass to charge ratio

‰ - Per mil

ANOVA - Analysis of variance

AA - Amino acid

AN - Ammonium nitrate

ANFO - Ammonium nitrate fuel oil

AOAC - Association of Analytical Communities

BMI - Body mass index

BSE - Bovine spongiform encephalopathy

BZP - Benzylpiperazine

CI - Confidence interval

CSIA - Compound-specific isotope analysis

DART-HRMS - Direct analysis in real time high-resolution mass spectrometry

DEA - Drug Enforcement Agency

DOF - Degrees of freedom

EA - Elemental analyzer

EA-IRMS - Elemental analyzer isotope ratio mass spectrometry

FMD - Foot-and-mouth disease

FTIR - Fourier-transform infrared spectroscopy

GC - Gas chromatography

GC/C/IRMS - Gas chromatography combustion isotope ratio mass spectrometry

GBL - γ-butyrolactone

GHB - γ-hydroxybutyric acid

IAEA - International Atomic Energy Agency

IAEA-600 - Caffeine standard

ICP-MS - Inductively coupled plasma mass spectrometry

IED - Improvised explosive device

IRMS - Isotope ratio mass spectrometry

HPLC - High-performance liquid chromatography

HSD – Honestly significant difference

LC - Liquid chromatography

LC-IRMS - Liquid chromatography isotope ratio mass spectrometry

LDA - Linear discriminant analysis

LOOCV - Leave-one-out cross-validation

LSVEC - Lithium carbonate reference standard

MAAH - Microwave-assisted acid hydrolysis

MANOVA - Multivariate analysis of variance

NBS-19 - Limestone reference standard

NIST - National Institute of Standards and Technology

NMR - Nuclear magnetic resonance

PE - Pentaerythritol

PETN - Pentaerythritol tetranitrate

PSIA - Position-specific isotope analysis

PTFE - Polytetrafluoroethylene

PVDF - Polyvinylidene fluoride

QQ - Quantile-quantile

SIA - Stable isotope analysis

TATP - Triacetone triperoxide

TFMPP - Trifluoromethylphenylpiperazine

TMAO - Trimethylamine N-oxide

USGS - United States Geological Survey

USGS 40 - L-glutamic acid reference standard

USGS 41 - L-glutamic acid reference standard

USGS 42 - Tibetan hair reference standard

USGS 43 - Indian hair reference standard

VPDB - Vienna Pee Dee Belemnite

XRF - X-ray fluorescence

INTRODUCTION

Stable isotope analysis (SIA) is a well-stablished research field that provides information about the source or fate of a substance based on the slight differences that exist in the natural abundance of stable isotopes of elements such as H, C, N, O and S. Isotope ratio mass spectrometry (IRMS) is a technique that unravels the source of chemically indistinguishable materials by measuring the differences in the natural isotope abundances in a per mil (or delta) scale. The robustness and excellent precision of IRMS has made it an indispensable tool in various fields of study, especially in forensic science. The theory behind this technique is based on isotope fractionation, which is the preferential incorporation of the heavy or light isotope of an element in one of the phases of a system undergoing a physical or chemical change. Fractionation most often occurs when a bond containing a heavier isotope is involved in a rate-limiting chemical transformation. The heavier isotope has a slightly higher bond dissociation energy than the lighter isotope, so the rate of chemical transformation of the heavier isotope is slightly slower. The slower rates of reaction of the heavier isotope leads to the preferential transformation of the lighter isotope into the reaction products. Isotope fractionation causes changes in the relative abundances of naturally occurring isotopes of an element and creates isotopic signatures that can inform an analyst about the source of a substance, or about the chemical and physical processes that a sample has undergone before analysis.

SIA can provide information ranging from travel history to health conditions of an individual. SIA can also indicate the geographic source and diet information from other lifeforms, such as plant and animal-based food, insects and animals. Bulk isotope ratios are the easiest and most precise type of isotopic measurement, but because the between-individuals variance within a species is not significantly larger than the within-individual variance, scientists are generally not able to use bulk

isotope ratios to distinguish between individuals of a species or determine metabolic information. This gap in knowledge has been partially filled through compound-specific isotope analysis (CSIA) of amino acids, which yields substantially more variables for comparison. When combined with multivariate analysis techniques, CSIA provides capabilities beyond anything possible with bulk IRMS. The results from this specific approach can significantly impact diverse fields of study, such as food authentication, forensic entomology, ecology, and clinical studies.

The overall goal of this dissertation is to demonstrate the power of CSIA in distinct forensic applications by working with proteinaceous biological materials to investigate: 1) the ability to link necrophagous blow flies in different life stages to their primary carrion diet; 2) the ability to identify the harvesting area of oysters for food authentication purposes; and 3) the ability to obtain biometric information of a human from their hair.

Chapter 1 is an extensive literature review that presents advances in the application of IRMS to materials of interest to the forensic community. Special attention is given to the natural abundance differences in the stable isotopes of carbon, nitrogen, hydrogen and oxygen because they are the most abundant and informative elements in typical forensic casework. Chapter 1 also presents some of the recent developments in normalization, error reporting and data analysis, which together provide a more scientific and robust foundation for admissibility in court. This chapter focusses on research published in the last decade and is organized into ten major sections, including human provenance, wildlife forensics, environmental forensics, seized drugs, ignitable liquids, explosives, food forensics, poisoning, questioned documents and miscellaneous applications.

Chapter 2 describes a forensic entomology and ecology project in which IRMS is used to understand the relationship between the $\delta^{13}C$ of amino acids in different carrion sources and the blow flies that feed on them. Adult blow flies are one of the first necrophagous insects to colonize fresh

carcasses. The eggs they lay hatch into larvae, which feed on the decomposing body. Like all organisms, blow flies are "what they eat", meaning that the isotopic composition of their body tissues reflects their diet. The analytical ability to link organisms from one trophic level to another using CSIA of amino acids could have wide-reaching consequences in a variety of other disciplines.

Chapter 3 combines IRMS and inductively coupled plasma-mass spectrometry (ICP-MS) to investigate the $\delta^{13}C$ and $\delta^{15}N$ bulk isotope ratios, carbon CSIA of amino acids, and cadmium and lead concentrations from extracted whole-body tissues of various samples of the Eastern oyster, *C. virginica*. These oysters were collected from the Gulf of Mexico coastal waters of Florida (FL), Louisiana (LA) and Texas (TX). The combinatory approach proposed in this chapter is a potentially valuable tool for oyster fisheries managers, wildlife and food safety enforcement officers, as well as to forensics and ecology research areas.

The last chapter describes the use of amino acid quantitation and amino-acid-specific isotope ratio analysis of scalp hair of American individuals to predict soft biometrics in humans. The results provide evidence that CSIA is a potent tool that transcends the capabilities of bulk isotope measurements in providing biometrics and routine/behavior traits of individuals.

Chapter 1 has been accepted for publication as a review article in *Forensic Chemistry*. Chapter 2 was published in *Analytical and Bioanalytical Chemistry* in the summer of 2018. Chapters 3 and 4 are in the final stages of preparation for submission.

CHAPTER 1: ISOTOPE RATIO MASS SPECTROMETRY IN FORENSIC SCIENCE APPLICATIONS

Reproduced in part with permission from Mayara P. V. Matos and Glen P. Jackson, *Forensic Chemistry*, accepted for publication, DOI: 10.1016/j.forc.2019.100154

1. Introduction

The ability to unravel the source of chemically indistinguishable substances has made isotope ratio mass spectrometry (IRMS) an indispensable tool in a variety of scientific disciplines, and especially in forensic science [1-3]. There are many excellent reviews and monologs on the theory, development, and application of stable isotope analysis (SIA) in different forensic science areas of study [4-13]. Herein, we do not attempt to be so comprehensive. Instead, we focus on the most recent, novel and impactful forensic applications, including new aspects of data analysis and reporting. In the last decade, IRMS, in combination with improved chromatographic techniques, has provided advances in diverse areas of forensic science, including sample preparation techniques that have enabled more reliable or meaningful discrimination between samples. The review is organized into ten major topical areas of forensic interest. Most of the citations are for applications that involve source provenance and sample classification, but some articles report on better understanding the fractionation of isotopes within or between certain substrates.

Since its foundation in 2002, the Forensic Isotope Ratio Mass Spectrometry Network (FIRMS) has spearheaded the application of IRMS to forensic casework. FIRMS has been organizing triennial conferences, providing forensic practitioner approvals, conducting inter-laboratory proficiency tests [2, 14], presenting guidance on suitable reference materials (RMs), and offering a "Good Practice Guide for IRMS" (GPG) to assist practitioners with the essential principles of the instrument operation, quality assurance, troubleshooting and data management [15]. The

FIRMS Network often publishes a special issue in an analytical or forensic science journal following each triennial conference, and these special editions are a rich source of forensically-relevant IRMS literature for anyone interested in the topic.

Relating to the FIRMS Network, Carter and Fry [16] conducted a series of inter-laboratory tests within FIRMS Network members to first assess the variance, quality control and quality assurance protocols of different laboratories, and then to guide improvements in the reproducibility of measurements between laboratories. Problems related to homogeneity in sample preparation, choice of reference materials and internal standards, as well as data reporting relative to delta (δ) scale, are among the identified deficiencies that required improvements to make IRMS results fit-for-purpose. Only a minority of labs were outside the expected range of the results. More recently, another inter-laboratory assessment was performed to compare the bulk isotope analysis of honey coming from diverse metrological institutes [17]. The results derived from forensic stable isotope laboratories within the FIRMS Network[18], and all the participating laboratories, provided $\delta^{13}C$ values for bulk honey that were within an acceptable range. The method by which each laboratory calculated and reported their measurement uncertainty was a notable point of discussion, however, because some laboratories report standard deviations instead of expanded measurement uncertainty, such as the 95% confidence interval. To align with international standards, the use of an expanded uncertainty instead of a standard deviation is recommended for reported results.

To assist practitioners in establishing expanding uncertainties, Dunn and coworkers [19] have suggested a simple and straightforward improvement to the Kragten spreadsheet published in the GPG [15], which complements the existing approaches and guidelines used for delta scale [20]. The new spreadsheet is quite practical, and it combines the different sources of isotope uncertainty to multiple samples in one spreadsheet. Note that analytical results can include human errors, which

are outside the random errors that are captured in uncertainty-budgeting spreadsheets. All researchers and practitioners should take preventative steps to promptly identify and mitigate sources of occasional mistakes, thereby enhancing the reliability of the any reported result [21, 22].

One of the biggest challenges in IRMS is the selection and use of appropriate—i.e. matrix matched—and well-characterized reference materials (RMs) [23]. The last few years have witnessed significant developments in RMs for calibration of δ^{2}H, δ^{18}O [24-27], δ^{13}C, δ^{15}N, and δ^{34}S values [28-30]. One RM is a mixture of three glycine solutions that are recommended for establishing multiple-point calibration curves for the δ^{13}C scale [29]. Another three sugar RMs (BEET-1, GALT-1, and FRUT-1) were developed for δ^{13}C normalization of sugar-based materials, although it can also be used for other organic materials [31]. The hair RMs USGS-42 and USGS-43 have been developed for measurements of hydrogen and oxygen stable isotopes, but are also appropriate for measurements involving C, N, and S of human and mammalian hair [28]. The use of (at least) a two-point calibration scale is now a minimum requirement for high-quality data [15, 23, 32, 33], and procedures are available with which to provide in-house isotope standards to help preserve the limited stocks of international materials [34].

Beyond the importance of accuracy, it is also important to report measures of precision or confidence intervals for forensic applications, and to provide estimates for the power of discrimination of forensic samples [35]. As examples of these approaches, several groups have used Bayesian networks to assess the value of IRMS data [36-38], and several groups have provided a method using likelihood ratios (LRs) as a measure of the strength of IRMS data [39-41]. Such developments in reporting are critical to the future of the forensic community. However, one potential problem with reporting results in terms of LRs is that when an LR weakly favors the prosecution, the LR can be totally misinterpreted by jurors as actually favoring the defense [42]!

Another way to interpret this observation is that jurors demand a very high threshold of confidence to find a suspect guilty, so a weakly favorable LR might not pass the cognitive threshold in the jurors' minds to warrant a severe penalty for the defendant. For a contextual understanding of the use of IRMS in legal applications, Ehleringer and Matheson have provided an excellent, comprehensive, clear review article that describes the admissibility of stable isotope analyses in court [43]. This foundational review is a profoundly important document for bridging the gap between the legal community and the research/practitioner communities, and there are many other forensic science disciplines that could benefit from such lucid a foundational document.

2. Human provenance

Many forensic stable isotope studies involve human subjects, and the goal of such investigations is usually to provide an investigative lead, such as insight into a person's geographic origin or travel history. Assisting these investigations, many IRMS studies have examined the relationship between the isotopic composition of human tissues and the geographic origin, health status or dietary interventions of the subjects. Such studies are useful for both paleo-archeological purposes and modern law enforcement investigations because both applications require the prediction of geographic origin of unidentified human remains [10, 11, 44-46].

A critical factor for strong geo-location inference is the establishment of reliable and high-resolution spatial maps for the precipitation and groundwater values for δ^2H and δ^{18}O [47, 48]. Such isotope landscapes, also known as Isoscapes [49], provide the framework for spatiotemporal movement of humans and other organisms [2, 47, 50]. In 2014, δ^2H and δ^{18}O measurements of 349 US tap water samples were made available in the largest public dataset to date. The samples included a broad geographic sampling and seasonal sampling [51]. Dr. Gabriel Bowen, from the University of Utah, has made the spatial variation metadata for water isotopes fully accessible through the Water

Isotopes Database (http://wateriso.utah.edu/waterisotopes/index.html) and through a recently developed mobile phone application called "wiSamples". Publicly-available data like this are critical for the validation and acceptance of Isoscapes for modern human provenancing, and some groups have successfully started using Isoscapes for such applications [52]. As a word of caution to prospective researchers in this area, one has to be especially careful with the calibration and interpretation of δ^{2}H measurements of proteinaceous material like hair, muscle and feathers [53]. The number of exchangeable hydrogens varies greatly depending on the protein composition, so it is critical to use of matrix-matched standards to obtain accurate isotope normalization [54].

For geographical provenance, biological samples must be representative of the organism and be chemically robust to provide meaningful isotope ratios, which is why bone, teeth, hair and nails are especially useful matrices. Hair and fingernails have the added advantages that they store a chronological record of diet and health of a person and that they can be non-invasively collected in the presence of a third party; i.e. witnessed [55, 56]. Hair and nails are both abundant in α-keratin—a protein that is extremely robust and insoluble in water under normal conditions. As an example of keratin's stability, a study by Koehler and Hobson showed that tanning of polar bear hides with sulfuric acid did not alter the δ^{13}C or δ^{15}N values of the hair in the hides but did alter the δ^{34}S values [57]. In another example, isotope ratio values of δ^{13}C, δ^{15}N and δ^{18}O in human hair were shown to be equally stable in a desiccator and freezer as they were spending ten months exposed to the natural environment [58]. However, as cautioned above, some δ^{2}H fractionation of hair was observed after prolonged storage times (e.g. 6 months). The general, chemical stability of keratins means that once they are formed, metabolic and chemical changes are minimal, and the isotopes of C, N and O are resistant to external influence.

A global database of $\delta^{13}C$ and $\delta^{15}N$ in hair and nails was recently compiled [59], and whereas the $\delta^{13}C$ values of hair and nail was shown to correlate strongly with the amount of C-4 plants in the diet—as determined by latitude and geography—the $\delta^{15}N$ values of hair and nail showed a much weaker correlation to geography. Instead, the $\delta^{15}N$ values correlated more strongly with fish/meat intake and coastal proximity (**Fig. 1.1**). Valenzuela *et al.* showed that, within the United States, $\delta^{34}S$ values of more than 206 human hair samples provided better geographic information than either $\delta^{13}C$ or $\delta^{15}N$ [60]. However, the samples in this particular study were almost devoid of coastal representation, which is where dietary factors are most likely to influence the $\delta^{13}C$ and $\delta^{15}N$ values.

Although most of the literature related to human provenancing focuses on the dietary components and geospatial movement of individuals [10, 11], non-dietary sources of phenotypic variance, such as sex, BMI and age, also enable the classification of subjects when performing compound-specific isotope analysis (CSIA) of hair [61]. One note of caution with hair and nail comparisons is that human hair is slightly enriched in ^{13}C and slightly depleted in ^{15}N relative to nail clippings from the same individual [62-64], so care must be taken when interpreting the isotope values between hair and nails.

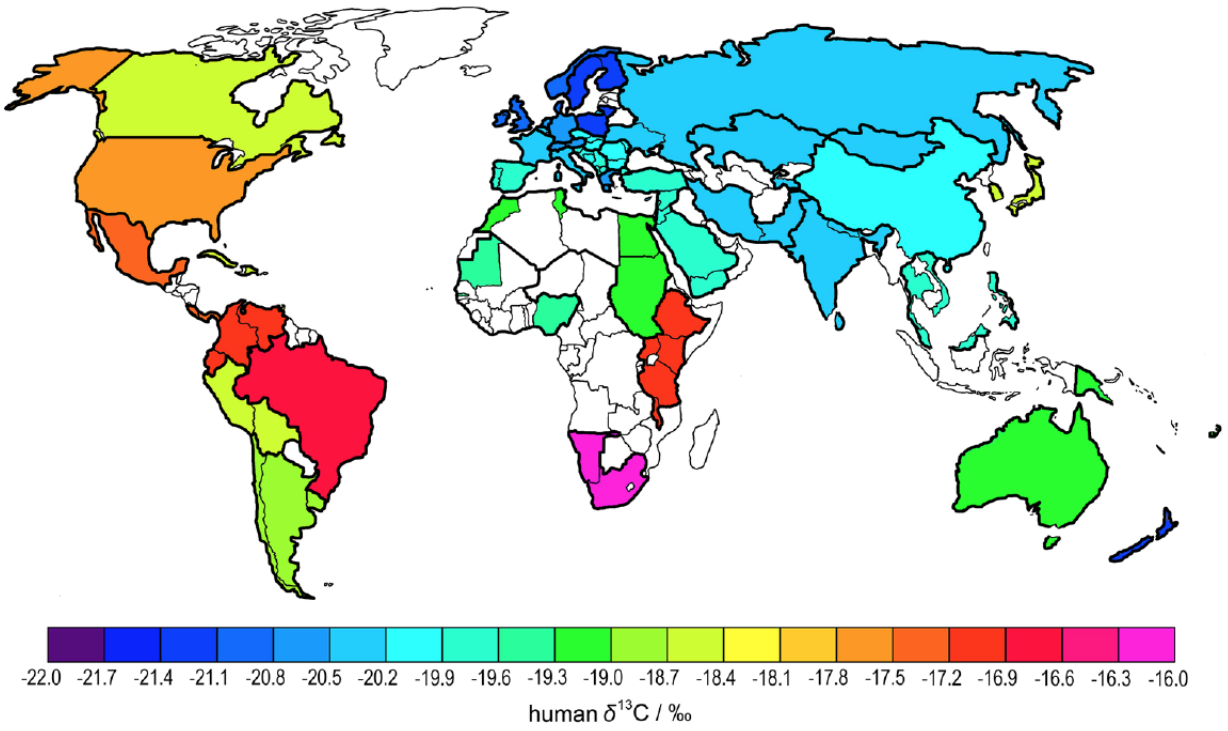

Fig. 1.1. Example of a global isotope database against which questioned samples can be compared. This map shows the spatial distribution of $\delta^{13}C$ values collected from more than 4,000 contemporary human hair and nail samples. Equatorial regions, especially on the African continent, are vastly under-represented. Image reprinted from reference [59]: F. Hulsemann, C. Lehn, S. Schneider, G. Jackson, S. Hill, A. Rossmann, N. Scheid, P.J. Dunn, U. Flenker, W. Schanzer, Global spatial distributions of nitrogen and carbon stable isotope ratios of modern human hair, Rapid Commun. Mass Spectrom. 29(22) (2015) 2111-21, Copyright (2015), with permission from John Wiley & Sons, Inc.

3. Wildlife forensics

Studies involving the illegal harvesting and the black-market trading of plants and animals are of great interest in the legal community. Illegal wildlife trade is a global problem estimated to circulate US$5-20 billion annually [65]. The determination of the geographic origin and movement of animals between different landscapes have both been successfully tracked using IRMS. For example, different isotopes are often used to unravel the trophic level of organisms and to establish the various flows of energy inside different food webs [66]. Such studies support a better understanding of the ecological behavior of animals and the development of effective conservational

strategies towards endangered species [67]. IRMS can also assist with wildlife crime investigations [67]. Even though IRMS can be very relevant in these particular forensic situations, there is formal delineation that divides forensic applications from "pure" ecological investigations. As with other cross-disciplinary studies, there are many benefits to maintaining an open dialog between forensic science and ecology application areas.

Carbon, nitrogen and, to a lesser extent, sulfur are the most studied isotopes for diet reconstruction, geographic origin determination, and the study of animal migration/foraging ecology in different habitats [68-72]. These applications also lead to a better understanding of illegal trading of wildlife products. Among these applications, elephant ivory and bone were the first wildlife materials where original source determination via multi-isotope analysis was combined with a forensic application [73-76]. More recently, δ^{13}C and δ^{15}N values were used to discriminate between the breeding of wild and captive Vietnamese endangered crocodile lizards of the taxon *Shinisaurus crocodilurus* [77]. SIA was also successful in determining the differences between wild vs. illegally traded/captive-bred African grey parrots (*Psittacus erithacus*) [78] and Burmese and reticulated pythons [79]. However, carbon and nitrogen trophic models are not trivial markers of energy flow through an ecosystem due to isotope fractionation. The term fractionation refers to the enrichment or depletion of isotope ratios when a substrate undergoes a physical or chemical transformation. Fractionation occurs when a bond containing a heavier isotope is involved in a rate-limiting chemical transformation, such as when an enzyme decarboxylates an amino acid during metabolism. The heavier isotope has a slightly higher bond dissociation energy than the lighter isotope, so the rate of chemical transformation of the heavier isotope is slightly slower, which leads to the preferential transformation of the lighter light isotope [80, 81].

Although measurable, isotopic fractionation between an organism and its food sources is not always predictable, especially in some highly dynamic and complex ecosystems like aquatic food webs [66]. For this reason, some researchers use isoscapes [82], and $^{87}Sr/^{86}Sr$ isotope ratios in addition to $\delta^{13}C$ and $\delta^{15}N$ values to predict an organism's movements. Such studies provide a better understanding of how SIA can be applied for wildlife conservation practices. Extra caution must be taken to ensure that the results are fit-for-purpose and devoid of fractionation [53, 54]. Meanwhile, when comparing high-resolution X-ray fluorescence (XRF) and $\delta^{13}C$ and $\delta^{15}N$ values of wild- and zoo-bred specimens of echidnas (*Tachyglossus aculeatus*), Brandis *et al.* reported 100% correct classification using the XRF data compared to 91.3% accuracy from the IRMS data [83]. Such studies are a reminder that IRMS measurements are not always the best or only tool in the analytical chemist's toolbox.

In the context of aquatic systems, some studies have investigated the influence of dietary water on the $\delta^{2}H$ values of different organisms' tissues, as well as how water signatures can be used to trace organic matter and migratory patterns [66, 84, 85]. For example, Soto and coworkers [86] performed an environmentally controlled experiment where the ambient water, dissolved O_2, food and tissue protein and lipids of two trophic level aquatic species—an insect and a fish—were analyzed for $\delta^{2}H$ and $\delta^{18}O$ values. The authors demonstrated that hydrogen and oxygen could serve as complementary tracers of diet and provenance in the aquatic ecosystem and pointed out the strengths and weaknesses of this approach. The lipid content of animal tissue is often reported as a source of variation in $\delta^{2}H$, $\delta^{13}C$ and $\delta^{15}N$ values from aquatic animals' tissues [84, 87-89]. Independent of the organism, the removal of lipids prior to bulk tissue analysis for their separated analysis or a posterior mathematical lipid normalization is a general recommendation in stable isotope ecology [86, 89, 90]. However, Patterson & Carmichael recently suggested that lipid

extraction may actually not be necessary for all taxa, but more important in glycogen storing species such as the Eastern oyster *Crassostrea virginica* [91]. This overall lipid correction practice should be reviewed in a species-specific and tissue-specific manner to avoid unnecessary sample handling, and misinterpretation of isotopic values in trophic ecology studies. In fact, Connan *et al.*'s recent study with fish samples showed that different pre-treatments widely used to remove interfering biological molecules (lipids, urea, TMAO) affect the isotopic data and suggested a more standardized pre-treatment approach to ensure the comparison and reproducibility of bulk SIA [92].

For terrestrial environments, the use of $\delta^{2}H$ and $\delta^{18}O$ analysis of tissues is not always tightly correlated with the precipitation $\delta^{2}H$ and $\delta^{18}O$ isoscapes, which might make geographic determinations more challenging. An example was reported with two North American carnivores, the bobcat (*Lynx rufus*) and the puma (*Puma concolor*), wherein both $\delta^{2}H$ and $\delta^{18}O$ values from hair samples of these felines lacked correlation with local isoscapes [93]. This study highlights the importance of additional investigations into isotopic fractionation and metabolic routing if IRMS is to find a stronger footing in wildlife forensics.

In recent work at the boundary between human provenance and wildlife forensics, two reports have investigated the light stable isotope composition of blowflies and their diets [94, 95]. Both studies showed isotope fractionation between the flesh and the blow flies that was significantly smaller than the isotopic variance that existed between the food sources, thereby enabling the discrimination of potential food sources. Through CSIA of amino acids in the different life stages of blow flies, the study by Matos *et al.* demonstrated that essential and non-essential amino acids are fractionated differently in the different life stages of the blow flies [95].

Regarding forest studies, Thomas *et al.* analyzed $\delta^{13}C$ and $\delta^{34}S$ values from red cedar (*Juniperus virginiana* L.) tree rings and presented a recent and gradual recovery of this species from

the decades-long acidic pollution that affected the Appalachian region [96]. Despite the direct correlation with forensics, this work revealed the effectiveness of stricter environmental legislation on human activity and also showed the potential of IRMS in forest ecosystems research.

Timber traceability coupled to initiatives against deforestation and illegal logging is another area that can strongly benefit from the use of stable isotope fingerprinting. The combination of $\delta^{15}N$, $\delta^{34}S$, $\delta^{18}O$ values, $^{87}Sr/^{86}Sr$ ratios, and radiocarbon dating was successful in identifying relocated South African cycad species removed from the wild, which supports the use of SIA as a prospective method to combat the illegal trading of endangered populations [97]. However, different isotopes have different inferential value depending on the species in question. For wood sourcing, or dendroprovenancing, of two Pinyon pines species in the southwestern United States, the $\delta^{13}C$ values from the tree rings proved to be a more precise and successful method than the analysis of ring widths by itself [98]. However, when working with Norway spruces (*Picea abies* Karst.) in and around the European Alps, carbon isotopes did not work as a proxy for their geolocation. In contrast, $\delta^{2}H$ and $\delta^{18}O$ values were more suitable for European spruces [99]. Stable isotopes have also been successful proxies in archaeological wood sourcing investigations [100], and could even be used for chronology determination of tropical trees with indistinct annual rings [101].

4. Environmental forensics

Environmental forensics covers a broad range of topics and involves the illegal contamination or damage of protected areas, whether intentional or not. A typical example would be the use of $\delta^{13}C$ values to determine the point source of an environmental pollutant. Due to the complexity that arises when investigating the source or fate of a contaminant release, it is usually necessary to use a variety of analytical techniques to resolve the issue, as shown in **Table 1.1** [102]. Compound-specific isotope analysis of $\delta^{13}C$, $\delta^{15}N$, $\delta^{2}H$, $\delta^{18}O$, $\delta^{37}Cl$, $\delta^{34}S$, and $\delta^{81}Br$ have been

comprehensively documented [103-107] alongside the advances and inherent challenges when applied to the micropollutants [108]. IRMS is mostly used in studies involving anthropogenic contamination because most pollutants are man-made and contain an isotope profile that differs significantly from natural sources of the same substance. Examples include chemical leaks and oil spills, which pose a major hazard to marine and coastal environments.

In a weathering simulation experiment of a simulated oil spill, GC-C-IRMS measured the $\delta^{13}C$ values of individual *n*-alkanes (C_{12}-C_{33}) in crude oil and showed that $\delta^{13}C$ values are generally unaltered by short-term weathering [109]. The lack of fractionation during mild weathering makes $\delta^{13}C$ analysis a suitable tool for oil fingerprinting such complex samples [110]. However, fractionation of hydrocarbons does occur in simulated fire debris samples, so the effects of elevated temperature, pyrolysis and combustion must be better understood before reliable inferences can be made between post-combustion residues and pre-combustion liquids from which they derived [111].

Table 1.1. Examples of instrumental platforms used for compound-specific isotope analysis of organic contaminants. Minimally adapted from reference [103]: T.B. Hofstetter, M. Berg, Assessing transformation processes of organic contaminants by compound-specific stable isotope analysis, Trends Anal. Chem. 30(4) (2011) 618-627, Copyright (2010), with permission from Elsevier.

Instrument	Separation	Interface system	Analyte	Ionization	Mass analysis/ ion detection	Isotopes	Reference example
GC/IRMS	GC GC x GC[c]	Comb[a] Comb/Red[d] Pyr[e]	CO_2 N_2 H_2	EI[b]	Magnetic sector/Faraday cups	$^{13}C/^{12}C$ $^{15}N/^{14}N$ $^{2}H/^{1}H$	[112-114] [113-115] [114]
LC/IRMS	LC	Wet oxidation	CO_2	EI	Magnetic sector/ Faraday cups	$^{13}C/^{12}C$	[116, 117]
GC/IRMS[f]	GC	none	Organics (PCE, TCE and DCE isomers; CH_3Br)	EI	Magnetic sector/ Faraday cups	$^{37}Cl/^{35}Cl$ $^{81}Br/^{79}Br$	[118] [119]
GC/qMS	GC	none	Organics (PCE, DDT and PCP)	EI	Quadrupole electron multiplier	$^{37}Cl/^{35}Cl$	[120]
GC/MC-ICP-MS	GC	ICP[g]	Cl Br S	ICP	Magnetic sector/Faraday cups	$^{37}Cl/^{35}Cl$ $^{81}Br/^{79}Br$ $^{34}S/^{32}S$	[121] [122] [123]
GC/CRDS[h]	GC	Comb	CO_2	none	Infrared spectroscopy	$^{13}C/^{12}C$	[124]

GC = Gas Chromatography, LC = Liquid Chromatography, IRMS = Isotope Ratio Mass Spectrometry, qMS = Quadrupole Mass Spectrometry, MC-ICPMS = Multicollector Inductively Coupled Plasma Mass Spectrometry, CRDS = Cavity Ring-Down Spectroscopy, PCE = tetrachloroethene, TCE = trichloroethene, DCE = dichloroethene, DDT= p,p′--dichlorodiphenyltrichloroethane, PCP = pentachlorophenol.

[a]Comb = Combustion at 900–950°C; [b]EI = Electron Ionization; [c]Applications reported exclusively for analysis of carbon isotopes; [d]Comb/Red = Combustions followed by reduction at 600–650°C; [e]Pyr = Pyrolysis at 1200–1450°C; [f]Direct injection GC/IRMS; [g] ICP = Inductively Coupled Plasma; [h]Also denoted as GC/C/CRDS owing to the use of a combustion interface.

5. Seized drugs

As stated in the 2013 National Survey on Drug Use and Health (NSDUH) report [125], approximately 24.6 million American people aged 12 or more self-declared illicit drug use in the previous year. Given the extent of novel psychoactive substances (NPSs) appearing on the market, IRMS has emerged as a potential technique to infer the cultivation location of drugs of plant origin, to establish trafficking routes, and to establish the synthetic pathways and chemical lots used in clandestine laboratories.

Cannabis sativa L., also known as cannabis or marijuana, is the most common plant-derived illicit drug in the United States and the world [126]. There were are approximately 19.8 million users in the US in 2013 [125], and its use has apparently skyrocketed since the legalization of medical and recreational marijuana in some US states [127]. With the additional announcement that the White House has alleviated restrictions on medical marijuana studies [128], scientists now have more legal support to conduct research in this area. For forensic purposes, IRMS has been mostly applied to infer cannabis source and distribution networks. Most of the data on large-scale drug trafficking samples is collected by the DEA special testing laboratory and it is unclear how much of the available data makes it to the public domain. This is not to criticize the DEA, but to highlight the point that the public domain probably does not contain all that has been learned about the isotopic composition of drug seizures from around the world.

Carbon and nitrogen stable isotopes are the most well explored isotopes for the origin determination and growth conditions assessment of *Cannabis* seized in different countries [129-131], and the DEA's database provides insight into trafficking, production and distribution networks [132]. Based on the differences in bulk $\delta^{13}C$ and $\delta^{15}N$ values from leaves and inflorescences of 554

marijuana samples, West *et al.* suggested an isotopic framework range to interpret the isotope ratio values [133]. An example is shown in **Fig. 1.2**. By combining parameters of indoor or outdoor growth and inorganic or organic fertilizer, West *et al.* demonstrated a linkage between isotopes and possible cultivation method beyond the correct geographical assignment of known seized samples [126, 134]. In a complementary work, Tipple and coworkers found that the study of chain length distributions, concentrations and $\delta^{13}C$ values of *n*-alkanes (n-C_{29}) from seized *Cannabis* inflorescences can also provide information about the cultivation settings of marijuana plants [135].

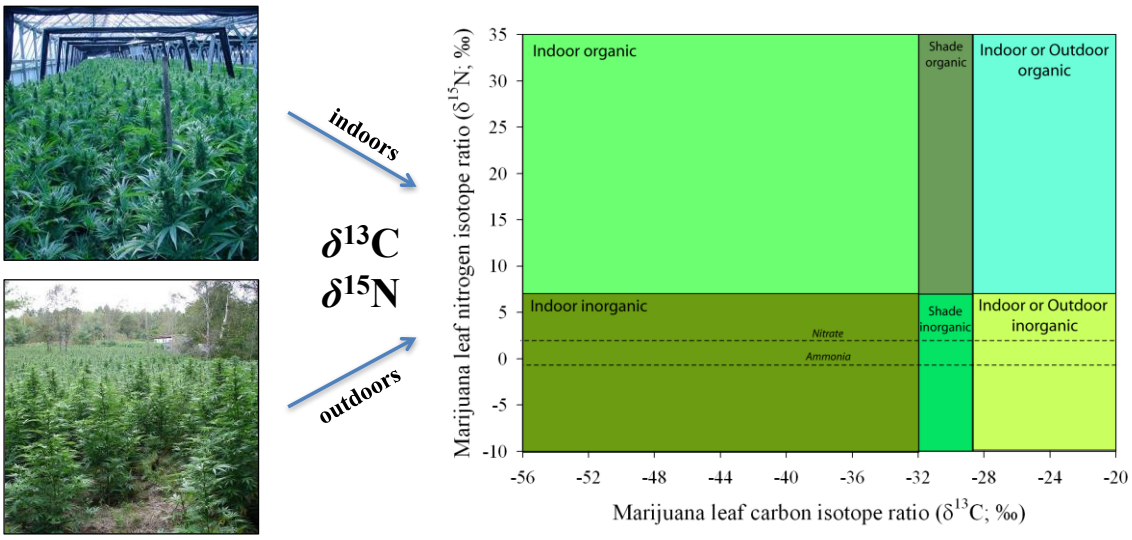

Fig. 1.2. Dual isotope approach for the inference of marijuana growth conditions. Image adapted from reference [133]: J.B. West, J.M. Hurley, J.R. Ehleringer, Stable isotope ratios of marijuana. I. Carbon and nitrogen stable isotopes describe growth conditions, J. Forensic Sci. 54(1) (2009) 84-9, Copyright (2008), with permission from John Wiley & Sons, Inc.

When characterizing marijuana samples seized in Alaska, Booth *et al.* demonstrated that multiple isotopes ($\delta^{13}C$, $\delta^{15}N$, $\delta^{2}H$ and $\delta^{18}O$) can be a useful approach to trace trafficking patterns [136], whereas other authors are exploring the $^{87}Sr/^{86}Sr$ ratios retained in marijuana leaves and inflorescences to achieve a similar goal [137]. A subsequent publication from the Jackson group

described the comparison of bulk $\delta^{13}C$ values of *Cannabis* plant samples to compound-specific $\delta^{13}C$ values of cannabinoids extracted from the same samples [138]. Although the advanced age of some of the samples had caused some isomerization and degradation of the cannabinoids, the results effectively showed that individual cannabinoids have unique $\delta^{13}C$ values relative to the bulk plant matter, which therefore makes it somewhat challenging to link extracted THC to a particular plant source.

Among all plant-derived drugs, cocaine's production and trafficking routes around the world are of particular interest to law enforcement agencies. In this context, SIA appears to be well-suited to the task because seized cocaine samples closely reflect the growth environment of coca plants. Mallette and coworkers [139] applied a multiple bulk isotope approach ($\delta^{13}C$, $\delta^{15}N$, $\delta^{2}H$ and $\delta^{18}O$) combined with trace alkaloids and multivariate statistics to discriminate cocaine coming from 19 major South American growing regions. A similar method was used to differentiate and determine the unique profile of the first illicit coca plantation in Mexico, showing that coca cultivation for cocaine production is expanding its limits outside South America [140]. Under controlled laboratory conditions, those same isotopes were investigated regarding their fractionation patterns in fractionally precipitated cocaine base. Interestingly, the authors observed an opposite trend to the usual Rayleigh fractionation because the earlier fractions of precipitated samples were more depleted than the later ones for all four isotopes. ^{15}N and ^{2}H were characterized by the largest fractionations [141].

γ-hydroxybutyric acid (GHB) is another illicit psychoactive drug that became very popular among young people at nightclubs or raves because of the desirable increase in euphoria and disinhibition. GHB use also provides less-desirable effects, including amnesia, which also made GHB attractive for use in drug-facilitated sexual assaults. The popularity caught the authorities'

attention because GHB, or its chemical precursors γ-butyrolactone (GBL) or 1,4-butanediol (1,4-BD) are colorless and odorless liquids, which makes them easy to spike into beverages of intended victims of drug-assisted sexual assault. Marclay and coworkers used GC/C/IRMS to investigate the effects of *in vivo* metabolism on δ^{13}C values of GHB [142]. Urinary GHB δ^{13}C values ranged from −25.06‰ to −24.81‰ for patients who had ingested prescribed pharmaceutical GHB, which was indistinguishable from the original δ^{13}C value of −24.99‰. Given that metabolism of GHB had no statistical influence on the isotopic ratio, comparison of a seized exogenous GHB and endogenous GHB from a victim can be used as a successful approach to incriminate/acquit a sexual assault suspect. In much the same way, IRMS can distinguish endogenous vs. exogenous sources of performance-enhancing hormones in athletes. Marclay and coworkers had previously used the same instrument to determine the source of 19 GBL samples obtained worldwide by measuring intra and inter-variability of their bulk carbon isotope signatures [143].

In other applications with synthetic drugs, IRMS elucidated different production batches of 23 seized tablets of the piperazine analogs benzylpiperazine (BZP) and trifluoromethylphenylpiperazine (TFMPP) [144], both synthetic stimulants sold as alternatives to ecstasy. In a parallel study, the same group reported the IRMS analysis three batches of benzylpiperazine hydrochloride (BZP·HCl) and its synthetic intermediates, which were synthesized from three different precursor suppliers [145]. Although all the intermediate samples were significantly different and correctly associated with their respective precursor suppliers, the increased variance in the measured δ^{13}C and δ^{15}N values for BZP·HCl meant that not all the BZP·HCl batches could be uniquely linked to the correct precursor suppliers. IRMS has also been used, in combination with other profiling techniques, to classify carfentanyl seizures [146].

A comprehensive discussion on the application of IRMS to methylamphetamine (also known as methamphetamine) and its precursors has already been provided by Gentile *et al.* [7] and will not be repeated in detail here. In another reviews, Collins and Salouros highlight the strategic importance of $\delta^{13}C$, $\delta^{2}H$ and $\delta^{15}N$ analysis as a complementary profiling technique to impurity profiling for the routine analysis of methylamphetamine seizures [12, 147]. **Fig. 1.3** demonstrates the range of $\delta^{13}C$ and $\delta^{2}H$ values obtained for 782 samples seized at the Australian border and the ability to distinguish semi-synthetic from natural or synthetic methylamphetamine. Other valuable work by Liu *et al.* compared the isotope ratios of ephedra plants, natural ephedrine, synthetic ephedrine and the partially- or totally-synthetic methamphetamine products [148]. Although the results enabled inferences to be made about the likely source of 987 methamphetamine casework samples, the ground truth for each casework sample was not known, so the casework-specific false positive and false negative rates could not be assessed.

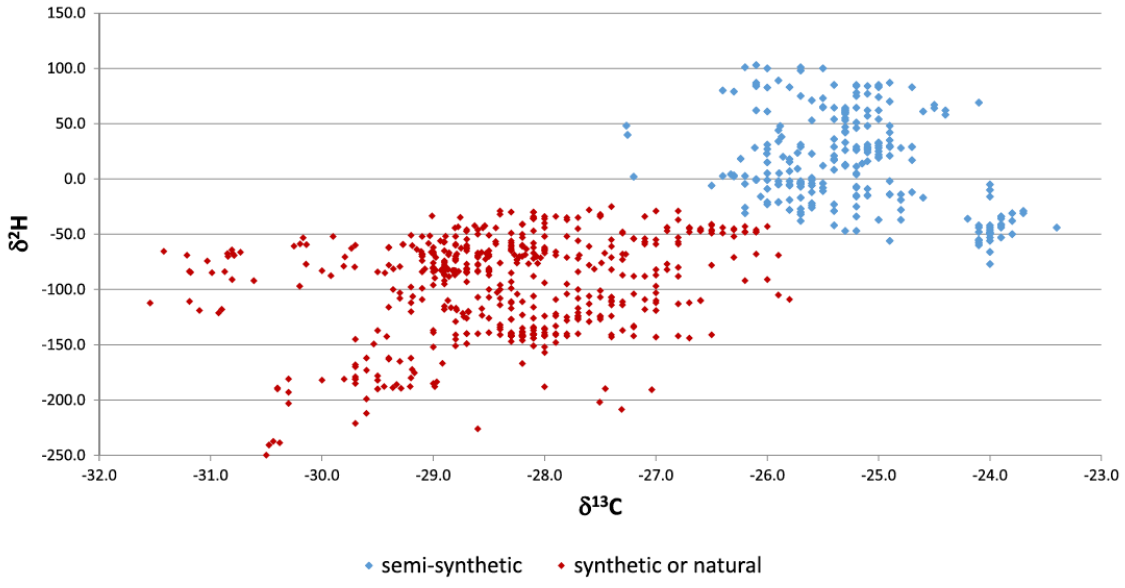

Fig. 1.3. Bivariate plot of the $\delta^{13}C$ and $\delta^{2}H$ values of 782 samples of methylamphetamine seized at the Australian Border. The blue data points in the upper right correspond with samples that were synthesized from ephedrine (pseudoephedrine), which was itself produced through a semi-synthetic process involving the fermentation of a sugar with benzaldehyde. The red data points in

the lower left include samples from natural origin (extracted from *Ephedra* plants) and the entirely-synthetic samples, which start with the bromination of propiophenone. Image reprinted from reference [147]: M. Collins, H. Salouros, A review of some recent studies on the stable isotope profiling of methylamphetamine: Is it a useful adjunct to conventional chemical profiling?, Sci. Justice 55(1) (2015) 2-9, Copyright (2014), with permission from Elsevier.

6. Ignitable liquids

According to the National Fire Protection Association (NFPA), around 282,600 intentional fires per year were reported to U.S. fire departments between 2007-2011, including 211,500 outside or unclassified fires, 50,800 structure fires and 20,400 vehicle fires [149]. Approximately 160,910 were found to be intentionally set with an ignitable liquid [150]. In spite of these statistics, and in contrast to the extensive use of IRMS on explosives, very few manuscripts have reported the analysis of ignitable liquids with IRMS [7].

Since 2009, diesel fuel has become a more frequently studied ignitable liquid [151-153] even though gasoline is the most commonly used ignitable liquid in arson cases [150]. In one study, Harvey *et al*. first isolated the *n*-alkanes from different diesel samples to ensure baseline resolution between each *n*-alkane and prevent any potential interference between peaks [151]. A following combination of δ^{2}H and δ^{13}C CSIA with multivariate statistics was then used to distinguish between the four diesel samples of different sources. Muhammad *et al*. examined a larger dataset of 45 diesel samples from various gas stations in New Zealand [152]. This study showed the difficulty of source attribution when there is only one major supplier of diesel to all the gas stations in the region. Source attribution was scientifically accurate, but of little forensic value.

Weathering and additives are the possible reasons for subtle differences in fuel isotopic compositions. By analyzing the fingerprint pattern of *n*-alkanes (e.g. nC_{12} to nC_{23}) via GC-IRMS, Muhammad *et al*. reaffirmed the discriminant power of CSIA. Moreover, following 21 days of

evaporation at room temperature (24 ± 2°C), hydrogen and carbon isotopic signatures of various *n*-alkanes in a diesel sample [153], the *n*-alkane underwent negligible fractionation for ^{13}C and varying degrees of fractionation of ^{2}H. For example, long-chain alkanes were not fractionated during evaporation, but the shorter chain alkanes nC_{12}–nC_{17} underwent significant ^{2}H fractionation.

Several groups have also reported evaporation effects on isotope ratios of different petroleum derivatives [154-156]. Whereas IRMS appears to be a suitable tool to predict potential common sources of pristine flammable liquid samples, Schwartz and coworkers showed that post-combustion residues in simulated fire debris undergo unpredictable extents of ^{13}C fractionation ranging from 0 to +10‰ relative to the same analytes in the pristine, unburned liquid [111]. The absence of any reliable trend in fractionation in simulated fires makes IRMS unsuitable for the comparison of pre-combustion compounds and their post-combustion residues. Not only do the analytes undergo fractionation during evaporation and pyrolysis, but pyrolysis products from the organic substrate (e.g. carpet) also contribute different weighted $\delta^{13}C$ values to different residues [157].

7. Explosives

Source determination of explosives has become a growing interest in a variety of government sectors, especially because of the daily use of a broad range of explosive devices in military actions, terrorism and insurgents' attacks. Recently, a combination of IRMS and inductively coupled plasma–mass spectrometry (ICP–MS) was used to provide a better discrimination between ammonium nitrate (AN) samples from distinct AN batches and manufacturers [158]. The low cost and easy access of AN as a fertilizer ensures that ammonium nitrate fuel oil (ANFO), consisting of a mixture of 94% AN and 6% fuel oil, is possibly still one of the most used materials employed in improvised explosive devices (IEDs) [159]. Brust *et al.* showed that ^{15}N and ^{18}O isotopic signatures

of AN samples could successfully distinguish between the different samples [158]. Carbon and hydrogen analyses were also performed, but low sample carbon contents and an observed influence of nitrogen on the δ^2H values made these two isotopes less useful. Benson *et al*. [160] achieved similar results when the source of Australian AN samples was differentiated based on their δ^2H, δ^{18}O, and δ^{15}N values [161].

Some challenges in working with nitrogen-rich organic compounds have been reported by other researchers. For example, incomplete reduction might cause the tailing in the N_2 peak of nitrates [162]. Caution must also be used when measuring organic substances against inorganic reference materials like IAEA-N1 and IAEA-N2 [162]. In addition, nitrogen-rich compounds can also influence the accuracy and precision of ^{2}H isotopic analysis [163]. Given that these compounds undergo thermochemical processes that are different from typical organic compounds in EA-IRMS, and that they tend to give lower than expected recoveries of nitrogen, Gentile *et al.* recommend a thermal decomposition method to remove of any external oxygen [162]. Additional results to this premise indicate that, compared to the usual EA combustion method, thermal decomposition provides more precise δ^{15}N and %N results for both organic and inorganic materials containing oxidized nitrogen. The thermal decomposition procedure did not have a deleterious effect on the measurement of %N, δ^{13}C or δ^{15}N values of materials containing reduced nitrogen [164]. Adjustments to this methodology would allow a more accurate, faster and cheaper way to analyze δ^{15}N materials using EA-IRMS. Other manuscripts have described that isotope analysis of each of the ion components of nitrogen-rich explosives (such as ammonium nitrate or urea nitrate) provides additional discriminatory power for the investigation of forensic samples [165-167].

Using samples synthesized in different conditions, Benson *et al*. presented the use of IRMS to differentiate triacetone triperoxide (TATP) samples, another common explosive in many terrorist

bombings [168]. Based on bulk $\delta^{13}C$ values, the samples were classified according to synthetic process. Also, carbon, hydrogen, and oxygen isotopic data were combined to classify the TATP samples to their common source. A global study by Howa *et al.* showed that $\delta^{13}C$ values of TATP correlate strongly with the $\delta^{13}C$ values of locally-available liquid acetone, the synthetic precursor to TATP [169].

Using bulk $\delta^{13}C$ and $\delta^{15}N$ values from a sample set containing the explosive pentaerythritol tetranitrate (PETN), Benson *et al.* showed the discrimination of PETN from detonating cord or cast PETN booster filling [168]. Howa and coworkers [170] investigated the factors that influence the carbon and nitrogen isotopic ratios of commercial PETN by isolating the explosive from the bulk sample of different manufacturers and observing the isotopic linkage between that substance and its reactants, pentaerythritol (PE) and nitric acid. The results showed that, whereas $\delta^{13}C$ values from PETN reflect the PE carbon signatures, PETN $\delta^{15}N$ values are influenced by both nitric acid $\delta^{15}N$ values and the deflagration reaction parameters. The authors suggested further experiments with controlled reaction conditions to provide a better understanding of the results.

The effectiveness and limitations of IRMS were also reported in studies involving RDX, HMX, TNT, HMTD, black powders and other pre- and post-blast materials from explosive devices [113, 171-176]. Whereas bulk analyses like these are extremely helpful for linking evidence in pre-detonation scenarios, there are significantly fewer reports linking post-detonation residues with pre-detonation samples. The CSIA of individual analytes in multi-component explosives would be helpful to connect the explosive precursor to the product samples. In this context, Chesson and coworkers provide a very useful step-by-step approach for the extraction and preparation of several explosive mixtures for IRMS **(Fig. 1.4)** [177]. The same group established a robust database that helps establish the use of explosive isotopic evidence in court [178].

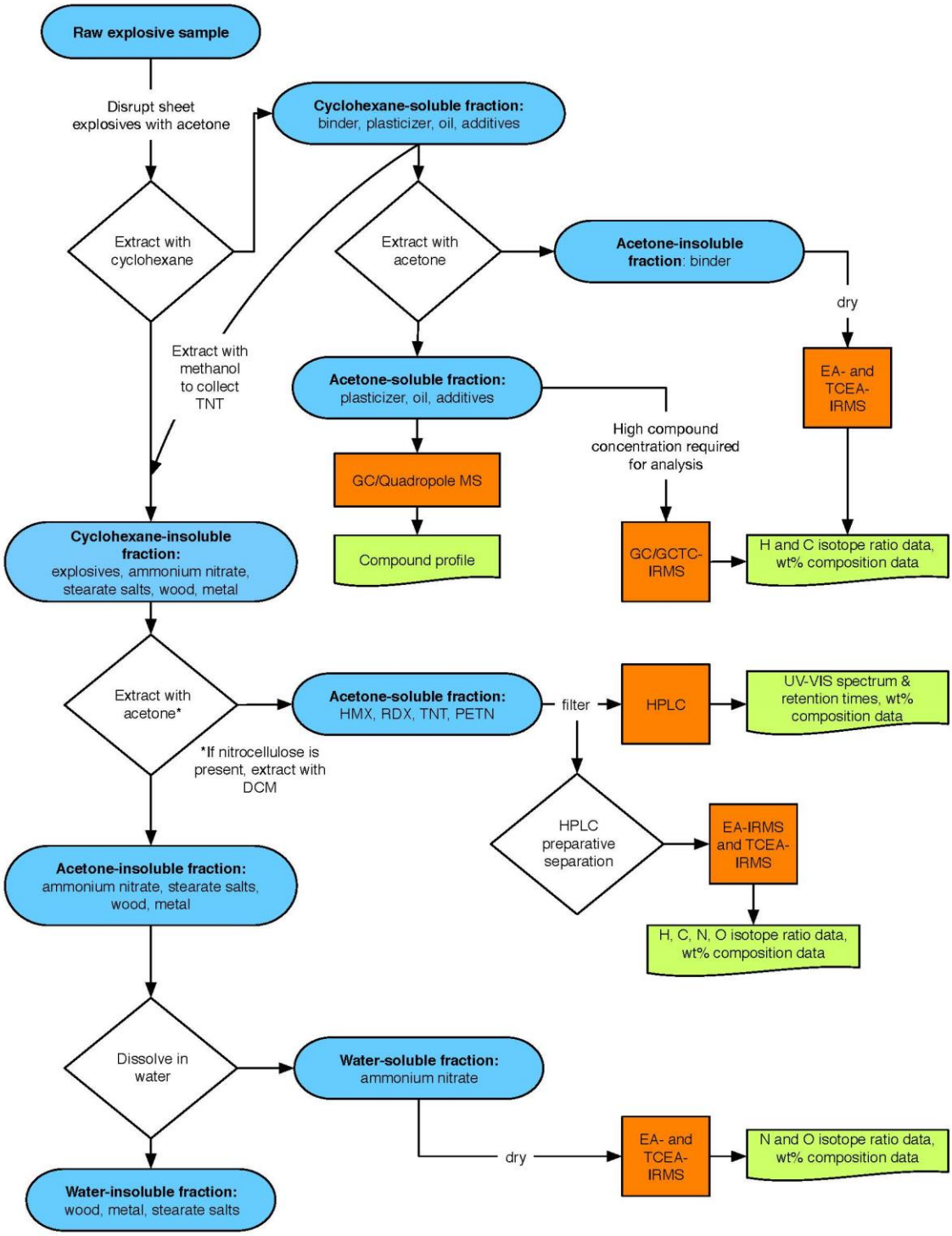

Fig. 1.4. Suggested workflow to isolate and prepare different components from explosive mixtures for measurement by IRMS and other analytical techniques. Image reprinted from reference [177]: L.A. Chesson, J.D. Howa, M.J. Lott, J.R. Ehleringer, Development of a methodological framework

for applying isotope ratio mass spectrometry to explosive components, Forensic Chem. 2 (2016) 9-14, Copyright (2016), with permission from Elsevier.

8. Food forensics

Since the 1990s, the application of SIA in several food adulteration/ safety studies has been recognized as an official method by AOAC International [179]. The use of isotopic techniques has also become prominent among the practiced methods to authenticate and protect citizens and businesses against a variety of legal issues involving foods and brands.

IRMS can provide insight regarding authenticity, provenance, and contamination of foodstuffs, and it has been used in a variety of legal cases [180]. Although counterfeit food is not always dangerous for consumption, counterfeiting is illegal and strongly affects the consumer confidence on the product or brand [181]. Food fraud is most prevalent when products are expensive to produce like premium-brand products. In such cases, black-market suppliers will typically employ cheaper, lower-quality ingredients and less labor-intensive manufacturing methods to produce the final product.

Honey is a commonly counterfeited product. Carbon bulk isotope analysis has been used for the detection of commercial honey adulteration (AOAC–C_4 Sugar Method 998.12) [182] because most authentic honey has a $\delta^{13}C$ value close to C_3 plants. However cheap substitutes include syrup sugars made from corn or sugar cane, which shift the $\delta^{13}C$ values towards C_4 plants values [183, 184]. The AOAC method identifies this adulteration because it requires the extraction of protein from honey and compares the differences between $\delta^{13}C$ values of honey protein vs. bulk honey ($\Delta\delta^{13}C$). Differences greater than 1‰ indicate that the honey has more than 7% adulteration with a C_4 syrup [185, 186]. However, elemental analysis by bulk IRMS is not very effective when honey is

diluted with cheap C_3-plant-derived sugars like sugar beet because the bulk isotope ratio would not be substantially different [186, 187]. One exception to the rule is the premium-priced New Zealand manuka honey, which naturally has a high level of C_4 sugar, and therefore has an isotope ratio that is indistinguishable from cane or corn syrup [188]. Because bulk IRMS cannot always identify adulteration in honey, LC-IRMS can provide more selectivity by providing compound-specific carbon isotope ratio measurements [189, 190]. Furthermore, the use of multi-isotope approaches to classify honey according to their botanical and/or geographical origin has also been reported **(Fig. 1.5)** [191, 192].

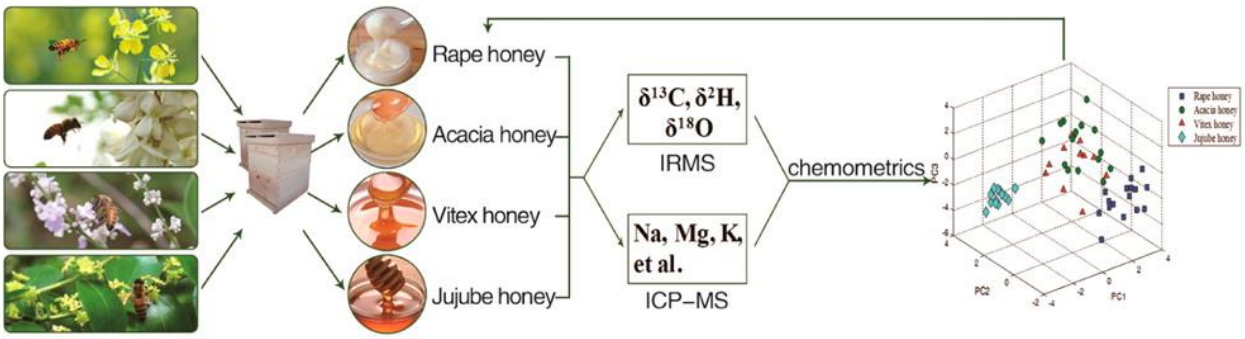

Fig. 1.5. Combination of IRMS, ICP-MS and chemometrics to classify Chinese honeys according to their botanical origins. Reprinted with permission from reference [192]: Z. Wu, L. Chen, L. Wu, X. Xue, J. Zhao, Y. Li, Z. Ye, G. Lin, Classification of Chinese honeys according to their floral origins using elemental and stable isotopic compositions, J. Agric. Food. Chem. 63(22) (2015) 5388-94. Copyright (2015) American Chemical Society.

Zhao *et al*. [193] and Camin *et al*. [180, 181] have both published thorough reviews about the applications of IRMS in authenticity and traceability of a variety of plant-based and animal-based foods. Another very comprehensive reading on the topic can be found in [194]. Isotope analysis has also contributed to the tracking of animal diets for the protection of premium products as well as for consumer health reasons. IRMS has been used to protect against bovine spongiform encephalopathy

(BSE), foot-and-mouth disease (FMD), and even avian influenza [193]. Most studies involve a multiple isotope approach and sometimes include additional analytical techniques. Applications include the determination of the primary diets of poultry [195-198], pigs [199, 200], beef [201], lamb [202, 203] and dairy products [204]. Other examples of food applications include the geographic origin of meat [205, 206], fish and shellfish [207-211], dairy [212-215], vegetables and fruits [216-219], grain-based food [220-225], chocolate [226], coffee [227], alcoholic and nonalcoholic drinks [228-233] and oils [234-237]. The influence of local ingredients on "global" foods, such as Big Mac® patties collected in 26 countries was also accessed via isotope analysis. The $\delta^{13}C$ values of hamburgers reflected the diets of the local cattle [238, 239].

Food fraud is a dynamic activity, however, and it poses a continuous challenge for researchers. Beyond the common use of $\delta^{13}C$ values for food authenticity and $\delta^{15}N$ values for the distinction of crops raised with organic or synthetic fertilizers, some groups are already incorporating the use of hydrogen and oxygen isotopes as valuable markers for geographic determination. For example, when investigating 436 commonly consumed meat samples from diverse terrestrial and marine animals, Chesson *et al.* reported that the correlations between $\delta^{2}H$ and $\delta^{18}O$ values from animal tissues reflect the consumed water similarly, independent of the animal taxa [240]. Hydrogen and oxygen isotopes were also applied to demonstrate that hamburgers sold at local restaurants are more likely to come from regionally raised cattle, while fast food chains rely on beef coming from further regions [13]. Interestingly, most food forensic articles apply some quite advanced chemometrics, which indicates a gradual change in the isotope community towards a more sophisticated interpretation of results.

The effect of cooking on the isotope ratios of foodstuff is not commonly investigated, although many consumed items in a human/animal diet are cooked before consumption. It was

recently reported that $\delta^{13}C$ and $\delta^{15}N$ values of grain-based desserts and yeast bread are not affected by baking or fermentation procedures, and the raw ingredients from processed food can be used to estimate the respective isotopic signatures [241]. Other research found that steaming, grilling and boiling of two types of fish (mackerel and haddock) did not have a significant effect on the bulk $\delta^{13}C$ and $\delta^{15}N$ values [242], although a small but significant effect on the $\delta^{13}C$ values has been reported for other fish species [243] Cooking processes such as boiling, frying or roasting also did not impact the $\delta^{13}C$ and $\delta^{15}N$ values of beef samples. However, $\delta^{2}H$ values became significantly enriched from 7.2‰ to 5.9‰ when compared to raw and processed beef [244]. Studies on how cooking methods affect stable isotope signatures are also a new and interesting venue to understand and reconstruct cultural habits and dietary routine of ancient human populations [245].

Given the increased retail sales and consumer demand for organic products [246], organic produce needs continual certification of authenticity. In this context, the difference between organic and conventionally produced food has become a hot topic in IRMS research. Regarding organic dairy products, chemical analysis of α-linolenic acid (C18:3ω3), phytanic acid diastereomer ratios (SRR/RRR), ^{1}H NMR- and ^{13}C NMR-spectroscopy data, $\delta^{15}N$ and $\delta^{13}C$ values of milk protein and fat identified cases of mislabeled organic dairy products [247-251]. Eggs [252], fish [253] and pork [254] have also been correctly identified by SIA as being produced under organic or conventional methods. The continued growth of organic foodstuff production is likely to continue the expansion in authentication involving IRMS. More information about the principles, applications and limitations of SIA in authenticating organic products from plant or animal origin can be found in [255, 256].

Isotope ratio analysis of $\delta^{15}N$ values can provide insight into the extent of man-made fertilizers. However, other factors can also influence the nitrogen signature in a crop, including soil

saturation levels, atmospheric nitrogen deposition, agricultural practices and the plant's internal nitrogen balance [257]. An important factor in food authentication is that the nitrogen isotope signature of cover crops composed of N_2-fixing leguminous plants is often similar to the signature of some synthetic fertilizers. For this reason, δ^{15}N analysis alone not a very suitable parameter for organic authentication [258, 259]. A combination of multiple isotopes, multivariate statistics, and other analytical techniques is therefore preferred. Successful multivariate approaches have included IRMS with ICP-MS [257] and IRMS with mid-infrared spectroscopy, (MIS) and Proton Nuclear Magnetic Resonance (^{1}H NMR) [260] to classify organic vs. conventionally-grown tomatoes. In addition, CSIA has also demonstrated good discriminatory power between plants that are grown under different conditions [258, 259, 261].

Besides all the benefits listed above, there are still some limitations for IRMS in real life food applications. The high costs to maintain the instrument itself are well known, but the lack of an extensive reference database containing products coming from a range of different diets, production conditions, locations and seasons is possibly the biggest problem [181]. Such a database would also have to be continually updated because of the dynamic nature of global food markets. To our knowledge, wine is the only product with a well stablished isotope databank, which was created in the early 1990s in the European Union [262]. Finally, one challenge in relating food forensics to forensic casework, such as nutritional studies of humans, is that even when controlled studies examine the consumption of large quantities of a certain food, like beer, the isotope signature of the intervention food group is so diluted by the natural variation in a person's diet that the dietary intervention may not be observable [263].

9. Poisoning

Although not as common as food authentication, IRMS is also used in poisoning investigations. Through the use of GC/C/IRMS, researchers in Japan analyzed $\delta^{13}C$ values in different samples of methamidophos (O, S-dimethyl phosphoramidothioate). High concentrations of this pesticide were identified in some frozen dumplings imported from China, which caused food poisoning in many Japanese citizens who consumed the product [264]. The comparison of Chinese and Japanese methamidophos isotopic values showed that the pesticide was not added in Japan. Subsequent investigations led a temporary worker in China to admit to the crime. Combining isotopes to investigate food contamination with pesticides for criminal or suicidal reasons have been reported by others. For example, Ehtesham *et al*. described the use of SIA in a case study of a deliberate contamination of milk powder with a pesticide (MFA) [265]. In another case, the comparison of $\delta^{15}N$ and $\delta^{13}C$ values of different methomyl (insecticide) products and a methomyl-containing Soju collected from a fatal poisoning incident in Korea was one of the investigative leads that enabled detectives to find the poison source and the suspect responsible for the crime [266]. $\delta^{15}N$ and $\delta^{18}O$ values were also used to show that a combination of horse manure, urine nitrification and intensive evaporation caused an accumulation of nitrates in a water-filled hole that eventually killed 71 wild horses [267].

In some situations, preventative steps have been taken to establish protocols to determine the isotopic ratios of potential poisons. For example, cyanide salts are easily available and highly toxic. Analyses of $\delta^{13}C$ and $\delta^{15}N$ values in several commercial NaCN and KCN batches, as well as extracted cyanide from food and medicine matrices, support the use of these two isotopes as forensic tools to distinguish different samples [268, 269]. Regarding the toxic protein ricin, which is a

Schedule I controlled substance from *Ricinus communis* (castor beans), the combination of $\delta^{13}C$, $\delta^{15}N$, $\delta^{18}O$, and $\delta^{2}H$ values provided powerful discrimination between different sources of castor beans even when the preparation method varied between acetone extraction, salt precipitation or affinity chromatography [270]. When a statistical integration approach was taken to join the four isotopes with $^{87}Sr/^{86}Sr$ ratios, the classification accuracy of castor seeds' geographic origin increased [37]. In other work involving the nerve agent, sarin, Moran *et al*. has shown that when the precursor methylphosphonic dichloride (DC) is converted to methylphosphonic difluoride (DF) during the synthesis, isotopic fractionation of carbon is minimal [271]. For this reason, nerve agents and their intermediates can be included in, or excluded from, the possibility of deriving from certain precursor feedstocks.

10. Questioned documents

Discrimination and source determination of documents remains a severe problem in forensic science. Such examinations include authenticating documents and signatures, document dating and threatening letters, among others [272-276]. Interest in the analysis of paper products was highlighted 2001 during the FBI's investigations of bioterrorist Anthrax letters in 2001 [277]. The likeness of envelopes used to mail the anthrax spores was investigated through SIA [43], but little discrimination was reported in that case.

Regarding paper examinations, in 2013, Jones and coworkers published a series of three manuscripts depicting the effectiveness of $\delta^{13}C$ analysis to distinguish the manufacturing source of document papers [278-280]. Using different brands of office papers collected in Australia and New Zealand, the authors evaluated intra and inter-variability of paper reams and suggested a confidence interval to discriminate documents. More recently, the same group has published two additional

manuscripts incorporating oxygen isotope values as well [281, 282]. Their results once again showed the potential of IRMS to discriminate paper samples, and a dual-isotope approach using carbon and oxygen was indicated as the next investigation step to optimize and ultimately validate an operation protocol suitable for paper document casework analysis. The results were consistent with previous IRMS results in which carbon, oxygen and hydrogen isotopes were able to discriminate 21 out of 25 European paper documents [283]. The combination of IRMS and XRF appeared to be even more effective at distinguishing between paper products. XRF instruments are more affordable and more-readily accessible to forensic labs and could offer an alternative approach to source attribution.

Regarding ink and toner analysis, Raman spectroscopy and Fourier-transform infrared spectroscopy (FTIR) are the most frequent, reliable and non-destructive methods to differentiate variations found in ballpoint and pens [284-286]. IRMS has only just begun to be explored for inks. For example, Chesson *et al*. described the first application of SIA of N, C, H, and O to characterize ballpoint and gel inks from pens purchased in the same package, pens from the same brand purchased in three different states, pens of different ages and ink on paper [287]. According to their results, within-package pens have statistically indistinguishable isotopic signatures, but between-package signatures of the same brand pens from different locations and ages were significantly different. In addition, when investigating ink on paper, nitrogen isotope values allowed the discrimination of the different inks. Additional method development is still required before IRMS can be used in questioned-document casework.

11. Miscellaneous

The implementation of IRMS in trace evidence studies involving clothing fibers is relatively understudied. Given the fact that alternative analytical methods struggle to provide information other

than the polymer type and color of fibers, isotope ratio analysis appears to be a prospective method to determine the source of similar fibers. $\delta^{13}C$, $\delta^{15}N$, and $\delta^{18}O$ values have enabled the discrimination between valuable natural fibers of cashmere and cheaper synthetic fibers that were used as a substitute for cashmere in the manufacturing process [288]. Using IRMS, a pilot multi-element study of carbon, hydrogen and oxygen isotopes also showed differences in un-dyed spun cotton fabric fibers from different countries [289]. The authors pointed out that for $\delta^{2}H$ and $\delta^{18}O$ values, a larger number of cotton fiber samples would be required to achieve more robust statistical results of within-region variability. To overcome this issue, a subsequent manuscript used hierarchical cluster analysis to compare the isotopic compositions of 17 raw cotton samples from many US states to 15 cotton fibers from different overseas regions [290]. Despite the promising results, some misidentified samples reaffirmed the necessity of a larger dataset and consideration of additional variables that influence results when IRMS is used. The $\delta^{2}H$ and $\delta^{18}O$ values of cotton can also be used to identify counterfeit currency, since cotton is a primary constituent of paper money. Cerling *et al*. [8] recently summarized results on how cotton isoscapes patterns provide unique geographic information to allow discrimination between genuine US bank notes vs. counterfeit notes.

In recent work by Nienaber *et al.*, SIA showed that within-batch isotope ratio values of cable ties were not significantly different, but that between-batch cable ties were significantly different, especially for $\delta^{2}H$ and $\delta^{15}N$ values of the nylon cable ties [41]. Along with IRMS measurements, other physical and chemical measurements enabled the discrimination of 19 of the 20 samples. The only two samples that could not be distinguished were unintentional replicates that shared the same lot number and supplier. Jones *et al.* surveyed the $\delta^{2}H$ and $\delta^{13}C$ values of 26 cling wraps and 26 packages of resealable bags in Australia [291]. Their work demonstrated a significant difference

between the within-sample variance and between-sample variance, the benefit of which was extolled in an example case study.

Plastic bags, cling film and adhesive packaging tapes are examples of other materials often associated with forensic situations. Examples include the packaging of drugs and explosives. SIA of plastic wraps have been demonstrated to contribute to the source elucidation of the illicit materials [292-296].

12. Summary

This review summarizes some of the SIA applications in different fields of forensic science. Good practices are readily available through the FIRMS Network, and they recommend reliable methods for calibration, normalization and the assessment and reporting of measurement uncertainties. In short, best practices require at least two isotopic standards per element and the reporting of confidence intervals instead of standard deviations.

Ecology and wildlife applications are the most challenging areas of interpretation, and species-specific techniques are often necessary to reveal trophic-level and food-web interactions. There are also big gaps in our understanding of how to interpret IRMS data involving migration patterns and foraging behavior of highly mobile animals. In biological applications, the dynamic nature of different organisms and the differences in metabolism within different organs of an organism are complicating factors in the interpretation of IRMS results. Special attention should be given to the type of tissues analyzed and their respective turnover rates [4], particularly if focusing in molecules such as amino acids. These are some of the reasons why amino acid isotope analysis became an active and promising research area in ecogeochemistry [297]. The continuous expansion of Isoscapes metadata and incorporation of other isotope ratios (e.g. $^{87}Sr/^{86}Sr$) show potential to

leverage the power of interpretations in multiple forensic areas. We expect this increase in data density to be reflected in future datasets, which, combined with advances in chemometrics, should provide a more solid structure for SIA in future casework.

Magnetic sector IRMS instruments still offer better abundance precision than new high resolution mass spectrometers like the Orbitrap [298], but analytical approaches that include techniques such as XRF, Raman spectroscopy, FTIR, NMR, ICP-MS, cavity ring-down spectroscopy, genetic markers, trace elements and fatty acids profiles tend to provide superior discrimination than IRMS values alone. The benefits derive from the inclusion of additional independent variables. The use of chemometrics and statistics in the data analysis has certainly flourished, but still requires further development.

CSIA is recognized as a more sophisticated, and more complex, approach than bulk IRMS. It provides more variables for discrimination, but these variables oftentimes are not true independent variables but covariates, which means a more careful consideration must be taken when interpreting the results. CSIA results provide additional source-level or metabolic information from the samples in question, which is potentially helpful in distinct forensic contexts [61, 95]. Baczynski *et al.* recently reported the development of a modified GC combustion interface that enables a two-order-of-magnitude reduction in the limits of detection [299]. The CSIA measurement of picomolar levels of organics in a mixture will no doubt open the door to new potential applications [299]. Position-specific isotope analysis (PSIA) of amino acids' carboxyl groups has also been introduced recently [300]. Continued development of PSIA and its applications is likely to provide more in-depth information about the source and metabolism of different amino acids and other metabolites [300]. The value of PSIA to forensic science is questionable at this point, but unless fundamental research

continues to push the boundaries of what is possible, we will never move beyond what is currently practicable.

CHAPTER 2: ANALYSIS OF THE ^{13}C ISOTOPE RATIOS OF AMINO ACIDS IN THE LARVAE, PUPAE, AND ADULT STAGES OF *Calliphora vicina* BLOW FLIES AND THEIR CARRION FOOD SOURCES

Reproduced in part with permission from Mayara P. V. Matos, Kateryna I. Konstantynova, Rachel M. Mohr, Glen P. Jackson, *Analytical and Bioanalytical Chemistry*, DOI 10.1007/s00216-018-1416-9

1. Introduction

The use of naturally occurring stable isotopes for the study of arthropods is a small but well explored field. For ecology applications, most of the studies are based on bulk isotope analysis for diet reconstruction and trophic position estimates [301-306]. Only a few studies have explored compound-specific isotope analysis (CSIA) to link amino acids from insects to their food sources [307-309]. Nonliving organisms (detritus) [310] have been often placed and studied as the base of food chains [311], but limited attention has been given to the category of detritus composed by decaying flesh of animal tissues, also known as carrion [312]. Animal decomposition plays an important role in the ecosystem when it influences the vegetation by releasing nitrogen-rich compounds into the soil [313] and increases insect activity in the area surrounding the carcass [312].

Among the necrophilous arthropods, the most commonly encountered and important colonizing insects are the blow flies (Diptera: Calliphoridae). In the US, adult blow flies are typically the first insects to arrive at a carcass, upon which they oviposit a clutch of eggs. The eggs hatch into larvae, commonly know as maggots, which actively feed upon the corpse tissues. After feeding, the larvae depart the corpse to burrow into soil or other protective detritus. There, the outermost layer of the larval epithelial chitin hardens into a puparium, inside which the pupa transforms from the larval to the winged adult stage. Once metamorphosis is complete, the adult emerges from the puparium and leaves it behind [314]. Although this process happens in a predictable fashion, the length of the

egg, larval, and pupal stages are highly dependent on environmental variables, particularly temperature. As a result, post-colonization interval estimation from immature insects can be highly contentious and is an area of active research in the field of forensic entomology [315-317].

The period of insect activity (PIA) is a proxy for the shortest possible time a corpse has been dead, so the standard practice in forensic entomology is to collect the oldest-appearing specimens on or around a corpse, thus avoiding an underestimation of the post-mortem interval (PMI) [318]. However, decaying carrion and the necrophilous insects that feed on it are part of the natural ecosystem and could potentially serve as sources of contamination for a corpse of forensic interest. For example the presence of larvae, pupae, or empty puparium from an preexisting carrion source could easily cause an estimate of the PIA [319]. Similarly, adult flies collected from a corpse could be either newly-arrived to feed or oviposit, indicating a short PMI, or might have hatched from larvae that originally fed on the corpse, indicating a much longer PMI. In cases with insect contamination, it is therefore critically important for a forensic entomologist to be able to positively associate the insects being used for estimating PMI and PIA with the decedent in question.

Forensic DNA analysis of tissues extracted from insect guts is one reliable method used to demonstrate that an insect larvae has fed upon a corpse [320, 321]. However, maggot saliva contains enzymes that also reach the gut region (specifically the crop) when combined with food [322], which can degrade DNA in a short period of time. Njau and coworkers [323] reported that human DNA could be recovered from larva crops only up to 48 h, or 96 h if maggots were starved. DNA recovery from the pupal or adult insect life stages would be impossible, although one case study did recover DNA from the exterior of a puparium [324]. An alternative method that works with a broader range of insect samples, in different life stages and points of preservation is needed. In this context, stable isotope analysis serves as a prospective methodology to link insects to their originating corpse.

In this study, we demonstrate the potential of stable isotope ratio analysis to link different blow fly life stages to carrion from different species, which could help resolve any uncertainty about the relationship between insects and corpses. Also, not many studies depict how the complex metabolic process that occurs during metamorphosis influence the isotopic signatures of insect life stages [304, 309, 325, 326]. Herein, we also depict how three life stages of a holometabolous insect can be distinguished from each other based on isotopic signatures of their amino acids.

Isotope ratio analysis is a powerful tool of forensic chemistry that has been used, for example, to predict the geographic origin of individuals based on the isotopic ratios of light elements in their hair [44, 327, 328]. Because stable isotopes originate from food, "you are what you eat". If, like people, blow flies *are* what they eat, the isotope ratios found in the fly specimens should allow identification of their developmental resource. Isotope ratio mass spectrometry (IRMS) should be particularly effective with blow flies developing on corpses because all of the biomolecules needed to complete blow fly growth and development are typically acquired from the tissue of a single individual. Proof of this hypothesis comes from a recent study using direct analysis in real time coupled to high-resolution mass spectrometry (DART-HRMS) used amino acid profiling of oviposited eggs to identify necrophagous fly species [329].

Several groups have shown that biological chemicals originating from different organs or different metabolic pools can have significantly different degrees of isotopic fractionation within the same organism [302, 306, 330]. However, isolation of these different chemical components of a specimen typically requires pooling specimens and conducting a significant number of wet-chemical processes. The resulting number of isotope measurement variables derived from such extensive work is typically limited to 3-4 variables per element, such as $\delta^{13}C$ values of lipids, protein (muscle) and chitin.

To maximize the number of isotopic variables and metabolic pools for chemical comparison, and to minimize the extent of wet chemical methods, we use amino-acid-specific isotope ratio analysis as a basis for comparing blow flies with the carrion from which they had fed. We examined the $\delta^{13}C$ values of amino acids derived from the different blow fly life stages and show that whereas the extent of $\delta^{13}C$ fractionation varies between amino acids and life stages, there is greater variance in $\delta^{13}C$ values of amino acids in the carrion. The results indicate that, among other capabilities, one may differentiate insects that grew and developed from on carrion from two different species.

2. Material and methods

2.1. Chemicals

Orthophosphoric acid (>85% purity), sodium persulfate (99% purity), sulfuric acid (>95% purity) and amino acids (98–99% purity) were purchased from Sigma-Aldrich (St. Louis, MO, USA). Isotope standards NBS-19, LSVEC, USGS-40, USGS-41, and IAEA-600 were purchased from NIST (Gaithersburg, MD, USA), USGS (Reston, VA, USA), and the IAEA (Vienna, Austria), respectively.

2.2. Blow fly treatment

Adult blow flies from a commercial strain of *Calliphora vicina* (Robineau-Desvoidy) (Diptera: Calliphoridae) oviposited under controlled conditions on three media. All of these were food-grade animal tissues obtained from a local grocery store: raw beef muscle, raw chicken liver and raw pork muscle. Larvae were allowed to feed *ad libitum* and develop normally into adult flies. Arbitrary individual insects were chosen from each treatment in three life stages. These stages were the post-feeding third instar (larvae) stage, the pupa and associated puparium—which combined were called pupae—and unfed adults. Adult flies were not permitted to feed before analysis.

2.3. Sample preparation

We analyzed a total of twelve replicates for each set of carrion type: carrion tissue (n=3), associated life stages larvae (n=3), pupae (n=3) and adult flies (n=3). Samples were individually pulverized in 2 mL polypropylene tubes containing four 3.2 mm chrome steel beads using a minibead beater (Biospec Products Inc., Bartlesville, OK, USA) for 5 min at 3450 rpm [61].

2.4. EA-IRMS

For bulk analysis, the different pulverized samples were precisely weighed to approximately 470 µg into tin capsules for posterior bulk $\delta^{13}C$ and $\delta^{15}N$ measurements. Samples were analyzed using a Flash HT Plus Elemental Analyzer (Thermo Fisher Scientific, Bremen, Germany) coupled to a Delta V Advantage Isotope Ratio Mass Spectrometer (Thermo Fisher Scientific, Bremen, Germany) via a Conflo IV interface (Thermo Fisher Scientific). Gases were ultra-high purtiy from Airgas (Morgantown, WV): >99.9999% He, 99.999% N_2, 99.997% CO_2, and 99.999% O_2.

Samples were measured relative to compressed CO_2 working gas and calibrated to the international scale, relative to VPDB, using a two-point normalization based on NBS-19 ($\delta^{13}C$= +1.950‰) and LSVEC ($\delta^{13}C$= -46.60‰). For nitrogen isotope ratio measurements, samples were measured relative to atmospheric air and converted to the "atmospheric nitrogen (air-N_2)" scale using USGS-40 ($\delta^{15}N$= -4.52‰) and USGS-41 ($\delta^{15}N$= +47.57‰) as two-point calibration standards [16]. IAEA-600 (caffeine; $\delta^{13}C$= -27.77‰, $\delta^{15}N$= +1.0‰) was run after every three or four samples as a quality control standard. The measurement uncertainty (95% confidence interval) from pooled replicates is estimated to be ± 0.2‰ for $\delta^{13}C$ measurements and ± 0.3‰ for $\delta^{15}N$ measurements. The following equation was used to express the relative difference of isotope ratios into the delta notation (per mil ‰) [15, 20]:

$$\delta_{\text{sample}}(‰) = \left(\frac{R\ sample}{R\ standard} - 1\right)$$

where R_{sample} is the specific isotope abundance ratio of the of the heavier isotope over the lighter for sample and $R_{standard}$ is the abundance ratio of the corresponding international standard.

2.5. LC-IRMS

For carbon compound-specific isotope analysis of insect amino acids (AA), we used a Dionex ICS5000 ion chromatography system (ICS) (Dionex, Sunnyvale, CA, USA) coupled through an LC-Isolink interface (Thermo Fisher Scientific, Bremen, Germany) to the same Delta V Advantage isotope ratio mass spectrometer described above. The LC-IRMS procedure used in this work has been used on numerous occasions for compound-specific isotope analysis of amino acids in proteinaceous material [5, 331-335], and more information about the method validation can be found in the previous articles [5, 331-335]. Aliquots of approximately 10 mg of each pulverized sample was hydrolyzed in 6 M hydrochloric acid for 24 h at 110 °C in a vacuum oven. This hydrolysis protocol does not cause significant $\delta^{13}C$ fractionation on the recovered amino acids [336]. The AA mixture was posteriorly evaporated to dryness at 40 °C in a Mivac evaporator (Genevac, Ipswich, UK). The dry residues were then reconstituted in 1 mL of deionized water and filtered with a 0.45 μm syringe filter to remove any non-hydrolysable body tissues. Like others, we observe that acid hydrolysis cause conversion of glutamine (Gln) and asparagine (Asn) to their respective dicarboxylic acids: glutamic acid (Glu) and aspartic acid (Asp). For this reason, the delta values reported for Glu and Asp include a small contribution from Gln and Asn, respectively [61, 337]. Methionine and cysteine were not observed after our acid hydrolysis.

A mixed-mode column Primesep A, 2.1 × 250 mm, 5 μm, 100 Å (SIELC Technologies, Prospect Heights, IL, USA) provided adequate separation of the recovered underivatized amino acids. The mobile phase was composed of 100% solvent A (100% deionized water [17.6 MΩ]) for the first 18.7 minutes. The mobile phase then underwent a linear gradient to 14% solvent B (0.03M

sulfuric acid in deionized water) at 40 minutes. The mobile phase then underwent another linear gradient elution to 100% solvent B at 95 minutes until the end of the separation at 120 minutes. The flow rate of the mobile phase was 260 μL/min. The HPLC eluent passed into the LC-Isolink interface, where wet chemical oxidation quantitatively converted all carbon containing compounds to CO_2. Oxidation took place in the aqueous phase at 99.9 °C using 10% sodium peroxodisulphate and 1.5 M phosphoric acid. These reagents were individually pumped into the Isolink two-head pump interface. The resulting gas mixture of CO_2 and water was removed from the cooled solution by a membrane exchanger and passed through two water traps before the effluent CO_2 stream was transferred to the attached IRMS. An Aura solvent degassing system with a 1.5 μm Teflon filter membrane (Sigma-Aldrich, St. Louis, MO, USA) filtered and degassed all mobile phase solvents and oxidation reagents for 30 min prior to use. To remove any external CO_2, all reagent solutions were continuously sparged with UHP helium before and during use.

Similar to the bulk IRMS measurements, samples were measured relative to CO_2 working gas and calibrated to the international scale relative to VPDB by using a two-point normalization based on USGS-40 ($\delta^{13}C$= -26.39‰) and USGA-41 ($\delta^{13}C$= 37.63‰). Caffeine IAEA-600 ($\delta^{13}C$= −27.77‰) was likewise used as quality control standard. Drift corrections were not necessary. Following the principle of identical treatment, a mixture of 17 pure standard amino acids of known isotopic composition were analyzed under the same conditions (except for the acid hydrolysis) to verify that chromatographic separation and instrument performance were being properly achieved without any significant fractionation. The measurement uncertainty (95% confidence interval) of pooled replicates was different for every amino acid (**Table 2.1**). More measurements should be performed to better estimate the individual precisions.

Table 2.1. Measurement uncertainty (95% CI) of $\delta^{13}C$ amino acid measurements when three separate samples of the same type are carried through the entire method (digestion, filtering, evaporation, reconstitution, separation and analysis). The uncertainties below are pooled uncertainties of triplicate measurements for each of three carrion sources and three life stages. Therefore, for each pooled value below, N=36, and DOF=21.

Amino Acid	Asp	Glu	Ser	Thr	Gly	Ala	Pro	Val	Ile/Leu	Tyr	Lys	His	Phe	Arg
± 95% C.I (‰)	1.2	0.5	0.5	0.4	0.8	0.6	0.8	1.1	1.3	1.6	1.3	1.5	1.5	1.9

2.6. Data analysis

For EA and LC-IRMS analyses, Isodat 3.0 software was used for data acquisition (Thermo Fisher Scientific) and SPSS 24 (IBM, Armonk, NY, USA) was used for statistical analysis. Statistical tests such as One-way ANOVA, Principal Component Analysis (PCA) and Canonical Discriminant Analysis (CDA) were performed following the definitions published in reference [61].

3. Results and Discussion

3.1. EA-IRMS

3.1.1. Nitrogen

In general, nitrogen fractionation occurred at each life stage of the blow flies. From carrion to larvae the average fractionation across all carrion sources was +3.7‰ (Figure 1), which is slightly higher than the general ^{15}N enrichment of +3.4‰ observed by others [338-340]. From the larvae to pupae life stages, the blow flies display an average fractionation of -1.0‰, but the uncertainty in the average fractionation is too large to be significantly different from the larvae. However, paired-sample T-tests revealed that within each carrion source, there was significant depletion in ^{15}N between the larvae and the pupae ($p<0.05$) (Figure 2). The metamorphic change from larvae to adult involves complex metabolic processes wherein the body tissues become more ^{15}N enriched in each life stage due to the release of depleted nitrogenous excreta [304, 341]. In this way, this apparent

depletion pattern from larvae to pupae between the carrion sources was a surprising result. It is worth mentioning that we did not separately analyze the puparium or meconium (post-emergence nitrogenous excreta) of the insects, which would provide a better understanding of the nitrogen fractionation during these stages.

Bulk nitrogen isotope ratios increased by an average of +2.5‰ from pupae to adult flies (Figure 1). The average enrichment of the adult flies relative to the average pupae or average larvae isotope ratios was significantly different, which was confirmed by paired-sample T-tests ($p<0.01$) within each carrion source (Figure 2). The total average fractionation from carrion to adult flies was +5.2‰, which was very significant (paired-samples T-test, $p<0.0001$). This overall $\delta^{15}N$ enrichment is usually a consequence of dietary influence or a reflection of the nitrogen waste during the insect development.

McCutchan *et al.* [342] observed that insects raised in high-protein diets depict a trophic shift (diet to consumer) that is higher than insects raised on invertebrate or plant-based diets. In our experiments, *C. vicina* was raised on a nearly-pure protein diet of vertebrate tissues. We speculate that the combination of diet and metamorphic effect might explain the average fractionation higher than the usual +3.4‰ [342]. Supporting this theory is that each life stage had an isotopic signature that was slightly different for each carrion source. In general, blow flies raised on beef depicted the most enriched nitrogen signatures, followed by blow flies raised on chicken and pork, respectively (Figure 2).

3.1.2. Carbon

Average bulk carbon isotope values showed an enrichment of +0.6‰ to +0.4‰ for larvae and pupae relative to carrion and a depletion of -1.2‰ for adult flies relative to carrion (**Figs. 2.1** and **2.2**), but only the adults were significantly different at the 95% confidence interval. Figure 1 shows that the average change in bulk carbon isotope ratio values is not significant between carrion and larvae or pupae. Trophic-level carbon fractionation results have been reported previously [342], and the $\Delta^{13}C$ shifts for most insect consumers were reported to be negligible or small; i.e. ranging from -2.7‰ to +3.4%, relative to the food source [89, 306].

In this study, the magnitude of carbon fractionation generally is less than 1‰. On the contrary, the isotope ratio differences between different carrion are as large as 8‰. The small degree of fractionation relative to the large difference between carrion sources suggests that ^{13}C values may be used to exclude certain sources of carrion as potential sources of food for blow flies measured at any life stage. For example, **Fig. 2.2** indicates that any life stage of a blow fly with a bulk ^{13}C value between -12‰ and -14‰ cannot have originated from either of the sources of chicken or pork used in this study. However, given the uncertainty in fractionation, a blow fly with a bulk ^{13}C value between -18 and -20‰ could have originated from either the pork sample or the chicken sample, but not from the beef sample.

These interpretations specifically relate to the individual samples of each food source used in this study, and not necessarily to every specimen of each food source. The average bulk ^{13}C value of the diets of different individuals within a species—and therefore the bulk ^{13}C value of individuals within a species—may vary by more than 10‰ [59], which means that more samples of each species should be analyzed before species-level determinations can be made. Given that dietary variations within species is likely to yield individuals that have similar bulk ^{13}C isotope ratios as individuals of

different species, bulk ^{13}C isotope ratio measurements are unlikely to be able to selectively identify the species-level food source of a particular blow fly. However, to provide more variables for statistical comparisons, and to thereby obtain better discriminating power, we explored the use of compound-specific ^{13}C measurements of different amino acids among life stages and tissue types.

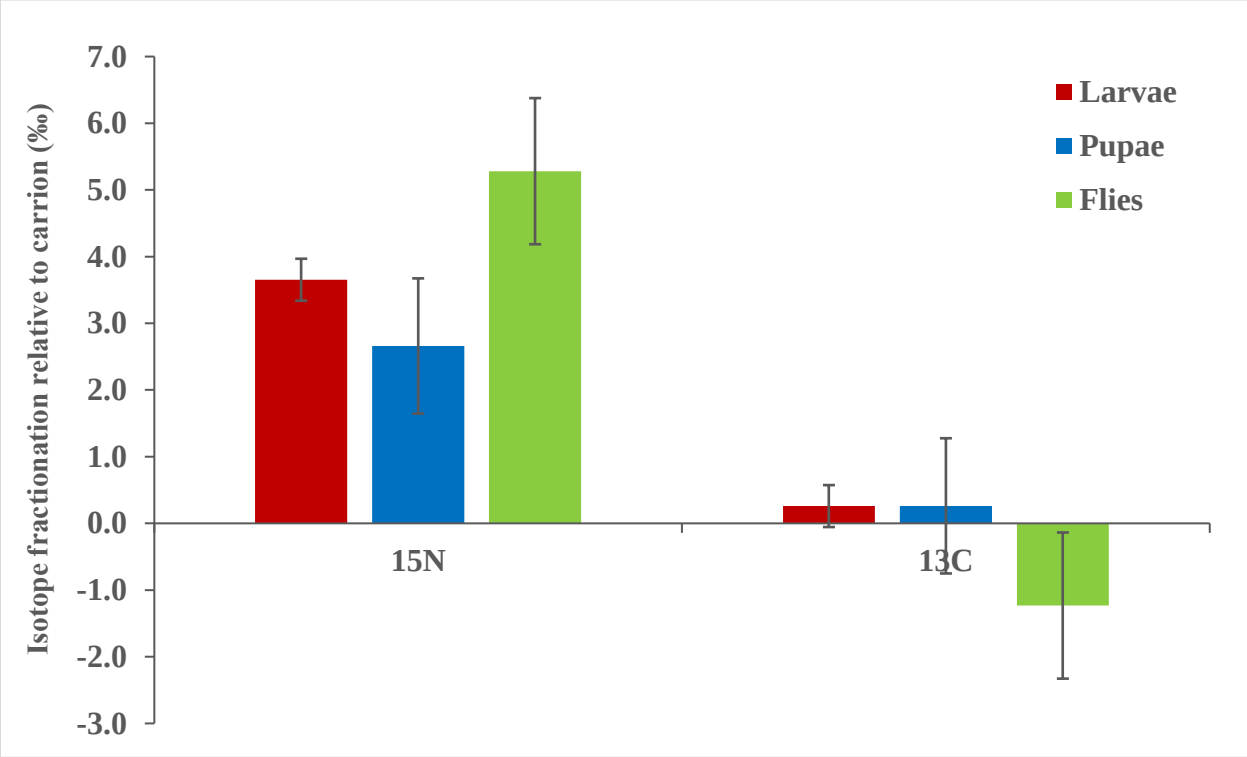

Fig. 2.1. Fractionation of bulk isotope ratio values for different life stages of blow flies, averaged across carrion sources (n=12). Error bars show the pooled 95% confidence intervals.

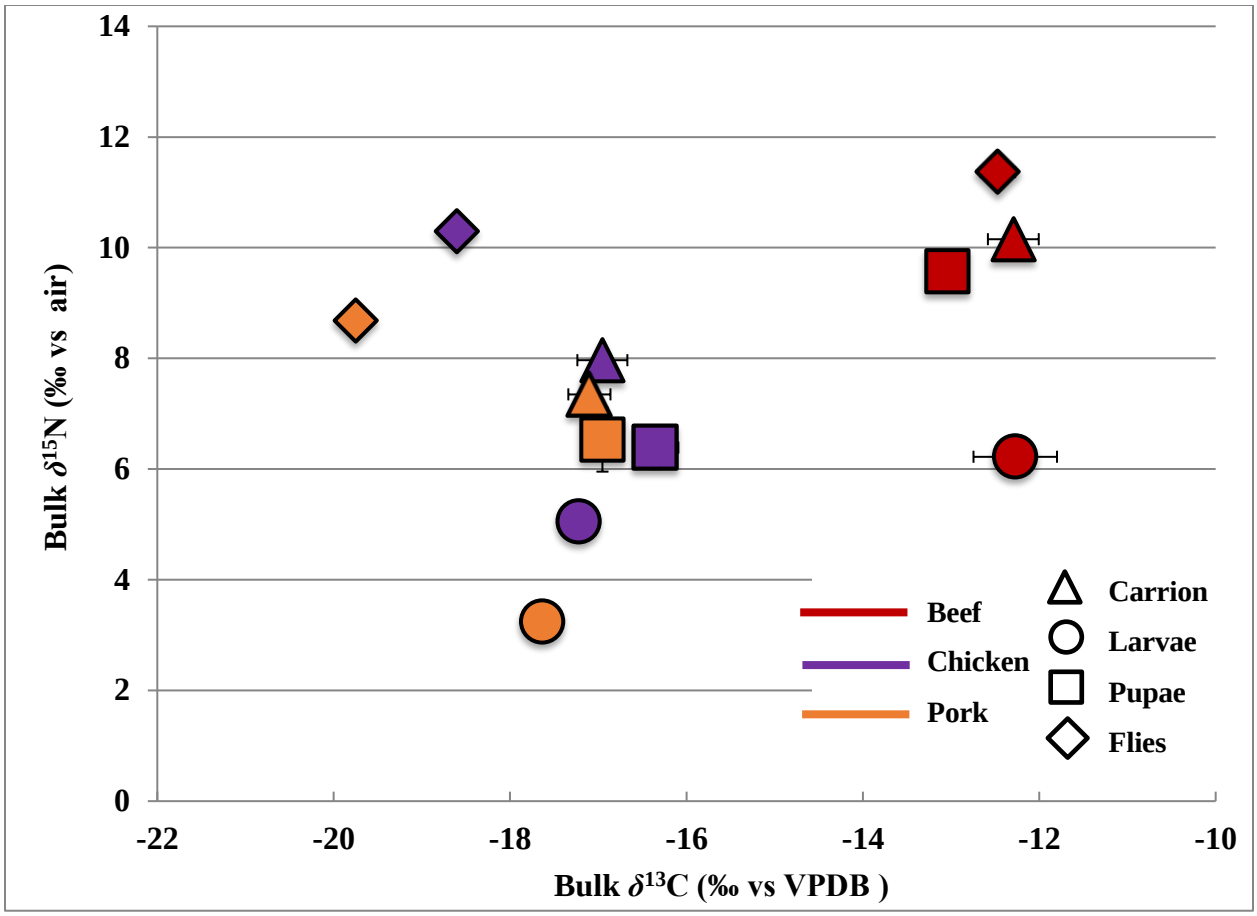

Fig. 2.2. Bivariate plot of bulk isotope ratio values for different life stages of blow flies that were raised on different sources of carrion (n=4 for each data point). Error bars show the measured 95% confidence intervals.

3.2. Compound-specific isotope analysis

To assess the isotopic fractionation between life stages, we plotted the average change in carbon isotope ratio values against each amino acid and life stage (**Fig. 2.3**, see Appendix **Fig. A2.1** and **Table A2.1**). The results show that the δ^{13}C values of the essential amino acids (His, Leu/Ile, Lys, Phe and Thr) at any life stage were not significantly different (at 95% CI) relative to the carrion (Figure 3). It is widely established that there is a carbon isotope shift of approximately +1‰ between trophic levels [306, 343, 344]. However, since essential amino acids cannot be synthesized by blow

flies, it is reasonable to expect that no carbon fractionation from diet to consumer should exist for essential amino acids [343], but that a greater extent of fractionation should exist for non-essential amino acids and other nutrients that can be chemically altered via metabolism in the blow flies. An exception to this trend was Val, which was significantly different (at 95% CI) relative to the carrion (**Fig. 2.3**). Based solely on our results, we could not find an explanation for valine being more enriched than the other essential amino acids. The assumption of an extra valine source coming from the insect's gut is a possible option because many fly species use metabolic products from symbiotic bacteria to enhance growth and development at early metamorphic stages [345]. If gut bacteria provide valine fractionation, one might expect the same valine enrichment in all three types of carrion, but enrichment seems to be less dramatic when insects were feed on chicken (see Appendix **Fig. A2.1**). To our knowledge, there are no references investigating the role of valine in a fly-bacteria symbiotic relationship. Because the number of replicate measurements is quite small (N=3), more experiments must be performed before any drawing and additional conclusions regarding valine metabolism. Nonetheless, it is still generally true that the essential amino acids can act as tracers that link the different fly life stages back to the specific consumed carrion, without concern for major fractionation.

In contrast to the essential amino acids, some non-essential amino acids in the blow flies showed measurably different isotope ratios relative to the food sources. This is an indication of *de novo* synthesis rather than direct routing from the diet [346]. For larvae and pupae, the isotopic ratios of serine, proline and glycine were enriched in ^{13}C relative to carrion by approximately +3.8‰, +4.5‰ and +7.2‰, respectively (**Fig. 2.3**). However, alanine showed $\delta^{13}C$ depletion of -2 to -3‰ for larvae and pupae relative to carrion. Although the magnitude of isotope enrichment of specific amino acids exceeds the typical trophic-level ^{13}C enrichment in whole animals [305, 306, 347], our

observations are consistent with bulk tissue or trophic-level fractionation, such as those reported by Webb *et al*. [330] for lipids and proteins (muscle).

We assume that some metabolic shifts during the growth and development of the insects influence the amino acid fractionation at different life stages of this species. *De novo* synthesis of non-essential amino acids is more energetically consuming than the direct routing of non-essential amino acids from the diet, the latter being favored when the diet contains high-protein content, such as carrion [346, 348, 349]. Our results showed the opposite trend, with a prevalence for the most energetically consuming via (*de novo* synthesis). Similar results were reported with birds [346], where the authors assumed that the non-direct routing from diet could be related to the fasting preceding feather synthesis. These metabolic shifts depicted in our results were most dramatic when the blow flies metamorphose from pupae to adult flies. For example, the non-essential amino acids (e.g. Ser, Pro, Gly, Ala and Glu) all showed ^{13}C depletion between the pupae and adult fly stages; the same pattern can be visualized in the plots for individual amino acids in the various diets (see Appendix **Fig. A2.1**). The greatest ^{13}C depletions from pupae to adult flies occurred for Ala (~3‰), Glu (~3‰) and Gly (~4‰) (**Fig. 2.3**).

The isotope depletions observed between pupae and adult flies do not seem to be correlated with the fractionation occurring between earlier life stages. For example, Glu did not show fractionation at all from carrion to larvae or carrion to pupae, Ala showed depletion in the first two life stages and other non-essential amino acids (Ser, Pro and Gly) all showed enrichment in the first two life stages relative to carrion.

Non-essential amino acids, except tyrosine, are synthesized from one of the intermediates of carbohydrate metabolism, such as pyruvate, oxaloacetate, α-ketoglutarate and 3-phosphoglycerate. Necrophagous insects, including *Calliphora vicina,* rely on diets containing virtually no

carbohydrates (animal tissues). Therefore, these insects probably use glucogenic amino acids and lipid catabolism to produce glucose via gluconeogenesis, a common metabolic pathway performed by all insects [350]. In insects, gluconeogenesis primarily occurs in the "fat body", an organ unique to arthropods, which is responsible for most of the synthesis, storage and utilization of biomolecules during insects' development [351, 352]. Usually, more than 50% of the fat body is composed of lipids [353], which are stored during the larval feeding stages of holometabolous insects such as flies for use during metamorphosis and as initial reserves for the young adults [351]. Thus, the dominance of gluconeogenesis in the larvae is probably responsible for the fractionations observed between carrion and larvae.

Another nutrient present in the fat body is glycogen, the main energy source of glucose during the post-feeding larval and pupal stages [351]. Within an organism, lipids generally present lower $\delta^{13}C$ values than carbohydrates and proteins because of a fractionation step associated with pyruvate dehydrogenase, the enzyme responsible for the oxidation of pyruvate to acetyl-CoA [354, 355]. The reason the adult flies are more depleted in ^{13}C than their previous stages is therefore likely to be because they mobilize their lipid reserves to synthesize their exoskeleton, organs, wings and reproductive organs, among other tissues. The known mechanisms do not seem to adequately explain why the earlier stages are so enriched in ^{13}C compared to the adults. One additional explanation is that the fractionation step required for the glycogen mobilization during the earlier stages make larvae and pupae enriched in ^{13}C due to the constant release of ^{12}C-enriched CO_2. Although the details remain to be resolved, the present results show that the $\delta^{13}C$ values of amino acids in blow flies correlate with that of their diets, but that each amino acid provides a unique pattern of fractionation during insect development.

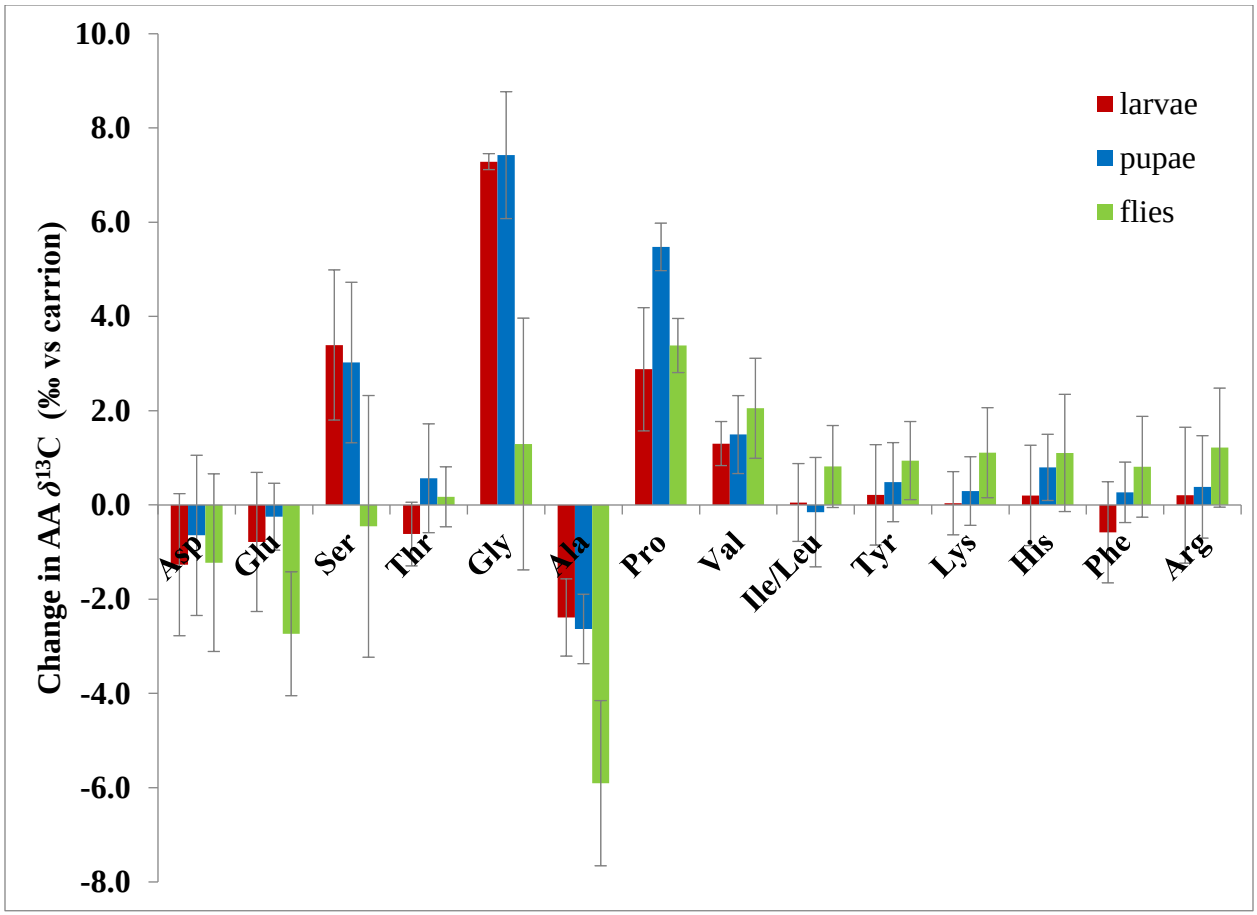

Fig. 2.3. Carbon fractionation between *C. vicina* life stages. When comparing the carbon isotopic ratio of larvae (n=9), pupae (n=9) and adult blow flies (n=9) relative to carrion, there was no significant difference for essential amino acids in between the different stages (95% CI). Non-essential and conditionally essential amino acids of larvae and pupae were more enriched in ^{13}C while adult flies were more depleted in ^{13}C, both relative to carrion. Bars represent mean ± 95% CI.

Pro and Glu showed quite unexpected signatures in that they differ from one another. Pro and Glu were different by 6‰ in larvae and pupae, but approximately 8‰ in adult flies. Proline is biosynthesized via a series of reactions that involve the cyclization of glutamate (deprotonated form of glutamic acid) as the precursor [356]. Because there are no carbon atoms involved in this process, we assumed there should be no carbon fractionation, so we expect Pro and Glu to have similar $\delta^{13}C$ values when Pro is not routed directly from the diet. However, Hare *et al.* [357] observed similar

disparity between Pro and Glu when investigating modern and fossil collagen; they suggest that proline might come directly from the diet rather than *de novo* synthesis.

Regardless of the underlying metabolic factors, we were interested to see how effective the amino-acid-specific isotope ratio values were in classifying blow flies with their carrion diets. We therefore performed some relatively simple multivariate approaches to understand the variance in isotope ratios within and between different grouping factors, like life stage.

3.2.1. Classification based on carrion

Individuals were first classified into groups based on the type of consumed carrion. Initially, principal component analysis (PCA) was conducted using the $\delta^{13}C$ values for fifteen amino acids extracted from each carrion and blow fly life stages as variables (**Fig. 2.4**). The data points include n=3 separate measurements for each sample. A separate measurement implies a unique sample, digestion and analysis step to provide independent input variables for each sample type.

One-way analysis of variance (One-way ANOVA) followed by Tukey's HSD post hoc test using carrion as the fixed factor (response variable) showed very significant differences between the within-group variance and between-group variance for every amino acid isotopic ratio (explanatory variable) (see Appendix **Table A2.2**). Ala was the only not statistically significant amino acid, with α value of 0.109. All the other amino showed α values less than 0.05. These significant alpha values demonstrate that the variance in isotope ratio values of amino acids between carrion sources is vastly larger than the variance captured within all the samples derived from a carrion source. In other words, fractionation of amino acids by the blow flies is negligible relative to the large difference that exists between the amino acids in the food source.

Principal component analysis (PCA) also showed a high degree of correlation between the variables. This fact was corroborated by the Kaiser-Meyer-Olkin measure of sampling adequacy (0.800), the Bartlett's test (<0.05). The variance explained by the first three principle components was 69.3% (PC1), 10.9% (PC 2) and 9.1% (PC3), which together explained ~89.3% of the total variance. Some natural clustering showed that individuals fed beef were separated into a distinct group, whereas insects fed pork and chicken were clustered together. Figure 4B is a bivariate plot of δ^{13}C values of Lys and Phe to show the contribution of just two amino acids to the variance in the isotope ratios between samples (blow flies or carrion source) derived from different carrion sources. One can clearly visualize the relative difference between within-group variance and between-group variance of δ^{13}C values of these two amino acids.

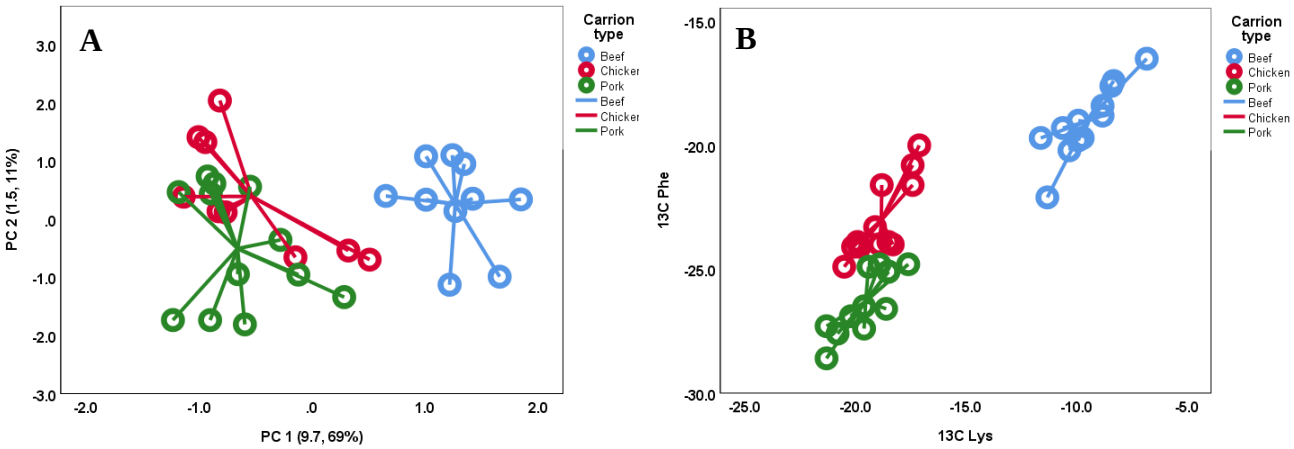

Fig. 2.4. A) Principal component analysis (PCA) plot to show some natural clustering when grouping blow fly stages to different carrion types. PCA used the non-averaged carbon isotope ratios of fifteen amino acids as the input variables. The absolute and percent variance explained by the first two PCA components are shown in the axis titles. **B)** Bivariate plot of δ^{13}C values of Lys and Phe to show the contribution of just two amino acids to the variance between samples (blow flies or original carrion source) derived from different carrion sources.

When using a supervised dimension reduction method—e.g. canonical discriminant analysis (CDA)—to examine the variance of blow flies and carrion, the results provided more useful

clustering. Using CDA, all samples derived from chicken and pork carrion could be separated using the first two canonical functions (Figure 5A). When predicting group memberships—e.g. to the original carrion source—100% of samples were correctly classified based on the CDA original rules, and 96.8% were accurately classified after leave-one-out cross-validation (LOOCV) (Figure 5B). The CDA original rules include every data point from the sample groups when performing the classification analysis. This approach is considered biased because a particular data point is used to build the classification rules which then attempt to predict its group membership. LOOCV is considered unbiased because the classification rules are based on all-but-one of the data points, and the rules are then used to predict the group membership of the held-out point. The process is repeated for every data point to assess the overall classification accuracy.

When Ala was omitted as variable, the original-rules accuracy and leave-one-out cross validation accuracy were both 100% accurate, which indicates that Ala does not provide any additional benefit for linking the blow flies to the carrion. As previously mentioned, one-way ANOVA showed Ala to be the only not significant variable, with a α value of 0.109.

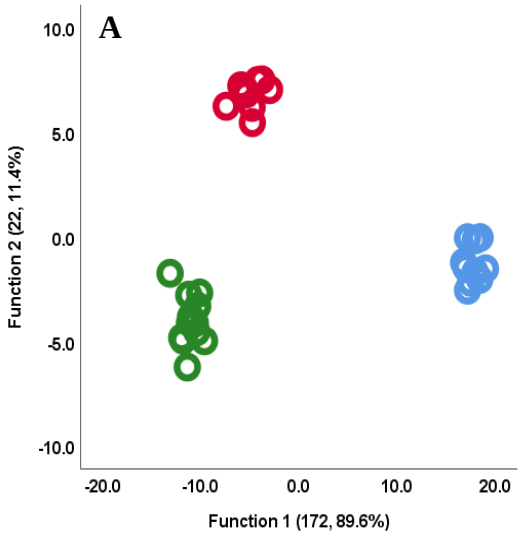

B

Classification Results[a,c]

		Carrion	Predicted Group Membership 1.0	2.0	3.0	Total
Original	Count	1.0	10	0	0	10
		2.0	0	9	0	9
		3.0	0	0	12	12
	%	1.0	100.0	.0	.0	100.0
		2.0	.0	100.0	.0	100.0
		3.0	.0	.0	100.0	100.0
Cross-validated[b]	Count	1.0	10	0	0	10
		2.0	0	8	1	9
		3.0	0	0	12	12
	%	1.0	100.0	.0	.0	100.0
		2.0	.0	88.9	11.1	100.0
		3.0	.0	.0	100.0	100.0

a. 100.0% of original grouped cases correctly classified.

b. Cross validation is done only for those cases in the analysis. In cross validation, each case is classified by the functions derived from all cases other than that case.

c. 96.8% of cross-validated grouped cases correctly classified.

Fig. 2.5. A) Canonical discriminant analysis (CDA) plot of not-averaged carbon isotope ratios of fifteen amino acids (14 variables) using carrion type as the classification factor. The absolute and percent variance explained by the first two functions are shown in the axis titles. **B)** Assignment to carrion groups based on CDA original rules and leave-one-out cross validation.

To test the classification scheme, and to ensure we are not overfitting the data, samples were assigned to four random groups instead of their carrion or sample type (i.e. life stage). The leave-one-out cross validation accuracy for predicting group membership of randomly-grouped samples was 25%, which is no better than guessing. As indicated by the ANOVA results, the successful clustering of all samples to their original carrion source is made possible by the small extent of amino acid fractionation relative to the large differences in amino acid isotope values between carrion. The amino acids that are most useful for carrion classification are those with the largest standardized canonical discriminant function coefficients, which—as one might expect—tend to be the essential amino acids that do not undergo fractionation (**Table 2.2**).

Table 2.2. Standardized canonical discriminant function coefficients for carrion as a discrimination factor. Variables with large absolute coefficient values have a bigger impact on the separation of carrion groups and successful classification. Highlighted variables are essential amino acids.

Standardized Canonical Discriminant Function Coefficients		
	Function	
	1	2
His	-1.689	-.426
Ile/Leu	.758	2.268
Lys	2.146	-1.243
Phe	.058	2.829
Thr	1.825	.660
Val	.198	-.103
Asp	-.140	-.537
Glu	-.180	.280
Ser	2.167	-.348
Ala	-.360	-.845
Pro	-.793	-1.604
Tyr	-.035	-1.490
Arg	-1.310	-1.558
Gly	-.698	2.139

The importance of each amino acid variable in the classification of blow flies to carrion source can also be understood through examination of the pooled within-group correlations between discriminating variables— i.e. the amino acids—and the standardized canonical discriminant functions (see Appendix **Table A2.3**). For example, the essential amino acids Thr, Lys and Val have the largest correlations with discriminant function 1, with correlations of 0.384, 0.304 and 0.229, respectively. These amino acids are most useful for distinguishing samples originating from beef from the other two carrion sources.

As a general rule, multivariate techniques should employ many more (e.g. >5x more) data points than variables. The use of fewer variables with successful classification gives strength to the statistical significance of the multivariate approach. Therefore, given the lack of fractionation for the essential amino acids, we repeated the CDA classification using only the eight non-essential amino acids as seven input variables for the 36 data points. Using His, Ile/Leu, Lys, Phe, Thr, Val and Arg, the first two discriminant functions explained 100% of the variance between samples from different carrion sources, and the leave-one-out cross-validation accuracy was also 100%. Classification accuracy remained at 100% (for LOOCV and original rules) when using the four essential amino acids Val, Arg, His and Phe. Classification works with fewer variables because there is a strong correlation between all the amino acids. For example, the isotope ratios of essential amino acids correlate with coefficients (R) that range between 0.785 for His and Phe and Ile/Leu to 0.976for Arg and Lys. In contrast, the use of only the non- essential amino acids (Ala, Asp, Glu, Ser, Gly and Pro) resulted in a LOOCV classification accuracy of 71%, probably because the metabolic fractionation of the non-essential amino acids adds extra variance to the isotope ratios at each life stage.

Cluster techniques were also investigated. Hierarchical cluster analysis showed that all the samples derived from beef readily clustered after the first branch points (see Appendix **Fig. A2.2**). The samples derived from pork and chicken did not naturally cluster at the next few branch points, presumably because of the similarity between the sample means for several of the amino acids.

3.2.2. Classification based on life stage

We also attempted to use $\delta^{13}C$ values of the fifteen amino acids to classify the different life stages regardless of the carrion type. Canonical discriminant analysis plot also showed very distinct

clustering for each of the life stages (**Fig. 2.6A**). We also included a variable called "tissue", which was the combination of all carrion meat. The first function was responsible for explaining ~81% of the variance. Using original rules, 100% of groups were correctly classified using the original rules, and 71% of the samples were correctly classified to tissue type after leave-one-out cross-validation (**Fig. 2.6B**). Of course, standard evidence collection procedures imply that it is unlikely that a sample would be analyzed without knowing the nature of the tissue sample or life stage of blow fly that was used. Still, this approach indicates that, regardless of diet, the fractionation of amino acids by the different life stages of the blow flies is sufficiently reproducible between the different carrion sources to permit life-stage determination. In the future, we will be interested to examine the correlation between fractionation of amino acids and the age of the larvae/blow flies. To date, the data are collected at discrete times during major developmental processes. It is possible that the changes in δ^{13}C values of certain amino acids could change quite reproducibly with time, which would then provide an objective, chemical method for establishing the age of a blow fly larvae. Variables with large absolute coefficients have a bigger impact on the discrimination scores. Highlighted variables are essential amino acids.

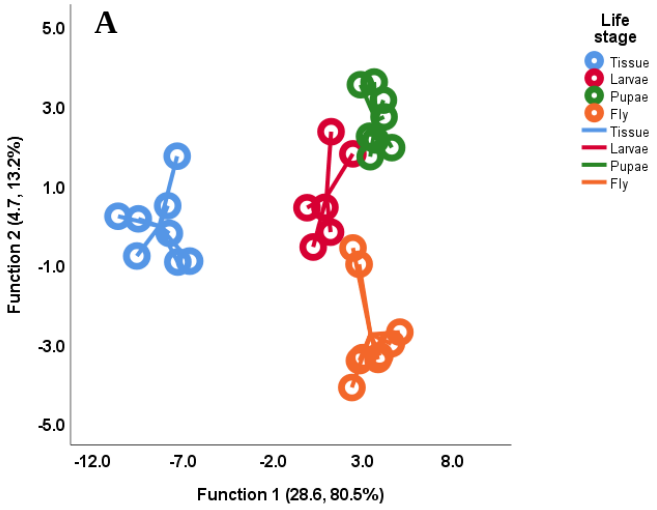

B

Classification Results[a,c]

		Life	Predicted Group Membership .0	1.0	2.0	3.0	Total
Original	Count	.0	8	0	0	0	8
		1.0	0	6	0	0	6
		2.0	0	0	8	0	8
		3.0	0	0	0	9	9
	%	.0	100.0	.0	.0	.0	100.0
		1.0	.0	100.0	.0	.0	100.0
		2.0	.0	.0	100.0	.0	100.0
		3.0	.0	.0	.0	100.0	100.0
Cross-validated[b]	Count	.0	7	1	0	0	8
		1.0	1	2	2	1	6
		2.0	0	3	5	0	8
		3.0	0	1	0	8	9
	%	.0	87.5	12.5	.0	.0	100.0
		1.0	16.7	33.3	33.3	16.7	100.0
		2.0	.0	37.5	62.5	.0	100.0
		3.0	.0	11.1	.0	88.9	100.0

a. 100.0% of original grouped cases correctly classified.

b. Cross validation is done only for those cases in the analysis. In cross validation, each case is classified by the functions derived from all cases other than that case.

c. 71.0% of cross-validated grouped cases correctly classified.

Fig. 2.6. A) Canonical discriminant analysis (CDA) plot not averaged carbon isotope ratios of fifteen amino acids using *C. vicina* life stages (larvae, pupae and adult fly) as the classification factor. Tissue corresponds to the combined diet signature (all carrions). The absolute and percent variance explained by the first two functions are shown in the axis titles. **B)** Assignment to life stage groups based on CDA original rules and leave-one-out cross validation. 0=tissue, 1=larvae, 2=pupae, 3=adult fly.

The underlying separation of groups based on life stage stems from the reproducible extent of fractionation for the different amino acids from the diet to the fly stages. Most of the largest absolute values in discriminant functions 1 and 2 were essential amino acids (His, Lys and Val for DF1; His, Lys, Thr and Arg for DF2) (**Table 3**). Arg is considered an essential AA for insects because they lost the ability to synthetize Arg during the evolutionary transition to uricotelism (excretion of uric acid) [358].

Table 2.3. Standardized canonical discriminant function coefficients table for life stage as discrimination factor.

Standardized Canonical Discriminant Function Coefficients			
	Function		
	1	2	3
His	4.429	-2.757	5.136
Ile/Leu	-1.607	.884	3.082
Lys	-4.762	-9.445	-6.982
Phe	-.937	.683	2.715
Thr	-.339	2.282	1.740
Val	2.005	.762	-.789
Asp	.172	.482	.382
Glu	1.271	.963	1.727
Ser	-.100	.454	-1.450
Ala	-2.487	.763	-.088
Pro	1.482	2.149	1.794
Tyr	-.338	-.865	-2.507
Arg	.109	4.788	-3.876
Gly	1.552	-.328	-.718

4. Conclusions

Bulk isotope ratio analyses were sufficient to identify blow flies fed on beef, chicken or pork. However, bulk isotope ratio analyses could not reliably distinguish blow flies raised on the latter two carrion. Amino-acid specific $\delta^{13}C$ analysis provided insight into the different types of metabolism at each of the major life stages. Essential amino acids tended not to undergo any fractionation because their structures and carbon-atom composition are unaffected by blow fly metabolic processes. However, the non-essential amino acids were enriched or depleted—depending

on life stage—by as much as ~8‰. Such insight could enhance the significance of blow flies for post-mortem interval determinations.

Additional compound-specific isotope experiments are necessary to better understand the fractionation patterns between the life stages of *C. vicina*. These studies could also assess any correlation between fractionation and time, which might then be useful for forensic PMI estimations, as well as for a better understanding of the biochemistry of amino acids during insect development. Because of the inter-individual isotopic variation in cattle, pigs, or chickens, it is difficult to draw any conclusions about how well this method might predict the species that a questioned fly has fed upon. However, this proof-of-principle study does indicate that amino-acid-specific isotope ratio analysis can be used to exclude the possibility that a particular food served as the primary diet for a blow fly in any of its life stages. More optimistically, these results indicate that if the within-species variance in isotope ratios is smaller than the between-species variance, then species-level determinations of carrion sources might be possible. Further research is being conducted to include human tissues in the pool of samples.

CHAPTER 3: ORIGIN DETERMINATION OF THE EASTERN OYSTER (*Crassostrea virginica*) USING A COMBINATION OF WHOLE-BODY COMPOUND-SPECIFIC ISOTOPE ANALYSIS AND HEAVY METAL ANALYSIS

Reproduced in part with permission from Mayara P. V. Matos, Marc E. Engel, John B. Mangrum and Glen P. Jackson, *Analytical Methods*, in preparation

1. Introduction

To protect consumers from harmful chemical and biological exposures, as well as to protect oyster fisheries from damage due to over harvesting, wildlife and food safety enforcement agencies have expressed a need for chemical or biological methods to identify the harvesting areas of oysters. Estuaries, where oysters grow, are characterized by having limited exchange of water from larger saltwater bodies, such as in the Gulf of Mexico (GOM), and they receive freshwater from rivers, streams and creeks that can be contaminated by local waste discharges and runoff from nearby industrial, agricultural and suburban areas. Therefore, the land use ascribed to the areas that drain into a given estuary greatly influences the chemical and biological content of the oysters that feed within its boundaries.

The greatest concern to human health from oysters is microbial contamination, especially when oysters are consumed without cooking. Water can carry bacteria and viruses into the estuary and especially so after heavy rainfall. Oysters contaminated with hepatitis A, norovirus [359], and salmonella are all known to cause illness in humans. However, the greatest concern associated with eating raw oysters is because of *Vibrio* sp., which is known to be prevalent in the GOM and South Eastern Atlantic waters [360-363]. In cases of *Vibrio vulnificus* infection, the fatality rate of infected patients is greater than 50% [362, 364]. Between 1981 and 1993, 690 Vibrio infections were reported in FL, and 72% of the reported cases mentioned that the patients had consumed raw oysters [361].

In 2011, the Centers for Disease Control (CDC) documented 117 cases of Vibrio infections in patients that had consumed oysters, and 107 of those cases had consumed raw oysters [365].

Estuaries are the nurseries for nearby marine ecosystems and therefore considered vital to the health of nearshore and offshore fisheries. Given the importance of estuary ecosystems, the harvest of estuarine species is managed by regulatory agencies. Among the regulated species are oysters, which play a significant role in the ecosystem by working as filter feeders and maintaining the nutrient balance of the estuary [366, 367]. Kellogg *et al*. reported that estuaries with fully restored oyster reefs, the oysters help improve the flux of nutrients like O_2, NH_4^+, nitrates and soluble reactive phosphorous in all seasons by more than an order of magnitude relative to areas that are not restored [366]. The oysters helped to assimilate a variety of nutrients, which benefited the ecosystem in question. Oysters are preyed upon by many estuarine inhabitants including: snails like the oyster drill (*Urosalpinx cinereal*); crab species like the stone crab (*Menippe* sp.) and mud crab (*Panopeus herbistii*); and fish such as the summer flounder (*Paralichthys denatus)*, black drum (*Pogonias cromis*), and sheepshead (*Archosargus probatocephalus*) [363, 368]. Oyster beds provide a habitat for other estuarine inhabitants (e.g. small fishes, crabs and other bivalves), making them a key component in the estuarine food web.

The GOM has been one of the largest commercial oyster fisheries in the USA. From 2000-2008, the GOM produced approximately 50% of the commercial oysters in the USA. During the same time, Apalachicola Bay in FL produced approximately 20% of commercial oysters harvested in the GOM. Since 2012, oyster production has been greatly reduced in Apalachicola Bay [363, 369, 370] in part due to significant reductions in water flows in the Apalachicola River. The reduced outflows are caused by the increased water needs of nearby urban and suburban areas and have contributed to the increased salinity of Apalachicola Bay, which has had a deleterious effect on the

oyster production. Since 2010, draught conditions in the southeastern USA, and a temporary increase in the number of oysters allowed for harvesting immediately after the BP Mercando well explosion, has further damaged the oyster fishery [363, 369].

The Florida Fish and Wildlife Conservation Commission (FWC) have authority for Bay closures to protect and manage the Apalachicola Bay oyster fishery and public health. The reduced availability of oysters due to environmental conditions and fishing pressure has led to harvesting restrictions on certain oyster reefs for certain times for the year. Despite the restrictions, oystermen are known to illegally harvest from the restricted areas and, when caught, claim that their catches come from waters that are legal to harvest [363, 369]. Between October 19th, 2018 and December 13th, 2018 the Florida Fish and Wildlife Conservation Commission reported four incidences where officers issued citations for oysters being harvested from restricted or prohibited areas [371]. Illegal oyster harvests from Apalachicola Bay hinders the recovery of the commercial fishery and poses a threat to the recovery of the Apalachicola Bay system.

Commercial oysters harvest areas may be closed when concerns for human health from either microbiological contamination or chemical contamination occur. Typically, these harvest areas are closed for short periods of time (5-10 days) due to heavy rainfall, because runoff from nearby freshwater sources increases the bacteria and virus levels in the water. However, oyster harvest areas and entire estuaries can be closed for months or years due to chemical contamination. For example, Lavaca Bay, TX is an area that has only recently been open to shellfish harvest after major restoration efforts were conducted to restore this once-highly-contaminated estuary [372].

The popular Eastern oyster, *C. virginica*, is a remarkably resilient species widely dispersed in many United States estuaries [373]. *C. virginica* has been one of the most popular species for the oyster harvesting business in the United States, despite its claimed reduced availability due to

excessive harvesting and some parasitic diseases [374]. Many studies involving this oyster are based on genetic analyses which aim to identify differentiation patterns in the distinct populations [375, 376], but little work has been done to explore the isotopic or elemental composition of this species as a way to determine geographic provenance.

Inductively coupled plasma–mass spectrometry (ICP-MS) and isotope ratio mass spectrometry (IRMS) have been successfully used to determine the geographic source of a variety of samples [377-381]. However, the few studies that combined both techniques focused on the ecology of a species or ecosystem changes due to seasonal or anthropogenic reasons [382, 383]. In this study we demonstrate the potential of lead (Pb) and cadmium (Cd) concentrations combined with bulk and compound-specific isotope analysis (CSIA) of *C. virginica* whole-body tissues to determine harvesting locations. Pb and Cd were chosen because they are primarily associated with anthropogenic activity and detected in almost all oysters tested in North America. Sources of these trace elements in the environment include fertilizers, the production of lead acid batteries and the mining and smelting of metals. Lead is still permitted in aviation fuel and also remains in the environment from legacy sources such as gasoline and lead-arsenic pesticides [384, 385]. The ability to use chemical signatures to identify harvest areas can play an important role in several areas, including: 1) the protection of consumers from the purchase of counterfeit oysters sold as "boutique" brand oysters, 2) to help regulatory agencies enforce harvesting regulations, and 3) to protect consumers from food-borne infections.

2. Experimental

2.1. Instrumentation

Cadmium and lead concentrations were determined by ICP-MS (PE Elan 6100 or PE Nexion, CT USA). Carbon and nitrogen bulk isotope ratio measurements ($\delta^{13}C$ and $\delta^{15}N$) were performed

using a Thermo Flash HT Plus elemental analyzer (EA) coupled to a Thermo Delta V Advantage isotope ratio mass spectrometer via a Conflo IV interface. For the $\delta^{13}C$ CSIA, we used a Dionex ICS5000 ion chromatography system (ICS) (Dionex, Sunnyvale, CA, USA) coupled through an LC-Isolink interface to a Delta V Plus isotope ratio mass spectrometer (Thermo Fisher Scientific, Bremen, Germany).

2.2. Sample collection

C. virginica oysters were sampled from Apalachicola Bay (Florida beds 1642 and 1662); Louisiana harvest area 28; and Copano and Galveston Bays, both in Texas (**Fig. 3.1** and **Figs. A3.1-A3.2**). These oysters were randomly collected, typically within days of harvest, from wholesale and retail outlets through 2011-2013. Ten oysters from each region were randomly selected for this project. Samples were placed in plastic bags, sealed, and shipped in coolers with cold packs overnight to the laboratory. All samples were stored in a -5 °C freezer until homogenization. In the laboratory, harvest areas were recorded from the sanitation tags that were included in the original inspection reports.

After defrosting, the oyster shells were first measured, then rinsed using metals-free water before shucking; rinsing helped avoid oyster tissue contamination from external debris. After shucking, the soft tissue weight was recorded, oysters were either segregated for the IRMS protocol or homogenized for the ICP-MS protocol. The homogenates were then stored in 50-mL screw top centrifuge tubes and frozen until digestion.

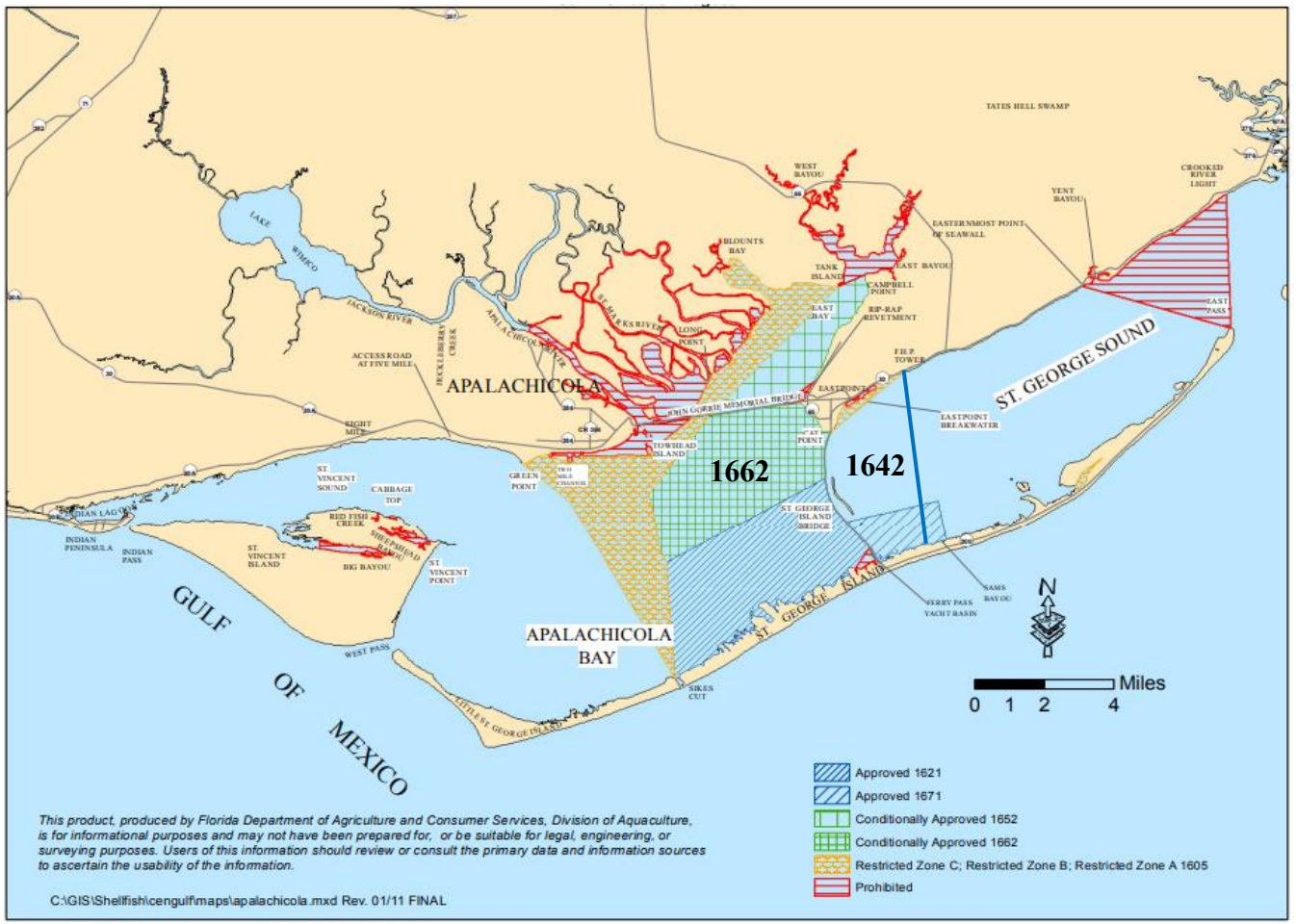

Fig. 3.1. Map of shellfish harvest areas in Apalachicola Bay, Florida. The two areas included in this study were FL 1642 and FL 1662. Source: Florida Department of Agriculture and Consumer Affairs.

2.3. ICP-MS analysis

Digestion and analysis were performed as previously described by Adams and Engel.[386] Briefly, approximately 0.5 g of homogenized tissue was digested in 5 mL of metals-free nitric acid. Samples were diluted to 100 mL with metals-free water, and the internal standards rhodium and lutetium were added prior to analysis of Cd and Pb using ICP-MS. The determination of metal concentrations (µg/g) was performed in duplicate following the described by Mudge *et al*. [387]. A laboratory reagent blank, a quality control sample, SRM 2976 Mussel Tissue (NIST, Gaithersburg, MD), and a calibration check standard (High Purity Standards, Charleston, SC) were analyzed after every ten samples.

2.4. EA-IRMS and LC-IRMS

Prior to stable isotope analysis, oyster soft tissues were lyophilized in microcentrifuge tubes for approximately 4 hours to remove any remaining water. The dried samples were placed in 2 mL polypropylene tubes containing four 3.2 mm chrome steel beads and pulverized for 5 min at a setting of 3450 rpm in a minibead beater (Biospec Products Inc., Bartlesville, OK, USA). This process creates more homogenous samples and facilitates the precise weighing in small aliquots, which leads to more reproducible results [328].

For bulk isotope analysis, samples of approximately 0.5 mg were weighed in tin capsules and placed in the instrument mentioned above. Isotopes were measured relative to the respective reference working gases (CO_2 and N_2, Matheson, Morgantown, WV). USGS-40 ($\delta^{13}C$= -26.39‰, $\delta^{15}N$= -4.52‰) and USGS-41 ($\delta^{13}C$= +37.63‰, $\delta^{15}N$= +47.57‰) (USGS, Reston, VA, USA) were used as two-point calibration standards to express the measured isotope values in the international scale against VPDB and Air, respectively [16]. Sulfanilamide was analyzed as a quality control every

12 samples. Isotope ratios were converted to the delta or per mil (‰) scale as suggested by IRMS guidelines [15, 20].

For CSIA, approximately 2 mg of each pulverized oyster was hydrolyzed in 6 M hydrochloric acid for 24 h at 110 °C in a vacuum oven to break the peptidic bonds. Afterwards, this mixture was filtered using a 0.45 µm PTFE syringe filter and evaporated to dryness at 60 °C under a stream of lab air. 1 mL of deionized water was used to re-dissolve the obtained dry residue, which was then filtered using a 0.45 µm PVDF syringe filter. Despite the destructive effect of HCl on some amino acids, the $\delta^{13}C$ values of the recovered ones are not considerably affected the hydrolysis conditions applied in this approach [61, 336, 388]. Amino acid chromatographic separation was performed in a Primesep A mixed-mode column (2.1 x 250 mm, 5 µm, 100 Å) (SIELC Technologies, Prospect Heights, IL, USA). For the first 18.7 minutes, mobile phase was composed by pure deionized water (at least 17.5 MΩ), followed by a successive decrease of pH through a gradient of pure deionized water with 0.03 M sulfuric acid. The flow rate of the mobile phase was 160 µL/min. Samples of commercial 17 standard amino acids (98–99% purity Sigma-Aldrich, St. Louis, MO, USA) were randomly analyzed throughout the sequences as a quality control for the chromatographic separation. All carbon-containing compounds eluted from the HPLC column were quantitatively oxidized to CO_2 in the LC-Isolink interface using wet chemical oxidation. This process occurred in the aqueous phase at 99.9 °C using sodium persulphate (100 g/L) and phosphoric acid (1.5 M). The resulting CO_2 was extracted from the cooled solution by a membrane exchanger, and any remaining water in the extracted CO_2 was removed in two water traps before the transfer to the IRMS system. Similar procedures using LC system for isotope analysis were previously reported [5, 61].

2.5. Data collection and statistical analysis

Isodat 3.0 was used as the data acquisition software, and IBM SPSS Statistics 25 was used in the statistical analyses. The normality of each oyster group was checked by the histograms and QQ-plots of residuals, the skewness and kurtosis of residuals and Shapiro–Wilk normality tests. For bulk isotope ratios, one-way analysis of variance (ANOVA) followed by Tukey's HSD post hoc test was performed to access the mean differences between each of the investigated harvest regions.

CSIA results were obtained for oysters collected in the Florida and Louisiana bays but not for Galveston and Copano bays. For this reason, we tested the multiple amino acid variables using one-way between-groups multivariate analysis of variance (MANOVA) followed by Games-Howell post hoc test, which does not assume equal variance of the data. General correlations and multicollinearity assessment were investigated using bivariate correlation coefficients. Linear discriminant analysis (LDA) using original discriminant rules and leave-one-out cross-validation (LOOCV) was performed to classify the oysters according to harvest area.

Statistical tests were performed on the bulk isotopic data ($\delta^{13}C$ and $\delta^{15}N$), Pb and Cd concentrations, and $\delta^{13}C$ values of nine amino acid peaks, including Asx, Glx, Ser, Gly, Val, Lys, Phe, Arg and Ile/Leu. Ile and Leu co-eluted, so the isotope ratio value for the co-eluting pair (Ile/Leu) was used as a variable in the model. The $\delta^{13}C$ values of aspartic acid (Asp) and glutamic acid (Glu) included a small contribution of asparagine (Asn) and glutamine (Gln), respectively, which were deaminated to their respective dicarboxylic acids during acid hydrolysis [61, 95, 337]. Because of deamidation, we reported these amino acid peaks as Asx and Glx.

3. Results and Discussion

3.1. Bulk $\delta^{13}C$ and $\delta^{15}N$ analysis

We tested Pb and Cd concentrations along with bulk and CSIA results of ten oyster tissue samples from each of the following areas: FL-1642 and FL-1662 areas (Apalachicola Bay); LA-28 area from Louisiana; Galveston and Copano bays, from Texas. The combined data was used to attempt the classification of samples based on their geographic origin. Bulk measurements of oyster tissues from each of the regions were normally distributed. Samples with missing data were removed from the analysis, making N= 9 or 10 samples per region. The mean $\delta^{13}C$ values ranged from -24.5‰ to -21.9‰, where LA 28 area gave the most depleted values and FL-1642 gave the most enriched values. For $\delta^{15}N$, values ranged from 8.8‰ to 15.1‰, where FL-1642 and Galveston bay were the most depleted and enriched, respectively (**Fig. 3.2**).

One-way ANOVA showed a statistically significant difference between the carbon and nitrogen bulk signatures of the harvest areas ($p<0.05$) (**Table A3.1**). Tukey's HSD post-hoc test (**Table A3.2**) revealed that the $\delta^{13}C$ values of FL 1642 oysters were significantly different from the samples from LA 28 ($p<0.05$) and FL 1662 ($p=0.06$), although the latter was different at the 94% confidence interval. On another hand, oysters from LA area 28 were significantly different from both Galveston and Copano bays ($p<0.05$). Oysters from Galveston and Copano bays were not distinguishable from each other. Regarding the nitrogen isotopes, all the areas were significantly different from Galveston bay ($p<0.05$), but not different from each other. Oyster tissues from Galveston area had a very enriched ^{15}N signature (~15‰) relative to the other bays. Galveston bay's $\delta^{15}N$ values, which exceed 10‰, indicate that Galveston bay receives an extra nutrient influx, most likely in the form of nitrate from some anthropogenic activity such as animal or sewage waste [389, 390].

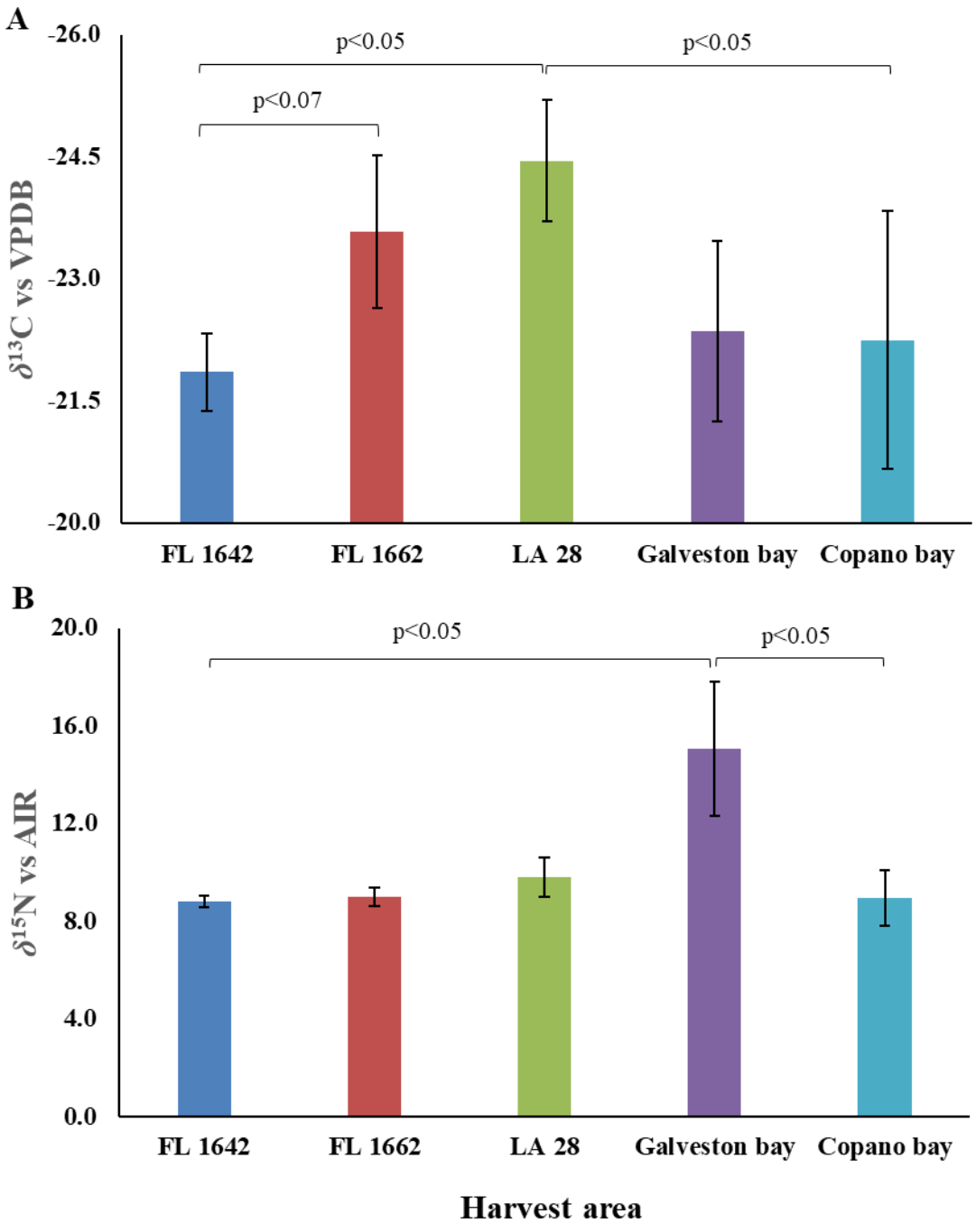

Fig. 3.2. A) Bulk δ^{13}C and **B)** δ^{15}N values of oyster tissue samples from five harvest areas. In A) LA 28 was significantly different from FL 1642, Galveston and Copano bays ($p<0.05$); FL 1642 statistically differed from FL 1662 ($p=0.06$). In B) Galveston bay was significantly different from all the other regions ($p<0.05$) (B). N=9 or 10 for each region. Error bars show the 95% confidence intervals of the means, assuming unequal variances.

Attempts to classify oysters based on geographic region using LDA of the bulk isotope ratio values showed that 54.2% of the samples were correctly classified to their harvest area after leave-one-out cross-validation (LOOCV) (**Table A3.3**). When using just Pb and Cd concentrations, the classification reached only 32% of accuracy, which is not much better than the random assignment probability of 20%. The combination of bulk isotope ratios with Pb and Cd concentrations increased the success of classification to ~63% after LOOCV. However, when using just Cd concentration along with the bulk isotope ratios, approximately 71% of the oysters were correctly classified to their geographic origin after LOOCV (**Table 3.1**). The first two canonical functions explained 92% of the total variance, which indicates that using a combination of bulk isotope ratios (of ^{13}C and ^{15}N) and the concentration of Cd shows better discrimination power to assign samples to specific sources than if working with only metal concentrations or only bulk isotope ratios.

Table 3.1. Linear discriminant analysis (classification) according to geographic origin using bulk $\delta^{13}C$ and $\delta^{15}N$ values and Cd concentration from whole-body oyster samples collected in different harvest areas.[a,c] N=9 or 10 for each region.

		Harvest Area	Predicted Group Membership					
			FL 1642	FL 1662	LA 28	Galveston bay	Copano bay	Total
Original	Count	FL 1642	9	0	0	0	1	10
		FL 1662	2	7	0	0	0	9
		LA 28	0	1	9	0	0	10
		Galveston bay	0	2	0	8	0	10
		Copano bay	3	0	2	0	4	9
	%	FL 1642	90.0	.0	.0	.0	10.0	100.0
		FL 1662	22.2	77.8	.0	.0	.0	100.0
		LA 28	.0	10.0	90.0	.0	.0	100.0
		Galveston bay	.0	20.0	.0	80.0	.0	100.0
		Copano bay	33.3	22.2	.0	.0	44.4	100.0
Cross-validated[b]	Count	FL 1642	9	0	0	0	1	10
		FL 1662	2	7	0	0	0	9
		LA 28	0	1	8	0	1	10
		Galveston bay	0	2	0	8	0	10
		Copano bay	3	1	3	0	2	9
	%	FL 1642	90.0	.0	.0	.0	10.0	100.0
		FL 1662	22.2	77.8	.0	.0	.0	100.0

	LA 28	.0	10.0	80.0	.0	10.0	100.0
	Galveston bay	.0	20.0	.0	80.0	.0	100.0
	Copano bay	33.3	11.1	33.3	.0	22.2	100.0

a. 77.1% of original grouped cases correctly classified.

b. Cross validation is done only for those cases in the analysis. In cross validation, each case is classified by the functions derived from all cases other than that case.

c. 70.8% of cross-validated grouped cases correctly classified.

3.2. Amino acid CSIA of $\delta^{13}C$

For multivariate analysis of CSIA data, the independent variable was the oysters' harvest area and the dependent variables were the $\delta^{13}C$ values of all the amino acid peaks. No serious violations were noted when testing the validity of the test assumptions. MANOVA results from the combination of the amino acids' carbon isotope ratios indicated a statistically significant difference between the difference harvest regions ($F=1.865$, $p=0.019$; partial eta squared=0.412), where the geographic harvest area explained 41% of the variance in the linear combination of $\delta^{13}C$ values of the amino acids. After further investigation of which amino acids were strongly influencing this model, Ser, Gly, Val, Ile/Leu, Lys, Phe and Arg were the most significant ($p<0.05$). However, we also noticed that the $\delta^{13}C$ values of Val, Ile/Leu, Lys, Phe and Arg were highly correlated among each other ($r>0.8$), indicating multicollinearity. Multicollinearity means that one of these variables can be used to predict the behavior of the others. The high degree of multicollinearity reduces the statistical power of any model that relies on mild correlation, like principal component analysis (PCA) and LDA, because too much variance is shared among the correlated variables [391, 392]. For this reason, we omitted the isotope values for Val, Ile/Leu, Lys, Phe and Arg from further multivariate analysis to avoid misinterpretation of results.

Games-Howell post hoc test revealed which harvest areas were statistically different from each other. Oysters from the two Apalachicola bays (FL 1642 and 1662) were significantly different at the 95% confidence level based on the $\delta^{13}C$ values of the two amino acids Ser ($p= 0.014$) and Gly ($p= 0.045$), but none of the other regions could be significantly distinguished using these two variables. To confirm this result, we built a binary logistic regression model using likelihood ratio method including the same variables, and the $\delta^{13}C$ values of Ser and Gly were significant predictors to distinguish between FL 1642 and FL 1662 areas at the 95% ($p=0.015$) and 90% confidence interval ($p=0.095$). The removal of those variables from the model were significant ($p=0.005$ and

p=0.025 for the $\delta^{13}C$ values of Ser and Gly, respectively), confirming the role of these terms in the prediction. We also investigated if the $\delta^{13}C$ values of amino acids would be helpful to the assignment of oysters to geographic harvest locations using LDA. Classification results of Asx, Glx, Ser and Gly $\delta^{13}C$ values (not highly correlated) showed that 65% of the samples were correctly classified based on the original rules of the method and only ~41% after leave-one-out cross-validation (LOOCV). After combining the isotope variables with respective Pb and Cd concentrations, the success rate improved to 77% based on original rules and 71% after LOOCV (**Fig. 3.3**), where 97% of the variance was explained by the first two canonical functions. Interestingly, correlation analysis did not reveal any significant linear correlations between metal concentrations and the isotope ratios ($p>0.05$). However, the first two linear functions used to discriminate between the regions were significant based on the Wilk's lambda significance test ($p<0.05$).

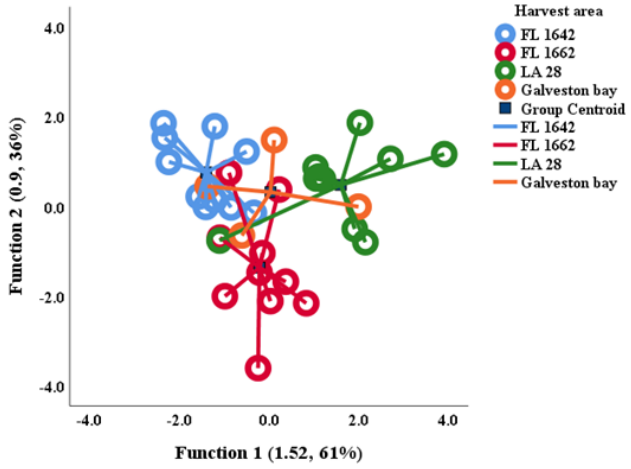

Classification Results[a,c]

		Region_code	Predicted Group Membership 1	2	3	4	Total
Original	Count	1	9	1	0	0	10
		2	1	8	0	1	10
		3	0	1	9	0	10
		4	2	1	1	0	4
	%	1	90.0	10.0	.0	.0	100.0
		2	10.0	80.0	.0	10.0	100.0
		3	.0	10.0	90.0	.0	100.0
		4	50.0	25.0	25.0	.0	100.0
Cross-validated[b]	Count	1	8	2	0	0	10
		2	1	7	2	0	10
		3	1	0	9	0	10
		4	2	1	1	0	4
	%	1	80.0	20.0	.0	.0	100.0
		2	10.0	70.0	20.0	.0	100.0
		3	10.0	.0	90.0	.0	100.0
		4	50.0	25.0	25.0	.0	100.0

a. 76.5% of original grouped cases correctly classified.

b. Cross validation is done only for those cases in the analysis. In cross validation, each case is classified by the functions derived from all cases other than that case.

c. 70.6% of cross-validated grouped cases correctly classified.

Fig. 3.3. Linear discriminant analysis (LDA) of CSIA δ^{13}C values of four amino acids (Asx, Glx, Ser and Gly), Pb and Cd concentrations from *C. virginica* oyster samples. The discrepancies between biased and unbiased classification rates indicate that a larger sample size would be more appropriate to improve the classification success based on harvest region.

These results support the assumption that the combinatory analysis of IRMS and ICP-MS variables strongly increases the correct discrimination of *C. virginica* geographic provenance. Regarding interpretation of the results, different nutritional conditions, temperatures, salinity and contaminants can all lead to different δ^{13}C values in the feedstock and fractionation of amino acids in the oysters [393]. Different micro-areas might exist within a bay depending upon the fresh water inflows and movement of sediments [394], making areas with similar water flow patterns and anthropogenic activities harder to differentiate. Despite the complexity our results showed that oysters sampled from within adjacent Apalachicola bay areas could be discriminated from each other. For example, the mean δ^{13}C values (± 95% confidence interval) for the amino acids Ser and Gly were -6.77 ± 1.55‰ and -8.67 ± 1.56‰ in area FL 1642, respectively, whereas the mean values in area FL 1662 were -10.97 ± 2.24‰ for Ser and -11.40 ± 1.47‰, for Gly. When comparing all the analyzed areas, FL 1642 and FL 1662 showed the most enriched δ^{13}C values of Ser and the most

depleted $\delta^{13}C$ values of Gly. From a regulatory point of view, an investigator could use these results to verify if the confiscated oysters were harvested in their reported area of origin, or an illegal area nearby. Based on the lower classification rates of only isotopes or Pb and Cd concentrations, it is unlikely that an unequivocal identification of the source could be achieved. The large variance in the bulk $\delta^{13}C$ data did not allow the separation within the Texas bays. However, compound-specific $\delta^{13}C$ values from these regions may provide a statistically significant difference, as seen for the Florida regions.

A few considerations must be taken when one is using these techniques. As discussed by Mudge *et al*. [387], shellfish elemental concentrations are highly affected by their site location, and also reflect seasonal and inter annual variability. Therefore, the proximity to waste disposal sites or changes in the oceanic currents can influence the ways in which shellfish are exposed to contaminants and nutrients. Our oyster samples included seasonal variance within each harvesting area, but it may be possible to achieve greater discrimination between areas if seasonal variations were controlled. To strengthen the predictive power of this approach, future studies should include a larger number of samples from each area, and a sufficient number of samples should be collected from each season to enable the effects of season to be controlled as a factor of isotopic variance.

4. Conclusions

This study examined the ability to discriminate the harvesting areas of *C. virginica* oysters by using contaminant heavy metals like Cd and Pb and bulk or CSIA measurements. Using leave-one-out cross validation of a database of ten oysters from four harvesting areas on the US shore of the Gulf of Mexico, harvesting areas could be correctly predicted with around 32% accuracy using the Cd and Pb concentrations alone, which is not much better than the random match probability of 20%. Using bulk $\delta^{13}C$ and $\delta^{15}N$ values, the reliability of predicting the harvesting area of oysters

increased to 50%, but only the oysters from Galveston bay could be differentiated from the other harvesting areas with significant confidence. The accuracy of harvesting area predictions improved to 65% using only the $\delta^{13}C$ values for amino acid peaks of Asx, Glx, Ser and Gly, and 71% by adding Cd and Pb concentrations. In summary, CSIA of the $\delta^{13}C$ values of amino acids in the oyster tissues yielded multivariate results for data analysis, which provided more accurate predictions than bulk ^{13}C and ^{15}N measurements. Site differentiation would certainly improve with a larger sample size and analysis of additional trace elements, such as nickel, silver, mercury, selenium, cadmium or zinc [386, 395-398], which were shown to be geographic markers for other marine organisms. The capability for high accuracy results and practical sample size requirements of this combinatory IRMS and ICP-MS approach make it a potentially valuable tool for oyster fisheries managers, wildlife and food safety enforcement officers, as well as to forensics and ecology research areas.

CHAPTER 4: COMPOUND-SPECIFIC ISOTOPE ANALYSIS OF HUMAN HAIR: METABOLISM, ROUTINE BEHAVIORS AND DISCRIMINATION BEYOND DIETARY FACTORS

Reproduced in part with permission from Mayara P. V. Matos and Glen P. Jackson, *Proceedings of National Academy of Sciences*, in preparation

1. Introduction

Isotope ratio mass spectrometry (IRMS) is a useful tool for the investigation of human origins and travel histories in forensic, archaeological and anthropological applications [10, 44, 50, 328, 399-402]. Most studies rely on dietary factors as the primary consideration for interpreting IRMS results, and metabolic processes are typically a secondary concern. In some studies, metabolic fractionation of isotope ratios has provided a source of considerable interference when interpreting stable isotope results [403-408], and few studies have investigated whether or not isotopes have an underlying role in defining biometric traits, such as sex. The goal of the present work is to provide insight into the relative contribution of behavioral and biometric traits on the isotope ratios of amino acids in human tissues. The present work focusses on human hair.

Scalp hair is a reliable investigative material because it is robust to diagenetic changes, easy and non-invasive to collect, it is quickly grown or regenerated, and it records a chronological relationship between the time of hair growth and the distance from the root [59, 409-411]. Another advantage to hair as a matrix is that because new hair is grown every day, the hair shaft does not suffer from isotopic turnover in the same manner as blood, muscle or bones [55, 412].

Hair is mainly composed by keratin, a family of proteins that account for 90-95% of hair dry mass [413]. The amino acids cysteine, serine, glutamic acid, threonine, glycine and leucine represent approximately 19%, 13%, 12%, 8% and 7% of the composition of hair shaft proteins, respectively [55], although the amino acids and co-enzymes required for keratin biosynthesis vary somewhat

during hair's growth cycle [327]. Carbon and nitrogen isotopic values for hair keratin are strongly related to diet, but are typically enriched by 1-2‰ and 2-3‰ than the food carbon and nitrogen, respectively [338, 343, 357, 410, 414] because the lighter isotopes are preferentially excreted during metabolism [80]. Additionally, hair growth can be influenced by the isotope ratios or concentration of the amino acids supplied by the circulatory blood [415].

Bulk measurements of tissues provide straightforward and robust isotope results, but the interpretation of its data is affected by the type of tissue, the physiological state of the organism and isotopic composition of the diet [340]. Bulk isotope analysis lacks the power to classify individuals into more specific groups, which can be limiting when studying organisms that constantly change resources and habitat [297], like humans. Analyzing stable isotopes from specific molecules instead of averaging isotopic signals from all contributing molecules in a sample improves the understanding of how isotope signatures are affected by metabolism. The molecular approach taken in compound-specific isotope analysis (CSIA) of amino acids provides unique isotopic values that can be linked to physiological states. Amino acids acquired only via diet are called essential, while those synthesized *in vivo* or routed (directly assimilated) into tissues from diet are called non-essential. The essential amino acids can be used as a proxy to infer human dietary sources whereas the non-essential amino acids reflect the metabolic status of a body. Importantly, some amino acids are defined as "conditionally" essential (e.g. Gly, Arg, Pro and Tyr) if their *de novo* synthesis depends on the availability of their natural amino acid precursors or on the physiological conditions of the organism [416-418].

Gas-chromatography combustion isotope ratio mass spectrometry (GC/C-IRMS) is the most commonly used separation method for CSIA of amino acids. One main disadvantage is that the derivatization steps required by this method introduce exogenous carbons to the amino acids, which

requires further individual correction factors to adjust the $\delta^{13}C$ values of each amino acid [419-421]. The separation of some co-eluting amino acids, and recovery of glutamine (Gln) and glutamic acid (Glu) was recently reported as positive side of NAIP derivatization method [388]. To avoid such complications, herein we used the alternative and well-stablished liquid chromatography-IRMS (LC-IRMS) method to perform CSIA of underivatized amino acids from scalp hair [61, 333, 334, 422, 423]. Our goal was to investigate different soft-biometric/endogenous factors and daily routine aspects as potential sources of isotopic variability between individuals.

2. Results and Discussion

2.1. Bulk isotope analysis (EA-IRMS)

Hair of 101 volunteers from around the US (30 males and 71 females) underwent $\delta^{13}C$ and $\delta^{15}N$ bulk isotope measurements. Some of these individuals self-reported dietary restrictions, such as vegan, ovo-lacto-vegetarian, pescatarian, paleo, low calorie or gluten-free diets. From these diet categories, only the vegans (average $\delta^{13}C$=-23.00‰, $\delta^{15}N$=6.97‰) clustered separately from the omnivorous population (average $\delta^{13}C$=-18.61‰, $\delta^{15}N$=9.67‰). Self-reported vegetarians gave average isotope values of -19.53‰ for carbon and 9.17‰ for nitrogen, which fell between vegans and omnivorous subjects, but not distinct enough to discriminate (**Fig. 4.1**).

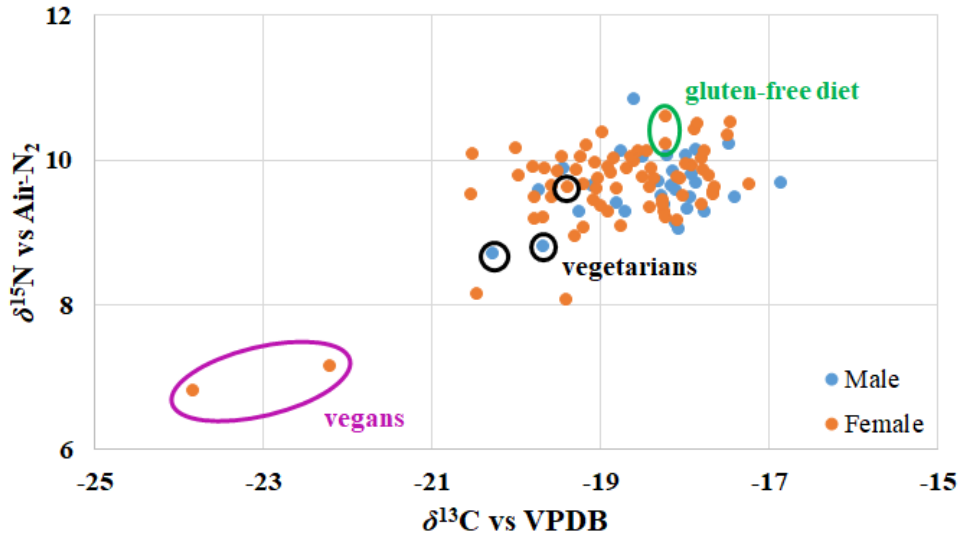

Fig. 4.1. Carbon and nitrogen bulk isotope measurements (EA-IRMS) of 101 subjects. Circled areas represent clustered groups of self-reported vegan, vegetarian or gluten-free dietary restrictions.

The hair of ovo-lacto-vegetarians is expected to be isotopically indistinguishable from omnivorous because the consumption of any animal-derived protein other than meat (e.g. eggs, milk) still reflects the isotopic signature of animal protein [410, 424]. We also confirmed the trend with δ^{15}N ratios, which increased from the hair of vegans to omnivorous [425, 426] due to the correlation with meat or marine fish dietary intake [427, 428]. True vegans had carbon and nitrogen values very distinct from the other groups, which is in accordance with the literature [410, 429]. We note that we do not know the length of time that each individual has maintained their dietary lifestyle, and it is possible that the dates of hair growth collected in the sampling procedure may have exceeded the boundaries of the claimed dietary habit. Despite these potential sources of variance, the two subjects under a gluten-free diet had very similar isotope values (average δ^{13}C=-18.22‰ and δ^{15}N=10.40‰). The other diet types presented no distinct pattern in this analysis.

Overall, females had average bulk isotope values of $\delta^{13}C$=-18.84‰ ± 0.25 and $\delta^{15}N$=9.62‰ ± 0.15 (95% confidence interval). After removing the two vegan subjects, females (n=69) had a bulk average of $\delta^{13}C$=-18.72‰ ± 0.19, $\delta^{15}N$=9.70‰ ± 0.11 (95% confidence interval). Males (n=30) were slightly more enriched in carbon having average bulk isotope values of -18.37‰ ± 0.28, but more depleted in $\delta^{15}N$ (9.61‰ ± 0.17). The difference between these groups was statistically significant for carbon (Student's t-test, p=0.045, two-sample assuming unequal variances), but not significant for nitrogen (Student's t-test, p=0.375, two-sample assuming unequal variances). Despite the significant difference between the sample means of males and females for ^{13}C, the significant overlap in the sample distributions infers that bulk isotope analysis of hair is unable to reliable differentiate the sex of an individual. Petzke *et al.* [425] reported females' hair to be more depleted than males for both bulk carbon and nitrogen isotopes, which is in general agreement with our findings. Interestingly, Kurle *et al*. [430] observed a higher bulk $\delta^{15}N$ value for females but almost no difference in the $\delta^{13}C$ values between the fur (and other tissues) of rats under a range of simulated omnivorous diets. They attributed the nitrogen differences to the longer growth period of male rats compared to females and that the retention of ^{14}N from dietary protein is usually more pronounced during growth periods or pregnancy [406]. In our results, the insignificant differences in nitrogen balance were probably masked by the presence of other variable and factors such as diet and age.

2.2. $\delta^{13}C$ CSIA of amino acids in hair

We analyzed a total of 101 subjects' hair via LC-IRMS. However, nineteen samples were not used because of the presence of matrix effects, which caused irregular, small, or co-eluting peaks for one or more amino acid. Of the 82 samples that were deemed acceptable in quality, 25 were males and 57 were females. The general characteristics of these individuals and the confidence interval of the measurements are shown in table A4.1. The measured amino acids were baseline

resolved: aspartic acid/asparagine (Asx), serine (Ser), glycine (Gly), valine (Val), tyrosine (Tyr), lysine (Lys), histidine (His), phenylalanine (Phe), and arginine (Arg). Methionine/cystine (Met/Cyt) and isoleucine/leucine (Ile/Leu) were measured as co-eluting pairs for a total of 11 variables (13 amino acids). The amino acids glutamic acid/glutamine (Glx), threonine (Thr), alanine (Ala) and proline (Pro) have been used in previous studies but were not used here because they either coeluted or were of insufficient abundance in many of the samples. Other amino acids were lost during acid hydrolysis (see SI text for details). By assuming complete oxidation in the Isolink interface, the relative peak areas of the CO_2 (*m/z* 44) of each amino acid were converted to the relative moles of carbon for each amino acid and ultimately to the relative moles of each amino acid in the original hair sample. Methionine oxidation could have occurred in these samples because oxygen was not removed from the vials before hydrolysis [61], so a major contribution of Cyt to the peak cannot be ruled out. This quantitative amino acid composition of hair worked as a second set of variables used to classify individuals into groups.

The essential amino acids were more depleted than the bulk $\delta^{13}C$ values of hair, but individually, Lys and His were more enriched in ^{13}C. They were also more depleted compared to non-essential amino acids. This general depletion pattern was observed in the comparison of single amino acids in British and American hair [414]. Non-essential amino acids followed the opposite trend; they were more enriched than the bulk $\delta^{13}C$ values, except for Tyr (**Table 4.1**). Overall, serine was the most enriched amino acid and phenylalanine was the most depleted. These patterns were the same for both sexes. The isotopic composition of amino acids with the lowest number of carbons, such as serine (3 carbons) and glycine (2 carbons), are more affected by metabolic events because transferring one carbon atom can significantly deplete or enrich the molecule in ^{13}C [431]. Others have reported glycine having the most enriched $\delta^{13}C$ value among all amino acids [62, 357, 425].

The observed enrichment of serine is supported by the fact that serine is a precursor for glycine [418]. In addition, 24% of α-amino N content of plasma is made of Gly and Ala, which suggests a central role of these amino acids in different metabolic routes [432]. Phe, Val and Ile/LeuIle/Leu shared the properties of being the most ^{13}C depleted amino acids. Plants also provide depleted values for Phe, Val and Ile/Leu because the many enzymes involved in their biosynthetic pathways are selective towards the isotopically lighter carbon isotope [357, 431]. Mammals cannot synthetize these three amino acids, so the isotopic imprint from the diet is reflected in the negligible fractionation from their ingested isotope values [425].

Table 4.1. Stable isotope signatures of bulk carbon and essential and non-essential amino acids in human hair. Met/Cyt were not included in this table because they are part of different amino acid categories and we analyzed them as one coeluted peak. Values are expressed as mean ± 95% confidence interval of the mean. N=81 (we did not have bulk isotope data for one of the 82 subjects)

Bulk $\delta^{13}C$ (‰)	**$\delta^{13}C$ Essential amino acids (‰)**		**$\delta^{13}C$ Non-essential amino acids (‰)**	
-18.68 ± 0.23	**VAL**	-23.82 ± 0.33	**ASX**	-16.40 ± 0.29
	ILE/LEU	-24.14 ± 0.28	**SER**	-9.46 ± 0.34
	LYS	-17.59 ± 0.55	**GLY**	-11.18 ± 0.41
	HIS	-10.78 ± 0.81	**TYR**	-23.02 ± 0.3
	PHE	-25.93 ± 0.49	**ARG**	-18.11 ± 0.32

Correlation analysis revealed significant positive correlations among the $\delta^{13}C$ values of different amino acids (**Table A4.2**), which were as good as r=0.707 ($p<0.01$) between Val and Arg. Some of the strong correlations have unidentified causes because, as exemplified for Val and Arg, they do not always possess direct metabolic relationships. For the amino acid quantities, correlations were not always positive, which makes sense given that the quantities were normalized relative to the sum of all the quantified amino acids. The coefficients of correlation ranged from r=-0.241

($p<0.05$) between Ile/Leu and Lys to $r=0.826$ ($p<0.01$) between Ile/Leu and Val (**Table A4.3**). The latter three amino acids (Ile, Leu and Val) are essential branched-chain amino acids (BCAAs) that share catabolic pathways [433], so the strong correlation is understandable. Some amino acids were expected to correlate but did not. For example, Phe is a metabolic precursor of Tyr [434], but their relative quantities in hair did not show a significant correlation.

Through one-way analysis of variance (ANOVA) and correlation analyses, several characteristic traits and biometric factors were found to contribute to the variance in the $\delta^{13}C$ values and relative quantities of amino acids in hair. For example, the variance of $\delta^{13}C$ values of essential amino acids is dominated by a subject's diet, so any small variance caused by another factor, such as phenotypic or metabolic effects, might not be observable relative to the effect of diet.

In another example, sex had the most significant effect on the relative quantities of amino acid in hair, and unless one accounts for the effect of sex on the relative quantities of amino acids, the smaller effects of other biometric factors (e.g. age) would be difficult to resolve. For these reasons, compound-specific isotope values were first corrected for the effect of diet before assessing the effect of secondary factors. To correct for the effect of diet, three different corrections were compared: 1) corrections based on meat intake in the self-reported questionnaire, 2) corrections based on the weighted average of the measured compound-specific $\delta^{13}C$ values of each individual, and 3) corrections based on bulk diet, which was assessed through off-line bulk $\delta^{13}C$ measurements of the same hair samples.

Preliminary assessments for normality, linearity, presence of univariate and multivariate outliers, homoscedascity, homogeneity of variance-covariance matrices, and multicollinearity were conducted prior to each statistical analysis to ensure no violation of each test's assumptions (SI text). Despite a total N=82 subjects, the number of subjects in each group changed depending upon which

biometric factor was under analysis. We assumed normality when there was a minimum of twenty subjects per group [435], and these assumptions were routinely supported by manual inspection. One 11-year-old boy was found to have very significantly different δ^{13}C values for Phe in his hair. His Phe δ^{13}C value measured -37.5‰, whereas the database values ranged from -21.6‰ to -30.3‰ (95% CI) with a mean value of 26.0‰. All the other amino acid δ^{13}C values and the concentration of Phe in his hair were within the normal range, so external contamination can be ruled out. The 11-year- had self-reported that he was diagnosed with autism and was taking prescription drugs including Risperidone. This medication, under the trade name Risperdal, is formulated with as much as 0.42 mg Phe per 1.5 mg dose of Risperidone (the dose taken by the subject).

The Phe in Risperdal is contained within the artificial sweetener aspartame, and the Phe content is significant enough to warrant a strong warning on the drug's label that patients with phenylketonuria should avoid the drug. Although we have not been able to analyze the subject's medication, we have a strong reason to believe that the depleted δ^{13}C value for Phe in this 11-year-old boy was caused by exogenous Phe from his prescription medication. Because of the unusual nature of his sample, this subject's data was not included in the 82 samples in the CSIA database. Of the remaining respondents, no correlation was found between the levels of artificial sweetener intake in their diets and Phe (or any other amino acid) δ^{13}C values.

2.2.1. Classification by sex

The presence of any relationship between sex and the 11 δ^{13}C variables was investigated through the Pearson product-moment correlation coefficients (**Table A4.4**). Following the strength of relationship guidelines proposed by Cohen [436], there was a small to medium positive correlation between sex and the δ^{13}C values of Gly ($r=0.355$, $p<0.01$), Val ($r=0.229$, $p<0.05$) and His ($r=0.232$,

p<0.05) in the original dataset. Correcting the $\delta^{13}C$ values for diet using each subject's bulk $\delta^{13}C$ measurements provided the strongest effect of sex $\delta^{13}C$ values. After correcting for bulk diet effects, the correlations between amino acids and sex improved for Gly (r=0.468, p<0.01), Val (r=0.457, p<0.01), and His (r=0.287, p<0.01), and became significant for Ser (r=0.338, p<0.01) and Arg (r=0.419, p<0.01).

We also tested if males and females differ in the carbon isotope values of their amino acids using a one-way between-groups multivariate analysis of variance (MANOVA). The independent variable was sex and the dependent variables were the $\delta^{13}C$ values of Asx, Ser, Gly, Val, Met/Cyt, Ile/Leu, Tyr, Lys, His, Phe and Arg. No serious violations were noted when testing the validity of the assumptions. Even without correcting for diet, a linear combination of all the amino acid's carbon isotope dependent variables indicated a statistically significant difference between males and females (F=3.594, p=4.5E-4; partial eta squared=0.361), where the sex of a donor explained 36% of the variance in the linear combination of $\delta^{13}C$ values. We further investigated which specific amino acids were dominant in the model. Table A4.5 shows that the $\delta^{13}C$ values reached statistical significance between males and females for Gly (F=11.562, p=0.001), Val (F=4.438, p=0.038) and His (F=4.541, p=0.036). The $\delta^{13}C$ value of Gly showed the strongest effect, with 13% of its variance explained by sex.

When comparing the three correction methods for diet, the method correcting for bulk $\delta^{13}C$ measurements provided the best improvement to the original (uncorrected) dataset results. After applying this correction, the sex of the donor explained 41% of the variance in the linear combination of $\delta^{13}C$ values (F=4.362, p=6E-5). Regarding the individual amino acids, the $\delta^{13}C$ values of Ser, Gly, Val, His and Arg were statistically significant different between males and females at α=0.05 (**Table A4.6**). To reduce the chance of type 1 errors, we applied a Bonferroni adjustment using an alpha

level of 4.5E-3 (original α=0.05 divided by the number of dependent variables analyzed) as a threshold for the significance [435]. The δ^{13}C values of non-essential amino acids Ser (F=10.167, p=0.002), Gly (F=22.119, p=1.07E-5) and Arg (F=16.829, p=9.86E-5), and the essential amino acid Val (F=20.873, p=1.78E-5) were responsible for the significant differences related to sex (**Table A4.6**). Gly and Val provided the largest F values, followed by Arg, suggesting they are the most valuable classifiers to predict the sex of a hair donor (**Fig. A4.1**).

The proportion of variance in the dependent variables (δ^{13}C values) that can be explained by the independent variable (sex) can be accessed in the effect size statistic provided by the partial eta squared values [392]. According to those value in Table S5, Gly has the largest effect size, followed by Val (partial eta squared=0.219 and 0.209, respectively), showing that approximately 22% and 21% of their variance was explained by sex, respectively. The difference in δ^{13}C mean scores for the two sex groups was between 1-2‰, where males were always more depleted than females in every statistically significant amino acid (**Table A4.7**). Because of the data correction, we can interpret these results are not being affected by food intake.

Linear canonical discriminant analysis (LDA) was also applied to classify individuals into males and females. According to the classification results, 81.5% of the subjects were classified into the correct sex based on the original rules of the method when using the δ^{13}C values of 13 amino acids corrected for bulk diet. Because LDA is a supervised classifier, we validated the results using leave-one-out cross validation (LOOCV) and obtained ~78% of classification accuracy using the same variables (**Table A4.8**). When using only the statistically significant variables from MANOVA (δ^{13}C values of Ser, Gly, Val, His and Arg), we obtained one Eigenvalue equal to 0.461 and a canonical correlation of 0.562. When inspecting the discrimination function coefficients obtained from this analysis, we observed that Gly has the greatest contributions to the discrimination score

(**Table A4.9**). In **Fig. 4.2** we observe that the results improved the classification to 83% correct based on the original rules and 80% based on LOOCV, showing 52% sensitivity (indication of false negatives) and 93% specificity (indication of false positives) after cross-validation.

A

Classification Results[a,c]

		Sex	Predicted Group Membership 1	2	Total
Original	Count	1	14	11	25
		2	3	53	56
	%	1	56.0	44.0	100.0
		2	5.4	94.6	100.0
Cross-validated[b]	Count	1	13	12	25
		2	4	52	56
	%	1	52.0	48.0	100.0
		2	7.1	92.9	100.0

a. 82.7% of original grouped cases correctly classified.

b. Cross validation is done only for those cases in the analysis. In cross validation, each case is classified by the functions derived from all cases other than that case.

c. 80.2% of cross-validated grouped cases correctly classified.

B

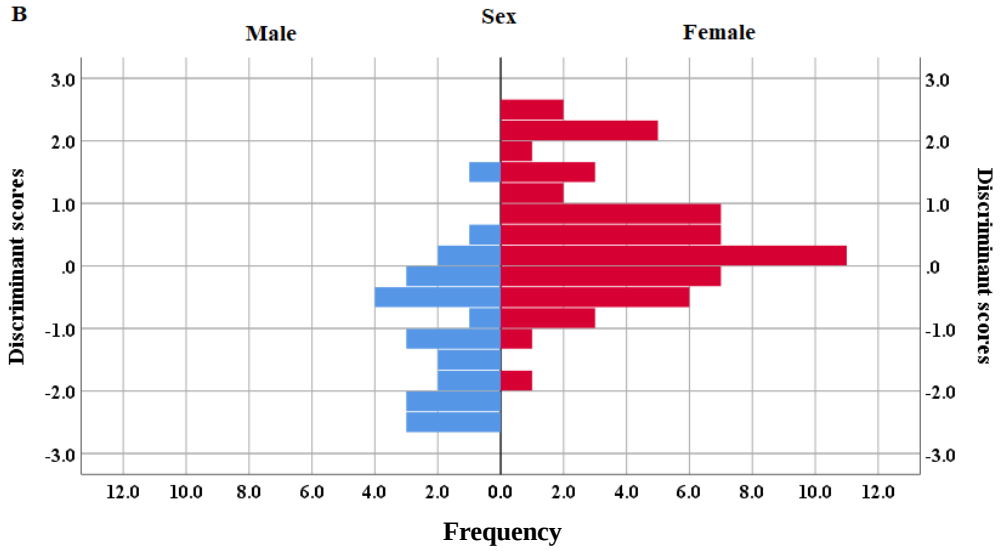

Fig. 4.2. A) Classification results from LDA of 81 hair samples (25 males, 56 females) according to sex. The variables were five amino-acid-specific $\delta^{13}C$ values (Ser, Gly, Val, His and Arg) corrected for the effect of diet. The leave-one-out cross-validation (LOOCV) accuracy for predicting sex is 80%. **B)** Frequency determination plot based on the discriminant scores for the LDA discriminant function.

Studies involving stable isotopes and binary human genders are often related to dietary differences linked to social identity status in the organization of ancient societies [437-440], but not many studies investigate inter-sex isotopic differences. In fact, the limited publications in this field suggest that sex differences do not interfere with the bulk isotope values [412, 441, 442]. Petzke *et al.* [425] reported the first results at the amino acid level, but again no differences were observed in the $\delta^{13}C$ and $\delta^{15}N$ values of individual amino acids from hair of a large cohort of German males and females. Herein, we found that different amino acids were not only isotopically different between sexes on the order of 1-2‰ but could be combined to predict sex with above 80% accuracy. Gly was, in general, one of the most ^{13}C enriched amino acids, and the most affected by sex. Interestingly, Morishita *et al.* [443] suggested that, in female rats, glycine is involved in the neural regulation of luteinizing hormone (LH) excretion. This hormone is directly related to male and female sex hormones, working in biochemical pathways that lead to the production and release of estrogen and testosterone. Considering that mammals share similar metabolic pathways, we hypothesize that a high demand for Gly to regulate the excretion of LH leads to an isotopic discrimination towards the light isotope, leaving this amino acid enriched in ^{13}C in human hair. In addition, glycine significantly improved menopause symptoms by showing a dose-dependent estrogen-like osteoprotective effect in *in vitro* and *in vivo* in menopausal animal models [444]. Hormonal factors strongly influence protein synthesis, and minimal changes are reflected in the hair due to the mitotically active cells in the hair follicle [413]. In this study we analyzed females with a broad age spectrum. If Gly was being recruited in the body or orally supplemented towards hormone regulation in those subjects, those changes would explain why this amino acid was more enriched in female subjects.

In addition to the study with $\delta^{13}C$, we investigated if the relative quantities of amino acids of each subject would also be helpful in discriminating the sex of a subject. After testing the validity of

the statistical assumptions, the quantities of Met/Cyt violated the multicollinearity assumption and were removed from further tests. This was unfortunate because cysteine is the most abundant amino acid in α-keratin hair [55] and is influenced by different biometric factors [445]. Therefore, here we show the results for the amino acid profiles of Asx, Ser, Gly, Val, Ile/Leu, Tyr, Lys, His, Phe and Arg (10 variables, 11 amino acids). When the relative abundance in the moles of amino acids are used, the term "mols" was included after each variable name to differentiate the relative quantities from the $\delta^{13}C$ values for each amino acid.

Sex explained 72% of the variance of a linear combination of 10 amino acid quantities (F=18.502, p=4.15E-16; partial eta squared=0.723). With the was reduced to six variables (Ser_mols, Val_mols, Ile/Leu_mols, Tyr_mols, Lys_mols and Arg_mols) the sex of a donor still explained 66% of the variance in the model (F=24.099, p=1.08E-15; partial eta squared=0.658). A Bonferroni adjustment (α=8.3E-3) revealed that only Val_mols (F=80.312, p=1.04E-13), Ile/Leu_mols (F=24.884, p=3E-6), Tyr_mols (F=19.816, p=2.7E-5) and Lys_mols (F=8.910, p=0.04) reached statistical significance between the two sex groups (**Table A4.10**). The average quantities of Val_mols and Ile/Leu_mols were more abundant in females than males, while Tyr_mols and Lys_mols were more abundant in males than females (**Fig. A4.2**). In this case, Val_mols had a very large F value, indicating the quantity of this amino acid in hair might be the most valuable classifier for sex. This was confirmed by its large effect size (partial eta squared=0.501), showing that approximately 50.1% of its variance was explained by sex. In a previous study by Rashaid *et al.* [445], Val was also more abundant in the hair of females and Try and Lys were more abundant in the hair of males. Rashaid *et al*. also reported Val was an important amino acid for sex discrimination, even though the subjects and analysis method were totally

independent; in the previous study, Rashaid *et al.* employed derivatization GC-MS to quantify the amino acids in the hair of 64 Jordanian subjects.

When attempting to predict the sex of a donor using the ten amino acid profiles, LDA showed ~94% of the subjects were classified into the correct sex based on the original rules when and the same value was obtained after LOOCV (**Table A4.11**). When using only the statistically significant variables from MANOVA (Val_mols, Ile/ Leu_mols, Tyr_mols, Lys_mols), we obtained one Eigenvalue equal to 1.335 and a canonical correlation of 0.756. According to the standardized discrimination function coefficients from this analysis, Val_mols provides the biggest absolute effect on the discrimination scores, followed by Ile/Leu and Tyr (**Table A4.12**). We show in Fig. 4.3 that discrimination based on only four variables was still very significant, being 89% correct based on the original rules and 89% based on LOOCV. This classification has higher sensitivity (80%), but equivalent specificity (93%) after cross-validation to the model using five δ^{13}C variables (**Fig. 4.2**).

A

Classification Results[a,c]

		Sex	Predicted Group Membership 1	2	Total
Original	Count	1	20	5	25
		2	4	53	57
	%	1	80.0	20.0	100.0
		2	7.0	93.0	100.0
Cross-validated[b]	Count	1	20	5	25
		2	4	53	57
	%	1	80.0	20.0	100.0
		2	7.0	93.0	100.0

a. 89.0% of original grouped cases correctly classified.

b. Cross validation is done only for those cases in the analysis. In cross validation, each case is classified by the functions derived from all cases other than that case.

c. 89.0% of cross-validated grouped cases correctly classified.

B

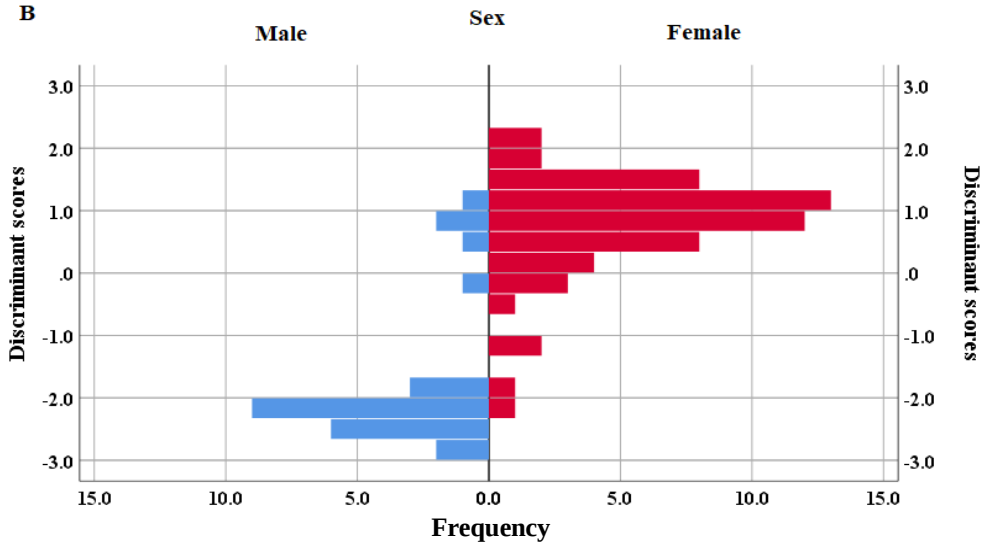

Fig. 4.3. A) Classification results from LDA of 82 hair samples (25 males, 57 females) according to sex. The variables were relative quantities of five amino acids Val, Ile/Leu, Tyr and Lys. The leave-one-out cross-validation (LOOCV) accuracy for predicting sex is 89%. **B)** Frequency determination plot based on the discriminant scores for the LDA discriminant function.

The literature on sex as an influencing factor in the composition of amino acids in human hair is rather convoluted. For example, some authors have found higher Cys/Cyt content in the scalp hair of males than females [445, 446], while others observed no relationship between this amino acid and the sex of the hair donors [447]. Additionally, male hair showed a higher concentration of Lys and Thr, while Phe was more concentrated in female hair r [445]. Despite the difference in AA composition, FTIR spectra of males and females' hair did not differ in secondary structure (α-helix and β-sheet) [448]. Whole-body leucine oxidation in muscle mass during exercise conditions was also reportedly distinct between males and females, where males oxidize leucine to a greater extent than females because males have greater muscle protein synthesis [449-451]. These results suggest that physical activity and different responses to fat and carbohydrate availabilities during endurance exercise might play a role on sexual dysmorphism [449]. Sex hormones also affect muscle protein metabolism [452]. In contrast, Dreyer *et al.* reported that muscle protein synthesis pathways are independent of sex [453].

In previous work, the quantities of Val, Phe and Pro were also reported as highly discriminating for sex [445]. In our study, the quantities of the essential amino acids Val, Ile/Leu, Lys and the conditionally essential Tyr were best for discriminating sex, where some of these had not been previously reported. Further research must be done to better understand which biochemical pathways influence the isotopic composition and concentrations of amino acid in human scalp hair, and if making comparisons based on hair from other mammals is a reliable extrapolation or not.

2.2.2. Age factor

We examined the relationship between the 11 δ^{13}C variables and age as a continuous variable or ordinal variable by grouping individuals into three arbitrary categories (≤25, 26-45 and ≥46 years old), respectively. The assumption of normality was violated when categorizing subjects because

there were less than 20 individuals in one of the age groups. Regarding age as a continuous variable, the only significant correlation found in the original (uncorrected for any effects) dataset was a small negative correlation with the δ^{13}C value of Lys (r=-0.256, p<0.05). After correcting the 11 δ^{13}C values for diet, the correlation between age and the δ^{13}C value of Lys increased to r=-0.312 (p<0.01) and the correlation between age and the δ^{13}C value of Ile/Leu became significant (r=0.245, p<0.05) (**Table A4.13**). Because sex has a significant effect on several of the δ^{13}C values, we also applied a correction for sex to the data that was corrected for diet. This correction for sex did not change the significance of the results relative to the diet-corrected data.

We also investigated the ability to predict age as a continuous dependent variable using the δ^{13}C values of the amino acids as multiple independent variables. No serious violations were noted after testing for normality, linearity, multicollinearity and homoscedasticity. The model with all 11 independent δ^{13}C variables explained approximately 26% of the variance in age, which exceeded the significance for correlation (p=0.023). Correcting for sex after the diet correction provided a slight improvement in the model, which then explained 28% of the variance (R^2=0.276, p=0.013). A second, simpler model using only five variables (Asx, Val, Ile/Leu, Lys and Arg) still explained 25% of the variance in age (R^2=0.251, p=4.4E-4), as shown in Fig. 4.4. Lys was the strongest contributing amino acid (Beta=-0.456, p=2E-4) at α=0.05 significance level, while Asx provided the second biggest contribution (Beta=-0.212, p=0.053). The standard deviation of this model's residual was 13.5, indicating that at the 95% confidence interval the predicted age of an individual is incorrect by about 27 years. This model does not have the precision required to be very useful as an investigative lead, but it can discriminate between the hair of individuals that are different in age by more than 27 years.

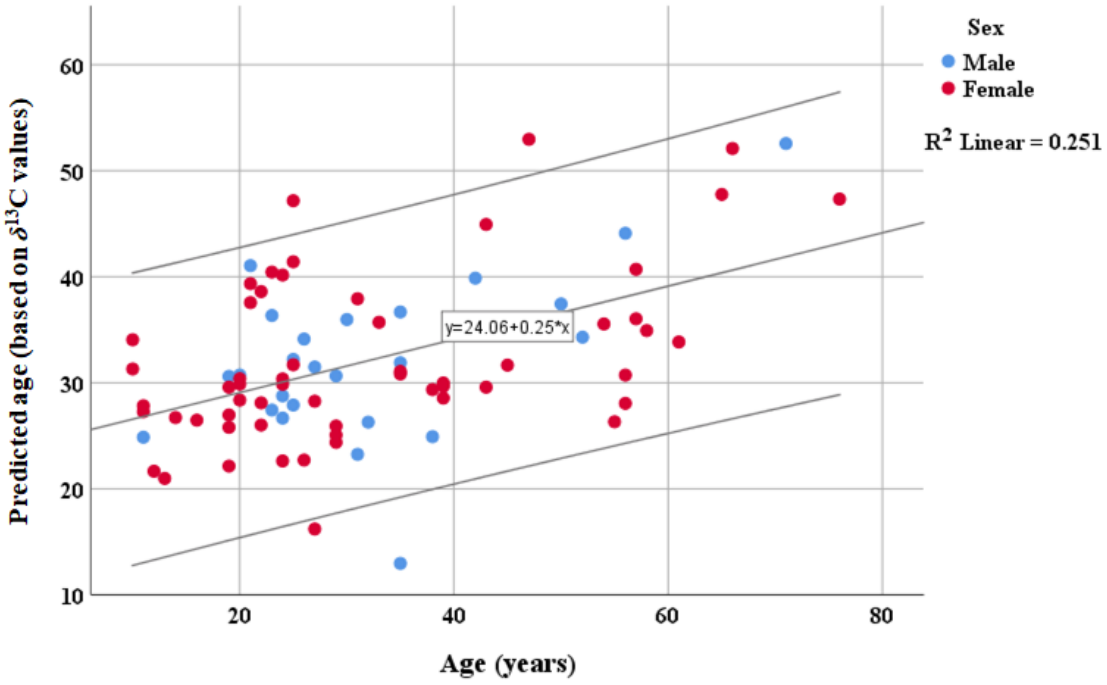

Fig. 4.4. Correlation between age and predicted age using a general linear model based on the $\delta^{13}C$ values of six amino acids (Asx, Val, Ile/Leu, Lys and Arg). This model explained 25% of the variance in age. The upper and lower lines show the 95% confidence interval for individual predictions.

The non-parametric Kruskal-Wallis test was used when age was separated into categories because we failed to meet the assumptions of normality and homogeneity of samples. This test revealed a statistically significant difference in the $\delta^{13}C$ values of Ile/Leu median ranks across the three age groups (≤25, N=38; 26-45, N=28; ≥46 years old, N=16), χ^2=8.959, p=0.011. A pairwise comparison using Dunn's post hoc test followed by a Bonferroni adjustment revealed that the $\delta^{13}C$ values of Ile/Leu were statistically distinct (p=0.008) between the age group 26-45 and ≥46 years old. The ≥46 years-old age group gave a more enriched median $\delta^{13}C$ value (-23.36‰, N=16) relative to the median of the 26-35-year-old group (-24.18‰, N=28). There was no evidence of a difference between the other age groups after the alpha adjustment. When working with the corrected (for diet) dataset, Kruskal-Wallis confirmed the result, showing $\delta^{13}C$ values of Ile/Leu as the only statistically

different across the three age groups (χ^2=8.697, p=0.013). Pairwise comparisons once again showed the difference was between the age group 26-45 and ≥46 years old (p=0.010), with the same pattern of ^{13}C enrichment for the older group (median=-23.81‰) compared to the younger age group (median=-24.29‰).

Another discriminant analysis was performed in attempt to classify individuals into the three age groups mentioned above. Using six $\delta^{13}C$ variables from the original dataset, 57% of the cases were correctly classified based on the original LDA rules and 52% after LOOCV. We then used the data corrected for diet and sex, reduced the number of $\delta^{13}C$ variables to three (Met/Cyt, Ile/Leu and Lys) and still reached 55% correct classification based on the original rules and 50% after LOOCV (**Fig. A4.3**). These classifications exceed the average random classification rate of 33.3%, but the classification rate is not sufficiently reliable as an investigative lead.

Not many studies have found associations between age and isotopic signature of mammalian tissues, but most studies have focused on bulk isotope measurements. Bulk $\delta^{13}C$ analysis of archaeological human bones with ages raging from newborn to around 60 years old indicated no evident age effect [442]. Similar results were found when testing bulk carbon and bulk nitrogen values of Japanese hair [441]. In the few cases where the authors reported an age effect on the isotope signatures of human samples, the interpretation was based on a correlation between age and dietary habits [454, 455]. Jackson *et al.* [61] reported the first attempt to classify individuals into age groups using compound-specific isotope analysis of amino acids in human hair. Their classification rate was 100% using a biased approach (in which samples in the database were predicted), but only reached 25% accuracy using LOOCV, which was not better than guessing. The small number of samples (20) in the previous study was insufficient to draw any meaningful conclusions.

Here, we increased the sample size from 20 to 82 subjects and increased the classification rate up to 50% using LOOCV. However, our linear combination of the predictor variables was still not successful in distinguishing the three age groups because of the small differences in the between-groups means, which are also a reflected of the small Eigenvalues associated with the two canonical functions (**Fig. A4.3**). Despite the poor classification rates, we did reveal new information about which amino acids correlate with age. Interestingly, essential amino acids were still the most affected by this factor, even after correcting for the effect of diet. These results suggest that age influences the mobilization of amino acids, which is reflected in significant enrichment in ^{13}C of certain essential amino acids with age.

In addition to the stable isotopes, we explored possible correlations between age and the quantities of amino acids. There were significant correlations between Ser_mols ($r=0.274$, $p<0.05$) and Gly_mols ($r=0.306$, $p<0.01$) and age as a continuous variable. Interestingly, we also observed a significant correlation with the arbitrarily-binned age categories for Asx_mols ($r=-0.226$, $p<0.05$), Ser_mols ($r=0.249$, $p<0.05$), Gly_mols ($r=0.237$, $p<0.05$) and Ile/Leu_mols ($r=-0.231$, $p<0.05$). Given that sex had known, measurable effect on the relative quantities of the amino acids, the models to predict age from amino acid quantities were examined before and after correcting for sex. In casework samples, the ground truth for the sex of a donor may not be known, so corrections for sex may not be possible. In applications were the sex of a donor is known, such as a mutilated victim, corrections for sex would be feasible.

To test if the quantities of amino acids would be able to explain any of the variance in age, the 11 variables were first assessed for validity. There were no major violations of the test assumptions, except for Met/Cyt_mols, which was again removed from the analysis. The general linear regression model with the relative mols of 10 amino acid variables explained approximately

27% of the variance in age (R^2=0.267, p=0.010). When the number of variables was reduced to the five variables with the greatest effect (Asx_mols, Ser_mols, Gly_mols, Ile/Leu_mols, and Tyr_mols), the simpler model still explained 22% of the variance in age (R^2=0.221, p=0.002). Tyr_mols provided the largest unique contribution to the model (Beta=0.358, p=0.009) at α=0.05, followed by Ile/Leu_mols (Beta=0.350, p=0.06), which was significant at α=0.1 significance level. The quantities of these two amino acids play a role in the age determination. The predicted age of an individual was incorrect by an average of 13.8 years based on the standard deviation of this model's residual, at the 0.05 significance level (**Fig. 4.5**). The model is more inaccurate after 40 years old. Intercept for the model was not significant when using α=0.05 (p=0.058).

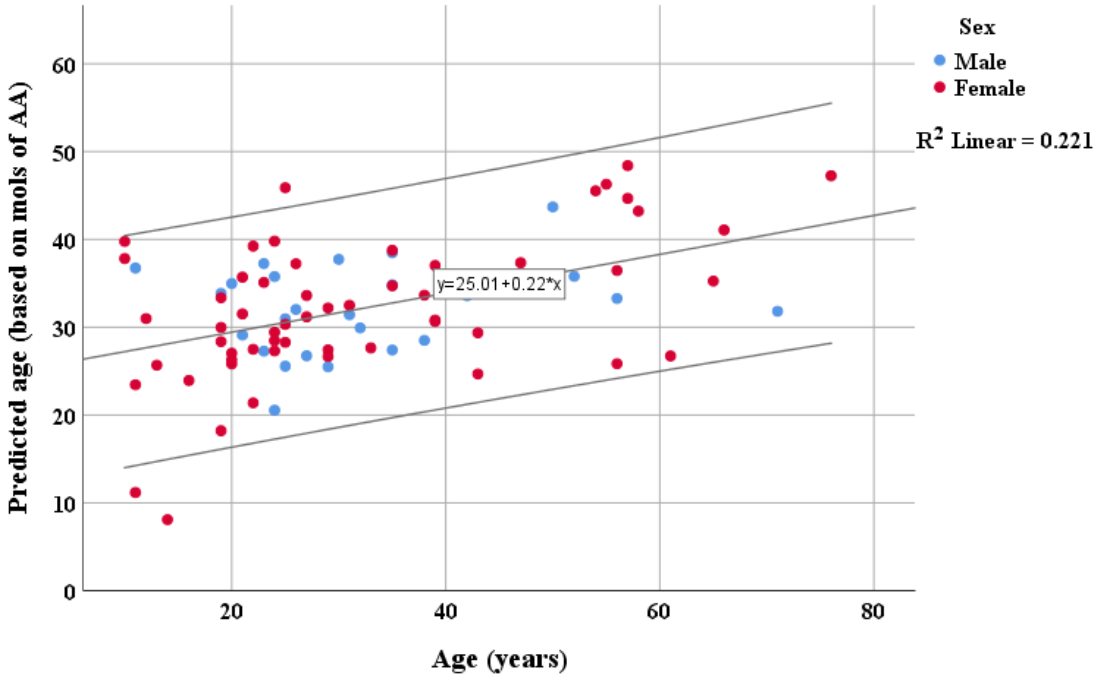

Fig. 4.5. Age prediction based on the relative molar quantities of five amino acid variables (Asx_mols, Ser_mols, Gly_mols, Ile/Leu_mols, and Tyr_mols). This general linear regression model explained 22% of the variance in age. The error bars show the 95% confidence interval for individual predictions.

When predicting the arbitrary age group of an individual using amino acid quantities, none of the amino acid quantities were statistically different across the three age groups at 95% significance level in the Kruskal-Wallis test, but some of them were significant at the 90% level. After a Dunn's post hoc test followed by Bonferroni adjustment, Ser_mols and Gly_mols were statistically different between the age groups ≤25 and ≥46 years old (p=0.065 and p=0.069). The difference in the medians was very small (3-5%): For Ser_mols, the median relative quantities were 3.91 for the ≤25 years-old group and 4.1 for the ≥46 years-old group. For Gly_mols, the median values for the <25-year-old and ≥46-year-old were 2.1 and 2.2, respectively. The variable Asx_mols was significantly different between the age groups ≤25 and ≥46 only at the 83% significance level (p=0.17), showing medians of 2.03 relative mols for the younger group compared to 2.01 relative mols for the older one. The variable Ile/Leu_mols was not able to discriminate between age groups up to the tested alpha level. Attempts to classify individuals into age groups was not very successful, reaching only 42.7% of cases after LOOCV due to the very low Eigenvalues associated with the two canonical functions (<0.3).

Rieck reported age-associated differences in the scalp hair of sisters between 1-24 years old [413]. Among other amino acids, Ser concentrations increased with age while Asp and Gly decreased with age. The differences were explained based on hormonal changes during puberty. We observed the same trend for Asp and Ser, but not for Gly, which was slightly more concentrated in the older group. In another study, Ala, Gly, Ile and Asp were more concentrated in people younger than 49 years old [445]. Herein we tested a much larger cohort and with groups covering more years of age than previous studies. Our age-dependent concentration differences were always for non-essential or conditionally essential between the youngest and oldest groups, which might also be mainly due to hormonal changes. Tryptophan (Trp) is another amino acid previously reported to change

concentration with age in human hair [413, 456], but we did not investigate Trp in this study. Ile/Leu was one of the only amino acid variables consistently related to age for both $\delta^{13}C$ values and quantities of amino acids.

Among other physiological functions, branched-chain amino acids (BCAAs), and especially leucine, are directly responsible for the stimulation of muscle protein synthesis and the reduction of protein degradation [457, 458]. During sarcopenia (progressive age-dependent loss of muscle mass), aging skeletal muscle might become less sensitive to the low physiological concentrations of BCAAs but it can be reverted by an oral supplement of leucine [459, 460]. We hypothesize that the recruitment of leucine to the skeleton muscle of older individuals was preferential toward the ^{12}C, which therefore left more enriched carbon signature in the hair of those subjects >46 years old.

2.2.3. BMI factor

For this factor we used values calculated from the self-reported questionnaire. We assigned subjects to four BMI categories: <18.5, 18.5-24.9, 25-29.9, and ≥30 that are related to the World Health Organization recommendations [461-463], where a BMI lower than 18.5 indicates a person is underweight; 18.5 to 24.9 is normal weight; 25 to 29.9 is overweight; and obese for BMI 30 or higher. We then tested the relationship between the 11 continuous $\delta^{13}C$ variables and BMI as a continuous or ordinal variable. Before correcting for diet, the $\delta^{13}C$ value of Asx was the only variable to correlate significantly with BMI (r=0.267, p=0.015). None of the corrections for diet or sex presented significant values at the 95% confidence level, but Asx and Arg were significant at the 90% confidence level. The sex correction on the diet corrected data revealed small positive correlations with BMI, with r=0.195 (p=0.079) for Asx and r=0.202 (p=0.068) for Arg. With an R^2=0.127, linear regression analysis confirmed these two amino acids had a weak correlation with

BMI (at α=0.1), but the combined model was not significant (p=0.520), so we cannot consider these results.

In reference [61], none of the individual amino acids could distinguish more than two BMI groups, but the $\delta^{13}C$ values of Thr could discriminate obese individuals from the other BMI groups. Threonine (Thr) was not investigated in this study because it tended to co-elute with glutamic acid (Glu) during the LC separation in many of our sample subjects. In the time allotted, we could not control the irregular retention of Thr, so we had to remove both amino acids from the analyses to keep the variables equivalent of all the subjects. When working with twenty female subjects, Jackson *et al*. [61] could classify individuals into correct BMI groups with 80% accuracy using LOOCV, where 97% of the variance was explained in one canonical function. In this larger cohort, we were unable to discriminate different BMI groups with such a high rate. Only 50% of the subjects were correctly classified using LOOCV.

Regarding the amino acid composition profile, Tyr_mols showed the only correlation with BMI as a continuous variable (r=0.288, p=0.009) and in BMI as categories (r=0.219, p=0.048). Normalizing for sex slightly improved the correlations for Tyr_mols with BMI as a continuous variable (r=0.297, p=0.007) or when binned (r=0.225, p=0.042). In the linear regression model, the linear combination of variables explained ~23% of the variance in BMI (R^2=0.234, p=0.030). Asx_mols (p=0.003) and Tyr_mols (p=0.001) were statistically significant predictors at the 95% CI, while Ile/Leu_mols and Arg_mols were significant at the 90% confidence level (p=0.082 and p=0.086, respectively). Tyr_mols provided the highest unique contribution to the model (Beta=0.662), followed by Asx_mols (Beta=-0.532). The significance of the model and useful variables did not change after correcting data for sex. When reducing the number of variables to four, we were only able to explain 13% of variance in BMI (R^2=0.131, p=0.027).

Only Tyr_mols was statistically different across the four BMI groups at 85% significance level in the Kruskal-Wallis test (χ^2=5.676, p=0.128). None of the variables were significant above this threshold. After a Dunn's post hoc test followed by Bonferroni adjustment, a modest difference was revealed to be between individuals with normal weight and obese (p=0.107), where the quantity in relative mols was higher for obese individuals (median=0.562 and 0.684 for normal and obese BMI, respectively). Elevated serum Tyr concentration was reported as one of the early biomarkers for adults (25-49 years old) prone to metabolic syndrome (e.g. obesity and insulin resistance (IR)) [464]. Here, Tyr concentration in hair of normal people was also very small, which indicates further studies should be performed before taking conclusions about this result and obesity. Discriminant analysis reached just 52.4% success in predicting BMI group membership after LOOCV (**Fig. A4.4**).

2.2.4. Effect of hair treatment

Twenty-six out of the 101 total subjects reported doing one of the following hair treatments: bleaching (5), chemical straightening (1), or coloring (25). All individuals were females. Subjects who bleached their hair also did coloring, but the opposite was not true. None of the participants reported doing baldness or Perm treatments. The two self-reported vegans also colored their hair. In table A4.14, we show that the different hair treatments did not show a significant difference among themselves in the bulk isotope values (Student's t-test, p=0.141 and p=0.876 for bulk carbon and nitrogen, respectively). There was also no statistical difference between females who bleached/died their hair and the ones who did not (Student's t-test, p=0.912 and p=0.173 for bulk carbon and nitrogen, respectively) (**Table A4.15**), indicating that bulk δ^{13}C and δ^{15}N values were unaffected by these treatments.

We also tested the population of females with no missing values for any of the amino acid isotope variables that could have been affected by a hair treatment. We observed no statistical

difference between the groups with (N=20) or without (N=37) hair treatment (**Table A4.16**). However, at the amino acid composition level, the original quantity of Gly in hair was the only amino acid statistically different between those group (Student's t-test, p=0.028) (**Table A4.17**). Some authors have described that cosmetic procedures in hair (chemical bleaching, alkaline straighteners, hair dyes, etc) can alter both C/N ratios and isotope values because these processes often cause fragmentation of proteins and conversion of amino acids to derivatives [465-467]. Cysteine is usually cited as the most affected amino acid, but we did not observe the same in our results because the Met/Cyt variable did not meet the multicollinearity assumptions.

2.2.5. Effect of alcohol consumption

We decided to test if alcohol consumption would also affect the compound-specific isotope data. Seventy-nine out of the 82 subjects reported their alcoholic drinking frequency. Subjects (number of subjects listed in parenthesis) were divided into five arbitrary categories based on their self-reported information: "drink daily, heavily" (1), "drink daily, some" (7), "drink weekly" (16), "drink occasionally" (31), "never drink" (24). Surprisingly, the isotopic ratios of some amino acids correlated with drinking habits. In the original dataset, the δ^{13}C value of Met/Cyt gave the highest negative Spearman correlation (r=-0.451, p<0.01), followed by Ser (r=-0.364, p<0.01) and Ile/Leu (r=-0.276, p<0.01). We used data normalized for sex and diet to access which correlations were related only to drinking frequency. The correlations between the δ^{13}Cvalues of Ser (r=-0.302, p<0.01) and Met/Cyt (r=-0.280, p<0.05) and alcohol consumption were confirmed.

Only one person claimed to a be a heavy alcoholic drinker, so we removed this category from further analysis to avoid statistical differences due to significant sample size differences. The Kruskal-Wallis test was again used because some samples failed the assumptions for a parametric test when working with categories. The only statistically significant differences across the four

drinking habits was for $\delta^{13}C$ value of the non-essential amino acid Ser (χ^2=8.593, p=0.035). After Dunn's post-hoc test and Bonferroni alpha adjustment, the difference between individuals with a daily drinking habit and the ones who never drink was significant at the 90% confidence level (p=0.089). The medians depicted a linear depletion of ~1.15‰ for $\delta^{13}C$ value of Ser as the frequency changed from daily drinking (median=-8.69‰) to no drinking (median=-9.83‰). Unfortunately, LDA was not successful in classifying individuals, showing only 50% of cases correctly classified into the drinking category according to the original rules, and ~49% after LOOCV. None of the quantities of amino acids were significant in any of the statistical tests.

The direct anti-alcohol effects of Ser and Gly were shown by Blum *et al.*[468] in an ethanol-induced animal model. The authors suggested the inhibitory effect was likely due to the role these amino acids play on the gastrointestinal tract, retarding ethanol absorption. L-serine was also shown to be a potential candidate to treat alcoholic fatty liver, an early-stage disease induced by chronic ethanol consumption [469]. The ^{13}C enrichment of Ser in the hair of daily alcoholic drinkers might reflect the preferential allocation of carbon-depleted molecules to delay alcohol absorption in the stomach. Further research with a large sample size of heavily alcohol drinkers will provide more conclusive evidence about the influence of this factor on isotope ratios.

2.2.6. Effect of sunlight exposure

We questioned the subjects about how much sunlight they were typically exposed per day. We divided the answers into four groups: ">2 h/day", "1-2 h/day", "<1 h/day" and "almost never". In the original dataset, we observed small but significant correlations between the $\delta^{13}C$ values of Tyr (r=0.252, p<0.05) and Lys (r=-0.335, p<0.01). After keeping sex and diet constant, the correlations changed to r=0.324 (p<0.01) for $\delta^{13}C$ of Tyr and r=-0.252 (p<0.05) for Lys. New correlations also appeared for the $\delta^{13}C$ of Ser (r=-0.248, p< 0.05) and Arg (r=0.271, p<0.05). Interestingly, when

attempting to find differences between groups, the $\delta^{13}C$ values of Ile/Leu, Lys and His showed a significant difference across the four groups in Kruskal-Wallis test at the 95% CI, while Ser and Tyr were significant at the 90% CI. However, there was no clear pattern of ^{13}C enrichment in these amino acids, suggesting that the statistical significance was probably not attributed to sunlight exposure.

Regarding the quantity of amino acids, the only significant correlation was found for Phe_mols ($r=-0.304$, $p<0.01$). When data was corrected for sex, the negative correlation was kept significant ($r=-0.294$, $p<0.01$). Overall, the number of Phe molecules in the scalp hair of the subjects was very small (<1 mol). This result was expected because ultraviolet radiation from sunlight exposure degrades aromatic amino acids via photo-degradation [467, 470], and most American individuals do not cover their heads when outdoors. It also supports the findings from Rashaid *et al*. [445], where hair of Jordanian females showed high abundance of Phe because the wearing of hijab avoided Phe degradation. LDA showed that 54% and 46% of the subjects were correctly classified into the sunlight exposure after LOOCV for isotope variables and quantities of amino acids, respectively. These values beat the random guessing probability of 25% but are still not sufficient for proper discrimination.

3. Conclusions

We performed bulk isotope analysis and amino acid compound-specific isotope analysis in 13 amino acids (individual and co-eluting pairs) from scalp hair of subjects from the US. We report the first successful classification of individuals based on sex using compound-specific isotope data and profiling of amino acids in human hair. Other soft-biometrics also presented correlations with the analyzed variables, but with lower classification rates. Alcohol consumption frequency was reflected in the isotope ratios of hair. After correcting the data for diet and sex, we did not observe

any statistically significant correlations between the $\delta^{13}C$ of amino acids and respective quantities for other factors such as smoking habits and consumption of soda/ sweeteners (data not shown).

4. Materials and methods

4.1. Study participants

After obtaining an approval from the WVU Institutional Review Board (nº 1702466936R001), we made a website page specifically to recruit volunteers willing to donate hair samples to this project. We distributed participation requests via a variety of distribution sites, including media blasts, Facebook, word-of-mouth, emails and flyers at conferences. We then mailed each volunteer an envelope containing informed consent forms, project information, instructions on how to collect hair and collection bags, and a questionnaire of approximately 45 questions about their hair treatments, physical health, medical history and diet. Individuals were asked to provide a minimum of 0.1 g of hair (for example: >30 hairs of 24" length or >60 hairs of 12" length). The subjects returned their signed consent forms, hair samples and completed questionnaires in pre-paid return envelopes sent by our group. Pregnant, cognitively impaired or incarcerated subjects were not included in this study. Pregnancy is known for affecting isotope balance [406, 407] and would be an extra confounding point among the other metabolic factors. We would not be able to access if cognitively impaired individuals fully understood the questionnaire or answered the questions based on their own choice. Finally, the recruitment of incarcerated subjects could lead to legal issues.

4.2. Sample preparation and Instrumental analysis

4.2.1. Hair cleaning

Each hair sample was soaked and vortexed in a solution of methanol: acetone: chloroform (1:1:1) (V:V:V) for 30 minutes, followed by two series of sonication in deionized water (30 min each) [61, 419, 425]. This procedure ensured the removal of external contaminants, such as lipids.

Following sonication in deionized water, the samples were dried in a vacuum oven at 60 °C for 4 hours. The previously dried samples were pulverized by placing them in a 2 mL polypropylene tube containing four 3.2 mm chrome steel beads for 6 min at 3450 rpm in a minibead beater (Biospec Products Inc., Bartlesville, OK, USA). Pulverized samples are more homogenous and easier to weigh precisely in small aliquots, which leads to more reproducible results [328].

4.2.2. Chemicals

Isotope standards USGS-40, USGS-41, USGS-42 and USGS-43 were purchased from USGS (Reston, VA, USA). Sodium persulfate (99% purity), Orthophosphoric acid (>85%purity), sulfuric acid (>95% purity), and amino acids (98–99% purity) and sulfanilamide were purchased from Sigma-Aldrich (St. Louis, MO, USA). Ultra-high purity gases were purchased from Airgas (Morgantown, WV): >99.9999% He, 99.999% N2, 99.997% CO2, and 99.999% O2.

4.3.3. EA-IRMS

Bulk isotope ratio measurements were performed to investigate $\delta^{13}C$ and $\delta^{15}N$ values. For this analysis, samples of approximately 0.5 mg were weighed in tin capsules and placed in a Thermo Flash HT Plus elemental analyzer (EA) coupled to the Thermo Delta V Advantage isotope ratio mass spectrometer via a Conflo IV interface. All isotopes were measured relative to the respective compressed working gas (CO_2 and N_2). USGS-40 ($\delta^{13}C$=-26.39‰, $\delta^{15}N$=-4.52‰) and USGS-41 ($\delta^{13}C$=+37.63‰, $\delta^{15}N$=+47.57‰) were used as two-point calibration standards to express the measured isotope values in the international scale against VPDB and Air, respectively, using a two-point calibration curve [16]. Triplicates of USGS-42 ($\delta^{13}C$=-21.09‰, $\delta^{15}N$=+8.05‰) and USGS-43 ($\delta^{13}C$=-21.28‰, $\delta^{15}N$=+8.44‰) were used to ensure the precision of EA measurements was within acceptable 95% confidence intervals. For quality control of the instrument stability, aliquots of the organic compound sulfanilamide ($C_6H_8N_2O_2S$) were run in triplicate every after 12 samples. The

following equation was used to convert isotope ratios to the delta scale or per mil (‰) [15, 20], where the ratio of the heavier over the lighter isotope for sample was defined as R_{sample}, and the abundance ratio of the corresponding international standard as $R_{standard}$.

$$\delta_{\text{sample}}\,(‰) = \left(\frac{\text{R sample}}{\text{R standard}} - 1\right)$$

4.3.4. LC-IRMS

For CSIA an aliquot (approximately 2 mg) of each pulverized hair sample were hydrolyzed in 6 M hydrochloric acid for 24 h at 110 °C in a vacuum oven. The mixture was then filtered using a 0.45 μm PTFE syringe filter and evaporated to dryness at 60 °C under a stream of lab air. The obtained dry residue was re-dissolved in 1 mL deionized water and filtered using a 0.45 μm PVDF syringe filter. Despite being the most common protocol to break peptidic bonds, acid hydrolysis can also be destructive to some AAs. The literature reports the decomposition of tryptophan and cysteine, oxidation of methionine, partial hydrolysis and low recovery of serine and threonine, loss of histidine and arginine that occurred during the process [471-474]. The reproducibility of studies that require recovery of individual AAs might be affected by these events. The $\delta^{13}C$ values of aspartic acid (Asp) and glutamic acid (Glu) included a small contribution of asparagine and glutamine, respectively, which were deaminated to their respective dicarboxylic acids during acid hydrolysis [61, 95, 337]. Because of this, we reported these AAs as Asx and Glx. Importantly, the hydrolysis conditions applied herein do not have a considerable effect on the ^{13}C enrichment, meaning that the $\delta^{13}C$ values of the recovered amino acids are not affected [61, 336, 388, 471].

For the analysis, we used a Dionex ICS5000 ion chromatography system (ICS) (Dionex, Sunnyvale, CA, USA) coupled through an LC-Isolink interface to a Delta V Plus isotope ratio mass spectrometer (Thermo Fisher Scientific, Bremen, Germany). AAs chromatographic separation was performed in a Primesep A mixed-mode column (2.1 x 250 mm) with a stationary phase particle size

of 5 µm, pore size 100 Å (SIELC Technologies, Prospect Heights, IL, USA). The mobile phase initiated with pure deionized water (at least 17.5 MΩ) for the first 18.7 minutes, followed by a successive decrease of pH through a gradient of pure deionized water with 0.03 M sulfuric acid. The flow rate of the mobile phase was 160 µL/min, which was the best result of the optimization performed on the method already reported by our group [61]. We ran samples of commercial 17 standard amino acids randomly spaced throughout the sequences as a quality control for the chromatographic separation. Using wet chemical oxidation, all carbon-containing compounds eluted from the HPLC column were quantitatively oxidized to carbon dioxide (CO_2) in the LC-Isolink interface. This process occurred in the aqueous phase at 99.9 °C using sodium persulphate (100 g/L) and phosphoric acid (1.5 M). The resulting CO_2 was removed from the cooled solution by a membrane exchanger, and remaining water was removed in two water traps before the transfer to the IRMS system. Similar procedures using LC system were previously reported [5].

4.3. Data analysis

For both EA and CSIA, Isodat 3.0 (Thermo Scientific, Waltham, MA) was used as the data acquisition software, and IBM SPSS Statistics 25 was used for the statistical analyses. Information collected in the questionnaires provided by each human subject allowed us to group individuals based on different biometric factors. The assumptions of normality, linearity, univariate and multivariate outliers, homogeneity of variance-covariance matrices, homoscedascity and multicollinearity were tested prior to each statistical analysis for compound-specific data.

Normality of each group was checked by the histograms and QQ-plots of residuals, skewness and kurtosis and Shapiro–Wilk normality test. Even though our total sample size was composed by 82 subjects, the number of subjects in each group changed depending upon which biometric factor was under analysis. We assumed the groups were normally distributed if there was a minimum of 20 subjects per group [435]. Scatterplots were used to test for linearity. Univariate outliers and

multivariate outliers were accessed via comparison of mean and 5% trimmed mean, box and whiskers plots and Mahalanobis distance, respectively. Homogeneity of variance-covariance matrices was tested using Box's test and when the results violated the test, we checked the more robust test Pillai's trace. This test also indicates if the linear combination of dependent variables generates any statistically significant difference among the tested groups. For multicollinearity, we analyzed if any of the variables showed correlation around 0.9 in the correlation matrix, which would be a reason for concern. In addition, we also checked values of Tolerance and Variance inflation factor (VIF) to ensure no multicollinearity was interfering in the results. The Levene's test for homoscedascity (equality) of variances was also performed before multivariate analysis of variance (MANOVA). If this assumption was violated, we performed the more robust Welch's test on the variables under question. According to the assumptions testing results, an appropriate parametric or nonparametric test was performed. In this study we used One-way ANOVA or MANOVA followed by Tukey HSD or Games-Howell test, independent t-test (Student's t-test), linear regression and linear discriminant analysis. Mann-Whitney U test, and Kruskal–Wallis test followed by Dunn's post hoc test were performed as nonparametric alternatives when samples were dichotomous or had three or more groups, respectively. Pearson correlation coefficient was used when the biometric factor was a continuous variable or had groups with >20 subjects (e.g. sex). Factors (e.g. age) in binned categories were tested via Spearman's rho correlation. A single factor ANOVA test was performed to test the null hypothesis that each δ^{13}C value or quantity of AA has no significant difference between groups using a same fixed factor (e.g. one of the biometric factors). Furthermore, MANOVA was used to test the same hypothesis but using more than one dependent variable at once. Furthermore, independent samples t-test (Student's t-test) and post-hoc pairwise comparisons (e.g. Tukey's HSD test or Games-Howell test) reduced the frequency of type 1 errors by comparing the

mean isotope ratios for individual groups when equal variances were assumed or not assumed, respectively. In both cases we applied an extra layer of correction to reduce type 1 errors via a Bonferroni adjustment. A cut-off significance value α=0.05 was used for all statistical tests, unless otherwise mentioned. A descriptive analysis with standard statistical parameters (number of samples, mean or median, standard deviation, standard error, 95% confidence interval) was also performed.

In prior research from our group, ANOVA of bulk isotope ratios of $\delta^{13}C$ and $\delta^{15}N$ values performed on 20 female Jordanian subjects indicated that isotope ratios could, to some extent, be used to differentiate hair of individuals [61]. Similarly, the same statistical tests were performed for CSIA. Single factor ANOVA was used to determine significant differences for an amino acid—which is a unique factor - whereas multiple factor ANOVA presented interactions between the different groups of organisms (various factors). MANOVA tested for interactions between the diverse response variables (amino acids). Also, linear discriminant analysis (LDA) using original discriminant rules and leave-one-out cross-validation (LOOCV) were applied to classify subjects into prior groups more accurately.

CONCLUSIONS AND FUTURE WORK

The ability to reveal the isotopic variations in chemically identical natural and manufactured materials, and investigate the source and history of a sample, has made stable isotope analysis (SIA) an important tool in disciplines including in forensic science, biology, archaeology and geochemistry. Here, we demonstrated the use of IRMS to investigate the isotope profiles of different proteinaceous samples for forensic applications.

IRMS is practiced in several forensic and research labs across the world, however most studies employ bulk isotope analysis as the primary way to perform isotope measurements because bulk analyses are so robust and easy to perform. Even though CSIA is gaining more popularity in the IRMS community, its application in forensic science is still in its early stages. In this dissertation, we showed the benefits and challenges of using CSIA as a methodology with capabilities that exceeds the limits of bulk IRMS analysis.

Whereas CSIA has some advantages over bulk analysis, it has some downsides. In the case of protein analysis, one limitation is that the acid hydrolysis step causes variable degradation of the amino acids cysteine, methionine, tyrosine and tryptophan. Also, asparagine and glutamine are converted to their respective acids, aspartic acid and glutamic acid. Even though acid hydrolysis is a major source of variability in the sample preparation, standard acid hydrolysis (110 °C for 24 h) is provides more efficient recoveries of amino acids relative to fast acid hydrolysis (150 °C for 70 min) [388]. Microwave-assisted acid hydrolysis (MAAH) could provide an improvement for future work because it is faster and equally efficient as standard heating methods [475, 476]. Another downside of CSIA is the instability of Thermo Scientific's Isolink interface and its software Isodat. Thermo's system is highly sensitive to the degassing level (removal of dissolved CO_2) and purity of the reagents, requires long stabilization times and frequent maintenance. The Isodat software is so temperamental that it is unreliable when operated in parallel with other software or an active internet

connection. The complexity and expertise required to obtain reproducible results in CSIA increases the need for high skilled users who can use and troubleshoot the instrument on a daily basis. Despite the capability of direct measurement of underivatized compounds, the need for aqueous-only mobile phases and limited flow rate (<700 µL/min) are two other constraints of the technique, where a single sample can take up to 2.5 h to be completely eluted. The slow HPLC separation times are an obvious target for future improvements. Reduced separation times could be achieved through the use of elevated temperatures, smaller (1-3 µm)-sized particles and alternative mixed-mode stationary phases that are compatible with aqueous-only mobile phases.

We concluded that even though bulk isotope ratio analyses could link *C. vicina* blow flies to their food source, it was inadequate to distinguish blow flies raised on chicken or pork. CSIA provided ^{13}C fractionation data for each amino acid at each of the major life stages. CSIA showed that essential amino acids undergo little or no fractionation between the food source and the blow fly, so they preserve the isotopic signature of the diet. In contrast, non-essential amino acids each undergo their own degrees of fractionation, which can be as large as ~8‰ relative to the food source. The results also indicated that a specific food source could be excluded from the possible primary diet options for a blow fly in any of its life stages.

The research on blow flies has significant potential, and there are many interesting questions to be answered now that we have answered some basic questions. For example, future work should include a larger sample size, collection of post-emergence residual exoskeleton, and analyses at different timeframes within each metamorphic stage to reveal more information about the biochemistry of amino acids during insect development. In addition, raising blow flies on human tissues instead of food-grade meat would enhance the forensic significance of this research. For

example, by showing that blow flies can be linked to certain humans or human tissues, the technique may become more valuable as a tool for supporting post-mortem interval determinations.

We also established that by using the $\delta^{13}C$ values of all 13 amino acid peaks, the harvesting area could be predicted with only 41% accuracy (LOOCV), but when combining these variables with lead and cadmium concentrations the success rate improves to 71% (LOOCV). Adjacent areas within the same Apalachicola bay could also be distinguished with greater than 90% accuracy (LOOCV) using only the $\delta^{13}C$ values of Ser and Gly. One of these areas is fishable in the winter season and the other is fishable in the summer season, so the ability to differentiate oysters from these two areas is a valuable capability for the Florida Department of Agriculture, which is responsible for code enforcement. Future work could seek to control for seasonality by collecting a larger number of samples within the same season within the different bay areas. Oysters are typically caught and sold within a few days, so it is likely that controlling for seasonal variation of $\delta^{13}C$ values within the harvesting areas could provide great accuracy in predicting the oysters' origin. An increase in sample size and the use of additional trace elements may also improve the discrimination power of our proposed approach. Also, the incorporation of $\delta^{13}C$ and, $\delta^{2}H$ and $\delta^{18}O$ analysis of the oyster shells may provide further insight about the environmental conditions of the estuaries, such as nutritional input, salinity, and water temperature.

Finally, we concluded that by using the $\delta^{13}C$ values of amino acids or their respective quantities from human scalp hair, we can predict the sex of an individual with 80% and 89% accuracy, respectively (LOOCV); a finding not yet reported for this methodology. We also found that diet influences the bulk $\delta^{13}C$ and $\delta^{15}N$ values of hair, and that these bulk values correlate with the amino-acid-specific isotope ratios. By controlling for the effect of diet on each amino acid, the variance in $\delta^{13}C$ values caused by other factors, like age or alcohol consumption, becomes more-

readily observable. In short, the variance caused by diet tends to mask the effects of other factors, but the effects of diet can be corrected to reveal the effects of the other factors. Despite the correlations between other soft-biometrics, such as age and BMI, with the analyzed variables, the classification rates were usually around 50% (LOOCV). We did not observe major effects of chemical treatments of hair on the isotope profiles. Routine behavior, such as alcohol consumption frequency, was surprisingly reflected in the isotope ratios of hair, but smoking habits and consumption of soda/ sweeteners were not. Future studies should focus on controlling some of the behavioral states or metabolic conditions of hair donors to better understand the metabolic pathways underlying the results. For example, one 11-year-old subject had abnormally depleted $\delta^{13}C$ values for Phe, and his medications contained enough aspartame to provide more than 40 mg of Phe per day. We hypothesize that his Phe isotope ratios were caused by extremely depleted $\delta^{13}C$ values from the exogenous phenylalanine in the aspartame, but this hypothesis could be further investigated.

First, future work could analyze the $\delta^{13}C$ values of Phe in different suppliers, pharmaceuticals, dietary supplements, foods and beverages. Second, future work could analyze the $\delta^{13}C$ values of Phe in the hair of subjects relative to a control study group in which the subjects in the response group are provided with isotopically depleted phenylalanine in the form of aspartame in their diets. Other controlled studies could involve small cohorts of subjects, like military team members or groups of people who do continuous and extended outdoors activities (e.g. hiking or biking trips that last weeks). These people could be given similar diets and exposed to similar exercise regimes during certain training periods or missions. Because factors such as age, diet and exercise would be quite controlled, the effect of sex would be readily discerned if half of the study group were male and half of the group were female.

Given that we found correlations between amino acid isotope ratios and alcohol consumption, a controlled CSIA of hair from alcoholic liver disease patients compared to a control group of non-alcohol drinkers could improve the comprehension of this interaction and propose this technique as a less invasive diagnostic approach for liver cirrhosis. The addition of δ^{15}N CSIA in parallel to the carbon analysis would facilitate the understanding of how the transamination of amino acids isotope ratios correlates with age or behavior, for example. Another interesting future study could be to compare the amino acid-specific isotope ratios from hair of individuals from distinct races/ethnicities. If differences are found, this technique could work in parallel to DNA analysis in the identification of victims or suspects in forensic situations.

Overall, the direct relevance of this dissertation was the presentation of a suitable alternative methodology to compare of diverse sample matrices in distinct forensic situations. We showed how different factors affect isotopic composition of hair, oysters and insects and provided some discussion about how metabolic factors in each scenario could be affecting those isotope profiles. In the future, CSIA of other proteinaceous materials could benefit criminal justice in its investigative leads for the ultimate identification of suspects and victims. In food forensics, CSIA could help assist with the risk assessment of oysters harvested in contaminated areas and food fraud involving mislabeled "boutique" oysters. We expect that the publications resultant from this dissertation project could extend the visibility of IRMS technique, increase successful reports in law enforcement, and benefit other fields of study on a long-term scale.

REFERENCES

[1] Z. Muccio, G.P. Jackson, Isotope ratio mass spectrometry, Analyst 134(2) (2009) 213-22.

[2] W. Meier-Augenstein, Stable isotope forensics: An introduction to the forensic application of stable isotope analysis, John Wiley & Sons, Chichester, UK, 2010.

[3] N. NicDaeid, H.A.S. Buchanan, K. Savage, J. Fraser, S.L. Cresswell, Recent advances in the application of stable isotope ratio analysis in forensic chemistry, Aust. J. Chem. 63(1) (2010) 3-7.

[4] S.S. Tobe, Determining the geographic origin of animal samples, in: A. Linacre (Ed.), Forensic Science in Wildlife Investigations, Taylor & Francis Group, LLC, Boca Raton, FL, 2009, pp. 127-156.

[5] J.S. McCullagh, Mixed-mode chromatography/isotope ratio mass spectrometry, Rapid Commun. Mass Spectrom. 24(5) (2010) 483-94.

[6] L.A. Chesson, B.J. Tipple, J.D. Howa, G.J. Bowen, J.E. Barnette, T.E. Cerling, J.R. Ehleringer, Stable isotopes in forensics applications, in: H.H. D., T.K. K. (Eds.), Treatise on Geochemistry, Elsevier, Oxford, 2014, pp. 285-317.

[7] N. Gentile, R.T.W. Siegwolf, P. Esseiva, S. Doyle, K. Zollinger, O. Delemont, Isotope ratio mass spectrometry as a tool for source inference in forensic science: A critical review, Forensic Sci. Int. 251 (2015) 139-158.

[8] T.E. Cerling, J.E. Barnette, G.J. Bowen, L.A. Chesson, J.R. Ehleringer, C.H. Remien, P. Shea, B.J. Tipple, J.B. West, Forensic stable isotope biogeochemistry, Annu. Rev. Earth Planet. Sci. 44(1) (2016) 175-206.

[9] L.A. Chesson, J.E. Barnette, G.J. Bowen, J.R. Brooks, J.F. Casale, T.E. Cerling, C.S. Cook, C.B. Douthitt, J.D. Howa, J.M. Hurley, H.W. Kreuzer, M.J. Lott, L.A. Martinelli, S.P. O'Grady, D.W. Podlesak, B.J. Tipple, L.O. Valenzuela, J.B. West, Applying the principles of isotope analysis in plant and animal ecology to forensic science in the Americas, Oecologia 187(4) (2018) 1077-1094.

[10] E.J. Bartelink, G.E. Berg, L.A. Chesson, B.J. Tipple, M.M. Beasley, J.R. Prince-Buitenhuys, H. MacInnes, A.T. MacKinnon, K.E. Latham, Applications of stable isotope forensics for geolocating unidentified human remains from past conflict situations and large-scale humanitarian efforts, in: K.E. Latham, E.J. Bartelink, M. Finnegan (Eds.), New Perspectives in Forensic Human Skeletal Identification, Academic Press2018, pp. 175-184.

[11] L.A. Chesson, B.J. Tipple, L.V. Youmans, M.A. O'Brien, M.M. Harmon, Forensic identification of human skeletal remains using isotopes: A brief history of applications from archaeological dig sites to modern crime scenes, in: K.E. Latham, E.J. Bartelink, M. Finnegan (Eds.), New Perspectives in Forensic Human Skeletal Identification, Elsevier,2018, pp. 157-173.

[12] H. Salouros, Illicit drug chemical profiling: Current and future state, Aust. J. Forensic Sci. 50(6) (2018) 689-696.

[13] J.R. Ehleringer, L.A. Chesson, L.O. Valenzuela, B.J. Tipple, L.A. Martinelli, Stable isotopes trace the truth: From adulterated foods to crime scenes, Elements 11(4) (2015) 259-264.

[14] <http://www.forensic-isotopes.org/>, 2016 (accessed Accessed August 20.2016).

[15] P.J.H. Dunn, J.F. Carter, Good Practice Guide for Isotope Ratio Mass Spectrometry, 2nd ed., FIRMS2018.

[16] J.F. Carter, B. Fry, Ensuring the reliability of stable isotope ratio data-beyond the principle of identical treatment, Anal. Bioanal. Chem. 405(9) (2013) 2799-814.

[17] P.J.H. Dunn, H. Goenaga-Infante, A.C. Goren, A. Şimşek, M. Bilsel, N. Ogrinc, P. Armishaw, L. Hai, CCQM-K140: Carbon stable isotope ratio delta values in honey, Metrologia 54(08005) (2017).
[18] P.J.H. Dunn, S. Hill, S. Cowen, H. Goenaga-Infante, M. Sargent, A.C. Gören, M. Bilsel, A. Şimşek, N. Ogrinc, D. Potočnik, P. Armishaw, L. Hai, L. Konopelko, Y. Chubchenko, L.A. Chesson, G. van der Peijl, C. Blaga, R. Posey, F. Camin, A. Chernyshev, S.A. Chowdhury, Lessons learned from inter-laboratory studies of carbon isotope analysis of honey, Sci. Justice 59(1) (2019) 9-19.
[19] P.J. Dunn, L. Hai, D. Malinovsky, H. Goenaga-Infante, Simple spreadsheet templates for the determination of the measurement uncertainty of stable isotope ratio delta values, Rapid Commun. Mass Spectrom. 29(22) (2015) 2184-6.
[20] T.B. Coplen, Guidelines and recommended terms for expression of stable-isotope-ratio and gas-ratio measurement results, Rapid Commun. Mass Spectrom. 25 (2011) 2538-2560.
[21] D.J. Hawke, J.C.S. Brown, S.J. Bury, B. Pracheil, The prevention and detection of human error in ecological stable isotope analysis, Methods Ecol. Evol. (2018).
[22] A.L. Plant, C.A. Becker, R.J. Hanisch, R.F. Boisvert, A.M. Possolo, J.T. Elliott, How measurement science can improve confidence in research results, PLoS Biol. 16(4) (2018) e2004299.
[23] W.A. Brand, T.B. Coplen, J. Vogl, M. Rosner, T. Prohaska, Assessment of international reference materials for isotope-ratio analysis (IUPAC Technical Report), Pure Appl. Chem. 86(3) (2014) 425-467.
[24] T.B. Coplen, H. Qi, L. Tarbox, J. Lorenz, B. Buck, USGS46 Greenland ice core water - A new isotopic reference material for δ^{2}H and δ^{18}O measurements of water, Geostand. Geoanalytical Res. 38(2) (2013) 153-157.
[25] H. Qi, T.B. Coplen, L. Tarbox, J.M. Lorenz, M. Scholl, USGS48 Puerto Rico precipitation - a new isotopic reference material for δ^{2}H and δ^{18}O measurements of water, Isotopes Environ. Health Stud. 50(4) (2014) 442-7.
[26] H. Qi, J.M. Lorenz, T.B. Coplen, L. Tarbox, B. Mayer, S. Taylor, Lake Louise water (USGS47): a new isotopic reference water for stable hydrogen and oxygen isotope measurements, Rapid Commun. Mass Spectrom. 28(4) (2014) 351-4.
[27] V. Faghihi, B.M.A.A. Verstappen-Dumoulin, H.G. Jansen, G. van Dijk, A.T. Aerts-Bijma, E.R.T. Kerstel, M. Gröning, H.A.J. Meijer, A new high-quality set of singly (^{2}H) and doubly (^{2}H and ^{18}O) stable isotope labeled reference waters for biomedical and other isotope-labeled research, Rapid Commun. Mass Spectrom. 29(4) (2015) 311-321.
[28] T.B. Coplen, H.P. Qi, USGS42 and USGS43: Human-hair stable hydrogen and oxygen isotopic reference materials and analytical methods for forensic science and implications for published measurement results, Forensic Sci. Int. 214(1-3) (2012) 135-141.
[29] D. Malinovsky, P.J.H. Dunn, G. Holcombe, S. Cowen, H. Goenaga-Infante, Development and characterisation of new glycine certified reference materials for SI-traceable ^{13}C/^{12}C isotope amount ratio measurements, J. Anal. At. Spectrom. 34(1) (2019) 147-159.
[30] H. Qi, T.B. Coplen, S.J. Mroczkowski, W.A. Brand, L. Brandes, H. Geilmann, A. Schimmelmann, A new organic reference material, l-glutamic acid, USGS41a, for δ^{13}C and δ^{15}N measurements - a replacement for USGS41, Rapid Commun. Mass Spectrom. 30(7) (2016) 859-66.
[31] M.M.G. Chartrand, J. Meija, P. Kumkrong, Z. Mester, Three certified sugar reference materials for carbon isotope delta measurements, Rapid Commun. Mass Spectrom. 33(3) (2019) 272-280.

[32] T.B. Coplen, Brand, W. A., Gehre, M., Groning, M., Meijer, H. A. J., Toman, B., Verkouteren, R. M., New Guidelines for $\delta^{13}C$ Measurements, Anal. Chem. 78(7) (2006) 2439-2441.
[33] W. Meier-Augenstein, A. Schimmelmann, A guide for proper utilisation of stable isotope reference materials, Isotopes Environ. Health Stud. (2018) 1-16.
[34] J.F. Carter, B. Fry, "Do it yourself" reference materials for $\delta^{13}C$ determinations by isotope ratio mass spectrometry, Anal. Bioanal. Chem. 405(14) (2013) 4959-62.
[35] Strengthening forensic science in the United States: A path forward, Committee on Identifying the Needs of the Forensic Sciences Community, National Research Council, The National Academy Press, 2009.
[36] C.D. Kennedy, G.J. Bowen, J.R. Ehleringer, Temporal variation of oxygen isotope ratios ($\delta^{18}O$) in drinking water: implications for specifying location of origin with human scalp hair, Forensic Sci. Int. 208(1-3) (2011) 156-66.
[37] B.J. Webb-Robertson, H. Kreuzer, G. Hart, J. Ehleringer, J. West, G. Gill, D. Duckworth, Bayesian integration of isotope ratio for geographic sourcing of castor beans, J. Biomed. Biotechnol. 2012 (2012) 8.
[38] G.J. Bowen, Z.F. Liu, H.B. Vander Zanden, L. Zhao, G. Takahashi, Geographic assignment with stable isotopes in IsoMAP, Methods Ecol. Evol. 5(3) (2014) 201-206.
[39] N. Farmer, W. Meier-Augenstein, D. Lucy, Stable isotope analysis of white paints and likelihood ratios, Sci. Justice 49(2) (2009) 114-9.
[40] J.F. Carter, S. Doyle, B.L. Phasumane, N. NicDaeid, The role of isotope ratio mass spectrometry as a tool for the comparison of physical evidence, Sci. Justice 54(5) (2014) 327-34.
[41] L.M. Nienaber, S.L. Cresswell, J.F. Carter, T. Peter, A comparison of plastic cable ties based on physical, chemical and stable isotopic measurements, Sci. Justice 58(1) (2018) 67-75.
[42] K.A. Martire, R.I. Kemp, M. Sayle, B.R. Newell, On the interpretation of likelihood ratios in forensic science evidence: Presentation formats and the weak evidence effect, Forensic Sci. Int. 240 (2014) 61-68.
[43] J.R. Ehleringer, S.M. Matheson Jr., Stable isotopes and courts, Utah Law Review No. 2 (2010) 385-442.
[44] E. Mutzel Rauch, C. Lehn, O. Peschel, S. Holzl, A. Rossmann, Assignment of unknown persons to their geographical origin by determination of stable isotopes in hair samples, Int. J. Legal Med. 123(1) (2009) 35-40.
[45] L. Font, G. van der Peijl, C. van Leuwen, I. van Wetten, G.R. Davies, Identification of the geographical place of origin of an unidentified individual by multi-isotope analysis, Sci. Justice 55(1) (2015) 34-42.
[46] C.A.M. France, D.W. Owsley, L.A.C. Hayek, Stable isotope indicators of provenance and demographics in 18th and 19th century North Americans, J. Archaeol. Sci. 42 (2014) 356-366.
[47] J.B. West, G.J. Bowen, T.E. Dawson, K.P. Tu, Isoscapes - Understanding movement, pattern, and process on Earth through isotope mapping, Springer Science+Business Media B.V., Springer Dordrecht Heidelberg London New York, 2010.
[48] A.G. West, E.C. February, G.J. Bowen, Spatial analysis of hydrogen and oxygen stable isotopes ("isoscapes") in ground water and tap water across South Africa, J. Geochem. Explor. 145 (2014) 213-222.
[49] G.J. Bowen, Isoscapes: Spatial pattern in isotopic biogeochemistry, Annu. Rev. Earth Planet. Sci. 38 (2010) 161-187.

[50] M.M. Warner, A.M. Plemons, N.P. Herrmann, L.A. Regan, Refining stable oxygen and hydrogen isoscapes for the identification of human remains in Mississippi, J. Forensic Sci. 63(2) (2018) 395-402.
[51] J.M. Landwehr, T.B. Coplen, D.W. Stewart, Spatial, seasonal, and source variability in the stable oxygen and hydrogen isotopic composition of tap waters throughout the USA, Hydrol. Process. 28(21) (2014) 5382-5422.
[52] C.J. Mancuso, J.R. Ehleringer, Resident and nonresident fingernail isotopes reveal diet and travel patterns, J. Forensic Sci. 64(1) (2019) 77-87.
[53] H.B. Vander Zanden, A. Reid, T. Katzner, D.M. Nelson, Effect of heat and singeing on stable hydrogen isotope ratios of bird feathers and implications for their use in determining geographic origin, Rapid Commun. Mass Spectrom. 32(21) (2018) 1859-1866.
[54] W. Meier-Augenstein, K.A. Hobson, L.I. Wassenaar, Critique: measuring hydrogen stable isotope abundance of proteins to infer origins of wildlife, food and people, Bioanalysis 5(7) (2013) 751-767.
[55] W. Meier-Augenstein, H.F. Kemp, Stable isotope analysis: hair and nails, Wiley Encyclopedia of Forensic Science, John Wiley & Sons, Ltd. (2012).
[56] I.M. Kempson, E. Lombi, Hair analysis as a biomonitor for toxicology, disease and health status, Chem. Soc. Rev. 40(7) (2011) 3915-40.
[57] G. Koehler, K.A. Hobson, Effects of tanning on the stable isotopic compositions of hair, Forensic Sci. Int. 292 (2018) 78-82.
[58] G.W. Gordon, T.B. Saul, D. Steadman, D.J. Wescott, K. Knudson, Preservation of hair stable isotope signatures during freezing and law enforcement evidence packaging, Forensic Chem. 11 (2018) 108-119.
[59] F. Hulsemann, C. Lehn, S. Schneider, G. Jackson, S. Hill, A. Rossmann, N. Scheid, P.J. Dunn, U. Flenker, W. Schanzer, Global spatial distributions of nitrogen and carbon stable isotope ratios of modern human hair, Rapid Commun. Mass Spectrom. 29(22) (2015) 2111-21.
[60] L.O. Valenzuela, L.A. Chesson, S.P. O'Grady, T.E. Cerling, J.R. Ehleringer, Spatial distributions of carbon, nitrogen and sulfur isotope ratios in human hair across the central United States, Rapid Commun. Mass Spectrom. 25(7) (2011) 861-8.
[61] G.P. Jackson, Y. An, K.I. Konstantynova, A.H.B. Rashaid, Biometrics from the carbon isotope ratio analysis of amino acids in human hair, Sci. Justice 55 (2015) 43-50.
[62] T.C. O'Connell, R.E.M. Hedges, M.A. Healey, A.H.R.W. Simpson, Isotopic comparison of hair, nail and bone: Modern analyses, J. Archaeol. Sci. 28(11) (2001) 1247-1255.
[63] C. Lehn, E. Mutzel, A. Rossmann, Multi-element stable isotope analysis of H, C, N and S in hair and nails of contemporary human remains, Int. J. Legal Med. 125(5) (2011) 695-706.
[64] T.C. O'Connell, C.J. Kneale, N. Tasevska, G.G. Kuhnle, The diet-body offset in human nitrogen isotopic values: a controlled dietary study, Am. J. Phys. Anthropol. 149(3) (2012) 426-34.
[65] G.E. Rosen, K.F. Smith, Summarizing the evidence on the international trade in illegal wildlife, EcoHealth 7(1) (2010) 24-32.
[66] J.C. Finlay, R.R. Doucett, C. McNeely, Tracing energy flow in stream food webs using stable isotopes of hydrogen, Freshw. Biol. 55(5) (2010) 941–951.
[67] J.A. Seminoff, S.R. Benson, K.E. Arthur, T. Eguchi, P.H. Dutton, R.F. Tapilatu, B.N. Popp, Stable isotope tracking of endangered sea turtles: validation with satellite telemetry and δ^{15}N analysis of amino acids, PLoS One 7(5) (2012) e37403.
[68] B.S. Graham, P.L. Koch, S.D. Newsome, K.W. McMahon, D. Aurioles, Using isoscapes to trace the movements and foraging behavior of top predators in oceanic ecosystems, in: J.B. West,

G.J. Bowen, T.E. Dawson, K.P. Tu (Eds.), Isoscapes: Understanding Movement, Pattern, and Process on Earth Through Isotope Mapping, Springer Science + Business Media B.V.,2010, pp. 299-318.
[69] R. Ramos, J. González-Solís, Trace me if you can: the use of intrinsic biogeochemical markers in marine top predators, Front. Ecol. Environ. 10(5) (2012) 258-266.
[70] H.B.V. Zanden, A.D. Tucker, K.M. Hart, M.M. Lamont, I. Fujisaki, D.S. Addison, K.L. Mansfield, K.F. Phillips, M.B. Wunder, G.J. Bowen, M. Pajuelo, A.B. Bolten, K.A. Bjorndal, Determining origin in a migratory marine vertebrate: a novel method to integrate stable isotopes and satellite tracking, Ecol. Appl. 25(2) (2015) 320-335.
[71] T. Tsutaya, Y. Fujimori, M. Hayashi, M. Yoneda, T. Miyabe-Nishiwaki, Carbon and nitrogen stable isotopic offsets between diet and hair/feces in captive chimpanzees, Rapid Commun. Mass Spectrom. 31(1) (2017) 59-67.
[72] T.E. Cerling, S.A. Andanje, F. Gakuya, J.M. Kariuki, L. Kariuki, J.W. Kingoo, C. Khayale, I. Lekolool, A.N. Macharia, C.R. Anderson, D.P. Fernandez, L. Hu, S.J. Thomas, Stable isotope ecology of black rhinos (*Diceros bicornis*) in Kenya, Oecologia 187(4) (2018) 1095-1105.
[73] N.J. van der Merwe, J.A. Lee-Thorp, J.F. Thackeray, A. Hall-Martin, F.J. Kruger, H. Coetzee, R.H.V. Bell, M. Lindeque, Source-area determination of elephant ivory by isotopic analysis, Nature 346 (1990) 744-746.
[74] T.E. Cerling, P. Omondi, A.N. Macharia, Diets of Kenyan elephants from stable isotopes and the origin of confiscated ivory in Kenya, Afr. J. Ecol. 45 (2007) 614-623.
[75] S. Ziegler, S. Merker, B. Streit, M. Boner, D.E. Jacob, Towards understanding isotope variability in elephant ivory to establish isotopic profiling and source-area determination, Biol. Conserv. 197 (2016) 154-163.
[76] J.C. Vogel, B. Eglington, J.M. Auret, Isotope fingerprints in elephant bone and ivory, Nature 346 (1990) 747-749.
[77] M. van Schingen, T. Ziegler, M. Boner, B. Streit, T.Q. Nguyen, V. Crook, S. Ziegler, Can isotope markers differentiate between wild and captive reptile populations? A case study based on crocodile lizards (*Shinisaurus crocodilurus*) from Vietnam, Glob. Ecol. Conserv. 6 (2016) 232-241.
[78] J. Alexander, C.T. Downs, M. Butler, S. Woodborne, C.T. Symes, Stable isotope analyses as a forensic tool to monitor illegally traded African grey parrots, Anim. Conserv. (2018).
[79] D.J.D. Natusch, J.F. Carter, P.W. Aust, N. Van Tri, U. Tinggi, Mumpuni, A. Riyanto, J.A. Lyons, Serpent's source: Determining the source and geographic origin of traded python skins using isotopic and elemental markers, Biol. Conserv. 209 (2017) 406-414.
[80] D.A. Schoeller, Isotope fractionation: Why aren't we what we eat?, J Archaeol Sci 26 (1999) 667–673.
[81] Z.D. Sharp, Principles of Stable Isotope Geochemistry, 2nd ed.2017.
[82] H.B. Vander Zanden, D.M. Nelson, M.B. Wunder, T.J. Conkling, T. Katzner, Application of isoscapes to determine geographic origin of terrestrial wildlife for conservation and management, Biol. Conserv. 228 (2018) 268-280.
[83] K.J. Brandis, P.J.B. Meagher, L.J. Tong, M. Shaw, D. Mazumder, P. Gadd, D. Ramp, Novel detection of provenance in the illegal wildlife trade using elemental data, Sci. Rep. 8(1) (2018) 15380.
[84] C.T. Graham, S.S.C. Harrison, C. Harrod, Differences in the contributions of dietary water to the hydrogen stable isotope ratios of cultured Atlantic salmon and Arctic charr tissues, Hydrobiologia 721(1) (2013) 45-55.

[85] H.B.V. Zanden, M.B. Wunder, K.A. Hobson, S.L. Van Wilgenburg, L.I. Wassenaar, J.M. Welker, G.J. Bowen, Contrasting assignment of migratory organisms to geographic origins using long-term versus year-specific precipitation isotope maps, Methods Ecol. Evol. 5(9) (2014) 891-900.
[86] D.X. Soto, L.I. Wassenaar, K.A. Hobson, Stable hydrogen and oxygen isotopes in aquatic food webs are tracers of diet and provenance, Funct. Ecol. 27(2) (2013) 535-543.
[87] I.C. Ansmann, J.M. Lanyon, J.M. Seddon, G.J. Parra, Habitat and resource partitioning among Indo-Pacific bottlenose dolphins in Moreton Bay, Australia, Mar. Mamm. Sci. 31(1) (2015) 211-230.
[88] F.A. Aya, I. Kudo, Isotopic shifts with size, culture habitat, and enrichment between the diet and tissues of the Japanese scallop *Mizuhopecten yessoensis* (Jay, 1857), Mar. Biol. 157(10) (2010) 2157-2167.
[89] W.J. Boecklen, C.T. Yarnes, B.A. Cook, A.C. James, On the use of stable isotopes in trophic ecology, Annu. Rev. Ecol. Evol. Syst. 42(1) (2011) 411-440.
[90] C.K. Weldrick, R. Trebilco, K.M. Swadling, Can lipid removal affect interpretation of resource partitioning from stable isotopes in Southern Ocean pteropods?, Rapid Commun. Mass Spectrom. (2019).
[91] H.K. Patterson, R.H. Carmichael, The effect of lipid extraction on carbon and nitrogen stable isotope ratios in oyster tissues: Implications for glycogen-rich species, Rapid Commun. Mass Spectrom. 30(24) (2016) 2594-2600.
[92] M. Connan, G. Hall, M. Smale, Effects of pre-treatments on bulk stable isotope ratios in fish samples: A cautionary note for studies comparisons, Rapid Commun. Mass Spectrom. 33(3) (2019) 291-302.
[93] S.J. Pietsch, K.A. Hobson, L.I. Wassenaar, T. Tutken, Tracking cats: problems with placing feline carnivores on $\delta^{18}O$, δD isoscapes, PLoS One 6(9) (2011) e24601.
[94] V. Bernhardt, T. Holdermann, N. Scheid, T. Schafer, M.A. Verhoff, J. Amendt, Same, same but different!-matching entomological traces to a human food source by stable isotope analysis, Int. J. Legal Med. 132(3) (2018) 915-921.
[95] M.P.V. Matos, K.I. Konstantynova, R.M. Mohr, G.P. Jackson, Analysis of the ^{13}C isotope ratios of amino acids in the larvae, pupae and adult stages of *Calliphora vicina* blow flies and their carrion food sources, Anal. Bioanal. Chem. 410(30) (2018) 7943-7954.
[96] R.B. Thomas, S.E. Spal, K.R. Smith, J.B. Nippert, Evidence of recovery of *Juniperus virginiana* trees from sulfur pollution after the Clean Air Act, Proc. Natl. Acad. Sci. U. S. A. 110(38) (2013) 15319-24.
[97] K. Retief, A.G. West, M.F. Pfab, Can stable isotopes and radiocarbon dating provide a forensic solution for curbing illegal harvesting of threatened cycads?, J. Forensic Sci. 59(6) (2014) 1541-51.
[98] A. Kagawa, S.W. Leavitt, Stable carbon isotopes of tree rings as a tool to pinpoint the geographic origin of timber, J. Wood Sci. 56(3) (2010) 175-183.
[99] Y. Gori, R. Wehrens, N. La Porta, F. Camin, Oxygen and hydrogen stable isotope ratios of bulk needles reveal the geographic origin of Norway spruce in the European Alps, PLoS One 10(3) (2015) 14.
[100] M. Bridge, Locating the origins of wood resources: a review of dendroprovenancing, Journal of Archaeological Science 39(8) (2012) 2828-2834.

[101] P.F. Poussart, M.N. Evans, D.P. Schrag, Resolving seasonality in tropical trees: multi-decade, high-resolution oxygen and carbon isotope records from Indonesia and Thailand, Earth. Planet. Sci. Lett. 218(3-4) (2004) 301-316.
[102] R.P. Philp, An overview of environmental forensics, Geol. Acta 12(4) (2014) 363-374.
[103] T.B. Hofstetter, M. Berg, Assessing transformation processes of organic contaminants by compound-specific stable isotope analysis, Trends Anal. Chem. 30(4) (2011) 618-627.
[104] T.B. Hofstetter, J. Bolotin, M. Skarpeli-Liati, R. Wijker, Z. Kurt, S.F. Nishino, J.C. Spain, Tracking transformation processes of organic micropollutants in aquatic environments using multi-element isotope fractionation analysis, Appl. Geochem. 26 (2011) S334-S336.
[105] A. Cincinelli, F. Pieri, Y. Zhang, M. Seed, K.C. Jones, Compound specific isotope analysis (CSIA) for chlorine and bromine: a review of techniques and applications to elucidate environmental sources and processes, Environ. Pollut. 169 (2012) 112-27.
[106] M. Thullner, F. Centler, H.-H. Richnow, A. Fischer, Quantification of organic pollutant degradation in contaminated aquifers using compound specific stable isotope analysis – Review of recent developments, Org. Geochem. 42(12) (2012) 1440-1460.
[107] W.J. Shin, S.W. Lee, S.Y. Heo, K.S. Lee, Stable isotopic fingerprinting for identification of the methyl tert-butyl ether (MTBE) manufacturer, Environ. Forensics 14(1) (2013) 36-41.
[108] M. Elsner, G. Imfeld, Compound-specific isotope analysis (CSIA) of micropollutants in the environment - current developments and future challenges, Curr. Opin. Biotechnol. 41 (2016) 60-72.
[109] Y. Li, Y. Xiong, W. Yang, Y. Xie, S. Li, Y. Sun, Compound-specific stable carbon isotopic composition of petroleum hydrocarbons as a tool for tracing the source of oil spills, Mar. Pollut. Bull. 58(1) (2009) 114-7.
[110] U.H. Yim, M. Kim, S.Y. Ha, S. Kim, W.J. Shim, Oil spill environmental forensics: the Hebei Spirit oil spill case, Environ. Sci. Technol. 46(12) (2012) 6431-7.
[111] Z. Schwartz, Y. An, K.I. Konstantynova, G.P. Jackson, Analysis of household ignitable liquids and their post-combustion weathered residues using compound-specific gas chromatography-combustion-isotope ratio mass spectrometry, Forensic Sci. Int. 233(1-3) (2013) 365-73.
[112] H.J. Tobias, G.L. Sacks, Y. Zhang, J.T. Brenna, Comprehensive two-dimensional gas chromatography combustion isotope ratio mass spectrometry, Anal. Chem. 80(22) (2008) 8613–8621.
[113] F. Gelman, A. Kotlyar, D. Chiguala, Z. Ronen, Precise and accurate compound-specific carbon and nitrogen isotope analysis of RDX by GC-IRMS, Int. J. Environ. Anal. Chem. 91(14) (2011) 1392-1400.
[114] S. Spahr, J. Bolotin, J. Schleucher, I. Ehlers, U. von Gunten, T.B. Hofstetter, Compound-specific carbon, nitrogen, and hydrogen isotope analysis of *N*-nitrosodimethylamine in aqueous solutions, Anal. Chem. 87(5) (2015) 2916-24.
[115] K. Schreglmann, M. Hoeche, S. Steinbeiss, S. Reinnicke, M. Elsner, Carbon and nitrogen isotope analysis of atrazine and desethylatrazine at sub-microgram per liter concentrations in groundwater, Anal. Bioanal. Chem. 405(9) (2013) 2857-67.
[116] D.M. Kujawinski, L. Zhang, T.C. Schmidt, M.A. Jochmann, When other separation techniques fail: compound-specific carbon isotope ratio analysis of sulfonamide containing pharmaceuticals by high-temperature-liquid chromatography-isotope ratio mass spectrometry, Anal. Chem. 84(18) (2012) 7656-63.
[117] D.M. Kujawinski, J.B. Wolbert, L. Zhang, M.A. Jochmann, D. Widory, N. Baran, T.C. Schmidt, Carbon isotope ratio measurements of glyphosate and AMPA by liquid

chromatography coupled to isotope ratio mass spectrometry, Anal. Bioanal. Chem. 405(9) (2013) 2869-78.
[118] O. Shouakar-Stash, R.J. Drimmie, M. Zhang, S.K. Frape, Compound-specific chlorine isotope ratios of TCE, PCE and DCE isomers by direct injection using CF-IRMS, Appl. Geochem. 21(5) (2006) 766-781.
[119] O. Shouakar-Stash, S.K. Frape, R.J. Drimmie, Determination of bromine stable isotopes using continuous-flow isotope ratio mass spectrometry, Anal. Chem. 77 (2005) 4027-4033.
[120] C. Aeppli, H. Holmstrand, P. Andersson, O. Gustafsson, Direct compound-specific stable chlorine isotope analysis of organic compounds with quadrupole GC/MS using standard isotope bracketing, Anal. Chem. 82(1) (2010) 420-426.
[121] M.R.M.D. Van Acker, A. Shahar, E.D. Young, M.L. Coleman, GC/multiple collector-ICPMS method for chlorine stable isotope analysis of chlorinated aliphatic hydrocarbons, Anal. Chem. 78(13) (2006) 4663-4667.
[122] D. Carrizo, M. Unger, H. Holmstrand, P. Andersson, Ö. Gustafsson, S.P. Sylva, C.M. Reddy, Compound-specific bromine isotope compositions of one natural and six industrially synthesised organobromine substances, Environ. Chem. 8(2) (2011) 127.
[123] A. Amrani, A.L. Sessions, J.F. Adkins, Compound-specific $\delta^{34}S$ analysis of volatile organics by coupled GC/multicollector-ICPMS, Anal. Chem. 81(21) (2009) 9027-9034.
[124] R.N. Zare, D.S. Kuramoto, C. Haase, S.M. Tan, E.R. Crosson, N.M. Saad, High-precision optical measurements of $^{13}C/^{12}C$ isotope ratios in organic compounds at natural abundance, Proc. Natl. Acad. Sci. U. S. A. 106(27) (2009) 10928-32.
[125] Results from the 2013 national survey on drug use and health: Mental health findings NSDUH Series H-49, HHS Publication No. (SMA) 14-4887. Rockville, MD: Substance Abuse and Mental Health Services Administration, 2014, p. 142.
[126] J.M. Hurley, J.B. West, J.R. Ehleringer, Tracing retail cannabis in the United States: geographic origin and cultivation patterns, Int. J. Drug Policy 21(3) (2010) 222-8.
[127] E.J. D'Amico, A. Rodriguez, J.S. Tucker, E.R. Pedersen, R.A. Shih, Planting the seed for marijuana use: Changes in exposure to medical marijuana advertising and subsequent adolescent marijuana use, cognitions, and consequences over seven years, Drug Alcohol Depend. 188 (2018) 385-391.
[128] Announcement of revision to the department of Health and Human Services guidance on procedures for the provision of marijuana for medical research as published on May 21, 1999, in: D.o.H.a.H. Services (Ed.) Federal Register 2015, pp. 35960-35961.
[129] T.M. Denton, S. Schmidt, C. Critchley, G.R. Stewart, Natural abundance of stable carbon and nitrogen isotopes in *Cannabis sativa* reflects growth conditions, Funct. Plant Biol. 28(10) (2001) 1005.
[130] E.K. Shibuya, J.E. Souza Sarkis, O.N. Neto, M.Z. Moreira, R.L. Victoria, Sourcing Brazilian marijuana by applying IRMS analysis to seized samples, Forensic Sci. Int. 160(1) (2006) 35-43.
[131] E.K. Shibuya, J.E. Sarkis, O. Negrini-Neto, L.A. Martinelli, Carbon and nitrogen stable isotopes as indicative of geographical origin of marijuana samples seized in the city of Sao Paulo (Brazil), Forensic Sci. Int. 167(1) (2007) 8-15.
[132] DEA, The official Drug Enforcement Agency authorized database. <https://deanumber.com/default.aspx?relID=33637>, 2019 (accessed February 2019.).
[133] J.B. West, J.M. Hurley, J.R. Ehleringer, Stable isotope ratios of marijuana. I. Carbon and nitrogen stable isotopes describe growth conditions, J. Forensic Sci. 54(1) (2009) 84-9.

[134] J.M. Hurley, J.B. West, J.R. Ehleringer, Stable isotope models to predict geographic origin and cultivation conditions of marijuana, Sci. Justice 50(2) (2010) 86-93.
[135] B.J. Tipple, B. Hambach, J.E. Barnette, L.A. Chesson, J.R. Ehleringer, The influences of cultivation setting on inflorescence lipid distributions, concentrations, and carbon isotope ratios of *Cannabis sp.*, Forensic Sci. Int. 262 (2016) 233-41.
[136] A.L. Booth, M.J. Wooller, T. Howe, N. Haubenstock, Tracing geographic and temporal trafficking patterns for marijuana in Alaska using stable isotopes (C, N, O and H), Forensic Sci. Int. 202(1-3) (2010) 45-53.
[137] J.B. West, J.M. Hurley, F.O. Dudas, J.R. Ehleringer, The stable isotope ratios of marijuana. II. Strontium isotopes relate to geographic origin, J. Forensic Sci. 54(6) (2009) 1261-9.
[138] Z. Muccio, C. Wockel, Y. An, G.P. Jackson, Comparison of bulk and compound-specific $\delta^{13}C$ isotope ratio analyses for the discrimination between Cannabis samples, J. Forensic Sci. 57(3) (2012) 757-64.
[139] J.R. Mallette, J.F. Casale, J. Jordan, D.R. Morello, P.M. Beyer, Geographically sourcing cocaine's origin - Delineation of the nineteen major coca growing regions in South America, Sci. Rep. 6 (2016) 23520.
[140] J.F. Casale, J.R. Mallette, Illicit coca grown in Mexico: An alkaloid and isotope profile unlike coca grown in South America, Forensic Chem. 1 (2016) 1-5.
[141] J.R. Mallette, J.F. Casale, L.M. Jones, D.R. Morello, The isotopic fractionation of carbon, nitrogen, hydrogen, and oxygen during illicit production of cocaine base in South America, Forensic Sci. Int. 270 (2017) 255-260.
[142] F. Marclay, C. Saudan, J. Vienne, M. Tafti, M. Saugy, Source inference of exogenous gamma-hydroxybutyric acid (GHB) administered to humans by means of carbon isotopic ratio analysis: novel perspectives regarding forensic investigation and intelligence issues, Anal. Bioanal. Chem. 400 (2011) 1105–1112.
[143] F. Marclay, D. Pazos, O. Delemont, P. Esseiva, C. Saudan, Potential of IRMS technology for tracing gamma-butyrolactone (GBL), Forensic Sci. Int. 198(1-3) (2010) 46-52.
[144] N.M. Beckett, S.L. Cresswell, D.I. Grice, J.F. Carter, Isotopic profiling of seized benzylpiperazine and trifluoromethylphenylpiperazine tablets using $\delta^{13}C$ and $\delta^{15}N$ stable isotopes, Sci. Justice 55(1) (2015) 51-6.
[145] N.M. Beckett, D.I. Grice, J.F. Carter, S.L. Cresswell, Precursor discrimination of designer drug benzylpiperazine using $\delta^{13}C$ and $\delta^{15}N$ stable isotopes, Sci. Justice 55(1) (2015) 57-62.
[146] J.F. Casale, J.R. Mallette, E.M. Guest, Analysis of illicit carfentanil: Emergence of the death dragon, Forensic Chem. 3 (2017) 74-80.
[147] M. Collins, H. Salouros, A review of some recent studies on the stable isotope profiling of methylamphetamine: Is it a useful adjunct to conventional chemical profiling?, Sci. Justice 55(1) (2015) 2-9.
[148] C.M. Liu, P.P. Liu, W. Jia, Y.F. Fan, Carbon and nitrogen stable isotope analyses of Ephedra plant and Ephedrine samples and their application for methamphetamine profiling, J. Forensic Sci. 63(4) (2018) 1053-1058.
[149] R. Campbell, Intentional fires, National Fire Protection Association - Fire Analysis and Research Division, 2014, p. 81.
[150] J.R. Hall Jr., Fires starting with flammable gas or flammable or combustible liquid, National Fire Protection Association - Fire Analysis and Research Division, 2014, p. 187.

[151] S.D. Harvey, K.H. Jarman, J.J. Moran, C.M. Sorensen, B.W. Wright, Characterization of diesel fuel by chemical separation combined with capillary gas chromatography (GC) isotope ratio mass spectrometry (IRMS), Talanta 99 (2012) 262-9.
[152] S.A. Muhammad, R.D. Frew, A.R. Hayman, Forensic differentiation of diesel fuels using hydrocarbon isotope fingerprints, Central European Geology 56(1) (2013) 19-37.
[153] S.A. Muhammad, A.R. Hayman, R. Van Hale, R.D. Frew, Assessing carbon and hydrogen isotopic fractionation of diesel fuel *n*-alkanes during progressive evaporation, J. Forensic Sci. 60(S1) (2015) S56-65.
[154] T. Kuder, P. Philp, J. Allen, Effects of volatilization on carbon and hydrogen isotope ratios of MTBE, Environ. Sci. Technol. 43(6) (2009) 1763-1768.
[155] W.J. Shin, K.S. Lee, Carbon isotope fractionation of benzene and toluene by progressive evaporation, Rapid Commun. Mass Spectrom. 24(11) (2010) 1636-40.
[156] Q. Xiao, Y. Sun, Y. Zhang, P. Chai, Stable carbon isotope fractionation of individual light hydrocarbons in the C_6–C_8 range in crude oil as induced by natural evaporation: Experimental results and geological implications, Org. Geochem. 50 (2012) 44-56.
[157] M.R. Williams, M.E. Sigman, J. Lewis, K.M. Pitan, Combined target factor analysis and Bayesian soft-classification of interference-contaminated samples: forensic fire debris analysis, Forensic Sci. Int. 222(1-3) (2012) 373-86.
[158] H. Brust, M. Koeberg, A. van der Heijden, W. Wiarda, I. Mugler, M. Schrader, G. Vivo-Truyols, P. Schoenmakers, A. van Asten, Isotopic and elemental profiling of ammonium nitrate in forensic explosives investigations, Forensic Sci. Int. 248 (2015) 101-12.
[159] A. Beveridge, Forensic investigation of explosions, 2nd ed., CRC Press, Taylor & Francis Group, LLC,2012.
[160] S.J. Benson, C.J. Lennard, P. Maynard, D.M. Hill, A.S. Andrew, C. Roux, Forensic analysis of explosives using isotope ratio mass spectrometry (IRMS)-discrimination of ammonium nitrate sources, Sci. Justice 49(2) (2009) 73-80.
[161] S.J. Benson, C.J. Lennard, D.M. Hill, P. Maynard, C. Roux, Forensic analysis of explosives using isotope ratio mass spectrometry (IRMS)-Part 1: instrument validation of the DELTA^{plus}XP IRMS for bulk nitrogen isotope ratio measurements, J. Forensic Sci. 55(1) (2010) 193-204.
[162] N. Gentile, M.J. Rossi, O. Delemont, R.T.W. Siegwolf, δ^{15}N measurement of organic and inorganic substances by EA-IRMS: a speciation-dependent procedure, Anal. Bioanal. Chem. 405(1) (2013) 159-76.
[163] W. Meier-Augenstein, H.F. Kemp, C.M. Lock, N_2: a potential pitfall for bulk ^{2}H isotope analysis of explosives and other nitrogen-rich compounds by continuous-flow isotope-ratio mass spectrometry, Rapid Commun. Mass Spectrom. 23(13) (2009) 2011-6.
[164] M.J. Lott, J.D. Howa, L.A. Chesson, J.R. Ehleringer, Improved accuracy and precision in $\delta^{15}N_{AIR}$ measurements of explosives, urea, and inorganic nitrates by elemental analyzer/isotope ratio mass spectrometry using thermal decomposition, Rapid Commun. Mass Spectrom. 29(15) (2015) 1381-8.
[165] R. Aranda IV, L.A. Stern, M.E. Dietz, M.C. McCormick, J.A. Barrow, R.F. Mothershead II, Forensic utility of isotope ratio analysis of the explosive urea nitrate and its precursors, Forensic Sci. Int. 206(1-3) (2011) 143-9.
[166] J.D. Howa, M.J. Lott, J.R. Ehleringer, Isolation and stable nitrogen isotope analysis of ammonium ions in ammonium nitrate prills using sodium tetraphenylborate, Rapid Commun. Mass Spectrom. 28(13) (2014) 1530-4.

[167] B.L. Grimm, L.A. Stern, A.J. Lowe, Forensic utility of a nitrogen and oxygen isotope ratio time series of ammonium nitrate and its isolated ions, Talanta 178 (2018) 94-101.
[168] S.J. Benson, C.J. Lennard, P. Maynard, D.M. Hill, A.S. Andrew, C. Roux, Forensic analysis of explosives using isotope ratio mass spectrometry (IRMS)-preliminary study on TATP and PETN, Sci. Justice 49(2) (2009) 81-6.
[169] J.D. Howa, J.E. Barnette, L.A. Chesson, M.J. Lott, J.R. Ehleringer, TATP isotope ratios as influenced by worldwide acetone variation, Talanta 181 (2018) 125-131.
[170] J.D. Howa, M.J. Lott, J.R. Ehleringer, Observations and sources of carbon and nitrogen isotope ratio variation of pentaerythritol tetranitrate (PETN), Forensic Sci. Int. 244 (2014) 152-7.
[171] N. Gentile, R.T.W. Siegwolf, O. Delémont, Study of isotopic variations in black powder: reflections on the use of stable isotopes in forensic science for source inference, Rapid Commun. Mass Spectrom. 23 (2009) 2559–2567.
[172] A.T. Quirk, J.M. Bellerby, J.F. Carter, F.A. Thomas, J.C. Hill, An initial evaluation of stable isotopic characterisation of post-blast plastic debris from improvised explosive devices, Sci. Justice 49(2) (2009) 87-93.
[173] D. Widory, J.J. Minet, M. Barbe-Leborgne, Sourcing explosives: a multi-isotope approach, Sci. Justice 49(2) (2009) 62-72.
[174] C.M. Lock, H. Brust, M. van Breukelen, J. Dalmolen, M. Koeberg, D.A. Stoker, Investigation of isotopic linkages between precursor materials and the improvised high explosive product hexamethylene triperoxide diamine, Anal. Chem. 84(11) (2012) 4984-92.
[175] J.D. Howa, M.J. Lott, L.A. Chesson, J.R. Ehleringer, Carbon and nitrogen isotope ratios of factory-produced RDX and HMX, Forensic Sci. Int. 240 (2014) 80-7.
[176] K. Bezemer, R. Woortmeijer, M. Koeberg, W. Wiarda, P. Schoenmakers, A. van Asten, Multicomponent characterization and differentiation of flash bangers - Part II: Elemental profiling of plastic caps, Forensic Sci. Int. 290 (2018) 336-348.
[177] L.A. Chesson, J.D. Howa, M.J. Lott, J.R. Ehleringer, Development of a methodological framework for applying isotope ratio mass spectrometry to explosive components, Forensic Chem. 2 (2016) 9-14.
[178] J.D. Howa, M.J. Lott, L.A. Chesson, J.R. Ehleringer, Isolation of components of plastic explosives for isotope ratio mass spectrometry, Forensic Chem. 1 (2016) 6-12.
[179] G.P. Danezis, A.S. Tsagkaris, F. Camin, V. Brusic, C.A. Georgiou, Food authentication: Techniques, trends & emerging approaches, TrAC, Trends Anal. Chem. 85 (2016) 123-132.
[180] F. Camin, M. Boner, L. Bontempo, C. Fauhl-Hassek, S.D. Kelly, J. Riedl, A. Rossmann, Stable isotope techniques for verifying the declared geographical origin of food in legal cases, Trends Food Sci. Technol. 61 (2017) 176-187.
[181] F. Camin, L. Bontempo, M. Perini, E. Piasentier, Stable isotope ratio analysis for assessing the authenticity of food of animal origin, Compr. Rev. Food Sci. Food Saf. 15(5) (2016) 868-877.
[182] AOAC, Official Method 998.12. C_4 plant sugars in honey, Official Methods of Analysis of AOAC International 2 (1999) 27-30.
[183] A. Simsek, M. Bilsel, A.C. Goren, $^{13}C/^{12}C$ pattern of honey from Turkey and determination of adulteration in commercially available honey samples using EA-IRMS, Food Chem. 130(4) (2012) 1115-1121.
[184] V. Berriel, C. Perdomo, Determination of high fructose corn syrup concentration in Uruguayan honey by ^{13}C analyses, LWT Food Sci. Technol. 73 (2016) 649-653.

[185] A.I. Cabanero, J.L. Recio, M. Ruperez, Liquid chromatography coupled to isotope ratio mass spectrometry: a new perspective on honey adulteration detection, J. Agric. Food. Chem. 54(26) (2006) 9719-27.
[186] A. Guler, H. Kocaokutgen, A.V. Garipoglu, H. Onder, D. Ekinci, S. Biyik, Detection of adulterated honey produced by honeybee (*Apis mellifera* L.) colonies fed with different levels of commercial industrial sugar (C_3 and C_4 plants) syrups by the carbon isotope ratio analysis, Food Chem. 155 (2014) 155-60.
[187] M. Tosun, Detection of adulteration in honey samples added various sugar syrups with $^{13}C/^{12}C$ isotope ratio analysis method, Food Chem. 138(2-3) (2013) 1629-32.
[188] K.M. Rogers, M. Grainger, M. Manley-Harris, The unique manuka effect: why New Zealand manuka honey fails the AOAC 998.12 C_4 sugar method, J. Agric. Food. Chem. 62(12) (2014) 2615-22.
[189] L. Elflein, K.-P. Raezke, Improved detection of honey adulteration by measuring differences between $^{13}C/^{12}C$ stable carbon isotope ratios of protein and sugar compounds with a combination of elemental analyzer - isotope ratio mass spectrometry and liquid chromatography - isotope ratio mass spectrometry (δ^{13}C-EA/LC-IRMS), Apidologie 39(5) (2008) 574-587.
[190] H. Dong, K. Xiao, Y. Xian, Y. Wu, Authenticity determination of honeys with non-extractable proteins by means of elemental analyzer (EA) and liquid chromatography (LC) coupled to isotope ratio mass spectroscopy (IRMS), Food Chem. 240 (2018) 717-724.
[191] A. Schellenberg, S. Chmielus, C. Schlicht, F. Camin, M. Perini, L. Bontempo, K. Heinrich, S.D. Kelly, A. Rossmann, F. Thomas, E. Jamin, M. Horacek, Multielement stable isotope ratios (H, C, N, S) of honey from different European regions, Food Chem. 121(3) (2010) 770-777.
[192] Z. Wu, L. Chen, L. Wu, X. Xue, J. Zhao, Y. Li, Z. Ye, G. Lin, Classification of Chinese honeys according to their floral origins using elemental and stable isotopic compositions, J. Agric. Food. Chem. 63(22) (2015) 5388-94.
[193] Y. Zhao, B. Zhang, G. Chen, A. Chen, S. Yang, Z. Ye, Recent developments in application of stable isotope analysis on agro-product authenticity and traceability, Food Chem. 145 (2014) 300-5.
[194] J.F. Carter, L.A. Chesson, Food forensics: stable isotopes as a guide to authenticity and origin, CRC Press, Boca Raton, 2017.
[195] L.D. Coletta, A.L. Pereira, A.A.D. Coelho, V.J.M. Savino, J.F.M. Menten, E. Correr, L.C. França, L.A. Martinelli, Barn vs. free-range chickens: Differences in their diets determined by stable isotopes, Food Chem. 131(1) (2012) 155-160.
[196] R.P. Oliveira, C. Ducatti, A.C. Pezzato, J.C. Denadai, V.C. Cruz, J.R. Sartori, A.S. Carrijo, F.R. Caldara, Traceability of poultry offal meal in broiler feeding using isotopic analysis (δ^{13}C and δ^{15}N) of different tissues, Brazilian Journal of Poultry Science 12(1) (2010) 13-20.
[197] C.N. Rhodes, J.H. Lofthouse, S. Hird, P. Rose, P. Reece, J. Christy, R. Macarthur, P.A. Brereton, The use of stable carbon isotopes to authenticate claims that poultry have been corn-fed, Food Chem. 118(4) (2010) 927-932.
[198] V.C. Cruz, P.C. Araujo, J.R. Sartori, A.C. Pezzato, J.C. Denadai, G.V. Polycarpo, L.H. Zanetti, C. Ducatti, Poultry offal meal in chicken: traceability using the technique of carbon ($^{13}C/^{12}C$)- and nitrogen ($^{15}N/^{14}N$)-stable isotopes, Poult. Sci. 91(2) (2012) 478-86.
[199] I. González-Martin, C. González-Pérez, M.J. Hernández, E. Marqués-Macias, S.F. Poveda, Use of isotope analysis to characterize meat from Iberian-breed swine, Meat Science 52 (1999) 437-441.

[200] I. González-Martin, C. González-Pérez, J.H. Méndez, C.S. González, Differentiation of dietary regimene of Iberian swine by means of isotopic analysis of carbon and sulphur in hepatic tissue, Meat Science 58 (2001) 25-30.
[201] M.T. Osorio, G. Downey, A.P. Moloney, F.T. Rohrle, G. Luciano, O. Schmidt, F.J. Monahan, Beef authentication using dietary markers: chemometric selection and modelling of significant beef biomarkers using concatenated data from multiple analytical methods, Food Chem. 141(3) (2013) 2795-801.
[202] T. Devincenzi, O. Delfosse, D. Andueza, C. Nabinger, S. Prache, Dose-dependent response of nitrogen stable isotope ratio to proportion of legumes in diet to authenticate lamb meat produced from legume-rich diets, Food Chem. 152 (2014) 456-61.
[203] L. Bontempo, F. Camin, L. Ziller, L. Biondi, M.G. D'Urso, V. Vasta, G. Luciano, Variations in stable isotope ratios in lamb blood fractions following dietary changes: a preliminary study, Rapid Commun. Mass Spectrom. 30(1) (2016) 170-4.
[204] E. Ehtesham, A. Hayman, R. Van Hale, R. Frew, Influence of feed and water on the stable isotopic composition of dairy milk, Int. Dairy J. 47 (2015) 37-45.
[205] B.L. Guo, Y.M. Wei, J.R. Pan, Y. Li, Stable C and N isotope ratio analysis for regional geographical traceability of cattle in China, Food Chem. 118(4) (2010) 915-920.
[206] G. Rees, S.D. Kelly, P. Cairns, H. Ueckermann, S. Hoelzl, A. Rossmann, M.J. Scotter, Verifying the geographical origin of poultry: The application of stable isotope and trace element (SITE) analysis, Food Control 67 (2016) 144-154.
[207] A. Trembaczowski, Use of sulphur and carbon stable-isotope composition of fish scales and muscles to identify the origin of fish, Mineralogia 42(1) (2011).
[208] J.F. Carter, U. Tinggi, X. Yang, B. Fry, Stable isotope and trace metal compositions of Australian prawns as a guide to authenticity and wholesomeness, Food Chem. 170 (2015) 241-8.
[209] M.P. Chaguri, A.L. Maulvault, M.L. Nunes, D.A. Santiago, J.C. Denadai, F.H. Fogaça, L.S. Sant'Ana, C. Ducatti, N. Bandarra, M.L. Carvalho, A. Marques, Different tools to trace geographic origin and seasonality of croaker (*Micropogonias furnieri*), LWT Food Sci. Technol. 61(1) (2015) 194-200.
[210] H. Kim, K. Suresh Kumar, K.-H. Shin, Applicability of stable C and N isotope analysis in inferring the geographical origin and authentication of commercial fish (Mackerel, Yellow Croaker and Pollock), Food Chem. 172C (2015) 523-7.
[211] I. Ortea, J.M. Gallardo, Investigation of production method, geographical origin and species authentication in commercially relevant shrimps using stable isotope ratio and/or multi-element analyses combined with chemometrics: an exploratory analysis, Food Chem. 170 (2015) 145-53.
[212] L.A. Chesson, L.O. Valenzuela, S.P. O'Grady, T.E. Cerling, J.R. Ehleringer, Hydrogen and oxygen stable isotope ratios of milk in the United States, J. Agric. Food. Chem. 58(4) (2010) 2358-2363.
[213] E. Ehtesham, A.R. Hayman, K.A. McComb, R. Van Hale, R.D. Frew, Correlation of geographical location with stable isotope values of hydrogen and carbon of fatty acids from New Zealand milk and bulk milk powder, J. Agric. Food. Chem. 61(37) (2013) 8914-23.
[214] R. Stevenson, S. Desrochers, J.-F. Hélie, Stable and radiogenic isotopes as indicators of agri-food provenance: Insights from artisanal cheeses from Quebec, Canada, Int. Dairy J. 49 (2015) 37-45.

[215] M. Nečemer, D. Potočnik, N. Ogrinc, Discrimination between Slovenian cow, goat and sheep milk and cheese according to geographical origin using a combination of elemental content and stable isotope data, J. Food Compost. Anal. 52 (2016) 16-23.
[216] F. Longobardi, G. Casiello, M. Cortese, M. Perini, F. Camin, L. Catucci, A. Agostiano, Discrimination of geographical origin of lentils (*Lens culinaris* Medik.) using isotope ratio mass spectrometry combined with chemometrics, Food Chem. 188 (2015) 343-9.
[217] T. Mimmo, F. Camin, L. Bontempo, C. Capici, M. Tagliavini, S. Cesco, M. Scampicchio, Traceability of different apple varieties by multivariate analysis of isotope ratio mass spectrometry data, Rapid Commun. Mass Spectrom. 29(21) (2015) 1984-90.
[218] E. de Rijke, J.C. Schoorl, C. Cerli, H.B. Vonhof, S.J. Verdegaal, G. Vivo-Truyols, M. Lopatka, R. Dekter, D. Bakker, M.J. Sjerps, M. Ebskamp, C.G. de Koster, The use of δ^{2}H and δ^{18}O isotopic analyses combined with chemometrics as a traceability tool for the geographical origin of bell peppers, Food Chem. 204 (2016) 122-8.
[219] M. Perini, L. Giongo, M. Grisenti, L. Bontempo, F. Camin, Stable isotope ratio analysis of different European raspberries, blackberries, blueberries, currants and strawberries, Food Chem. 239 (2018) 48-55.
[220] N.S. Podio, M.V. Baroni, R.G. Badini, M. Inga, H.A. Ostera, M. Cagnoni, E.A. Gautier, P.P. Garcia, J. Hoogewerff, D.A. Wunderlin, Elemental and isotopic fingerprint of Argentinean wheat. Matching soil, water, and crop composition to differentiate provenance, J. Agric. Food. Chem. 61(16) (2013) 3763-73.
[221] D. Luo, H. Dong, H. Luo, Y. Xian, J. Wan, X. Guo, Y. Wu, The application of stable isotope ratio analysis to determine the geographical origin of wheat, Food Chem. 174 (2015) 197-201.
[222] Y. Wu, D. Luo, H. Dong, J. Wan, H. Luo, Y. Xian, X. Guo, F. Qin, W. Han, L. Wang, B. Wang, Geographical origin of cereal grains based on element analyser-stable isotope ratio mass spectrometry (EA-SIRMS), Food Chem. 174 (2015) 553-7.
[223] I.M. Chung, J.K. Kim, M. Prabakaran, J.H. Yang, S.H. Kim, Authenticity of rice (*Oryza sativa* L.) geographical origin based on analysis of C, N, O and S stable isotope ratios: a preliminary case report in Korea, China and Philippine, J. Sci. Food Agric. 96(7) (2016) 2433-9.
[224] I.M. Chung, J.K. Kim, K.J. Lee, S.K. Park, J.H. Lee, N.Y. Son, Y.I. Jin, S.H. Kim, Geographic authentication of Asian rice (*Oryza sativa* L.) using multi-elemental and stable isotopic data combined with multivariate analysis, Food Chem. 240 (2018) 840-849.
[225] L. Bontempo, F. Camin, M. Paolini, C. Micheloni, K.H. Laursen, Multi-isotopic signatures of organic and conventional Italian pasta along the production chain, J. Mass Spectrom. 51(9) (2016) 675-83.
[226] M. Bononi, G. Quaglia, F. Tateo, Easy extraction method to evaluate δ^{13}C vanillin by liquid chromatography-isotopic ratio mass spectrometry in chocolate bars and chocolate snack foods, J. Agric. Food. Chem. 63(19) (2015) 4777-81.
[227] J.F. Carter, H.S. Yates, U. Tinggi, Isotopic and elemental composition of roasted coffee as a guide to authenticity and origin, J. Agric. Food. Chem. 63(24) (2015) 5771-9.
[228] L.A. Chesson, L.O. Valenzuela, S.P. O'Grady, T.E. Cerling, J.R. Ehleringer, Links between purchase location and stable isotope ratios of bottled water, soda, and beer in the United States, J. Agric. Food. Chem. 58(12) (2010) 7311-6.
[229] S. Rummel, S. Hoelzl, P. Horn, A. Rossmann, C. Schlicht, The combination of stable isotope abundance ratios of H, C, N and S with ^{87}Sr/^{86}Sr for geographical origin assignment of orange juices, Food Chem. 118(4) (2010) 890-900.

[230] S.V. Dutra, L. Adami, A.R. Marcon, G.J. Carnieli, C.A. Roani, F.R. Spinelli, S. Leonardelli, R. Vanderlinde, Characterization of wines according the geographical origin by analysis of isotopes and minerals and the influence of harvest on the isotope values, Food Chem. 141(3) (2013) 2148-53.
[231] M. Perini, F. Camin, $\delta^{18}O$ of ethanol in wine and spirits for authentication purposes, J. Food Sci. 78(6) (2013) C839-44.
[232] J.F. Carter, H.S. Yates, U. Tinggi, A global survey of the stable isotope and chemical compositions of bottled and canned beers as a guide to authenticity, Sci. Justice 55(1) (2015) 18-26.
[233] J.F. Carter, H.S. Yates, U. Tinggi, Stable isotope and chemical compositions of European and Australasian ciders as a guide to authenticity, J. Agric. Food. Chem. 63(3) (2015) 975-82.
[234] M. Horacek, K. Hansel-Hohl, K. Burg, G. Soja, W. Okello-Anyanga, S. Fluch, Control of origin of sesame oil from various countries by stable isotope analysis and DNA based markers-A pilot study, PLoS One 10(4) (2015) 12.
[235] H. Jeon, S.C. Lee, Y.J. Cho, J.H. Oh, K. Kwon, B.H. Kim, A triple-isotope approach for discriminating the geographic origin of Asian sesame oils, Food Chem. 167 (2015) 363-9.
[236] F. Camin, A. Pavone, L. Bontempo, R. Wehrens, M. Paolini, A. Faberi, R.M. Marianella, D. Capitani, S. Vista, L. Mannina, The use of IRMS, ^{1}H NMR and chemical analysis to characterise Italian and imported Tunisian olive oils, Food Chem. 196 (2016) 98-105.
[237] F. Chiocchini, S. Portarena, M. Ciolfi, E. Brugnoli, M. Lauteri, Isoscapes of carbon and oxygen stable isotope compositions in tracing authenticity and geographical origin of Italian extra-virgin olive oils, Food Chem. 202 (2016) 291-301.
[238] L.A. Martinelli, G.B. Nardoto, L.A. Chesson, F.D. Rinaldi, J.P.H.B. Ometto, T.E. Cerling, J.R. Ehleringer, Worldwide stable carbon and nitrogen isotopes of Big Mac® patties: An example of a truly "glocal" food, Food Chem. 127(4) (2011) 1712-1718.
[239] L.A. Chesson, Flesh foods, or What can stable isotope analysis reveal about the meat you eat?, in: J.F. Carter, L.A. Chesson (Eds.), Food forensics: stable isotopes as a guide to authenticity and origin, CRC Press, Boca Raton, 2017, pp. 115–152.
[240] L.A. Chesson, L.O. Valenzuela, G.J. Bowen, T.E. Cerling, J.R. Ehleringer, Consistent predictable patterns in the hydrogen and oxygen stable isotope ratios of animal proteins consumed by modern humans in the USA, Rapid Commun. Mass Spectrom. 25(24) (2011) 3713-3722.
[241] J.N. Bostic, S.J. Palafox, M.E. Rottmueller, A.H. Jahren, Effect of baking and fermentation on the stable carbon and nitrogen isotope ratios of grain-based food, Rapid Commun. Mass Spectrom. 29(10) (2015) 937-47.
[242] R. Fernandes, J. Meadows, A. Dreves, M.-J. Nadeau, P. Grootes, A preliminary study on the influence of cooking on the C and N isotopic composition of multiple organic fractions of fish (mackerel and haddock), J. Archaeol. Sci. 50 (2014) 153-159.
[243] B. Doering, Measuring the potential influence of cooking on the carbon and nitrogen isotopic composition of spawning Chinook salmon, Journal of Archaeological Science: Reports 12 (2017) 491-498.
[244] J. Zhou, B. Guo, Y. Wei, G. Zhang, S. Wei, Y. Ma, The effect of different cooking processes on stable C, N, and H isotopic compositions of beef, Food Chem. 182 (2015) 23-6.
[245] A. Royer, V. Daux, F. Fourel, C. Lecuyer, Carbon, nitrogen and oxygen isotope fractionation during food cooking: Implications for the interpretation of the fossil human record, Am. J. Phys. Anthropol. 163(4) (2017) 759-771.

[246] H. Willer, J. Lernoud, The world of organic agriculture. Statistics and emerging trends 2016. , Research Institute of Organic Agriculture (FiBL), Frick, and IFOAM – Organics International, Bonn, 2016.
[247] J. Molkentin, A. Giesemann, Follow-up of stable isotope analysis of organic versus conventional milk, Anal. Bioanal. Chem. 398(3) (2010) 1493-500.
[248] J. Molkentin, Applicability of organic milk indicators to the authentication of processed products, Food Chem. 137(1-4) (2013) 25-30.
[249] I.M. Chung, I. Park, J.Y. Yoon, Y.S. Yang, S.H. Kim, Determination of organic milk authenticity using carbon and nitrogen natural isotopes, Food Chem. 160 (2014) 214-8.
[250] S. Kaffarnik, M. Schröder, K. Lehnert, T. Baars, W. Vetter, δ^{13}C values and phytanic acid diastereomer ratios: combined evaluation of two markers suggested for authentication of organic milk and dairy products, Eur. Food Res. Technol. 238(5) (2014) 819-827.
[251] S. Erich, S. Schill, E. Annweiler, H.U. Waiblinger, T. Kuballa, D.W. Lachenmeier, Y.B. Monakhova, Combined chemometric analysis of ^{1}H NMR, ^{13}C NMR and stable isotope data to differentiate organic and conventional milk, Food Chem. 188 (2015) 1-7.
[252] K.M. Rogers, Stable isotopes as a tool to differentiate eggs laid by caged, barn, free range, and organic hens, J. Agric. Food. Chem. 57(10) (2009) 4236-42.
[253] J. Molkentin, I. Lehmann, U. Ostermeyer, H. Rehbein, Traceability of organic fish – Authenticating the production origin of salmonids by chemical and isotopic analyses, Food Control 53 (2015) 55-66.
[254] Y. Zhao, S. Yang, D. Wang, Stable carbon and nitrogen isotopes as a potential tool to differentiate pork from organic and conventional systems, J. Sci. Food Agric. 96(11) (2016) 3950-5.
[255] C.T. Inácio, P.M. Chalk, A.M.T. Magalhães, Principles and Limitations of Stable Isotopes in Differentiating Organic and Conventional Foodstuffs: 1. Plant Products, Crit. Rev. Food Sci. Nutr. 55(9) (2015) 1206-1218.
[256] C.T. Inácio, P.M. Chalk, Principles and limitations of stable isotopes in differentiating organic and conventional foodstuffs: 2. Animal products, Crit. Rev. Food Sci. Nutr. 57(1) (2017) 181-196.
[257] S.D. Kelly, A.S. Bateman, Comparison of mineral concentrations in commercially grown organic and conventional crops – Tomatoes (*Lycopersicon esculentum*) and lettuces (*Lactuca sativa*), Food Chem. 119(2) (2010) 738-745.
[258] K.H. Laursen, A. Mihailova, S.D. Kelly, V.N. Epov, S. Berail, J.K. Schjoerring, O.F. Donard, E.H. Larsen, N. Pedentchouk, A.D. Marca-Bell, U. Halekoh, J.E. Olesen, S. Husted, Is it really organic? - Multi-isotopic analysis as a tool to discriminate between organic and conventional plants, Food Chem. 141(3) (2013) 2812-20.
[259] M. Paolini, L. Ziller, K.H. Laursen, S. Husted, F. Camin, Compound-Specific δ^{15}N and δ^{13}C Analyses of Amino Acids for Potential Discrimination between Organically and Conventionally Grown Wheat, J. Agric. Food. Chem. 63(25) (2015) 5841-50.
[260] M. Hohmann, Y. Monakhova, S. Erich, N. Christoph, H. Wachter, U. Holzgrabe, Differentiation of organically and conventionally grown tomatoes by chemometric analysis of combined data from proton nuclear magnetic resonance and mid-infrared spectroscopy and stable isotope analysis, J. Agric. Food. Chem. 63(43) (2015) 9666-75.
[261] A. Mihailova, N. Pedentchouk, S.D. Kelly, Stable isotope analysis of plant-derived nitrate - novel method for discrimination between organically and conventionally grown vegetables, Food Chem. 154 (2014) 238-45.

[262] N. Christoph, A. Hermann, H. Wachter, 25 Years authentication of wine with stable isotope analysis in the European Union – Review and outlook, BIO Web of Conferences 5 (2015) 02020.
[263] H. Chen, B.H. Shen, S.J. Zhang, P. Xiang, X.Y. Zhuo, M. Shen, Alcohol consumption or contamination: A preliminary study on the determination of the ethanol origin by stable carbon isotope analysis, Forensic Sci. Int. 289 (2018) 374-380.
[264] H. Kawashima, The measurement of stable carbon isotope ratios of eight methamidophos samples, J. Forensic Sci. 60(5) (2015) 1360-4.
[265] E. Ehtesham, F. Camin, L. Bontempo, R.D. Frew, Stable isotope measurements and modeling to verify the authenticity of dairy products, in: J.F. Carter, L.A. Chesson (Eds.), Food Forensics: Stable Isotopes as a Guide to Authenticity and Origin, CRC Press, Boca Raton, 2017, pp. 239–256.
[266] B.Y. Song, S. Gwak, M. Jung, G. Nam, N.Y. Kim, Tracing the source of methomyl using stable isotope analysis, Rapid Commun. Mass Spectrom. 32(3) (2018) 235-240.
[267] G. Michalski, S. Earman, C. Dahman, R.L. Hershey, T. Mihevc, Multiple isotope forensics of nitrate in a wild horse poisoning incident, Forensic Sci. Int. 198(1-3) (2010) 103-9.
[268] H.W. Kreuzer, J. Horita, J.J. Moran, B.A. Tomkins, D.B. Janszen, A. Carman, Stable carbon and nitrogen isotope ratios of sodium and potassium cyanide as a forensic signature, J. Forensic Sci. 57(1) (2012) 75-9.
[269] I. Tea, I. Antheaume, B.L. Zhang, A test to identify cyanide origin by isotope ratio mass spectrometry for forensic investigation, Forensic Sci. Int. 217(1-3) (2012) 168-73.
[270] H.W. Kreuzer, J.B. West, J.R. Ehleringer, Forensic applications of light-element stable isotope ratios of *Ricinus communis* seeds and ricin preparations, J. Forensic Sci. 58 Suppl 1 (2013) S43-51.
[271] J.J. Moran, C.G. Fraga, M.K. Nims, Stable-carbon isotope ratios for sourcing the nerve-agent precursor methylphosphonic dichloride and its products, Talanta 186 (2018) 678-683.
[272] V. Causin, C. Marega, A. Marigo, R. Casamassima, G. Peluso, L. Ripani, Forensic differentiation of paper by X-ray diffraction and infrared spectroscopy, Forensic Sci. Int. 197(1-3) (2010) 70-4.
[273] T. Trejos, A. Flores, J.R. Almirall, Micro-spectrochemical analysis of document paper and gel inks by laser ablation inductively coupled plasma mass spectrometry and laser induced breakdown spectroscopy, Spectrochim. Acta, Pt. B: Atom. Spectrosc. 65(11) (2010) 884-895.
[274] C. Neumann, R. Ramotowski, T. Genessay, Forensic examination of ink by high-performance thin layer chromatography - The United States Secret Service Digital Ink Library, J. Chromatogr. A 1218(19) (2011) 2793-811.
[275] C.E. Berger, D. Ramos, Objective paper structure comparison: assessing comparison algorithms, Forensic Sci. Int. 222(1-3) (2012) 360-7.
[276] J.A. Green, Reliability of paper brightness in authenticating documents, J. Forensic Sci. 57(4) (2012) 1003-7.
[277] Review of the scientific approaches used during the FBI's investigation of the 2001 anthrax letters, The National Academies Press, Washington, DC, 2011.
[278] K. Jones, S. Benson, C. Roux, The forensic analysis of office paper using carbon isotope ratio mass spectrometry - Part 1: understanding the background population and homogeneity of paper for the comparison and discrimination of samples, Forensic Sci. Int. 231(1-3) (2013) 354-63.
[279] K. Jones, S. Benson, C. Roux, The forensic analysis of office paper using carbon isotope ratio mass spectrometry -Part 2: method development, validation and sample handling, Forensic Sci. Int. 231(1-3) (2013) 364-74.

[280] K. Jones, S. Benson, C. Roux, The forensic analysis of office paper using carbon isotope ratio mass spectrometry. Part 3: Characterizing the source materials and the effect of production and usage on the $\delta^{13}C$ values of paper, Forensic Sci. Int. 233(1-3) (2013) 355-64.
[281] K. Jones, S. Benson, C. Roux, The forensic analysis of office paper using oxygen isotope ratio mass spectrometry. Part 1: Understanding the background population and homogeneity of paper for the comparison and discrimination of samples, Forensic Sci. Int. 262 (2016) 97-107.
[282] K. Jones, S. Benson, C. Roux, The forensic analysis of office paper using oxygen Isotope Ratio Mass Spectrometry, part 2: Characterising the source materials and the effect of production and usage on the $\delta^{18}O$ values of cellulose and paper, Forensic Sci. Int. 268 (2016) 151-158.
[283] A. van Es, J. de Koeijer, G. van der Peijl, Discrimination of document paper by XRF, LA–ICP–MS and IRMS using multivariate statistical techniques, Sci. Justice 49(2) (2009) 120-126.
[284] A. Braz, M. Lopez-Lopez, C. Garcia-Ruiz, Raman spectroscopy for forensic analysis of inks in questioned documents, Forensic Sci. Int. 232(1-3) (2013) 206-12.
[285] A. Braz, M. Lopez-Lopez, C. Garcia-Ruiz, Studying the variability in the Raman signature of writing pen inks, Forensic Sci. Int. 245C (2014) 38-44.
[286] C.K. Muro, K.C. Doty, J. Bueno, L. Halamkova, I.K. Lednev, Vibrational spectroscopy: recent developments to revolutionize forensic science, Anal. Chem. 87(1) (2015) 306-27.
[287] L.A. Chesson, B.J. Tipple, J.E. Barnette, T.E. Cerling, J.R. Ehleringer, The potential for application of ink stable isotope analysis in questioned document examination, Sci. Justice 55(1) (2015) 27-33.
[288] Y. Suzuki, R. Kobe, R. Nakashita, A novel method to discriminate between natural and synthetic fibers by stable carbon, nitrogen, and oxygen isotope analyses, Chem. Lett. 41(3) (2012) 242-243.
[289] N.N. Daeid, W. Meier-Augenstein, H.F. Kemp, Investigating the provenance of un-dyed spun cotton fibre using multi-isotope profiles and chemometric analysis, Rapid Commun. Mass Spectrom. 25(13) (2011) 1812-6.
[290] W. Meier-Augenstein, H.F. Kemp, E.R. Schenk, J.R. Almirall, Discrimination of unprocessed cotton on the basis of geographic origin using multi-element stable isotope signatures, Rapid Commun. Mass Spectrom. 28(5) (2014) 545-52.
[291] K. Jones, F. Koens, T. Simpson, Background survey of polyethylene in the Australian Capital Territory - A demonstration of variability in isotopic abundance values and their application to forensic casework, Sci. Justice 58(4) (2018) 276-281.
[292] F.A. Idoine, J.F. Carter, R. Sleeman, Bulk and compound-specific isotopic characterisation of illicit heroin and cling film, Rapid Commun. Mass Spectrom. 19(22) (2005) 3207-3215.
[293] J.F. Carter, R. Sleeman, J.C. Hill, F. Idoine, E.L. Titterton, Isotope ratio mass spectrometry as a tool for forensic investigation (examples from recent studies), Sci. Justice 45(3) (2005) 141-149.
[294] E. Taylor, J.F. Carter, J.C. Hill, C. Morton, N.N. Daeid, R. Sleeman, Stable isotope ratio mass spectrometry and physical comparison for the forensic examination of grip-seal plastic bags, Forensic Sci. Int. 177(2-3) (2008) 214-20.
[295] J.F. Carter, P.L. Grundy, J.C. Hill, N.C. Ronan, E.L. Titterton, R. Sleeman, Forensic isotope ratio mass spectrometry of packaging tapes, Analyst 129(12) (2004) 1206-10.
[296] M. Horacek, J.S. Min, S. Heo, J. Park, W. Papesch, The application of isotope ratio mass spectrometry for discrimination and comparison of adhesive tapes, Rapid Commun. Mass Spectrom. 22(11) (2008) 1763-6.

[297] K.W. McMahon, S.D. Newsome, Amino acid isotope analysis: A new frontier in studies of animal migration and foraging ecology, in: K.A. Hobson, L.I. Wassenaar (Eds.), Tracking Animal Migration with Stable Isotopes, Academic Press2019, pp. 173-190.
[298] S. Khodjaniyazova, M. Nazari, K.P. Garrard, M.P.V. Matos, G.P. Jackson, D.C. Muddiman, Characterization of the spectral accuracy of an orbitrap mass analyzer using Isotope Ratio Mass Spectrometry, Anal. Chem. 90(3) (2018) 1897-1906.
[299] A.A. Baczynski, P.J. Polissar, D. Juchelka, J. Schwieters, A. Hilkert, R.E. Summons, K.H. Freeman, Picomolar-scale compound-specific isotope analyses, Rapid Commun. Mass Spectrom. 32(9) (2018) 730-738.
[300] B. Fry, J.F. Carter, K. Yamada, N. Yoshida, D. Juchelka, Position-specific $^{13}C/^{12}C$ analysis of amino acid carboxyl groups - automated flow-injection analysis based on reaction with ninhydrin, Rapid Commun. Mass Spectrom. 32(12) (2018) 992-1000.
[301] P.H. Ostrom, M. Colunga-Garcia, S.H. Gage, Establishing pathways of energy flow for insect predators using stable isotope ratios: field and laboratory evidence, Oecologia 109 (1997) 108-113.
[302] C. Gratton, A.E. Forbes, Changes in delta 13C stable isotopes in multiple tissues of insect predators fed isotopically distinct prey, Oecologia 147(4) (2006) 615-24.
[303] R. Hood-Nowotny, B.G.J. Knols, Stable isotope methods in biological and ecological studies of arthropods, Entomol. Exp. Appl. 124(1) (2007) 3-16.
[304] T.M. Tibbets, L.A. Wheeless, C.M. del Rio, Isotopic enrichment without change in diet: an ontogenetic shift in δ15N during insect metamorphosis, Funct. Ecol. 22 (2008) 109-113.
[305] P.M. Wehi, B.J. Hicks, Isotopic fractionation in a large herbivorous insect, the Auckland tree weta, J. Insect Physiol. 56(12) (2010) 1877-82.
[306] F. Hyodo, Use of stable carbon and nitrogen isotopes in insect trophic ecology, Entomol. Sci. 18(3) (2015) 295-312.
[307] D.M. O'Brien, M.L. Fogel, C.L. Boggs, Renewable and nonrenewable resources: amino acid turnover and allocation to reproduction in Lepidoptera, Proc. Natl. Acad. Sci. U. S. A. 99(7) (2002) 4413-8.
[308] D.M. O'Brien, C.L. Boggs, M.L. Fogel, Pollen feeding in the butterfly Heliconius charitonia: isotopic evidence for essential amino acid transfer from pollen to eggs, Proc. Biol. Sci. 270(1533) (2003) 2631-6.
[309] Y. Chikaraishi, N.O. Ogawa, H. Doi, N. Ohkouchi, 15N/14N ratios of amino acids as a tool for studying terrestrial food webs: a case study of terrestrial insects (bees, wasps, and hornets), Ecol. Res. 26(4) (2011) 835-844.
[310] M.J. Swift, O.W. Heal, J.M. Anderson, Decomposition in terrestrial ecosystems, University of California Press, Berkeley and Los Angeles, CA, 1979.
[311] J.C. Moore, E.L. Berlow, D.C. Coleman, P.C. Ruiter, Q. Dong, A. Hastings, N.C. Johnson, K.S. McCann, K. Melville, P.J. Morin, K. Nadelhoffer, A.D. Rosemond, D.M. Post, J.L. Sabo, K.M. Scow, M.J. Vanni, D.H. Wall, Detritus, trophic dynamics and biodiversity, Ecol. Lett. 7(7) (2004) 584-600.
[312] Carrion Ecology, Evolution, and their Applications, CRC Press, Boca Raton, FL, 2015.
[313] L.H. Yang, Periodical cicadas as resource pulses in North American forests, Science 306 (2004) 1565–1567.
[314] Forensic Entomology: the utility of arthropods in legal investigations, 2nd ed. ed., Taylor & Francis: Boca Raton2009.

[315] R.M. Mohr, J.K. Tomberlin, Development and validation of a new technique for estimating a minimum postmortem interval using adult blow fly (Diptera: Calliphoridae) carcass attendance, Int. J. Legal Med. 129(4) (2015) 851-9.
[316] A.M. Tarone, M.R. Sanford, Is PMI the hypothesis or the null hypothesis?, J. Med. Entomol. 54(5) (2017) 1109-1115.
[317] J.K. Tomberlin, R. Mohr, M.E. Benbow, A.M. Tarone, S. VanLaerhoven, A roadmap for bridging basic and applied research in forensic entomology, Annu. Rev. Entomol. 56 (2011) 401-21.
[318] J. Amendt, C.P. Campobasso, E. Gaudry, C. Reiter, H.N. LeBlanc, M.J. Hall, E. European Association for Forensic, Best practice in forensic entomology-standards and guidelines, Int. J. Legal Med. 121(2) (2007) 90-104.
[319] M.S. Archer, M.A. Elgar, C.A. Briggs, D.L. Ranson, Fly pupae and puparia as potential contaminants of forensic entomology samples from sites of body discovery, Int. J. Legal Med. 120(6) (2006) 364-8.
[320] R. Zehner, J. Amendt, R. Krettek, STR typing of human DNA from fly larvae fed on decomposing bodies, J. Forensic Sci. 49(2) (2004) 1-4.
[321] J.D. Wells, F.J. Introna, G. Di Vella, C.P. Campobasso, J. Hayes, F.A.H. Sperling, Human and insect mitochondrial DNA analysis from maggots, J. Forensic Sci. 46(3) (2001) 685-687.
[322] R.P. Hobson, Studies on the nutrition of blow-fly larvae: III. The liquefaction of muscle, J. Exp. Biol. 9 (1932) 359–365.
[323] D.G. Njau, E.K. Muge, P.W. Kinyanjui, C.O.A. Omwandho, S. Mukwana, STR analysis of human DNA from maggots fed on decomposing bodies: Assessment of the time period for successful analysis, Egypt J Forensic Sci 6(3) (2016) 261-269.
[324] D. Marchetti, E. Arena, I. Boschi, S. Vanin, Human DNA extraction from empty puparia, Forensic Sci. Int. 229(1-3) (2013) e26-9.
[325] J.M. Patt, S.C. Wainright, G.C. Hamilton, D. Whittinghill, K. Bosley, J. Dietrick, J.H. Lashomb, Assimilation of carbon and nitrogen from pollen and nectar by a predaceous larva and its effects on growth and development, Ecol. Entomol. 28 (2003) 717-728.
[326] K.O. Spence, J.A. Rosenheim, Isotopic enrichment in herbivorous insects: A comparative field-based study of variation, Oecologia 146 (2005) 89-97.
[327] I. Fraser, W. Meier-Augenstein, R.M. Kalin, The role of stable isotopes in human identification: a longitudinal study into the variability of isotopic signals in human hair and nails, Rapid Commun. Mass Spectrom. 20(7) (2006) 1109-16.
[328] W. Meier-Augenstein, I. Fraser, Forensic isotope analysis leads to identification of a mutilated murder victim, Sci. Justice 48(3) (2008) 153-9.
[329] J.E. Giffen, J.Y. Rosati, C.M. Longo, R.A. Musah, Species identification of necrophagous insect eggs based on amino acid profile differences revealed by direct analysis in real time-high resolution mass spectrometry, Anal. Chem. 89(14) (2017) 7719-7726.
[330] S.C. Webb, R.E.M. Hedges, S.J. Simpson, Diet quality influences the δ13C and δ15N of locusts and their biochemical components, J. Exp. Biol. 201 (1998) 2903-2911.
[331] J.S. McCullagh, D. Juchelka, R.E. Hedges, Analysis of amino acid 13C abundance from human and faunal bone collagen using liquid chromatography/isotope ratio mass spectrometry, Rapid Commun. Mass Spectrom. 20(18) (2006) 2761-8.
[332] J.P. Godin, L.B. Fay, G. Hopfgartner, Liquid chromatography combined with mass spectrometry for 13C isotopic analysis in life science research, Mass Spectrom. Rev. 26(6) (2007) 751-74.

[333] C.I. Smith, B.T. Fuller, K. Choy, M.P. Richards, A three-phase liquid chromatographic method for delta C-13 analysis of amino acids from biological protein hydrolysates using liquid chromatography-isotope ratio mass spectrometry, Anal. Biochem. 390(2) (2009) 165-172.
[334] M. Raghavan, J.S.O. McCullagh, N. Lynnerup, R.E.M. Hedges, Amino acid δ^{13}C analysis of hair proteins and bone collagen using liquid chromatography/isotope ratio mass spectrometry: paleodietary implications from intra-individual comparisons, Rapid Commun. Mass Spectrom. 24(5) (2010) 541-548.
[335] J.P. Godin, J.S. McCullagh, Review: Current applications and challenges for liquid chromatography coupled to isotope ratio mass spectrometry (LC/IRMS), Rapid Commun. Mass Spectrom. 25(20) (2011) 3019-28.
[336] S. Jim, V. Jones, M.S. Copley, S.H. Ambrose, R.P. Evershed, Effects of hydrolysis on the delta13C values of individual amino acids derived from polypeptides and proteins, Rapid Commun. Mass Spectrom. 17(20) (2003) 2283-9.
[337] M.R. Howland, L.T. Corr, S.M.M. Young, V. Jones, S. Jim, N.J. Van Der Merwe, A.D. Mitchell, R.P. Evershed, Expression of the dietary isotope signal in the compound-specific d13C values of pig bone lipids and amino acids, International Journal of Osteoarchaeology 13(1-2) (2003) 54-65.
[338] M.J. DeNiro, S. Epstein, Influence of diet on the distribution of nitrogen isotopes in animals, Geochim. Cosmochim. Acta 45 (1981) 341-351.
[339] M. Minagawa, E. Wada, Stepwise enrichment of 15N along food chains: Further evidence and the relation between d15N and animal age, Geochim. Cosmochim. Acta 48 (1984) 1135-1140.
[340] D.M. Post, Using stable isotopes to estimate trophic position: Models, methods, and assumptions, Ecology 83(3) (2002) 703-718.
[341] H. Doi, E. Kikuchi, S. TaKagi, S. Shikano, Changes in carbon and nitrogen stable isotopes of chironomid larvae during growth, starvation and metamorphosis, Rapid communications in mass spectrometry : RCM 21 (2007) 997-1002.
[342] J.H. McCutchan, W.M. Lewis, C. Kendall, C.C. McGrath, Variation in trophic shift for stable isotope ratios of carbon, nitrogen, and sulfur, Oikos 102 (2003) 378-390.
[343] M.J. DeNiro, S. Epstein, Influence of diet on the distribution of carbon isotopes in animals, Geochim. Cosmochim. Acta 42 (1978) 495-506.
[344] B.J. Peterson, B. Fry, Stable isotopes in ecosystem studies, Annu. Rev. Ecol. Syst. 18 (1987) 293-320.
[345] J.K. Tomberlin, T.L. Crippen, A.M. Tarone, M.F.B. Chaudhury, B. Singh, J.A. Cammack, R.P. Meisel, A Review of Bacterial Interactions With Blow Flies (Diptera: Calliphoridae) of Medical, Veterinary, and Forensic Importance, Ann. Entomol. Soc. Am. 110(1) (2017) 19-36.
[346] K.W. McMahon, M.J. Polito, S. Abel, M.D. McCarthy, S.R. Thorrold, Carbon and nitrogen isotope fractionation of amino acids in an avian marine predator, the gentoo penguin (Pygoscelis papua), Ecol. Evol. 5(6) (2015) 1278-90.
[347] G.A. Langellotto, J.A. Rosenheim, M.R. Williams, Enhanced carbon enrichment in parasitoids (Hymenoptera): a stable isotope study, Ann. Entomol. Soc. Am. 98(2) (2005) 205-213.
[348] S. Jim, V. Jones, S.H. Ambrose, R.P. Evershed, Quantifying dietary macronutrient sources of carbon for bone collagen biosynthesis using natural abundance stable carbon isotope analysis, Br. J. Nutr. 95(06) (2006) 1055.
[349] K.W. McMahon, M.L. Fogel, T.S. Elsdon, S.R. Thorrold, Carbon isotope fractionation of amino acids in fish muscle reflects biosynthesis and isotopic routing from dietary protein, J. Anim. Ecol. 79(5) (2010) 1132-41.

[350] R.F. Chapman, The Insects: Structure and Function, 5th ed., Cambridge University Press, New York, United States of America 2013.
[351] E.L. Arrese, J.L. Soulages, Insect fat body: Energy, metabolism, and regulation, Annu. Rev. Entomol. 55 (2010) 207-25.
[352] J.H. Law, M.A. Wells, Insects as biochemical models, J. Biol. Chem. 264(28) (1989) 16335-16338.
[353] A.R. Gilby, Lipids and their metabolism in insects, Annu. Rev. Entomol. 10 (1965) 141-160.
[354] M.J. DeNiro, S. Epstein, Mechanism of carbon isotope fractionation associated with lipid synthesis, Science 197(4300) (1977) 261-263.
[355] J.M. Hayes, Factors controlling 13C contents of sedimentary organic compounds: Principles and Evidence, Mar. Geol. 113 (1993) 111-125.
[356] H. Tapiero, G. Mathé, P. Couvreur, K.D. Tew, II. Glutamine and glutamate, Biomed. Pharmacother. 56 (2002) 446-457.
[357] P.E. Hare, M.L. Fogel, T.W. Stafford, A.D. Mitchell, T.C. Hoering, The isotopic composition of carbon and nitrogen in individual amino acids isolated from modern and fossil proteins, J Archaeol Sci 18(3) (1991) 277-292.
[358] S.R.R. Reddy, J.W. Campbell, Arginine metabolism in insects - Role of arginase in proline formation during silkmoth development, Biochem. J. 115 (1969) 495-503.
[359] A.J. Hall, V.G. Eisenbart, A.L. Etingüe, L.H. Gould, B.A. Lopman, U.D. Parashar, Epidemiology of foodborne norovirus outbreaks, United States, 2001-2008, Emerg. Infect. Dis. 18(10) (2012) 1566-1573.
[360] S.F. Altekruse, R.D. Bishop, L.M. Baldy, S.G. Thompson, S.A. Wilson, B.J. Ray, P.M. Griffin, Vibrio gastroenteritis in the US Gulf of Mexico region: the role of raw oysters, Epidemiol. Infect. 124 (2000) 489-495.
[361] W.G. Hlady, K.C. Klontz, The Epidemiology of Vibrio Infections in Florida, 1981-1993, J. Infect. Dis. 173(5) (1996) 1176-1183.
[362] R.L. Shapiro, S. Altekruse, L. Hutwagner, R. Bishop, R. Hammond, S. Wilson, B. Ray, S. Thompson, R.V. Tauxe, P.M. Griffin, G. Vibrio Working, The Role of Gulf Coast Oysters Harvested in Warmer Months in Vibrio vulnificus Infections in the United States, 1988-1996, The Journal of Infectious Diseases 178(3) (1998) 752-759.
[363] S. VanderKooy, M.E. Berrigan, B. Randall, L. Robinson, J. Herrmann, B. Lezina, C. O'Brien, R. Goodrich, T. Herrington, C. Nelson, W. Keithly, W. P., J. Supan, S.P. Geiger, B. Arnold, R. Fulford, E.N. Powell, The oyster fishery of the Gulf of Mexico United States: A regional management plan-2012 revision. Publication No. 202, in: S. VanderKooy (Ed.) Gulf States Marine Fisheries Commission, Ocean Springs, Mississippi, 2012, pp. 6-1-6-10.
[364] N.A. Daniels, Vibrio vulnificus Oysters: Pearls and Perils, Clin. Infect. Dis. 52(6) (2011) 788-792.
[365] Summary of Human Vibrio Cases Reported to CDC, 2011, Centers for Disease Control and Prevention (CDC), National Enteric Disease Surveillance: COVIS Annual Summary, 2011.
[366] M.L. Kellogg, J.C. Cornwell, M.S. Owens, K.T. Paynter, Denitrification and nutrient assimilation on a restored oyster reef, Mar. Ecol. Prog. Ser. 480 (2013) 1-19.
[367] C.J. Langdon, R.I.E. Newell, Digestion and nutrition in larvae and adults, in: V.S. Kennedy, R.I.E. Newell, A.F. Eble (Eds.), The Eastern Oyster: Crassostrea virginica, Maryland Sea Grant College, College Park, MD, 1996, pp. 231-269.

[368] M.E. White, E.A. Wilson, Predators, Pests and Competitors, in: V.S. Kennedy, N.R.I. E., A.F. Eble (Eds.), The Eastern Oyster: Crassostrea virginica, Maryland Sea Grant College, College Park, MD, 1996, pp. 559-575.
[369] K. Havens, M. Allen, E. Camp, T. Irani, A. Lindsey, J.G. Morris, A. Kane, D. Kimbro, S. Otwell, B. Pine, C. Walters, Apachicola Bay Oyster Situation Report, National Oceanic and Atmospheric Administration - U. S. Department of Commerce, 2014.
[370] Apalachicola Bay oyster conservation-based changes remain in effect through summer season. Florida Fish and Wildlife Conservation Commission. <https://myfwc.com/news/all-news/oyster-conservation/ >, 2017 (accessed February 2019.).
[371] Florida Fish and Wildlife Conservation Commission Field Operations Weekly Reports. <https://myfwc.com/about/inside-fwc/le/weekly-reports/ >, 2019 (accessed February 2019.).
[372] Celebrating the Completion of the Lavaca Bay, Texas, Restoration. U.S. Fish & Wildlife Service. <https://www.fws.gov/home/feature/2007/lavacabayrestoration.pdf>, 2007 (accessed February 2019.).
[373] P.J. Erbland, G. Ozbay, A comparison of the macrofaunal communities inhabiting a *Crassostrea virginica* oyster reef and oyster aquaculture gear in Indian River Bay,
Delaware, J. Shellfish Res. 27(4) (2008) 757-768.
[374] C. Wilson, L. Scotto, J. Scarpa, A. Volety, S. Laramore, D. Haunert, Survey of water quality, oyster reproduction and oyster health status in the St. Lucie estuary, J. Shellfish Res. 24(1) (2005) 157-165.
[375] Status review of the Eastern oyster (*Crassostrea virginica*), in: E.O.B.R. Team (Ed.) Report to the National Marine Fisheries Service, Northeast Regional Office. NOAA Tech. Memo. NMFS F/SPO-88, 105 p., 2007, p. 105.
[376] M. Espiñeira, N. González-Lavín, J.M. Vieites, F.J. Santaclara, Development of a method for the genetic identification of commercial bivalve species based on mitochondrial 18S rRNA sequences., J. Agric. Food. Chem. 57 (2009) 495-502.
[377] S. Kelly, M. Baxter, S. Chapman, C. Rhodes, J. Dennis, P. Brereton, The application of isotopic and elemental analysis to determine the geographical origin of premium long grain rice, Eur. Food Res. Technol. 214(1) (2002) 72-78.
[378] C.D. Judd, K. Swami, ICP-MS determination of lead isotope ratios in legal and counterfeit cigarette tobacco samples, Isotopes Environ. Health Stud. 46(4) (2010) 484-494.
[379] P.W. Holder, K. Armstrong, R. Van Hale, M.A. Millet, R. Frew, T.J. Clough, J.A. Baker, Isotopes and trace elements as natal origin markers of Helicoverpa armigera -an experimental model for biosecurity pests, PLoS One 9(3) (2014) e92384.
[380] D.M.A.M. Luykx, S.M. van Ruth, An overview of analytical methods for determining the geographical origin of food products, Food Chem. 107(2) (2008) 897-911.
[381] F. Ricardo, L. Genio, M. Costa Leal, R. Albuquerque, H. Queiroga, R. Rosa, R. Calado, Trace element fingerprinting of cockle (Cerastoderma edule) shells can reveal harvesting location in adjacent areas, Sci. Rep. 5 (2015) 11932.
[382] M.L. Carroll, B.J. Johnson, G.A. Henkes, K.W. McMahon, A. Voronkov, W.G. Ambrose, Jr., S.G. Denisenko, Bivalves as indicators of environmental variation and potential anthropogenic impacts in the southern Barents Sea, Mar. Pollut. Bull. 59(4-7) (2009) 193-206.
[383] L. Bougeois, M. de Rafélis, G.-J. Reichart, L.J. de Nooijer, F. Nicollin, G. Dupont-Nivet, A high resolution study of trace elements and stable isotopes in oyster shells to estimate Central Asian Middle Eocene seasonality, Chem. Geol. 363 (2014) 200-212.

[384] H. Abadin, A. Ashizawa, Y.W. Stevens, F. Llados, G. Diamond, G. Sage, M. Citra, A. Quinones, S.J. Bosch, S.G. Swarts, Toxicological profile for lead, U.S. Department of Health and Human Services, Agency for Toxic Substances and Disease Registry (ATSDR) Toxicological Profiles, 2007, p. 582.
[385] O. Faroon, A. Ashizawa, S. Wright, P. Tucker, K. Jenkins, L. Ingerman, C. Rudisill, Toxicological profile for cadmium, U.S. Department of Health and Human Services, Agency for Toxic Substances and Disease Registry (ATSDR) Toxicological Profiles, 2012, p. 279.
[386] D.H. Adams, M.E. Engel, Mercury, lead, and cadmium in blue crabs, Callinectes sapidus, from the Atlantic coast of Florida, USA: A multipredator approach, Ecotoxicol. Environ. Saf. 102 (2014) 196-201.
[387] J.F. Mudge, M.E. Engel, C.N. Ryan, D.M. Klein, Monte Carlo-based distance analysis using Unit Mass Resolution ICP-MS data for shellfish of origin verification, Integr. Environ. Assess. Manag. 11(3) (2015) 515-6.
[388] K.L. Enggrob, T. Larsen, M. Larsen, L. Elsgaard, J. Rasmussen, The influence of hydrolysis and derivatization on the determination of amino acid content and isotopic ratios in dual-labeled (^{13}C, ^{15}N) white clover, Rapid Commun. Mass Spectrom. 33(1) (2019) 21-30.
[389] T.H.E. Heaton, Isotopic studies of nitrogen pollution in the hydrosphere and atmosphere: A review, Chem. Geol. 59 (1986) 87-102.
[390] L.E. Graniero, E.L. Grossman, A. O'Dea, Stable isotopes in bivalves as indicators of nutrient source in coastal waters in the Bocas del Toro Archipelago, Panama, PeerJ 4 (2016) e2278.
[391] J.F. Hair Jr., W.C. Black, B.J. Babin, R.E. Anderson, Multivariate data analysis, Pearson New International - 7th ed., Pearson, London, UK, 2014.
[392] J. Pallant, SPSS survival manual: A step by step guide to data analysis using SPSS program, 6th ed., McGraw-Hill Education, London, UK, 2016.
[393] H.G. Close, Compound-Specific Isotope Geochemistry in the Ocean, Ann. Rev. Mar. Sci. 11 (2019) 27-56.
[394] P.S. Harikumar, U.P. Nasir, Ecotoxicological impact assessment of heavy metals in core sediments of a tropical estuary, Ecotoxicol. Environ. Saf. 73(7) (2010) 1742-7.
[395] N. Pourang, C.A. Richardson, S.R. Chenery, H. Nasrollahzedeh, Assessment of trace elements in the shell layers and soft tissues of the pearl oyster Pinctada radiata using multivariate analyses: a potential proxy for temporal and spatial variations of trace elements, Environ. Monit. Assess. 186(4) (2014) 2465-85.
[396] M. Fukushima, H. Tamate, Y. Nakano, Trace element determination in soft tissues of marine bivalves by activation analysis, J. Radioanal. Nucl. Chem. 255(2) (2003) 231-234.
[397] A.M. Azad, S. Frantzen, M.S. Bank, B.M. Nilsen, A. Duinker, L. Madsen, A. Maage, Effects of geography and species variation on selenium and mercury molar ratios in Northeast Atlantic marine fish communities, Sci. Total Environ. 652 (2019) 1482-1496.
[398] D.F. Pavlov, J. Bezuidenhout, M.V. Frontasyeva, Z.I. Goryainova, Differences in Trace Element Content between Non-Indigenous Farmed and Invasive Bivalve Mollusks of the South African Coast, American Journal of Analytical Chemistry 06(11) (2015) 886-897.
[399] E. Rauch, S. Rummel, C. Lehn, A. Buttner, Origin assignment of unidentified corpses by use of stable isotope ratios of light (bio-) and heavy (geo-) elements--a case report, Forensic Sci. Int. 168(2-3) (2007) 215-8.
[400] A.L. Lamb, Stable isotope analysis of soft tissues from mummified human remains, Environ Archaeol 21(3) (2016) 271-284.

[401] C. Lehn, A. Rossmann, M. Graw, Provenancing of unidentified corpses by stable isotope techniques - presentation of case studies, Sci. Justice 55(1) (2015) 72-88.
[402] P.E. Hare, M.L. Fogel, T.W. Stafford, T.C. Hoering, A.D. Mitchell, Stable isotopes in amino-acids from fossil bones and their relationship to ancient diets, Abstr Pap Am Chem S 193 (1987) 17-Hist.
[403] K.J. Petzke, T. Feist, W.E. Fleig, C.C. Metges, Nitrogen isotopic composition in hair protein is different in liver cirrhotic patients, Rapid Commun. Mass Spectrom. 20 (2006) 2973-2978.
[404] K.J. Petzke, A. Freudenberg, S. Klaus, Beyond the role of dietary protein and amino acids in the prevention of diet-induced obesity, Int. J. Mol. Sci. 15(1) (2014) 1374-91.
[405] K.J. Petzke, B.T. Fuller, C.C. Metges, Advances in natural stable isotope ratio analysis of human hair to determine nutritional and metabolic status, Curr. Opin. Clin. Nutr. Metab. Care 13(5) (2010) 532-40.
[406] B.T. Fuller, J.L. Fuller, N.E. Sage, D.A. Harris, T.C. O'Connell, R.E. Hedges, Nitrogen balance and δ^{15}N: why you're not what you eat during pregnancy, Rapid Commun. Mass Spectrom. 18(23) (2004) 2889-96.
[407] B.T. Fuller, J.L. Fuller, N.E. Sage, D.A. Harris, T.C. O'Connell, R.E. Hedges, Nitrogen balance and δ^{15}N: why you're not what you eat during nutritional stress, Rapid Commun. Mass Spectrom. 19(18) (2005) 2497-506.
[408] V. Balter, A. Nogueira da Costa, V.P. Bondanese, K. Jaouen, A. Lamboux, S. Sangrajrang, N. Vincent, F. Fourel, P. Telouk, M. Gigou, C. Lecuyer, P. Srivatanakul, C. Brechot, F. Albarede, P. Hainaut, Natural variations of copper and sulfur stable isotopes in blood of hepatocellular carcinoma patients, Proc. Natl. Acad. Sci. U. S. A. 112(4) (2015) 982-5.
[409] Z.D. Sharp, V. Atudorei, H.O. Panarello, J. Fernandez, C. Douthitt, Hydrogen isotope systematics of hair: Archeological and forensic applications, J Archaeol Sci 30(12) (2003) 1709-1716.
[410] S.A. Macko, M.H. Engel, V. Andrusevich, G. Lubec, T.C. O'Connell, R.E.M. Hedges, Documenting the diet in ancient human populations through stable isotope analysis of hair, Philos Trans R Soc London B Biol Sci 354(1379) (1999) 65-76.
[411] G. Lubec, G. Nauer, K. Seifert, E. Strouhal, H. Porteder, J. Szilvassy, M. Teschler, Structural stability of hair over three thousand years, J Archaeol Sci 14(2) (1987) 113-120.
[412] H.P. Schwarcz, M.J. Schoeninger, Stable isotope analyses in human nutritional ecology, Am. J. Phys. Anthropol. 34 (1991) 283-321.
[413] W. Rieck, Age-dependent measurements of amino acids in human hairs - a longitudinal study, Arch. Gerontol. Geriatr. 25(1) (1997) 59-71.
[414] J.S. McCullagh, J.A. Tripp, R.E. Hedges, Carbon isotope analysis of bulk keratin and single amino acids from British and North American hair, Rapid Commun. Mass Spectrom. 19(22) (2005) 3227-31.
[415] A.H. Rashaid, B. Harrington Pde, G.P. Jackson, Profiling amino acids of Jordanian scalp hair as a tool for diabetes mellitus diagnosis: A pilot study, Anal. Chem. 87(14) (2015) 7078-84.
[416] M. Womack, W.C. Rose, The role of proline, hydroxyproline, and glutamic acid in growth, J. Biol. Chem. 171 (1947) 37-50.
[417] A.A. Jackson, The glycine story, Eur. J. Clin. Nutr. 45 (1991) 59-65.
[418] P.J. Reeds, Dispensable and indispensable amino acids for humans, J. Nutr. 130(7) (2000) 1835S-40S.

[419] Y. An, Z. Schwartz, G.P. Jackson, δ^{13}C analysis of amino acids in human hair using trimethylsilyl derivatives and gas chromatography/combustion/isotope ratio mass spectrometry, Rapid Commun. Mass Spectrom. 27(13) (2013) 1481-9.
[420] L.T. Corr, R. Berstan, R.P. Evershed, Optimisation of derivatisation procedures for the determination of δ^{13}C values of amino acids by gas chromatography/combustion/isotope ratio mass spectrometry, Rapid Commun. Mass Spectrom. 21(23) (2007) 3759-71.
[421] L.T. Corr, R. Berstan, R.P. Evershed, Development of N-acetyl methyl ester derivatives for the determination of δ13C values of amino acids using gas chromatography-combustion-isotope ratio mass spectrometry, Anal. Chem. 79 (2007) 9082-9090.
[422] J.P. Godin, J. Hau, L.B. Fay, G. Hopfgartner, Isotope ratio monitoring of small molecules and macromolecules by liquid chromatography coupled to isotope ratio mass spectrometry, Rapid Commun. Mass Spectrom. 19(18) (2005) 2689-98.
[423] J.P. Godin, T. Stellingwerff, L. Actis-Goretta, A.F. Mermoud, S. Kochhar, S. Rezzi, The role of liquid chromatography and flow injection analyses coupled to isotope ratio mass spectrometry for studying human in vivo glucose metabolism, Rapid Commun. Mass Spectrom. 25 (2011) 2989–2994.
[424] D.M. Roy, R. Hall, A.C. Mix, R. Bonnichsen, Using stable isotope analysis to obtain dietary profiles from old hair: A case study from Plains Indians, Am. J. Phys. Anthropol. 128(2) (2005) 444-452.
[425] K.J. Petzke, H. Boeing, S. Klaus, C.C. Metges, Carbon and nitrogen stable isotopic composition of hair protein and amino acids can be used as biomarkers for animal-derived dietary protein intake in humans, J. Nutr. 135(6) (2005) 1515-1520.
[426] F. Huelsemann, K. Koehler, H. Braun, W. Schaenzer, U. Flenker, Human dietary δ^{15}N intake: Representative data for principle food items, Am. J. Phys. Anthropol. 152(1) (2013) 58-66.
[427] M.J. Schoeninger, M.J. Deniro, Nitrogen and carbon isotopic composition of bone-collagen from marine and terrestrial animals, Geochim. Cosmochim. Acta 48(4) (1984) 625-639.
[428] F. Huelsemann, U. Flenker, K. Koehler, W. Schaenzer, Effect of a controlled dietary change on carbon and nitrogen stable isotope ratios of human hair, Rapid Commun. Mass Spectrom. 23(16) (2009) 2448-54.
[429] K.J. Petzke, H. Boeing, C.C. Metges, Choice of dietary protein of vegetarians and omnivores is reflected in their hair protein ^{13}C and ^{15}N abundance, Rapid Commun. Mass Spectrom. 19(11) (2005) 1392-400.
[430] C.M. Kurle, P.L. Koch, B.R. Tershy, D.A. Croll, The effects of sex, tissue type, and dietary components on stable isotope discrimination factors (δ^{13}C and δ^{15}N) in mammalian omnivores, Isotopes Environ. Health Stud. 50(3) (2014) 307-21.
[431] M.L. Fogel, N. Tuross, Extending the limits of paleodietary studies of humans with compound specific carbon isotope analysis of amino acids, Journal of Archaeological Science 30(5) (2003) 535-545.
[432] G.E. Gutman, B. Alexander, Studies of amino acid metabolism: I. Blood glycine and alanine and their relationship to the total amino acids normal subjects, J. Biol. Chem. 168 (1947) 527-536.
[433] J.T. Cole, Metabolism of BCAAs, in: R. Rajendram, V.R. Preedy, V.B. Patel (Eds.), Branched Chain Amino Acids in Clinical Nutrition, Springer Science+Business Media, New York, 2015, pp. 13-24.
[434] S. Udenfriend, J.R. Cooper, The enzymatic conversion of phenylalanine to tyrosine, J. Biol. Chem. 194 (1952) 503-511.

[435] B.G. Tabachnick, L.S. Fidell, Using multivariate statistics, 6th ed., Pearson Education, Boston, 2013.
[436] J. Cohen, Statistical power analysis for the behavioral sciences, 2nd ed., Lawrence Erlbaum Associates, Hillsdale, N.J, 1988.
[437] J.H. Barrett, M.P. Richards, Identity, gender, religion and economy: New isotope and radiocarbon evidence for marine resource intensification in early historic Orkney, Scotland, UK, European Journal of Archaeology 7(3) (2004) 249-271.
[438] C.D. White, Gendered food behaviour among the Maya - Time, place, status and ritual, J Soc Archaeol 5(3) (2005) 356-382.
[439] L.J. Reitsema, G. Vercellotti, Stable isotope evidence for sex- and status-based variations in diet and life history at medieval Trino Vercellese, Italy, Am. J. Phys. Anthropol. 148(4) (2012) 589-600.
[440] A.D. Somerville, P.S. Goldstein, S.I. Baitzel, K.L. Bruwelheide, A.C. Dahlstedt, L. Yzurdiaga, S. Raubenheimer, K.J. Knudson, M.J. Schoeninger, Diet and gender in the Tiwanaku colonies: Stable isotope analysis of human bone collagen and apatite from Moquegua, Peru, Am. J. Phys. Anthropol. 158(3) (2015) 408-22.
[441] M. Minagawa, Reconstruction of human diet from $\delta^{13}C$ and $\delta^{15}N$ in contemporary Japanese hair: a stochastic method for estimating multi-source contribution by double isotopic tracers, Appl. Geochem. 7 (1992) 145-158.
[442] N.C. Lovell, D.E. Nelson, H.P. Schwarcz, Carbon isotope ratios in palaeodiet: Lack of age or sex effect, Archaeometry 28(1) (1986) 51-55.
[443] H. Morishita, T. Hashimoto, K. Kishi, K. Nakago, H. Mitani, M. Tomioka, S. Kuroiwa, Y. Miyauchi, Effects of glycine on serum gonadotropins and estradiol and on concentrations of free amino acids in the middle hypothalamus in female rats, Gynecol. Obstet. Invest. 12(4) (1981) 187-196.
[444] M.H. Kim, H.M. Kim, H.J. Jeong, Estrogen-like osteoprotective effects of glycine in in vitro and in vivo models of menopause, Amino Acids 48(3) (2016) 791-800.
[445] A.H.B. Rashaid, P.B. Harrington, G.P. Jackson, Amino acid composition of human scalp hair as a biometric classifier and investigative lead, Analytical Methods 7(5) (2015) 1707-1718.
[446] R.C. Clay, K. Cook, J.I. Routh, Studies in the composition of human hair, J. Am. Chem. Soc. 62(10) (1940) 2709–2710.
[447] R.H. Wilson, H.B. Lewis, The cystine content of hair and other epidermal tissues, J. Biol. Chem. 73 (1927) 543-553.
[448] H. Panayiotou, Vibrational spectroscopy of keratin fibres - A forensic approach, Physical and Chemical Sciences, Queensland University of Technology, 2004.
[449] L.S. Lamont, A.J. McCullough, S.C. Kalhan, Gender differences in the regulation of amino acid metabolism, J. Appl. Physiol. 95 (2003) 1259–1265.
[450] S. Phillips, S. Atkinson, M. Tarnopolsky, J. MacDougall, Gender differences in leucine kinetics and nitrogen balance in endurance athletes, J. Appl. Physiol. 75 (1993) 2134–2141.
[451] M.M. Markofski, E. Volpi, Protein metabolism in women and men: similarities and disparities, Curr. Opin. Clin. Nutr. Metab. Care 14(1) (2011) 93-7.
[452] K.D. Tipton, Gender differences in protein metabolism, Curr. Opin. Clin. Nutr. Metab. Care 4(6) (2001) 493-498.
[453] H.C. Dreyer, S. Fujita, E.L. Glynn, M.J. Drummond, E. Volpi, B.B. Rasmussen, Resistance exercise increases leg muscle protein synthesis and mTOR signalling independent of sex, Acta Physiol. (Oxf.) 199(1) (2010) 71-81.

[454] M.A. Katzenberg, S.R. Saunders, W.R. Fitzgerald, Age differences in stable carbon and nitrogen isotope ratios in a population of prehistoric maize horticulturists, Am. J. Phys. Anthropol. 90 (1993) 267-281.
[455] J.C. Sealy, N.J. van der Merwe, Social, spatial and chronological patterning in marine food use as determined by ä 13 C measurements of Holocene human skeletons from the south-western Cape, South Africa, World Archaeology 20(1) (1988) 87-102.
[456] A. Bertazzo, M. Biasiolo, C.V.L. Costa, E. Cardin de Stefani, G. Allegri, Tryptophan in human hair: correlation with pigmentation, Farmaco 55(8) (2000) 521-5.
[457] S.R. Kimball, L.S. Jefferson, Signaling pathways and molecular mechanisms through which branched-chain amino acids mediate translational control of protein synthesis, J. Nutr. 136(1 Suppl) (2006) 227S-31S.
[458] A. Valerio, G. D'Antona, E. Nisoli, Branched-chain amino acids, mitochondrial biogenesis, and healthspan: an evolutionary perspective, Aging (Albany NY) 3(5) (2011) 464-78.
[459] D. Dardevet, I. Rieu, P. Fafournoux, C. Sornet, L. Combaret, A. Bruhat, S. Mordier, L. Mosoni, J. Grizard, Leucine: a key amino acid in ageing-associated sarcopenia?, Nutr. Res. Rev. 16(1) (2003) 61-70.
[460] S. Fujita, E. Volpi, Amino acids and muscle loss with aging, J. Nutr. 136(1 Suppl) (2006) 277S-80S.
[461] WHO, Physical Status: the use and interpretation of anthopometry, WHO Technical Report Series, 841, World Health Organization, Geneva, Switzerland, 1995.
[462] WHO, Consultation on obesity. Obesity: Preventing and managing the global epidemic, World Health Organization Geneva, Switzerland, 2000.
[463] WHO, Appropriate body-mass index for Asian populations and its implications for policy and intervention strategies, Lancet 363(9403) (2004) 157.
[464] N. Mohorko, A. Petelin, M. Jurdana, G. Biolo, Z. Jenko-Praznikar, Elevated serum levels of cysteine and tyrosine: early biomarkers in asymptomatic adults at increased risk of developing metabolic syndrome, Biomed Res Int 2015 (2015) 418681.
[465] N. Baba, Y. Nakayama, F. Nozaki, T. Tamura, Denaturation and release of amino acids in hairs treated with cold-waving lotions, hair-dyes, hair-bleaching solutions and depilatories, J Hyg Chem 19(2) (1973) 47-52.
[466] T.C. O'Connell, R.E.M. Hedges, Investigations into the effect of diet on modern human hair isotopic values, Am. J. Phys. Anthropol. 108(4) (1999) 409-425.
[467] C.R. Robbins, Chemical composition of different hair types, Chemical and physical behavior of human hair, Springer-Verlag Berlin Heidelberg2012, p. 724.
[468] K. Blum, J.E. Wallace, R.N. Friedman, Reduction of acute alcoholic intoxication by α-amino acids: glycine and serine, Life Sci. 14 (1974) 557-565.
[469] W.C. Sim, H.Q. Yin, H.S. Choi, Y.J. Choi, H.C. Kwak, S.K. Kim, B.H. Lee, L-serine supplementation attenuates alcoholic fatty liver by enhancing homocysteine metabolism in mice and rats, J. Nutr. 145(2) (2015) 260-7.
[470] A.C. Nogueira, L.E. Dicelio, I. Joekes, About photo-damage of human hair, Photochem Photobiol Sci 5(2) (2006) 165-9.
[471] A.H.B. Rashaid, G.P. Jackson, P.B. Harrington, Quantitation of Amino Acids in Human Hair by Trimethylsilyl Derivatization Gas Chromatography-Mass Spectrometry, Enliven: Bio analytical Techniques 1(1) (2014) 1-12.
[472] C.J. Rayner, Protein Hydrolysis of Animal Feeds for Amino Acid Content, J. Agric. Food Chem. 33 (1985) 722-725.

[473] M. Fountoulakis, H.-W. Lahm, Hydrolysis and amino acid composition analysis of proteins, J. Chromatogr. A 826 (1988) 109-134.
[474] P. Roberts, D.L. Jones, Critical evaluation of methods for determining total protein in soil solution, Soil Biol. Biochem. 40(6) (2008) 1485-1495.
[475] N. Wang, L. Li, Reproducible microwave-assisted acid hydrolysis of proteins using a household microwave oven and its combination with LC-ESI MS/MS for mapping protein sequences and modifications, J. Am. Soc. Mass. Spectrom. 21(9) (2010) 1573-87.
[476] M. Damm, M. Holzer, G. Radspieler, G. Marsche, C.O. Kappe, Microwave-assisted high-throughput acid hydrolysis in silicon carbide microtiter platforms--a rapid and low volume sample preparation technique for total amino acid analysis in proteins and peptides, J. Chromatogr. A 1217(50) (2010) 7826-32.

APPENDIX

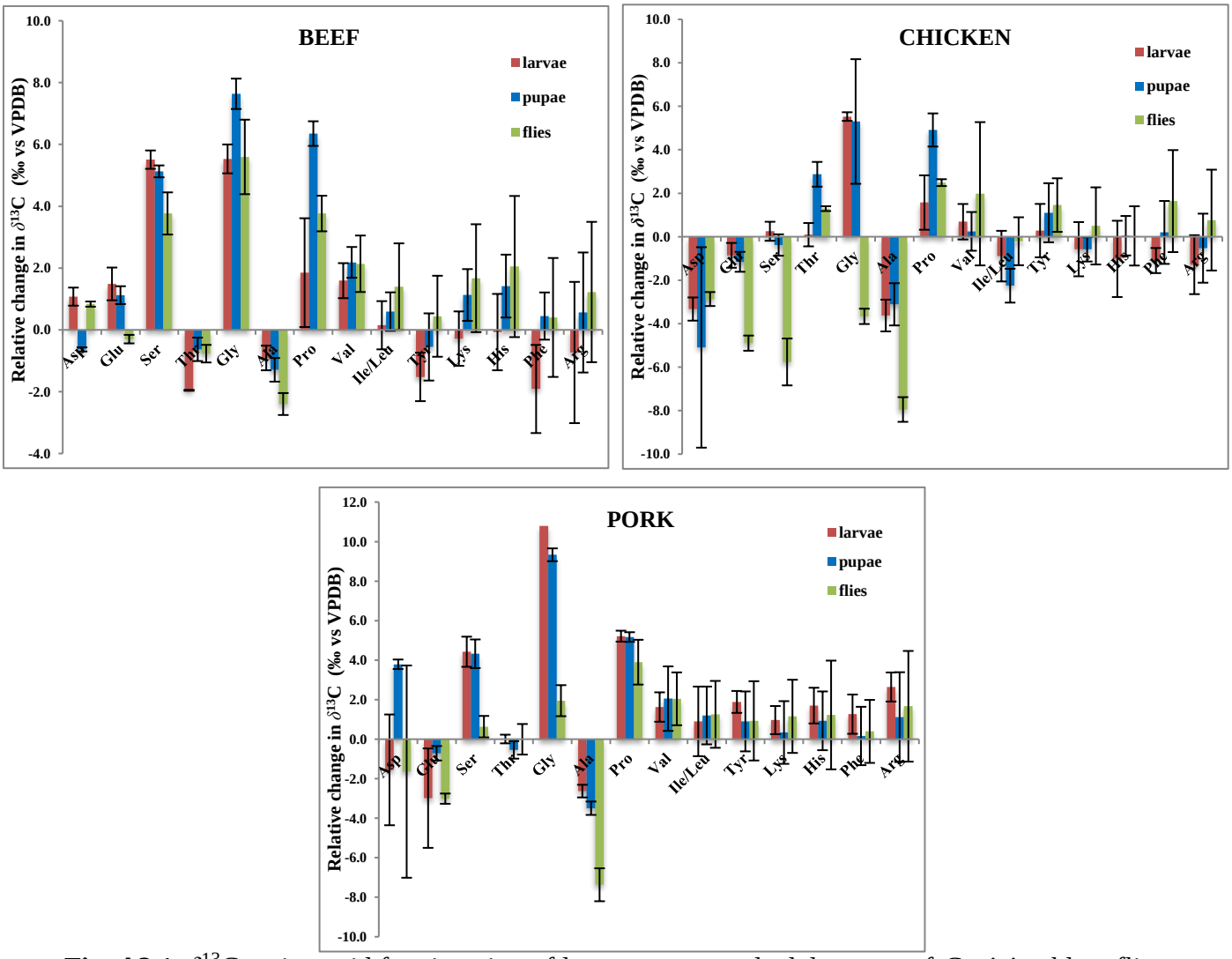

Fig. A2.1. δ^{13}C amino acid fractionation of larvae, pupae and adult stages of *C. vicina* blow flies in each of the carrion food sources they fed on. Bars represent mean ± 95% CI.

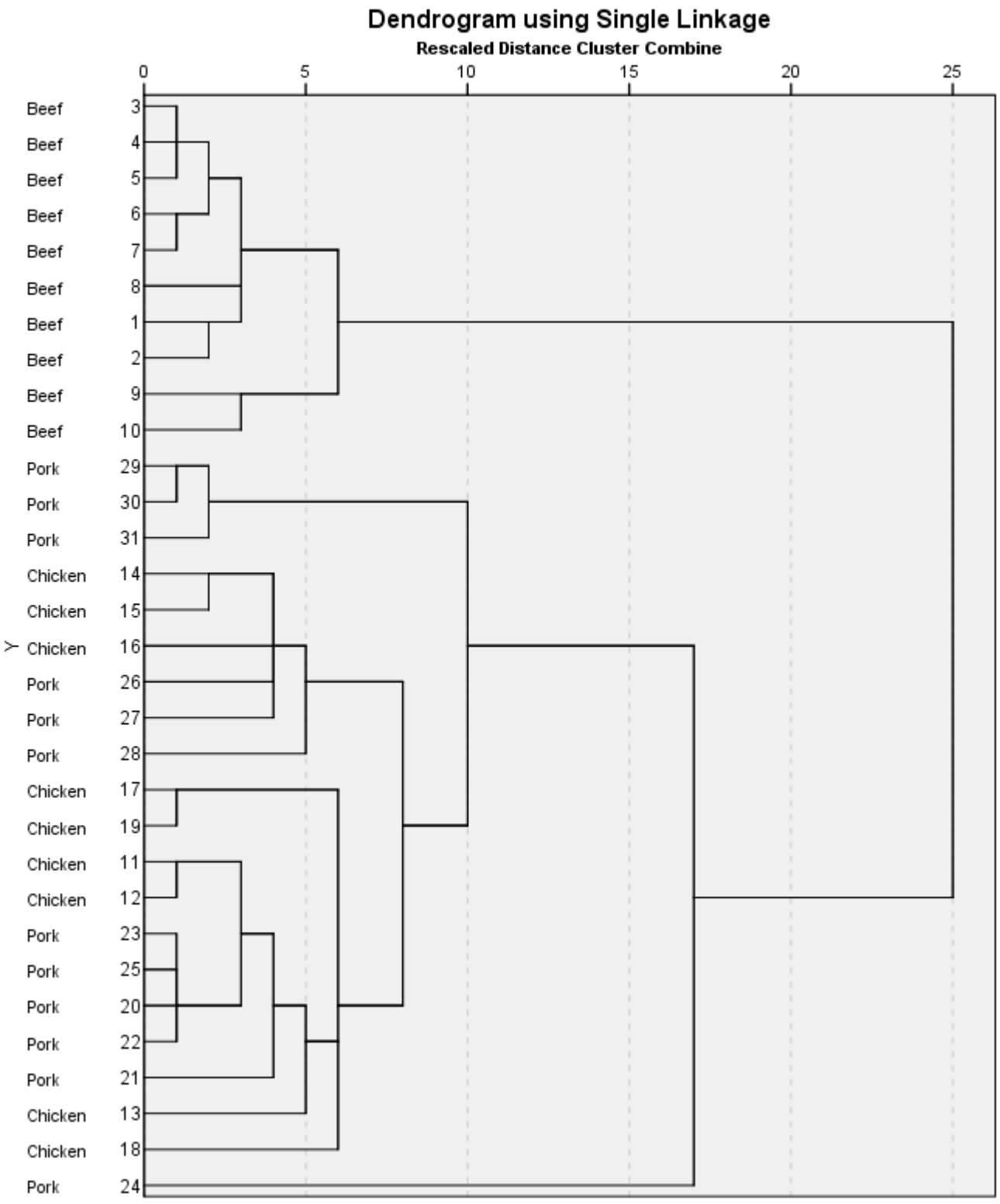

Fig. A2.2. Hierarchical Cluster analysis results using all the amino acids as variables. Delta ^{13}C values were standardized to z-scores before analysis. The cluster method used between-groups linkage and the measure is the squared Euclidian distance.

Table A2.1. Absolute $\delta^{13}C$ changes in fifteen amino acids from different life stages of *C. vicina* blow flies and the respective carrion sources used as their diet. No viable adult flies were obtained from the human carrion diet.

Carrion type	Life stage	Asp	Glu	Ser	Thr	Gly	Ala	Pro	Val	Ile/Leu	Tyr	Lys	His	Phe	Arg
Beef	tissue	-6.16	-6.00	-2.21	-3.35	-3.44	-10.19	-13.60	-16.71	-18.01	-14.11	-10.15	-10.03	-18.78	-10.35
	larvae	-5.08	-4.51	3.30	-5.31	2.09	-11.10	-11.75	-15.11	-17.86	-15.63	-10.44	-10.10	-20.69	-11.09
	pupae	-6.79	-4.88	2.92	-3.98	4.19	-11.48	-7.25	-14.52	-17.42	-14.66	-9.03	-8.61	-18.33	-9.79
	flies	-5.33	-6.30	1.56	-4.12	2.15	-12.59	-9.84	-14.57	-16.61	-13.67	-8.48	-7.98	-18.38	-9.13
Chicken	tissue	-9.66	-7.46	0.23	-13.13	0.33	-9.50	-17.31	-23.24	-21.34	-21.83	-18.64	-15.88	-23.20	-18.60
	larvae	-12.99	-8.32	0.49	-13.04	5.86	-13.13	-15.73	-22.55	-22.23	-21.55	-19.22	-16.90	-24.30	-19.88
	pupae	-14.75	-8.62	-0.15	-10.26	5.63	-12.61	-12.40	-22.99	-23.59	-20.73	-19.22	-15.83	-23.01	-19.12
	flies	-12.53	-12.36	-5.53	-11.84	-3.33	-17.45	-14.82	-21.26	-21.55	-20.38	-18.15	-15.84	-21.57	-17.83
Pork	tissue	-10.19	-7.57	-5.71	-12.92	-9.06	-9.90	-19.12	-24.97	-24.62	-24.06	-20.15	-16.95	-26.76	-19.62
	larvae	-11.74	-10.56	-1.29	-12.91	1.74	-12.52	-13.90	-23.34	-23.72	-22.17	-19.19	-15.25	-25.49	-16.98
	pupae	-6.40	-8.29	-1.39	-13.47	0.28	-13.39	-13.95	-22.92	-23.42	-23.16	-19.81	-16.02	-26.60	-18.50
	flies	-11.83	-10.58	-5.08	-12.93	-7.11	-17.27	-15.22	-22.93	-23.37	-23.13	-19.00	-15.72	-26.36	-17.96

Table A2.2. Analysis of variance of $\delta^{13}C$ values of fifteen amino acids in carrion and blow flies using carrion source as the fixed factor. The blow fly samples include 3 separate individuals from each life stage: larva, pupae and adult fly.

		Sum of Squares	df	Mean Square	F	Sig.
ASP	Between Groups	234.011	2	117.005	9.453	.001
	Within Groups	383.719	31	12.378		
	Total	617.730	33			
GLU	Between Groups	111.748	2	55.874	21.578	.000
	Within Groups	82.861	32	2.589		
	Total	194.610	34			
SER	Between Groups	135.909	2	67.954	11.961	.000
	Within Groups	187.487	33	5.681		
	Total	323.396	35			
THR	Between Groups	565.352	2	282.676	353.233	.000
	Within Groups	26.408	33	.800		
	Total	591.760	35			
GLY	Between Groups	198.341	2	99.170	5.718	.008
	Within Groups	537.615	31	17.342		
	Total	735.955	33			
ALA	Between Groups	28.051	2	14.025	2.370	.109
	Within Groups	195.265	33	5.917		
	Total	223.316	35			
PRO	Between Groups	178.484	2	89.242	16.685	.000
	Within Groups	176.505	33	5.349		
	Total	354.989	35			
VAL	Between Groups	492.922	2	246.461	141.728	.000
	Within Groups	57.386	33	1.739		
	Total	550.307	35			

ILE/LEU	Between Groups	258.416	2	129.208	87.636	.000
	Within Groups	48.654	33	1.474		
	Total	307.070	35			
TYR	Between Groups	485.469	2	242.734	86.621	.000
	Within Groups	92.474	33	2.802		
	Total	577.943	35			
LYS	Between Groups	746.062	2	373.031	244.898	.000
	Within Groups	50.266	33	1.523		
	Total	796.328	35			
HIS	Between Groups	290.154	2	145.077	27.309	.000
	Within Groups	175.312	33	5.312		
	Total	465.466	35			
PHE	Between Groups	317.057	2	158.529	74.283	.000
	Within Groups	70.426	33	2.134		
	Total	387.483	35			
ARG	Between Groups	576.647	2	288.323	96.543	.000
	Within Groups	98.553	33	2.986		
	Total	675.200	35			

Table A2.3. Pooled within-groups correlations between discriminating variables and standardized canonical discriminant functions. Results refer to carrion type as a classification factor.

Structure Matrix		
	Function	
	1	2
Thr	.384*	-.098
Lys	.304*	-.105
Val	.229*	-.055
His	.196*	-.111
Ile/Leu	.189*	.039
Arg	.185*	-.112
Tyr	.174*	.014
Phe	.160*	.135
Glu	.084*	-.057
Pro	.082*	-.031
Ser	.069*	.025
Ala	.025*	-.010
Gly	.036	.084*
Asp	.047	-.077*

Pooled within-groups correlations between discriminating variables and standardized canonical discriminant functions

Variables ordered by absolute size of correlation within function.

*. Largest absolute correlation between each variable and any discriminant function

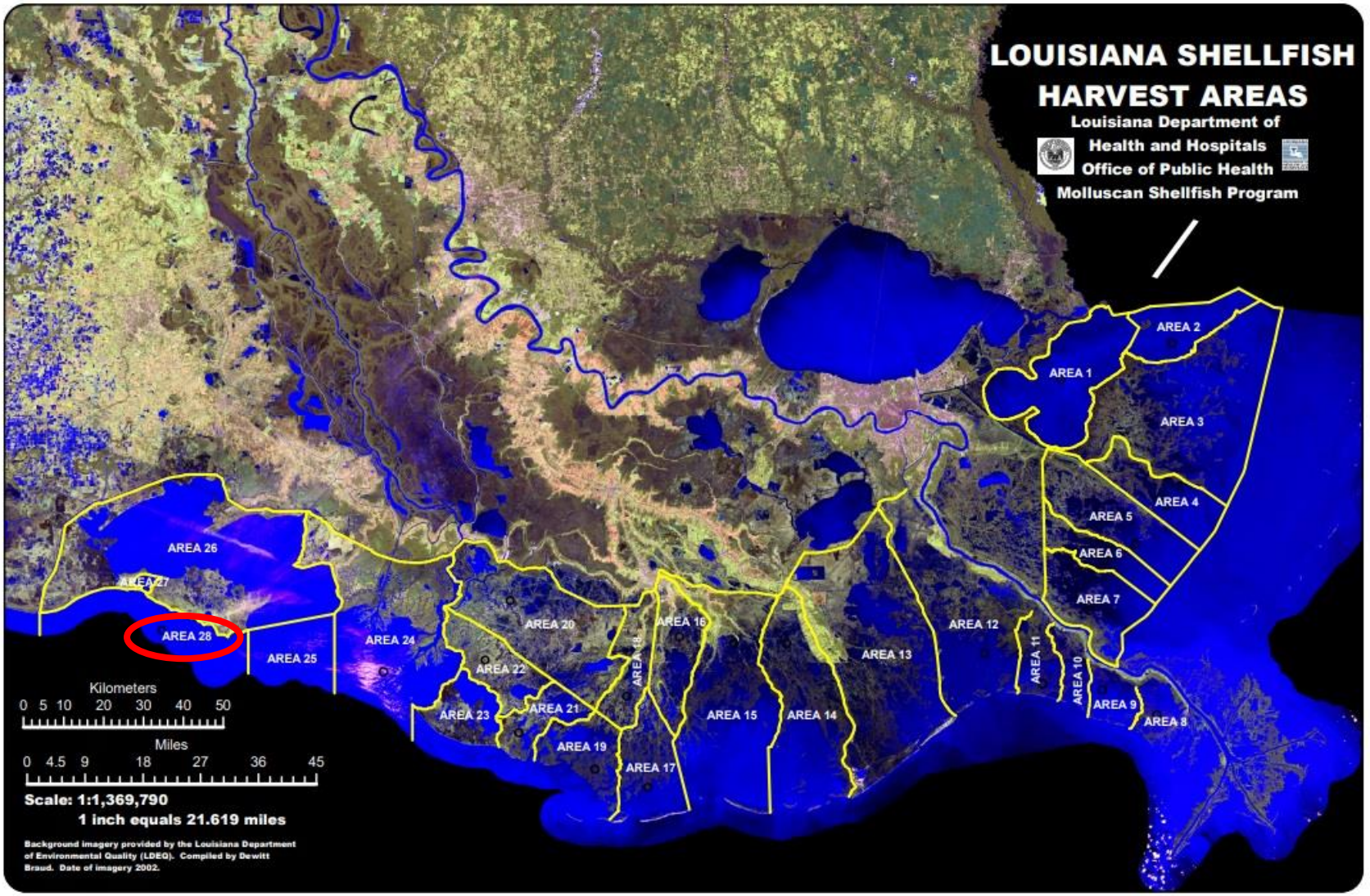

Fig. A3.1. Map of shellfish harvest areas in Louisiana. Red circle indicates the area included in this study, LA area 28. Source: Louisiana Department of Health and Hospitals, Office of Public Health, Molluscan Shellfish Program.

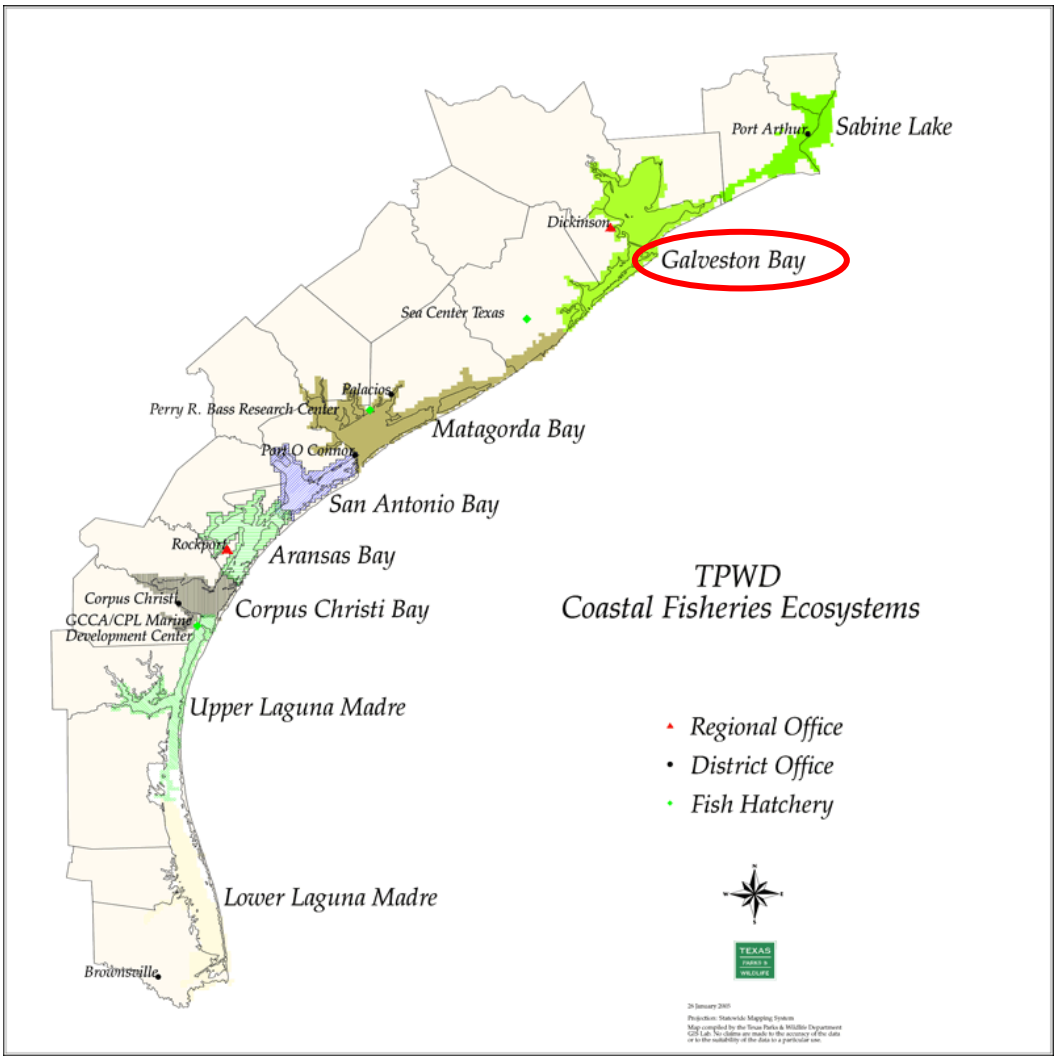

Fig. A3.2. Map of Texas bays inclusing shellfish harvest areas. Red circle indicates one of the areas included in this study, Galveston Bay. The other area was Copano Bay, which is a small unimpacted bay within the Aransas Bay. Source: Texas Parks and Wildlife.

Table A3.1. One-way ANOVA of bulk $\delta^{13}C$ and $\delta^{15}N$ values of oyster samples from five different harvest areas. N=9 or 10 for each region.

ANOVA

		Sum of Squares	df	Mean Square	F	Sig.
$\delta^{13}C$	Between Groups	46.414	4	11.604	6.011	.001
	Within Groups	84.931	44	1.930		
	Total	131.345	48			
$\delta^{15}N$	Between Groups	282.358	4	70.589	18.443	6.84e-9
	Within Groups	164.579	43	3.827		
	Total	446.937	47			

Table A3.2. One-way ANOVA followed by Tukey's HSD post-hoc test of of bulk $\delta^{13}C$ and $\delta^{15}N$ values of oyster samples revealed which samples could be statistically discriminated from one region to another. N=9 or 10 for each region.

Multiple Comparisons

Tukey HSD

Dependent Variable	(I) Harvest Area	(J) Harvest Area	Mean Difference (I-J)	Std. Error	Sig.	95% Confidence Interval	
						Lower Bound	Upper Bound
$\delta^{13}C$	FL 1642	FL 1662	1.73	.62	.059	-.041	3.49
		LA 28	2.60*	.62	.001	.83	4.36
		Galveston bay	.52	.62	.927	-1.27	2.27
		Copano bay	.39	.64	.972	-1.42	2.21
	FL 1662	FL 1642	-1.73	.62	.059	-3.49	.041
		LA 28	.87	.62	.630	-.90	2.64
		Galveston bay	-1.22	.62	.297	-2.99	.54
		Copano bay	-1.33	.64	.242	-3.15	.48
	LA 28	FL 1642	-2.60*	.62	.001	-4.36	-.83
		FL 1662	-.87	.62	.630	-2.64	.90
		Galveston bay	-2.10*	.62	.013	-3.86	-.33
		Copano bay	-2.21*	.64	.010	-4.02	-.39
	Galveston bay	FL 1642	-.50	.62	.927	-2.27	1.27
		FL 1662	1.22	.62	.297	-.53	2.99
		LA 28	2.09*	.62	.013	.33	3.90
		Copano bay	-.11	.64	1.000	-1.93	1.70
	Copano bay	FL 1642	-.39	.64	.972	-2.21	1.42
		FL 1662	1.33	.64	.242	-.48	3.15
		LA 28	2.21*	.64	.010	.39	4.02

		Galveston bay	.11	.64	1.000	-1.70	1.93
δ^{15}N	FL 1642	FL 1662	-.19	.90	1.000	-2.75	2.37
		LA 28	-.98	.87	.795	-3.47	1.51
		Galveston bay	-6.24*	.87	.000	-8.73	-3.75
		Copano bay	-.12	.904	1.000	-2.68	2.43
	FL 1662	FL 1642	.19	.90	1.000	-2.37	2.74
		LA 28	-.79	.90	.902	-3.35	1.77
		Galveston bay	-6.05*	.90	.000	-8.61	-3.49
		Copano bay	.06	.92	1.000	-2.56	2.69
	LA 28	FL 1642	.98	.87	.795	-1.51	3.47
		FL 1662	.79	.90	.902	-1.77	3.35
		Galveston bay	-5.26*	.87	.000	-7.75	-2.77
		Copano bay	.86	.90	.874	-1.70	3.42
	Galveston bay	FL 1642	6.24*	.87	.000	3.75	8.73
		FL 1662	6.05*	.90	.000	3.49	8.61
		LA 28	5.26*	.87	.000	2.77	7.75
		Copano bay	6.117522*	.90	.000	3.56	8.68
	Copano bay	FL 1642	.12	.90	1.000	-2.43	2.68
		FL 1662	-.06	.92	1.000	-2.69	2.56
		LA 28	-.857	.90	.874	-3.42	1.70
		Galveston bay	-6.12*	.90	.000	-8.68	-3.56

*. The mean difference is significant at the 0.05 level.

Table A3.3. Linear discriminant analysis (classification) according to geographic origin using bulk $\delta^{13}C$ and $\delta^{15}N$ values from whole-body oyster samples collected in different harvest areas. N=9 or 10 for each region.

			Predicted Group Membership					
		Harvest Area	FL 1642	FL 1662	LA 28	Galveston bay	Copano bay	Total
Original	Count	FL 1642	8	0	0	0	2	10
		FL 1662	0	2	4	0	3	9
		LA 28	0	3	7	0	0	10
		Galveston bay	0	1	1	8	0	10
		Copano bay	5	1	1	0	2	9
	%	FL 1642	80.0	.0	.0	.0	20.0	100.0
		FL 1662	.0	22.2	44.4	.0	33.3	100.0
		LA 28	.0	30.0	70.0	.0	.0	100.0
		Galveston bay	.0	10.0	10.0	80.0	.0	100.0
		Copano bay	55.6	11.1	11.1	.0	22.2	100.0
Cross-validated[b]	Count	FL 1642	8	0	0	0	2	10
		FL 1662	0	2	4	0	3	9
		LA 28	0	3	6	0	1	10
		Galveston bay	0	1	1	8	0	10
		Copano bay	5	1	1	0	2	9
	%	FL 1642	80.0	.0	.0	.0	20.0	100.0
		FL 1662	.0	22.2	44.4	.0	33.3	100.0
		LA 28	.0	30.0	60.0	.0	10.0	100.0
		Galveston bay	.0	10.0	10.0	80.0	.0	100.0
		Copano bay	55.6	11.1	11.1	.0	22.2	100.0

a. 56.3% of original grouped cases correctly classified.

b. Cross validation is done only for those cases in the analysis. In cross validation, each case is classified by the functions derived from all cases other than that case.

c. 54.2% of cross-validated grouped cases correctly classified.

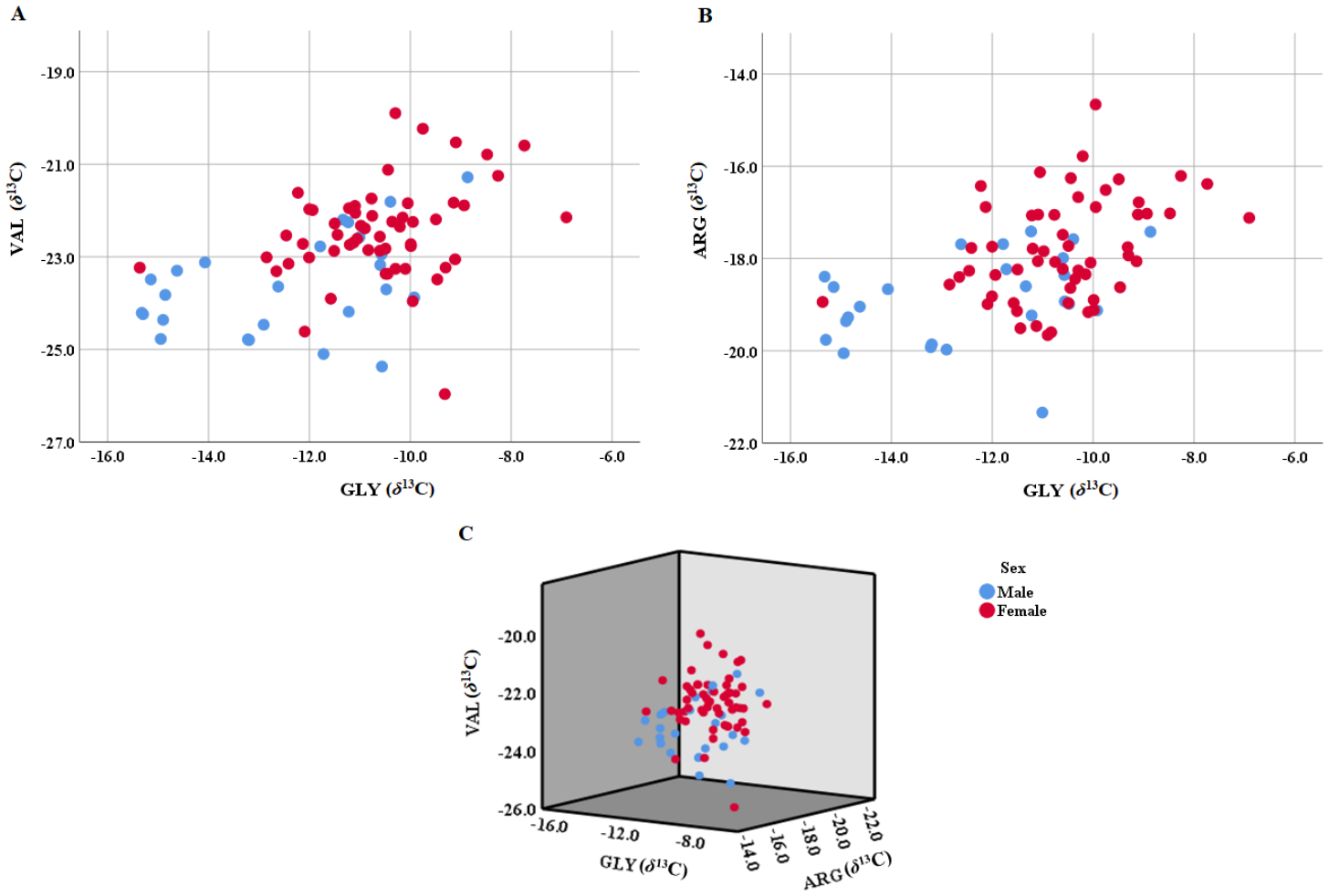

Fig. A4.1. Bivariate plot of the δ^{13}C of the amino acids with the highest F values in MANOVA test using SEX as independent variable. **A)** δ^{13}C values of Gly and Val (F= 22.119 and F= 20.873, respectively), and **B)** δ^{13}C values of Gly and Arg (F= 16.829). **C)** 3D scatterplot of the carbon isotope values from the three amino acids with the most significant influence on the classification based on sex.

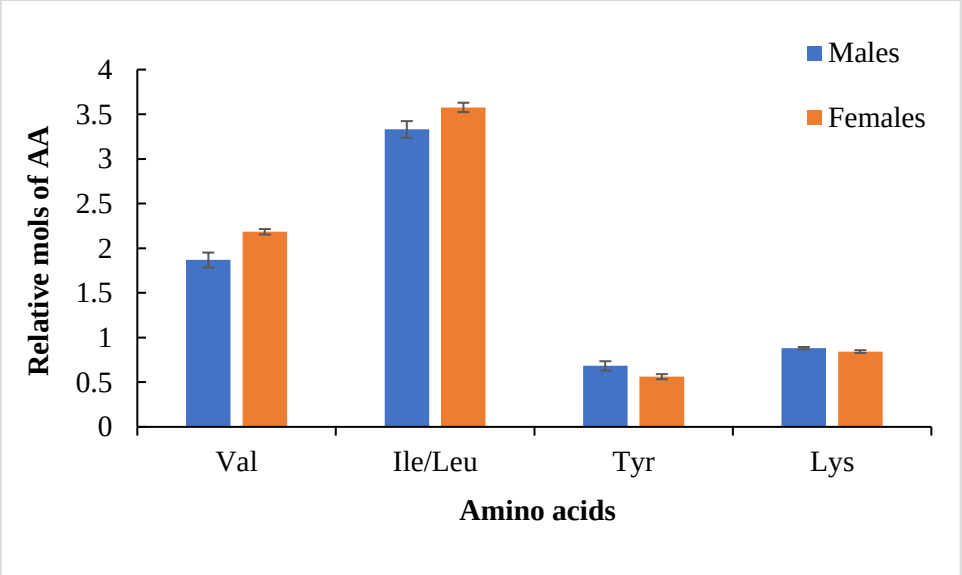

Fig. A4.2. Relative amino acid composition in the hair of males and female subjects. Val was more abundant in females, showing an average of 2.18 ± 0.03 and 1.86 ± 0.08 for males. Ile/Leu showed the same pattern, having an average of 3.57 ± 0.05 for females and 3.33 ± 0.09 for males. Tyr and Lys presented the opposite trend, being more abundant in males (0.68 ± 0.05 and 0.88 ± 0.01, respectively) than in females (0.56 ± 0.03 and 0.84 ± 0.02). Values are expressed as mean ± 95% confidence interval of the mean.

A

Classification Results[a,c]

		Age (Binned) in 3 groups	Predicted Group Membership <= 25	26 - 45	46+	Total
Original	Count	<= 25	28	6	4	38
		26 - 45	16	11	1	28
		46+	9	1	6	16
	%	<= 25	73.7	15.8	10.5	100.0
		26 - 45	57.1	39.3	3.6	100.0
		46+	56.3	6.3	37.5	100.0
Cross-validated[b]	Count	<= 25	26	7	5	38
		26 - 45	18	9	1	28
		46+	9	1	6	16
	%	<= 25	68.4	18.4	13.2	100.0
		26 - 45	64.3	32.1	3.6	100.0
		46+	56.3	6.3	37.5	100.0

a. 54.9% of original grouped cases correctly classified.

b. Cross validation is done only for those cases in the analysis. In cross validation, each case is classified by the functions derived from all cases other than that case.

c. 50.0% of cross-validated grouped cases correctly classified.

B

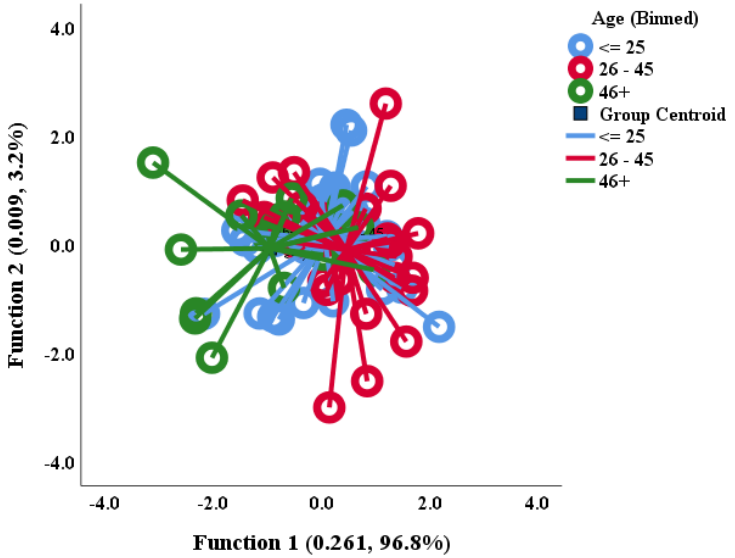

Fig. A4.3. A) LDA results using AGE as the classification factor and $\delta^{13}C$ values of three amino acids after data was corrected for diet and sex. We obtained approximately 50% of correct classification after LOOCV. **B)** LDA plots for 82 subjects using isotope ratios of Met/Cyt, Ile/Leu and Lys. The variables were chosen based on their higher canonical discriminant functions compared to the other amino acids. The two discriminant functions have very small Eigenvalues (<1), which is the possible reason for the poor classification.

A

Classification Results[a,c]

			Predicted Group Membership				
		BMI (Binned)	<= 18.4	18.5 - 24.9	25.0 - 29.9	30.0+	Total
Original	Count	<= 18.4	0	5	0	0	5
		18.5 - 24.9	0	38	2	2	42
		25.0 - 29.9	0	15	6	2	23
		30.0+	0	5	2	5	12
	%	<= 18.4	.0	100.0	.0	.0	100.0
		18.5 - 24.9	.0	90.5	4.8	4.8	100.0
		25.0 - 29.9	.0	65.2	26.1	8.7	100.0
		30.0+	.0	41.7	16.7	41.7	100.0
Cross-validated[b]	Count	<= 18.4	0	4	0	1	5
		18.5 - 24.9	2	35	2	3	42
		25.0 - 29.9	0	15	5	3	23
		30.0+	0	6	3	3	12
	%	<= 18.4	.0	80.0	.0	20.0	100.0
		18.5 - 24.9	4.8	83.3	4.8	7.1	100.0
		25.0 - 29.9	.0	65.2	21.7	13.0	100.0
		30.0+	.0	50.0	25.0	25.0	100.0

a. 59.8% of original grouped cases correctly classified.

b. Cross validation is done only for those cases in the analysis. In cross validation, each case is classified by the functions derived from all cases other than that case.

c. 52.4% of cross-validated grouped cases correctly classified.

B

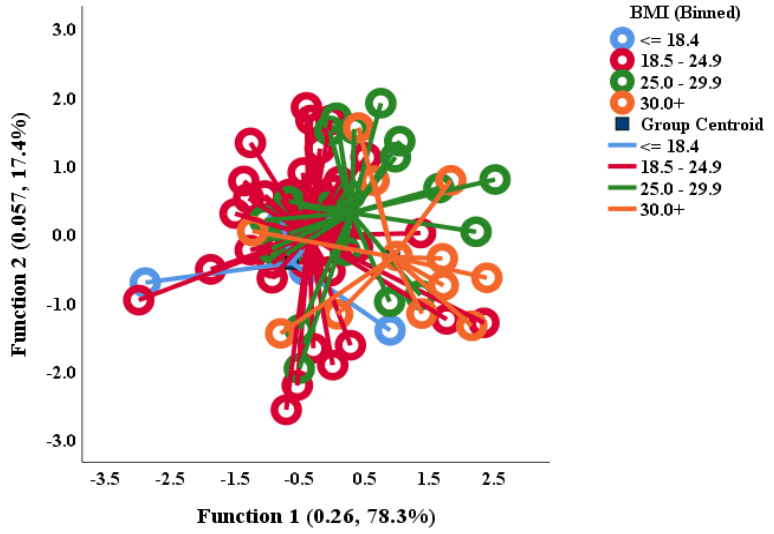

Fig. A4.4. A) LDA results using BMI as classification factor and relative quantities in mols of six amino acid variables. Leave one-out cross-validation reached just 50% of accuracy in discriminating the cases into the BMI groups. **B)** LDA plots for 82 subjects using Asx_mols, Gly_mols, Ile/Leu_mols,Tyr_mols, Lys_mols and Arg_mols as predictor variables. The variables were chosen based on their higher canonical discriminant functions compared to the other quantities of amino acids. Eigenvalues were very small (<1) and not helpful in the classification.

Table A4.1. Summary of self-reported characteristics for bulk hair analysis and compound-specific isotope analysis of American volunteers. Data is reported as mean ± expanded uncertainty of the measurements (2σ).

	BULK (N=101)		**CSIA (N=82)**	
	Males (mean ± 95% CI)	**Females (mean ± 95% CI)**	**Males (mean ± 95% CI)**	**Females (mean ± 95% CI)**
N	30	71	25	57
Age (years)	33 ± 26	32 ± 30	33 ± 27	32 ± 32
Weight (Kg)	81 ± 38	68 ± 43	82 ± 41	68 ± 46
Height (cm)	178 ± 22	164 ± 20	179 ± 24	164 ± 21
BMI	26 ± 8	25 ± 13	26 ± 9	25 ± 14

Table A4.2. Person product-moment correlation coefficient among the $\delta^{13}C$ values of 13 amino acids (11 variables). The correlations ranged from r=0.226 to r=0.707. * indicates correlation was significant at the 0.05 level (2-tailed), ** correlation was significant at the 0.01 level (2-tailed). N= 82.

		ASX	SER	GLY	VAL	MET/ CYT	ILE/LEU	TYR	LYS	HIS	PHE	ARG
ASX	Pearson Correlation	1	.499**	.363**	.409**	.465**	.454**	.365**	.159	.160	.170	.496**
	Sig. (2-tailed)		.000	.001	.000	.000	.000	.001	.155	.150	.127	.000
SER	Pearson Correlation	.499**	1	.494**	.541**	.587**	.655**	.120	.314**	.188	.139	.537**
	Sig. (2-tailed)	.000		.000	.000	.000	.000	.283	.004	.091	.213	.000
GLY	Pearson Correlation	.363**	.494**	1	.560**	.326**	.310**	.374**	.084	.254*	-.106	.554**
	Sig. (2-tailed)	.001	.000		.000	.003	.005	.001	.456	.021	.341	.000
VAL	Pearson Correlation	.409**	.541**	.560**	1	.314**	.705**	.555**	.226*	.540**	.107	.707**
	Sig. (2-tailed)	.000	.000	.000		.004	.000	.000	.041	.000	.340	.000
MET/ CYT	Pearson Correlation	.465**	.587**	.326**	.314**	1	.570**	.333**	.292**	.082	.237*	.458**
	Sig. (2-tailed)	.000	.000	.003	.004		.000	.002	.008	.462	.032	.000
ILE/LEU	Pearson Correlation	.454**	.655**	.310**	.705**	.570**	1	.447**	.398**	.327**	.326**	.604**
	Sig. (2-tailed)	.000	.000	.005	.000	.000		.000	.000	.003	.003	.000
TYR	Pearson Correlation	.365**	.120	.374**	.555**	.333**	.447**	1	.006	.358**	.015	.661**
	Sig. (2-tailed)	.001	.283	.001	.000	.002	.000		.960	.001	.896	.000
LYS	Pearson Correlation	.159	.314**	.084	.226*	.292**	.398**	.006	1	-.086	.361**	.101

	Sig. (2-tailed)	.155	.004	.456	.041	.008	.000	.960		.443	.001	.369
HIS	Pearson Correlation	.160	.188	.254*	.540**	.082	.327**	.358**	-.086	1	.122	.488**
	Sig. (2-tailed)	.150	.091	.021	.000	.462	.003	.001	.443		.273	.000
PHE	Pearson Correlation	.170	.139	-.106	.107	.237*	.326**	.015	.361**	.122	1	.176
	Sig. (2-tailed)	.127	.213	.341	.340	.032	.003	.896	.001	.273		.114
ARG	Pearson Correlation	.496**	.537**	.554**	.707**	.458**	.604**	.661**	.101	.488**	.176	1
	Sig. (2-tailed)	.000	.000	.000	.000	.000	.000	.000	.369	.000	.114	

Table A4.3. Person product-moment correlation coefficient among the quantities of 13 amino acids (11 variables). The correlations ranged from r=-0.241 to r=0.826. * indicates correlation was significant at the 0.05 level (2-tailed), ** correlation was significant at the 0.01 level (2-tailed). N= 82.

		ASX_mols	SER_mols	GLY_mols	VAL_mols	MET/ CYT_mols	ILE/LEU_ mols	TYR_mols	LYS_mols	HIS_mols	PHE_mols	ARG_mols
ASX_mols	Pearson Correlation	1	-.066	-.109	.104	-.776**	.369**	-.023	-.009	-.351**	.260*	.476**
	Sig. (2-tailed)		.558	.331	.353	.000	.001	.834	.936	.001	.018	.000
SER_mols	Pearson Correlation	-.066	1	.356**	-.545**	.079	-.615**	.285**	.067	.079	-.063	.129
	Sig. (2-tailed)	.558		.001	.000	.481	.000	.009	.547	.481	.573	.248
GLY_mols	Pearson Correlation	-.109	.356**	1	-.024	.009	-.186	-.001	.026	-.114	-.179	-.187
	Sig. (2-tailed)	.331	.001		.832	.933	.095	.991	.816	.307	.108	.092
VAL_mols	Pearson Correlation	.104	-.545**	-.024	1	-.408**	.826**	-.729**	-.203	-.311**	-.180	-.109
	Sig. (2-tailed)	.353	.000	.832		.000	.000	.000	.068	.004	.106	.332
MET/ CYT_mols	Pearson Correlation	-.776**	.079	.009	-.408**	1	-.523**	.147	-.033	.287**	-.269*	-.492**
	Sig. (2-tailed)	.000	.481	.933	.000		.000	.188	.772	.009	.015	.000
ILE/LEU_m ols	Pearson Correlation	.369**	-.615**	-.186	.826**	-.523**	1	-.662**	-.241*	-.391**	-.090	-.066
	Sig. (2-tailed)	.001	.000	.095	.000	.000		.000	.029	.000	.420	.557
TYR_mols	Pearson Correlation	-.023	.285**	-.001	-.729**	.147	-.662**	1	-.078	.176	-.050	.153
	Sig. (2-tailed)	.834	.009	.991	.000	.188	.000		.488	.114	.655	.169

LYS_mols	Pearson Correlation	-.009	.067	.026	-.203	-.033	-.241*	-.078	1	.323**	.666**	-.156
	Sig. (2-tailed)	.936	.547	.816	.068	.772	.029	.488		.003	.000	.162
HIS_mols	Pearson Correlation	-.351**	.079	-.114	-.311**	.287**	-.391**	.176	.323**	1	.188	-.196
	Sig. (2-tailed)	.001	.481	.307	.004	.009	.000	.114	.003		.090	.077
PHE_mols	Pearson Correlation	.260*	-.063	-.179	-.180	-.269*	-.090	-.050	.666**	.188	1	.079
	Sig. (2-tailed)	.018	.573	.108	.106	.015	.420	.655	.000	.090		.482
ARG_mols	Pearson Correlation	.476**	.129	-.187	-.109	-.492**	-.066	.153	-.156	-.196	.079	1
	Sig. (2-tailed)	.000	.248	.092	.332	.000	.557	.169	.162	.077	.482	

Table A4.4. Person product-moment correlation coefficient for SEX factor vs. $\delta^{13}C$ values of 13 amino acids (11 variables). The strength of correlation and significance increased when the data was corrected for diet. * indicates correlation was significant at the 0.05 level (2-tailed), ** correlation was significant at the 0.01 level (2-tailed). N= 82 for original data and all diet corrections, except bulk diet correction (N= 81).

Amino acid	Correlation coefficient	Original $\delta^{13}C$ dataset	Diet correction for meat intake	Weighted diet correction	Bulk diet correction
		Sex	**Sex**	**Sex**	**Sex**
ASX	Pearson Correlation	-0.132	-0.097	-0.183	0.021
	Sig. (2-tailed)	0.237	0.385	0.100	0.850
SER	Pearson Correlation	0.190	**0.218***	**0.238***	**0.338****
	Sig. (2-tailed)	0.087	**0.049**	**0.031**	**0.002**
GLY	Pearson Correlation	**0.355****	**0.363****	**0.398****	**0.468****
	Sig. (2-tailed)	**0.001**	**0.001**	**0.000**	**0.000**
VAL	Pearson Correlation	**0.229***	**0.281***	**0.329****	**0.457****
	Sig. (2-tailed)	**0.038**	**0.010**	**0.003**	**0.000**
MET/CYT	Pearson Correlation	-0.072	-0.075	-0.110	0.097
	Sig. (2-tailed)	0.518	0.501	0.325	0.390
ILE/LEU	Pearson Correlation	0.008	0.067	-0.007	0.196
	Sig. (2-tailed)	0.946	0.548	0.952	0.080
TYR	Pearson Correlation	-0.082	-0.025	-0.113	0.061
	Sig. (2-tailed)	0.466	0.827	0.314	0.591
LYS	Pearson Correlation	0.032	0.049	0.030	0.135
	Sig. (2-tailed)	0.774	0.660	0.792	0.230
HIS	Pearson Correlation	**0.232***	**0.224***	**0.243***	**0.287****
	Sig. (2-tailed)	**0.036**	**0.043**	**0.028**	**0.009**
PHE	Pearson Correlation	0.058	0.061	0.056	0.157
	Sig. (2-tailed)	0.604	0.584	0.616	0.163
ARG	Pearson Correlation	0.209	**0.255***	**0.324****	**0.419****
	Sig. (2-tailed)	0.059	**0.021**	**0.003**	**0.000**

Table A4.5. MANOVA tests of between-subjects effects on the original $\delta^{13}C$ dataset (uncorrected) using SEX as independent variable and $\delta^{13}C$ values of 13 amino acids (11 variables) as dependent variables. There was a statistically significant difference between the $\delta^{13}C$ values of Gly, Val and His of males and females. N= 82 (25 males, 57 females), α=0.05.

Source		Type III Sum of Squares	df	Mean Square	F	Sig.	Partial Eta Squared
Sex	ASX	2.451	1	2.451	1.422	0.237	0.017
	SER	8.459	1	8.459	3.010	0.087	0.036
	GLY	36.217	1	36.217	**11.562**	**0.001**	**0.126**
	VAL	9.390	1	9.390	**4.438**	**0.038**	**0.053**
	MET_CYT	0.488	1	0.488	0.422	0.518	0.005
	ILE/LEU	0.008	1	0.008	0.005	0.946	0.000
	TYR	1.043	1	1.043	0.537	0.466	0.007
	LYS	0.550	1	0.550	0.083	0.774	0.001
	HIS	58.321	1	58.321	**4.541**	**0.036**	**0.054**
	PHE	1.332	1	1.332	0.272	0.604	0.003
	ARG	7.324	1	7.324	3.658	0.059	0.044

Table A4.6. MANOVA tests of between-subjects effects on the data corrected with individual bulk carbon measurements using SEX as independent variable and $\delta^{13}C$ values of 13 amino acids (11 variables) as dependent variables. After the correction for diet, there was a statistically significant difference between the $\delta^{13}C$ values of Ser, Gly, Val, His and Arg of males and females. Using a Bonferroni adjusted α= 4.5E-3 (α value/ number of dependent variables), the $\delta^{13}C$ value of His was not significant anymore. N= 81 (25 males, 56 females), α=0.05.

Source		Type III Sum of Squares	df	Mean Square	F	Sig.	Partial Eta Squared
Sex	ASX	0.043	1	0.043	0.036	0.850	0.000
	SER	15.713	1	15.713	**10.167**	***0.002***	**0.114**
	GLY	56.889	1	56.889	**22.119**	***1.07e-5***	**0.219**
	VAL	22.643	1	22.643	**20.873**	***1.78e-5***	**0.209**
	MET_CYT	1.018	1	1.018	0.748	0.390	0.009
	ILE/LEU	3.191	1	3.191	3.143	0.080	0.038
	TYR	0.434	1	0.434	0.292	0.591	0.004
	LYS	8.542	1	8.542	1.463	0.230	0.018
	HIS	85.925	1	85.925	**7.108**	**0.009**	**0.083**
	PHE	9.713	1	9.713	1.987	0.163	0.025
	ARG	19.203	1	19.203	**16.829**	***9.86e-5***	**0.176**

Table A4.7. Descriptive statistics of the data corrected with individual bulk carbon measurements using SEX as independent variable and $\delta^{13}C$ values of 13 amino acids (11 variables) as dependent variables. The difference in the mean scores for males and females was at most 2‰.

AA	Sex	Mean	Std. Deviation	N
SER	Male	**-10.120**	1.387	25
	Female	**-9.166**	1.175	56
	Total	-9.460	1.312	81
GLY	Male	**-12.432**	1.996	25
	Female	**-10.617**	1.399	56
	Total	-11.177	1.803	81
VAL	Male	**-23.610**	1.065	25
	Female	**-22.465**	1.031	56
	Total	-22.819	1.164	81
HIS	Male	**-12.321**	3.104	25
	Female	**-10.091**	3.628	56
	Total	-10.779	3.607	81
ARG	Male	**-18.860**	.974	25
	Female	**-17.806**	1.107	56
	Total	-18.131	1.169	81

Table A4.8. Linear discriminant analysis (classification) of 81 subjects (25 males, 56 females) according to SEX after data correction for diet. We used the $\delta^{13}C$ values of Asx, Ser, Gly, Val, Met/Cyt, Ile/Leu, Tyr, Lys, His, Phe and Arg (11 variables, 13 amino acids) as variables. Subjects were correctly classified as males or females with approximately 78% accuracy after leave-one-out cross validation.

			Predicted Group Membership		
		Sex	**Male**	**Female**	**Total**
Original	**Count**	**1**	14	11	25
		2	4	52	56
	%	**1**	56.0	44.0	100.0
		2	7.1	92.9	100.0
Cross-validated[c]	**Count**	**1**	13	12	25
		2	6	50	56
	%	**1**	52.0	48.0	100.0
		2	10.7	89.3	100.0

a. 81.5% of original grouped cases correctly classified.

b. 77.8% of cross-validated grouped cases correctly classified.

c. Cross validation is done only for those cases in the analysis. In cross validation, each case is classified by the functions derived from all cases other than that case.

Table A4.9. Standardized canonical discriminant function coefficients using SEX as a discrimination factor. $\delta^{13}C$ variables with large absolute coefficient values have a bigger impact on the separation of subject into sex groups and successful classification. The data was corrected for diet using individual bulk measurements prior to analysis.

Standardized Canonical Discriminant Function Coefficients	
AA	**Function 1**
SER	.230
GLY	.473
VAL	.380
HIS	.134
ARG	.240

Table A4.10. MANOVA tests of between-subjects effects using SEX as independent variable and the quantities of 7 amino acids as dependent variables. Using a Bonferroni adjusted α= 8.3E-3 (α=0.05/ number of dependent variables), Ser and Arg were not significant anymore. The word "mols" was added to each variable to differentiate them from the names used with carbon isotopes. N= 82 (25 males, 57 females).

Source	Dependent Variable	Type III Sum of Squares	df	Mean Square	F	Sig.	Partial Eta Squared
Sex	SER_mols	.361	1	.361	5.044	.027	.059
	VAL_mols	1.729	1	1.729	**80.312**	***1.04e-13***	**.501**
	ILE/LEU_mols	1.056	1	1.056	**24.884**	***3e-6***	**.237**
	TYR_mols	.254	1	.254	**19.816**	***2.7e-5***	**.199**
	LYS_mols	.025	1	.025	**8.910**	**.004**	**.100**
	ARG_mols	.045	1	.049	4.503	.037	.053

Table A4.11. Linear discriminant analysis (classification) of 82 subjects (25 males, 57 females) according to SEX. We used the quantities of Asx, Ser, Gly, Val, Ile/Leu, Tyr, Lys, His, Phe and Arg (10 variables, 11 amino acids) as variables. Subjects were correctly classified as males or females with approximately 94% accuracy after leave-one-out cross validation.

			Predicted Group Membership		
		Sex	**Male**	**Female**	**Total**
Original	**Count**	**1**	22	3	25
		2	2	55	57
	%	**1**	88.0	12.0	100.0
		2	3.6	96.5	100.0
Cross-validated[c]	**Count**	**1**	22	3	25
		2	2	55	57
	%	**1**	88.0	12.0	100.0
		2	3.5	96.5	100.0

a. 93.9% of original grouped cases correctly classified.

b. 93.9% of cross-validated grouped cases correctly classified.

c. Cross validation is done only for those cases in the analysis. In cross validation, each case is classified by the functions derived from all cases other than that case.

Table A4.12. Standardized canonical discriminant function coefficients using SEX as a discrimination factor. Mols of AA with large absolute coefficient values have a bigger impact on the separation of subject into sex groups and successful classification.

Standardized Canonical Discriminant Function Coefficients

AA	Function 1
VAL_mols	1.374
ILE/LEU_mols	-.626
TYR_mols	.009
LYS_mols	-.396

Table A4.13. Person product-moment correlation coefficient for AGE factor vs. $\delta^{13}C$ values of 13 amino acids (11 variables). The strength of correlation and significance slightly increased after corrections for diet. There were no significant correlations when age was separated in groups (results not shown). * indicates correlation was significant at the 0.05 level (2-tailed), ** correlation was significant at the 0.01 level (2-tailed). N= 82 for original data and all diet corrections, except bulk diet correction (N= 81).

Amino acid	Correlation coefficient	Original $\delta^{13}C$ dataset	Diet correction for meat intake	Weighted diet correction	Bulk diet correction	Sex correction after weighted diet correction	Sex correction after bulk diet correction
		Age	**Age**	**Age**	**Age**	**Age**	**Age**
ASX	Pearson Correlation	-0.091	-0.092	-0.18	-0.069	-0.184	-0.068
	Sig. (2-tailed)	0.416	0.41	0.105	0.542	0.098	0.544
SER	Pearson Correlation	0.012	0.013	-0.051	-0.003	-0.052	0.004
	Sig. (2-tailed)	0.914	0.905	0.651	0.981	0.644	0.969
GLY	Pearson Correlation	-0.098	-0.115	-0.152	-0.135	-0.165	-0.142
	Sig. (2-tailed)	0.382	0.305	0.174	0.23	0.139	0.206
VAL	Pearson Correlation	-0.011	-0.015	-0.082	-0.001	-0.086	0.009
	Sig. (2-tailed)	0.924	0.892	0.466	0.994	0.443	0.934
MET/CYT	Pearson Correlation	0.021	0.019	-0.052	0.041	-0.052	0.043
	Sig. (2-tailed)	0.854	0.865	0.643	0.719	0.641	0.705
ILE/LEU	Pearson Correlation	0.171	**0.219***	**0.245***	**0.242***	**0.245***	**0.251***
	Sig. (2-tailed)	0.125	**0.048**	**0.026**	**0.029**	**0.026**	**0.024**
TYR	Pearson Correlation	0.082	0.109	0.043	0.109	0.043	0.111
	Sig. (2-tailed)	0.464	0.328	0.701	0.332	0.7	0.326
LYS	Pearson Correlation	**-0.256***	**-0.267***	**-0.312****	-0.197	**-0.312****	-0.197
	Sig. (2-tailed)	**0.02**	**0.015**	**0.004**	0.077	**0.004**	0.079
HIS	Pearson Correlation	0.076	0.072	0.062	0.076	0.064	0.086
	Sig. (2-tailed)	0.5	0.52	0.582	0.499	0.568	0.448
PHE	Pearson Correlation	0.104	0.104	0.081	0.161	0.081	0.166
	Sig. (2-tailed)	0.352	0.35	0.472	0.152	0.47	0.139
ARG	Pearson Correlation	0.023	0.025	-0.036	0.038	-0.037	0.051
	Sig. (2-tailed)	0.834	0.821	0.75	0.74	0.74	0.654

Table A4.14. Independent sample t-tests (Student's t-test) comparing the carbon and nitrogen bulk isotope values of females who did different different hair treatments.The one subject who did chemical straithening was not included in this analysis. However, its value (δ^{13}C=-18.682, δ^{15}N=9.863) was not vastly different from the other treatments mean. N=25, two-sample assuming unequal variance, α= 0.05.

	Average TRUE δ^{13}C - Bleach and coloring	***Average TRUE δ^{13}C - Coloring***
Mean	-18.329	-18.998
Variance	0.308	2.582
Observations	5	20
Hypothesized Mean Difference	0	
df	20	
t Stat	1.531	
P(T<=t) one-tail	0.071	
t Critical one-tail	1.725	
P(T<=t) two-tail	**0.141**	
t Critical two-tail	2.086	

	Average TRUE δ^{15}N - Bleach and coloring	***Average TRUE δ^{15}N - Coloring***
Mean	9.418	9.456
Variance	0.072	0.901
Observations	5	20
Hypothesized Mean Difference	0	
df	22	
t Stat	-0.157	
P(T<=t) one-tail	0.438	
t Critical one-tail	1.717	
P(T<=t) two-tail	**0.876**	
t Critical two-tail	2.074	

Table A4.15. Independent sample t-tests (Student's t-test) comparing the carbon and nitrogen bulk isotope values of females who did any of the hair treatments vs. the ones who did not. N= 71, two-sample assuming unequal variance, $\alpha = 0.05$.

	Average TRUE $\delta^{13}C$ - no hair treatment	***Average TRUE $\delta^{13}C$ - with hair treatment***
Mean	-18.823	-18.857
Variance	0.646	2.085
Observations	45	26
Hypothesized Mean Difference	0	
df	34	
t Stat	0.111	
P(T<=t) one-tail	0.456	
t Critical one-tail	1.691	
P(T<=t) two-tail	**0.912**	
t Critical two-tail	2.032	

	Average TRUE $\delta^{15}N$ - no hair treatment	***Average TRUE $\delta^{15}N$ - with hair treatment***
Mean	9.715	9.465
Variance	0.240	0.703
Observations	45	26
Hypothesized Mean Difference	0	
df	35	
t Stat	1.392	
P(T<=t) one-tail	0.086	
t Critical one-tail	1.690	
P(T<=t) two-tail	**0.173**	
t Critical two-tail	2.030	

Table A4.16. Independent sample t-tests (Student's t-test) comparing the δ^{13}C values of females who did any of the hair treatments vs. the ones with untreated hair. N= 57, two-sample assuming unequal variance, α= 0.05.

Null hypothesis	t	Sig.
The distribution of δ^{13}C ASX is the same across categories of Hair treatment	-0.147	0.884
The distribution of δ^{13}C SER is the same across categories of Hair treatment	0.044	0.966
The distribution of δ^{13}C GLY is the same across categories of Hair treatment	1.400	0.172
The distribution of δ^{13}C VAL is the same across categories of Hair treatment	1.091	0.284
The distribution of δ^{13}C MET/ CYT is the same across categories of Hair treatment	0.519	0.607
The distribution of δ^{13}C ILE/LEU is the same across categories of Hair treatment	0.811	0.426
The distribution of δ^{13}C TYR is the same across categories of Hair treatment	1.436	0.161
The distribution of δ^{13}C LYS is the same across categories of Hair treatment	0.297	0.769
The distribution of δ^{13}C HIS is the same across categories of Hair treatment	1.670	0.102
The distribution of δ^{13}C PHE is the same across categories of Hair treatment	1.716	0.094
The distribution of δ^{13}C ARG is the same across categories of Hair treatment	1.486	0.148

Table A4.17. Independent sample t-tests (Student's t-test) comparing the quantities of amino acids in females who did any of the hair treatments vs. the ones with untreated hair. N= 57, two-sample assuming unequal variance, $\alpha = 0.05$.

Null hypothesis	t	Sig.
The distribution of ASX_mols is the same across categories of Hair treatment	0.414	0.681
The distribution of SER_mols is the same across categories of Hair treatment	-1.122	0.268
The distribution of GLY_mols is the same across categories of Hair treatment	**-2.256**	**0.028**
The distribution of VAL_mols is the same across categories of Hair treatment	-0.635	0.529
The distribution of ILE/LEU_mols is the same across categories of Hair treatment	0.987	0.328
The distribution of TYR_mols is the same across categories of Hair treatment	-0.135	0.893
The distribution of LYS_mols is the same across categories of Hair treatment	-0.732	0.469
The distribution of HIS_mols is the same across categories of Hair treatment	-0.413	0.682
The distribution of PHE_mols is the same across categories of Hair treatment	-1.170	0.247
The distribution of ARG_mols is the same across categories of Hair treatment	-0.488	0.628